Doctor Thesis

博士論文

Structural Analysis of Troponin Complex
: Crystallization and Biochemical Studies

トロポニン複合体の構造解析：結晶化と生化学的研究

by

SOICHI TAKEDA

武田　壮一

Submitted to Nagoya University

名古屋大学大学院　理学研究科　生物学専攻

Thesis supervisor: Professor Hiroshi Hayashi

March 1997

①

Doctor Thesis

博士論文

Structural Analysis of Troponin Complex
: Crystallization and Biochemical Studies

トロポニン複合体の構造解析：結晶化と生化学的研究

by

SOICHI TAKEDA

武田　壮一

Submitted to Nagoya University

名古屋大学大学院　理学研究科　生物学専攻

Thesis supervisor: Professor Hiroshi Hayashi

March 1997

要旨

トロポニン複合体は TnT, TnI, TnC の 3 つのサブユニットから成り、骨格筋及び心筋に於いてカルシウムイオンによる収縮の調節に重要な役割を担っている。この調節機構を理解するためにはトロポニン複合体の三次元立体構造を明らかにすることが重要な課題となっている。現在のところ TnC についてはその三次元立体構造が、X 線結晶解析法及び多次元核磁気共鳴法によってカルシウム結合数が 2 のものと 4 のものとが報告されている。カルシウムイオンによる調節の仕組みを立体構造の上から明らかにするには、他のサブユニットとの相互作用部位さらには複合体としての構造とその変化を捉える必要がある。しかし TnT 及び TnI、あるいは複合体としての構造解析は今のところ成功していない。その理由として、TnT 及び TnI 単体では溶解度が低く安定性がない事、また筋肉より精製したトロポニン複合体は多くのアイソフォームを含み、結晶化に要求される均一な試料を得る事が難しいという点が挙げられる。結晶化は蛋白質構造解析の第一歩であり、測定及び解析技術の進歩の著しい今日に於いては良質の結晶を得る事が構造解析へのボトルネックとなっていると言え、良質な結晶を得るための一般的な方法論の確立は構造学者のみならず、多くの生物学者の望むところとなっている。本研究ではトロポニン複合体の X 線結晶解析を目的として、結晶化試料の設計から得られた結晶の改良までの各段階について様々な新しい試みを行った。その結果、解析レベルの結晶を含むいくつかの複合体の結晶化に成功した。本学位論文では次に示す五章にこれら新しい試みを含むトロポニン複合体の結晶化への計略とその結果及び考察についてまとめる。

第一章では結晶化試料の設計に関して、蛋白質分解酵素によるトロポニン複合体の限定分解を行った結果を記載する。多くの蛋白質において限定分解によって切り出された機能ドメインの結晶化及びその構造解析が成功している。限定分解を行うことで、結晶化の弊害となる一次構造を含む構造の異種性あるいは構造の不安定な領域を取り除くことが結晶化に有効であろうと考えられる。結晶化試料の設計を目的として、これらの実験を始めたが、トロポニン複合体

のドメイン構造と機能との関わりについて新たな知見が得られた。ウサギ骨格筋より調製したトロポニン複合体をカルシウム存在下でキモトリプシンで限定分解することで、TnT の C 末端側 159-259 残基、TnI の N 末端側 1-134 残基、TnC から成り、アクトミオシン ATPase をカルシウムイオン濃度依存的に調節する機能的なコアドメインを単離する事が出来た。また、カルシウム不在下の同様の処理で TnT の C 末端側 159-259 残基、TnI の N 末端側 1-116 残基、TnC から成るコアが単離出来たが、カルシウム調節能は失われていた。これらの結果から、カルシウムイオンによるアクトミオシン ATPase 調節に必須な領域(TnI 残基 117-134)を明らかにすることが出来、また２状態(筋中での活性化状態と定常状態に相当する２状態)間での構造の違いをキモトリプシンによる TnI の切断位置の違いとして捉えることができた。また得られた TnI 断片を用いる事で、TnI の C 末端側にアクチン－トロポミオシンとの結合部位が存在している事を明らかにした。

第二章では第一章で特徴付けた新しく見出した TnI 断片を精製するための詳しい方法について記載する。かつては、この様な長さの TnI 断片を得るには、大腸菌で発現された蛋白質を用いる方法しか知られていなかったが、本研究では TnI 断片 1-116 及び 1-134 残基を効率よくかつ高い純度で得る方法を確立した。

第三章では実際に結晶化が成功したものについて、分子の設計から初期解析さらに今後の展望について記述する。第一節ではこれまでトロポニンの機能ドメインと考えられていた TnT2-TnC-TnI 三量体の結晶について述べる。PEG4000、4-10%及び $ZnCl_2$、1-10mM 存在下、pH 8 で菱面体状の結晶を得る事に成功した。現在のところ分解能 8-10Å程度のものしか得られていないが、トロポニン三量体の結晶としては初めての報告であり、結晶の改善についての展望を記述する。第二節ではトロポニン複合体及びトロポミオシンの断片を含む $Tm_{141-284}$-TnT25k-TnC-TnI 複合体(Tm 141-284 残基、TnT 53-260 残基と TnC 及び TnI 計５ペプチドを含む複合体)の結晶について述べる。かつて　ロポニン－トロポミオシンから成る活性トロポミオシンの結晶が報告されたが、高分解能

の解析はなされていない。重合したトロポミオシンがネット状の格子を形成し、含水量を高めている事が問題として考えられている。我々は重合しないトロポミオシンを用いる事で、新しい結晶を得る事に成功した。現在のところ 20 μm 程度の大きさのものしか得られていないが、超薄切片の電子顕微鏡観察により、蛋白質から成る結晶であることが確かめられている。第三節では TnI 断片 1-47 残基と TnC を含む TnC-TnI_{1-47} 二量体の結晶について記述する。TnI の N 末は TnC と強い相互作用する事が知られており、筋繊維中でのトロポニン分子の安定化に重要な役割を担っていると考えられている。我々はこの複合体を異なる 2 条件で結晶化する事に成功し、さらにクエン酸ナトリウムより生じた結晶はその後の条件の最適化により 2.3Åの分解能の回折像を示した。

第四章では第三章に於いて用いた結晶化試料の調整法について述べる。結晶化に用いた試料は全て大腸菌で大量発現させたトロポニン各成分とその断片を用いている。第一節では TnT25k、TnI、TnC 各成分の菌体からの精製法を、第二、第三節ではメチオニン、及びシステイン残基特異的な化学的切断法による、TnT2 及び TnI_{1-47} 断片の調整法と TnT2-TnC-TnI 三量体及び TnC-TnI_{1-47} 二量体の調整法を、第四節ではトロポミオシン断片 141—284 の精製法と $Tm_{141-284}$-TnT25k-TnC-TnI 複合体の調整法について記載する。本研究では特定部位の変異体蛋白質を用い化学的切断法により目的の断片を効率良く得る事に成功した。これら方法では大腸菌での直接発現が困難でありかつ合成では不可能な長さのペプチドを高い純度で得ることが可能である。これらの手法の結晶化試料への適用については本研究が初めての報告であるが実際に高分解の回折能を有する結晶を得る事に成功した事により、結晶化試料の調整法の一つとして他の蛋白質への応用が期待される。

第五章では蛋白質工学的手法による結晶化へのアプローチについて記載する。本研究では二つの手法の可能性と問題点の検討を行った。第一節ではリジン残基の還元的メチル化について記載する。Rayment らによるミオシン S-1 の構造解析に於いては、リジン残基を特異的に化学修飾し、蛋白質の表層構造を変える事で良質の結晶を得る事に成功した。本研究ではこの手法をトロポニ

ン複合体に適用し結晶化を試みた。結果としては結晶を得るに至らなかったが、新たに考案した、修飾した蛋白質をリジルエンドペプチダーゼで消化し修飾されたリジン残基を検出する方法について記載する。またこの手法を用いた蛋白質相互作用部位の同定法を考案した。第二節では他の遺伝子産物との融合蛋白質を結晶化試料として用いた場合について記載する。本研究ではではマルトース結合蛋白質(MBP)を TnT の C 末断片 TnT2 との融合蛋白質(MBP-TnT2)として発現及び精製し、TnC 及び TnI との複合体として再構成したものの結晶化を行った。

ABSTRACT

Troponin (Tn), consisting of three subunits, TnT, TnC and TnI, plays a crucial role in the calcium-dependent regulation of vertebrate striated muscle contraction. In order to understand the mechanism of regulation of muscle contraction, it is essentially important to know the three dimensional structure of the Tn complex at an atomic resolution. Although crystal structure of avian TnC has been available for a decade, the molecular structures of TnT and TnI are still unknown. Tn complex isolated from muscle contains many isoforms, has never given rise to well diffracting crystals. In order to obtain crystals of Tn complex, several kinds of Tn complex have been designed, optimized purification procedures and allowed to be crystallized. In addition, limited proteolysis have been used not only to obtain the structural information but also clarify the structural and functional domains within the troponin complex. We also made attempt to crystallize troponin complex by the use of two different protein engineering techniques.

The thesis consists of following five parts.

In part I, structural and functional domains of troponin complex, which are derived from the studies based on the limited proteolysis, are described. Not only the functional core domain of the troponin complex was clarified but also conformational difference of troponin under different conditions (the activated and the resting state) was detected by limited chymotryptic digestion of the ternary troponin complex.

In part II, Purification procedures for the troponin components and the fragments (which are characterized in part 1) from rabbit skeletal muscle are described in detail.

In part III, crystallization and preliminary crystallographic analysis of the troponin complex are described. Following three species of the complexes were reproducibly crystallized. III-1, TnT2-TnC-TnI ternary complex (TnT res.159-259); III-2, $Tm_{141-284}$-TnT25k-TnC-TnI complex (Tm res.141-284; TnT res. 53-260); III-3, TnC-TnI_{1-47} (TnI res. 1-47) binary complex.

In part IV, Purification procedures for *E.coli* expressed troponin components, fragments and tropomyosin fragments, and also the methods to reconstitute the complexes used in the crystallization trials described in part III are described.

In part V, the discussions about the applicability of protein engineering techniques for crystallization of proteins are described: (V-1) reductive methylation of lysine residues of troponin complex and (V-2) crystallization of troponin complex as a fusion protein.

CONTENTS

The abbreviations used are:

Tn, troponin; Tm, tropomyosin; S1, myosin subfragment 1; MBP, maltose binding protein;
EDTA, ethylenediaminetrtraacetic acid;
EGTA, ethyleneglycol bis(2-aminoethylether)tetraacetic acid;
HEPES, N-hydroxyethylpiperazine-N'-2-ethanesulfonic acid;
HPLC, high performance liquid chromatography;
MES, 2-(N-morpholino)ethanesulfonic acid;
MOPS, 4-morpholineethanesulfonic acid;
PAGE, polyacrylamide gel electrophoresis;
PEG, polyethyleneglycol;
PIPES, piperazine-N,N'-bis(2-ethanesulfonic acid);
SDS, sodium dodecyl sulfate;
TLCK, Nα-tosyl-L-lysyl ahloromethyl keton;
Tris, tris(hydroxymethyl)aminomethane;

INTRODUCTION

Cellular calcium

Ionized calcium (Ca^{2+}) is a ubiquitous intracellular second messenger molecule controlling a wide array of cellular processes, including secretion, contraction, metabolic adjustment, changes in gene expression and cell proliferation (for reviews, see Berrige, 1993; Claphan, 1995). Ca^{2+} is required for life, although prolonged presence of high concentration of Ca^{2+} leads to cell death. Ca^{2+} cannot be metabolized like other second messenger molecules, *e.g.* cyclic nucleotides, inositol phosphates, and so on. The presence of binding proteins or extracting systems must be required for keeping the concentration of Ca^{2+} low, at 10^{-7} to 10^{-8}M in the resting cell. It is notable that the vertebrate skeletal muscle cell is not only the most extensively studied but also the first system where the Ca^{2+} is recognized as a key regulator of cellular process (for review, see Ebashi and Endo, 1968).

Muscle cell and calcium regulation

The contractile machinery of vertebrate striated muscle shows an elaborate framework. According to the sliding filament model of muscle contraction (Fig. 0-1), the contraction of muscle is due to the interaction of myosin located in the thick filament with filamentous actin which forms the thin filament together with other molecules. The contraction of striated muscle is regulated by the concentration of cytoplasmic Ca^{2+}, which in turn is regulated by the sarcoplasmic reticulum (SR). The electric depolarization of the plasma membrane elicited by a nerve impulse led to release Ca^{2+} from the SR. The Ca^{2+} flooding into the cytosol then initiates the contraction of each myofibril. The increase in Ca^{2+} concentration in the cytosol is transient because the Ca^{2+} is rapidly pumped back into the SR by an abundant Ca^{2+}-ATPase in its membrane. The Ca^{2+} dependence of myofibril contraction within the skeletal muscle cell is due entirely to a set of specialized accessory proteins closely associated with actin filament (Fig. 0-2). One of these accessory proteins is a muscle form of tropomyosin, a rod-shaped molecule that binds in the groove of the actin helix. Almost all part of the molecule is made of α-helical coiled-coil. The other major accessory protein involved in the Ca^{2+} regulation of vertebrate skeletal muscle is troponin. It has been shown that troponin plays an essential role in Ca^{2+} regulation of striated muscle contraction.

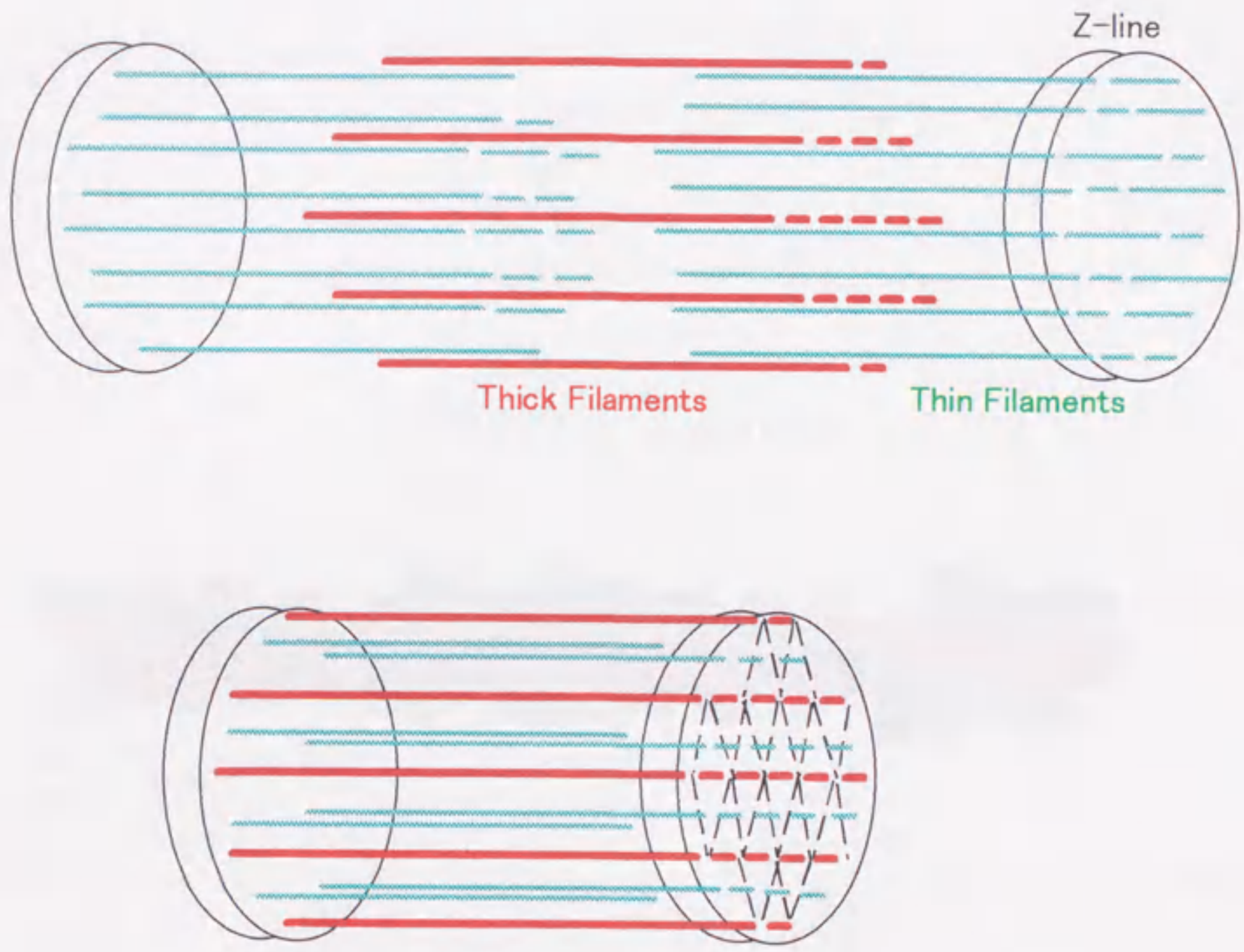

Figure 0-1 Sliding filament model. In 1950's, two groups of investigators independently proposed a *sliding-filament model* on the basis of x-ray, light-microscopic, and electron-microscopic studies. The essential futures of this model, which was proposed by Andrew Huxley and Ralph Niedergerke and by Hugh Huxley and Jean Hanson, are:

1. The length of the thick and thin filaments do not change during muscle contraction.
2. In stead, the length of the sarcomere decreases during contraction because the two types of filaments overlap more.
3. The force of contraction is generated by a process that actively moves one type of the filament past the neighboring filament of the other type.

(From Stryer, L. (1988) in *Biochemistry third edition* pp.923, W. H. Freeman and company, New York, with modification)

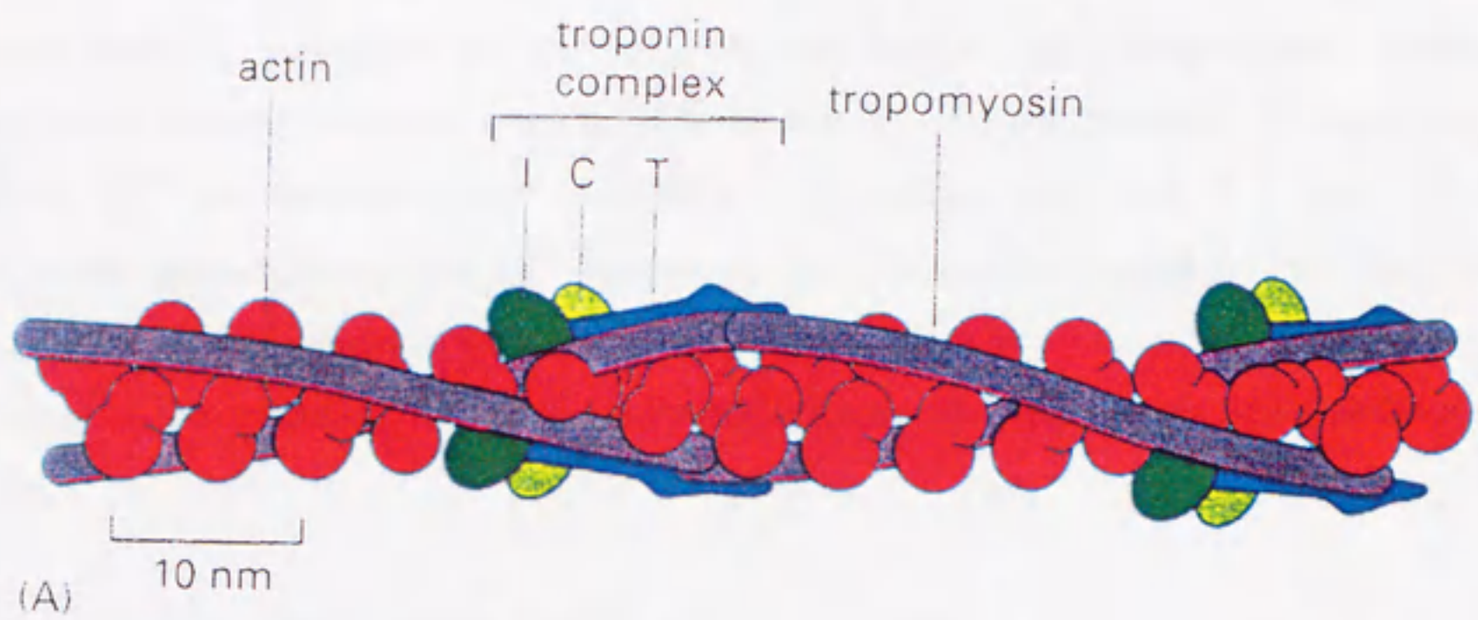

Figure 0-2. Model of a thin filament. The troponin complex consists of three components: TnI (green), TnC (light green), and TnT (blue).

(From Arbert et al., (1994) in *Molecular Biology of the Cell third edition* pp854, Garland Publishing, Inc. New York.)

Discovery of Troponin

It was early in 1960s, a new protein factor which was necessary for the Ca^{2+} sensitivity of actomyosin was discovered by Ebashi and colleagues (Ebashi, 1963; Ebashi and Ebashi, 1964). This protein factor was named native tropomyosin, because of its similarities in amino acid composition, biochemical and physical properties to tropomyosin. Tropomyosin was discovered and isolated in the 1940s by Bailey (Bailey, 1948), although no physiological role was known until the finding of a new protein termed troponin from native tropomyosin by Ebashi and colleagues (Ebashi and Kodama, 1965). The mixture of purified troponin with purified tropomyosin reconstituted the physico-chemical properties and physiological activities of native tropomyosin. Unlike other myofibrillar proteins, troponin was shown to be able to bind and release Ca^{2+} depending on the cellular Ca^{2+} concentrations which are utilized in the calcium regulation, and when reconstituted with tropomyosin-actin-myosin, Ca^{2+} dependence of superprecipitation and ATPase were observed. These findings and numerous others confirmed that troponin was the real Ca^{2+}-sensitizing protein involved in the regulation of the skeletal muscle contraction (for review, see Ebashi and Endo, 1968).

The components of the troponin complex

Greaser and Gergely (1971, 1973) established that troponin exists as a complex of three non-identical subunits. Subsequent investigations of the functions of the individual subunits led to the following terminology: TnC is the Ca^{2+}-binding subunit; TnI inhibits actomyosin ATPase activity; and TnT binds to tropomyosin and thereby attaches the troponin complex to the thin filament (for reviews, see Leavis and Gergely, 1984; Ohtsuki *et al.*, 1986; Zot and Potter, 1987; Tobacman, 1996).

TnC from rabbit skeletal muscle is composed of 159 residues and a very acidic protein (pI~4.3) owing to its high contents of glutamic acid and aspartic acid residues (Collins *et al.*, 1977, Zot *et al.*, 1987). The crystal structure of avian skeletal TnC revealed a dumb-bell shaped structure with two globular lobes connected by a central helix (Fig. 0-3; Herzberg and James, 1985, 1988; Sundaralingam *et al.*, 1985) and the overall appearance was turned out to be very similar to that of calmodulin (Babu, *et al.*, 1985). Structural similarities of TnC with myosin light chains were also shown (Rayment, *et al.*, 1991; Xie, *et al.*, 1994). It is interesting from an evolutionary point of view that each of these Ca^{2+}-binding protein functions as a key regulator of contraction in different types of muscle cell: troponin in the vertebrate striated muscle, myosin light chains in the molluscs muscle and calmodulin in the vertebrate smooth muscle together with myosin light chain kinase.

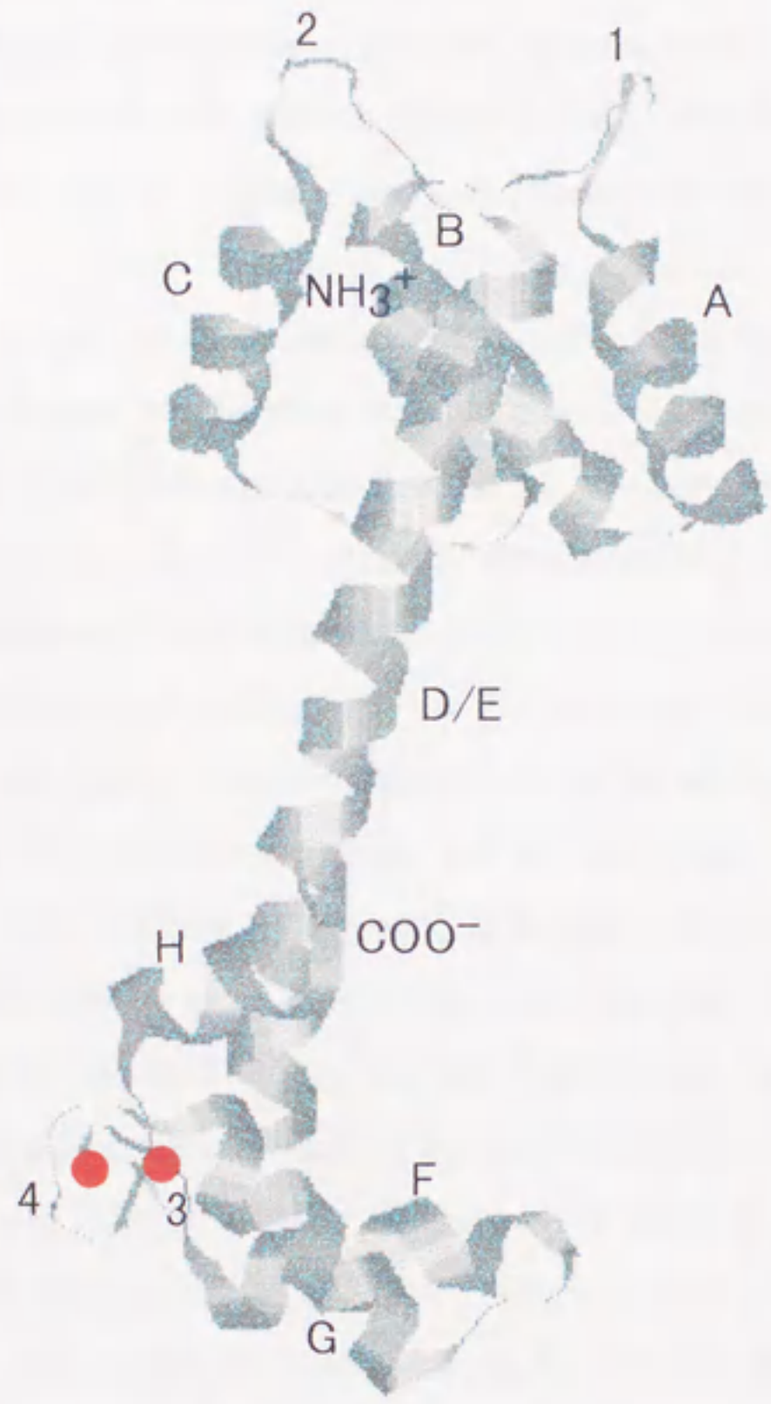

Figure 0-3 Ribbon representation of skeletal muscle TnC crystal structure (after Herzberg and James, 1985), generated by RASMOL. Helices are labeled A through H; Ca^{2+}-binding domains are labeled 1through 4.

These proteins are particularly interesting subjects for comparative sequence studies because their diverse functional properties have evolved from a common origin (for review, see Collins, 1991). While globular lobes in each protein contain a pair of potential Ca^{2+}-binding sites, the number of sites which really bind metal ions is varied among the muscle Ca^{2+}-binding proteins. In the case of TnC, it has been revealed that the Ca^{2+}-binding sites in the N-terminal domain are specific for Ca^{2+} and responsible for the regulation of muscle contraction. On the other hand, the C-terminal two Ca^{2+}-binding sites show higher affinity for Ca^{2+} as well as for Mg^{2+} and they are believed to always filled with Ca^{2+} or Mg^{2+} in the muscle cell (for reviews, see Grabarek *et al.*, 1992; Farah and Reinach, 1995).

TnI from rabbit skeletal muscle consists of 181 amino acids and has two segments with extremely basic amino acid sequences: Residues 102-135 contain 12 basic side chains and residues 5-27 contain six basic side chains (Wilkinson and Grand, 1978; Sheng *et al.*, 1992). Both of these segments are significant in the regulatory thin filament interactions. The interface between TnI and TnC has been focused on by many researchers because it is likely a primary site for transmission of the effect of Ca^{2+}-binding to the regulatory sites of TnC to other thin filament components. By the use of synthetic peptides, chemically cleaved fragments and truncated mutant molecules of TnI, major TnC-binding regions of TnI have been assigned. The N-terminal region of TnI (residues, 1-40) interacts with the C-terminal domain of TnC and contributes to stabilize the TnC-TnI binary complex (Syska *et al.*, 1976; Sheng *et al.*, 1992; Ngai and Hodges, 1992; Farah *et al.*, 1994). Segment corresponding to residues 96-116, so-called the "inhibitory region", of TnI was shown to bind not only to TnC but also to actin and retained the inhibitory activity of actomyosin ATPase (Syska *et al.*, 1976; Talbot and Hodges, 1981). The mutant TnI which has a deletion in this region failed to regulate acto-S1 ATPase (Farah *et al.*, 1994). There has been no known roles in the C-terminal region of TnI on the regulatory mechanism of Tn until the recent report by Farah *et al.*(1994). The mutant TnIs with C-terminus truncations greatly reduced the inhibitory activity. They concluded that the inhibitory region and C-terminal region of TnI (especially residues 103-156) were involved in both TnI's inhibitory effect on the actomyosin ATPase and its Ca^{2+}-dependent interactions with the regulatory N-terminal domain of TnC (Farah *et al.*, 1994; Farah and Reinach, 1995).

TnT is the largest of the troponin subunits and consists of 259 amino acid residues (Pearlstone *et al.*, 1977). TnT is a highly polar molecule, with a concentration of acidic side chains near its N-terminus (residue 1-39) and predominance of basic residues near its C-terminus (residue 221-259). It has been shown that TnT serves as a major link between troponin and tropomyosin. Circular dichroism data (Pearlstone and Smillie, 1978) showed a high helical content in residues 71-151 of TnT which was shown to bind tropomyosin (Jackson *et al.*, 1975). Although a proposal was

made that this segment interacts with tropomyosin by forming a coiled coil or triple-stranded coiled coil (Nagano *et al.*, 1980; Nagano and Miyamoto, 1982), the proposal remains to be proved.

Troponin complex - the overall appearance and functional domains

Some experimental evidences have suggested that a troponin complex has elongated appearance with a globular part along the tropomyosin molecule. It also suggested that this asymmetric morphology is mainly due to TnT by an electron microscopic study of rotary shadowed molecules (Flicker *et al.*, 1982) and an X-ray crystallographic analysis of Tn complex and TnT fragments which were diffused into a tropomyosin crystal (White *et al.*, 1987). Studies of the altered reactivities of lysine or tyrosine residues of tropomyosin upon binding to troponin (Hitchcock *et al.*, 1988; Mak and Smillie, 1981) have also shown to confirm this idea. Immunoelectron microscopic analysis showed that anti-TnT antibodies bound to the thin filaments formed striations which are much wider than those formed by anti-TnC or by anti-TnI antibodies (Ohtsuki, 1979). The results may be indicative of a wider distribution of TnT, while Ohtsuki interpreted the wider striation in terms of the large size of antibodies and the TnT exposure to the solution through two distinct surface areas.

It has been shown that chymotrypsin cleaved TnT into two fragments; N-terminal part, T1 and C-terminal part, T2. Both T1 and T2 can bind to tropomyosin, but only T2 is able to bind to TnC and TnI (Ohtsuki, 1979; Tanokura *et al.*, 1983; Pearlstone and Smillie, 1982, 1983). A complex containing T2, TnC and TnI retained the function of Ca^{2+}-regulation of actomyosin ATPase and Ca^{2+}-sensitive superprecipitation (Ohtsuki, *et al.*, 1981). These findings suggest that the globular part which is mainly composed of T2, TnC and TnI must be the functional domain of the troponin complex and binds to tropomyosin at around Cys-190.

The T1 part could be elongated to cover almost one third of the C-terminus of tropomyosin and may extend to the N-terminus of the adjacent tropomyosin molecule (Mak *et al.*, 1983; White *et al.*, 1987), and could serve to add a structural stability for troponin complex on the thin filament, but the extension of T1 to the adjacent Tm molecule remains to be solved (reviews, see Ohtsuki *et al.*, 1986; Zot and Potter, 1987). The function of N-terminus of T1 region has not been known. Deletion in the N-terminal region of T1 part have shown no obvious differences in function of regulating acto-S1 ATPase activity compared to intact molecule (Ohtsuki *et al.*, 1984; Pan *et al.*, 1991; Tobacman, 1987; Willadsen *et al.*, 1992; Fujita *et al.*, 1992).

A low resolution model of TnC-TnI complex has been proposed based on small-angle X-ray and neutron scattering studies (Olah *et al.*, 1994; Olah and Trewhella, 1994). According to this model, almost all region of the primary structure of TnI is involved in the interaction with TnC. Together with other recent experiments (Kobayashi *et al.*, 1995; Leszyk *et al.*, 1990; Farah *et al.*,

1994; Kobayashi *et al.*, 1994; Krudy *et al.*, 1994), TnC-TnI interaction sites can be summarized as follows: the central region (residues ~50-130 of TnI) winds around the full length of TnC, and each of the two end regions binds either to the outer edge of the N- or to that of the C-terminal domain of TnC in an antiparallel manner.

Ca^{2+} induced conformational changes in troponin complex

Ca^{2+}-binding to the regulatory sites of TnC must cause a change in the protein-protein interactions within the Tn complex, which transmits to other thin filament components and ultimately changes the interaction of actin with myosin. In order to understand the molecular mechanism of the Ca^{2+}-regulation by troponin, conformational transition of Tn complex upon Ca^{2+}-binding to the regulatory sites of TnC has been investigated using various methods: Chemical modification of Lys side chains (Hitchcock, 1981; Hitchcock *et al.*, 1981; Hitchcock-DeGregori, 1982), chemical cross-linking (Sutoh, 1980; Wang *et al.*, 1990), fluorescence energy transfer experiments (Schulzki *et al.*, 1990; Zhao *et al.*, 1995). Recently, by multidimensional NMR, the Ca^{2+}-saturated form of TnC structure has been solved (Slupsky and Sykes, 1995). As proposed originally by Herzberg *et al.* (1986), in the Ca^{2+}-bound form, a hydrophobic patch is exposed in the N-terminal domain by relative movement of helices B and C with respect to helices N, A and D. This hydrophobic surface in the N-terminal domain of TnC has been suggested to represent a Ca^{2+}-dependent binding site for TnI and/or TnT.

As described above, the TnI segment residues 96-116 is of special interest because it also binds to actin and can inhibit acto-S1 ATPase activity (Syska *et al.*, 1976). Subsequent studies with smaller synthetic peptides from this segment of TnI (Nozaki *et al*, 1980; Talbot and Hodges, 1981; Van Eyk and Hodges, 1988) have confirmed that it binds to either actin or TnC, but not to both simultaneously; these studies narrowed the segment required for the inhibitory activity to residues 105-114. By the use of mutidimentional NMR, the structure of inhibitory region (residues 105-114) bound to TnC was revealed amphiphilic α-helix, distorted around the two central proline residues (Campbell and Sykes, 1991). On the other hand, the synthetic peptide corresponding to N-terminal segment of actin (resides 1-28) was shown to interact with both TnC and myosin S1 (Van Eyk and Hodges, 1991; Van Eyk *et al.*, 1991). These synthetic peptides have been successfully used to investigate the mechanism of regulation. Van Eyk *et al.* (1991) proposed a model which explains the protein interactions during muscle regulation (Fig. 0-4). In their model, N-terminal region of actin (residues 1-28) and inhibitory region of TnI (residues 104-115) are two of the Ca^{2+}-dependent switches that control the relaxation and contraction. In the absence of Ca^{2+}, $TnI_{104-115}$ interacts with $actin_{1-28}$ causing inhibition of acto-S1 ATPase. On the other hand, in the presence of Ca^{2+}, $TnI_{104-115}$ interacts with TnC and $actin_{1-28}$ interacts with S1, and causing the activation of S1 ATPase activity. Synthetic peptides are powerful tools to investigate such a complicated phenomenon, but results

obtained by the use of synthetic peptides should be treated with cautions, because fragments very often show different properties from the native molecule.

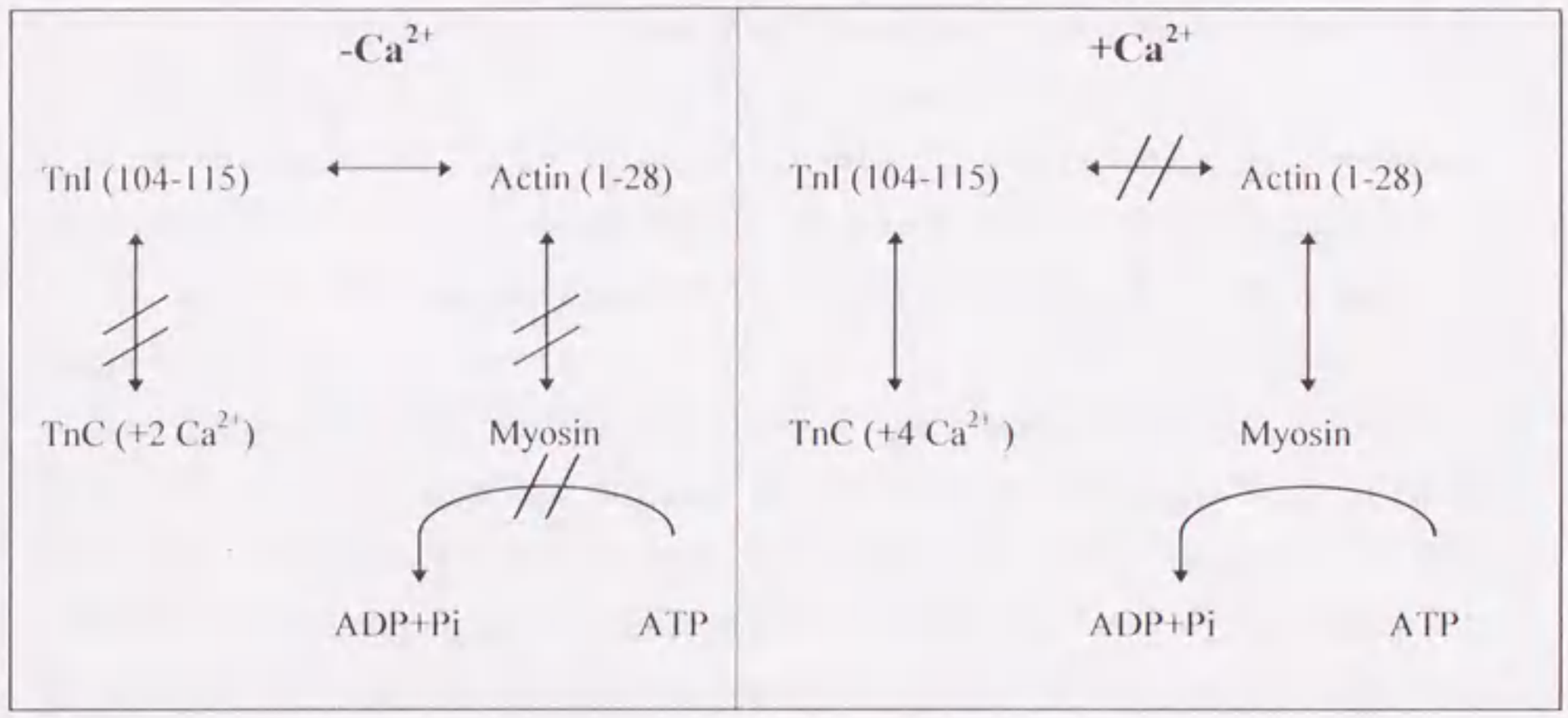

Figure 0-4. The model for the protein interactions during muscle regulation proposed by Van Eyk *et al.* (From Van Eyk *et al.*, 1991 In: Ruegg, J. C., ed, *Peptide as probes in muscle reserch*, Heidelberg, Germany: Springer-Verlag, pp. 15-31.)

Regulation by tropomyosin -troponin

In 1970's, based on the interpretation of X-ray diffraction patterns, the steric blocking hypothesis was proposed in order to explain the mechanism of calcium regulation (Haselgrove, 1973; Huxley, 1973; Parry and Squire, 1973). The hypothesis assumes that the tropomyosin strand can be located at one of two positions on the actin strand. In the "off" state, tropomyosin strand at one position sterically blocks the acto-S1 interaction, while in the "on" state, the strand at the other position does not. The transition of tropomyosin strand between the two positions is solely induced by Ca^{2+}-binding to troponin. Recently, Lehman *et al.* (1994) visualized two different positions of tropomyosin on actin by using the three-dimensional reconstitution of electron micrographs on the assumption that the whole structure is of helical symmetry. Although analysis by X-ray and EM have suggested models of filament structure, unambiguous interpretation have not been possible for many years. The problems associated with both the X-ray and EM studies which are describe above are two fold. Firstly, only layer lines of lower orders are included in the model building. Secondly, possible intensities which could be indexed based on the 2 / 1 helices of an axial pitch of c. 770 Å

(which would come from the mass of Tn complex, if they were located on ideal 2 / 1 helical symmetry) are completely neglected for technical reasons. Consequently, non of these models represent the mass associated with the Tn complex. For the same reasons, in the model, the position of tropomyosin strands relative to the actin strands could be different from the reality.

Changes in the diffraction patterns must reflect changes within the thin filament structure. It is obvious that not only tropomyosin but also troponin and actin must undergo structural changes upon Ca^{2+}-binding to TnC. At the present stage, however, it is technically difficult to construct a model of the thin filament with considerable troponin mass by helical image reconstruction method. And the attachment of the myosin head to the thin filament should also change the structure of thin filament.

Although the steric blocking model is simple and intuitively pleasing, it never agree with biochemical and physiological data. The steric blocking model predicts that in the absence of Ca^{2+} the degree of association of S1 much weaker with regulated actin (actin + native tropomyosin) than unregulated actin. Eisenberg and colleagues showed that steady stated ATPase rate reduced 96% in the absence of Ca^{2+}, while the association constant of S1 with regulated actin was virtually the same in the presence of Ca^{2+} as in the presence of EGTA, by stopped flow absorbance measurements (Chalovich *et al.*, 1981), and by direct measurements of the binding by ultracentrifuge (Chalovich and Eisenberg, 1982). Increasing evidences showed that in addition to the primary role of S1 as the force generator and enzyme, it is also involved in the regulation process (Morris and Lehrer, 1982). Solution studies have indicated that myosin heads (S1) function as the primary switch and facilitate the process (for review, see Chalovich, 1992). The allosteric/cooperative model which was first formulated by Hill and colleagues (1980) based on solution studies of reconstituted thin filaments, do not appear to agree with the steric blocking model on the molecular event. Recently Lehrer (1994) proposed a testable schematic model for regulatory process that incorporates the three 2-state systems. The model can be summarized as follow: Ca^{2+} and myosin heads are both involved in regulation, with Ca^{2+} as the allosteric effector and the myosin head-induced tropomyosin off-on transition as the switch.

Further studies are required for understanding the structure function relationship of the muscle thin filament as an allosteric protein complex. For this purpose, it is essentially important to relate each state of the filament which is proposed by biochemical analysis with the model structure which is constructed based on X-ray and/or electron diffraction analysis. Although an atomic structure of the entire thin filament has been desired, it has not yet obtained either by X-ray fiber diffraction analysis or by image analysis of electron micrographs. If the structure of the troponin complex is available, it will be advantageous for modeling the thin filament structure. Therefore, for the first step to understand the molecular mechanism of Ca^{2+}-regulation, it is essential to elucidate an

atomic structure of the troponin complex.

The aim of the present study

In order to elucidate the molecular mechanisms of striated muscle regulation, it is essentially important to obtain the three-dimensional structure of troponin complex at an atomic resolution. It is remarkable that the principal actors in the contractile apparatus, actin (Kabsch *et al.*, 1990), myosin (Rayment *et al.*, 1993), have been separately crystallized and analyzed at an atomic resolution. On the contrary, no one has produced well diffracting crystals of the regulatory protein complex for more than a couple of decades since its discovery by Ebashi and colleagues.

The goal of the present study is to elucidate the three-dimensional structure of troponin complex by X-ray crystallography. Production of well diffracting crystals is the key step in this work. In the following section, I describe our strategies for obtaining the crystals of the troponin complex.

Strategies and experimental designs for obtaining crystals of troponin complex

Our strategies for designing the protein samples for crystallization are as follows.

Firstly, our aim is to elucidate the structure-function relationships of Ca^{2+}-regulation, therefore we have to know the whole structure of troponin complex rather than an individual subunit or a part of the complex. Furthermore, troponin exerts its function only in the presence of tropomyosin, therefore the interface between troponin and tropomyosin must also be important. Therefore, we have designed troponin complex and tropomyosin fragment as target systems to be crystallized ($Tm_{141-284}$-TnT25k-TnC-TnI).

Secondly, we think that it is vary advantageous for crystallizing a new protein to work with truncated proteins rather than the native molecules, because of protein solubility, size, stability, or complexity. For these reasons, we chose TnT2-TnC-TnI complex, which retains biological significance of troponin complex, as the most suitable for our purpose.

Thirdly, isolated structural core domains would be good candidate for crystallization because of its stability. We made the binary complex consisting of TnC and TnI fragment (res.1-47). This complex does not contain TnI segment of considerable importance in the inhibition of actomyosin ATPase, but contains the structurally important interface between TnC and TnI. Also, this complex is rather easily obtained and stable for a long period of storage, thus this complex is very suited for crystallization experiments.

In this thesis, being divided into five parts, the results of experiments undertaken based on these strategies will be presented and discussed.

In part 1, limited proteolysis of the ternary troponin complex will be described. This study

was aimed at identifying structural domains within the complex. The results would also be useful for designing stable sample for crystallization. In this study, we have found out the structural and functional core domain of troponin complex by the use of limited chymotryptic digestion, and also clarified the functions of the segments of TnI; residues 117-134 (117-140) are necessary for Ca^{2+}-dependent inhibitory action of TnI and residues 134-181 (140-181) are involved in interaction with actin-tropomyosin.

In part II, detailed purification procedures for the proteins used in part I will be described.

In part III, crystals of three different types of complex, which have been obtained for the first time in the present study, will be described and preliminary X-ray diffraction data will be presented. Based on our new findings and previous ones by others, stable and homogenous samples, which retains some part of the functions of the original troponin complex, have been designed and prepared for crystallization trials. In conclusion, among the various designed troponin complex, three kinds of complex protein have been reproducibly crystallized; TnT2-TnC-TnI complex (III-1), $Tm_{141-284}$TnT25k-TnC-TnI complex (III-2) and TnC-TnI_{1-47} complex (III-3). For production of these crystals, bacterially expressed subunits were individually purified and reconstituted into the complexes consisting of subunits at an equimolar ratio. Also for obtaining the homologous and stable individual subunits or its fragments, site specific point mutations were introduced into the original molecules. For example, amino acid substitution of cysteine residues to alanine or serine residues to prevent inter-or intramolecular cross-linkings, insertion of methionine or cysteine residues for obtaining desired fragments by the use of specific chemical cleavages. So far, we have obtained well diffracting crystals of TnC-TnI_{1-47} complex, and the structural analysis is now under way.

In part IV, detailed purification procedures for the proteins used in part III will be described.

In part V, our trials of reductive methylation of the troponin complex and application of fusion protein techniques to our system will be described, and general applicability of these methods will be discussed. Crystallization is the first obstacle which everybody encounters when starts the X-ray crystallography of a new protein. Because production of crystals with high quality is still based upon "trials and errors". The situation has been improved in recent years by introducing numerous new methodologies into this field (for reviews, see McPharson, 1990; Forest and Schutt, 1992; MacPherson *et al.*, 1995; Giegé *et al.*, 1994). In the present study, we employed two different approaches to improve a chance to obtain crystals: reductive methylation of lysine side chains to change the surface properties of the proteins which may allow to make crystalline contacts (V-1); crystallization of troponin complex as a fusion protein (V-2). So far, we have not yet obtained any crystal of the troponin complex along these lines, general applicability of these methods to other

molecules are discussed.

【Part I】

Structural and Functional Domains of Troponin Complex

SUMMARY

Limited proteolysis have been applied for troponin complex in order to detect conformational differences of Tn under different conditions. We found that not only TnT but also TnI was susceptible to chymotryptic digestion and that cleavage sites of TnI were dependent on the Ca^{2+}-occupancy of TnC. In addition, we characterized the effects of the depletion of the C-terminal part of TnI on the acto-S1 ATPase activity and the binding to tropomyosin-actin. The TnT2-TnC-$TnI_{Ca\text{-}frag}$ (TnI res. 1-134 and 1-140) complex, which was produced in the presence of $CaCl_2$ and $MgCl_2$, retains the activating and inhibitory capabilities of whole Tn on acto-S1 ATPase activity, while TnT2-TnC-$TnI_{Mg\text{-}frag}$ (TnI res. 1-116) complex, which was obtained in the presence of $MgCl_2$ and EGTA, lost its ability to activate acto-S1 ATPase activity. We also showed that, in contrast to the TnC-TnI binary complex, the TnC-TnI fragment complexes did not bind to actin-tropomyosin even at low concentration of Ca^{2+}. The results indicate that the segment residues 117-134 or 117-140 of TnI is necessary for the Ca^{2+}-dependent inhibitory action of the Tn complex on acto-S1 ATPase activity, while residues 135-181 or 141-181 of TnI are involved in the interaction of Tn with the tropomyosin-actin filament.

EXPERIMENTAL PROCEDURES

Proteins

All myofibrillar proteins used in this study were prepared from rabbit fast skeletal muscle. Troponin and its components were purified according to the method by Ebashi *et al.*, (1971) with slight modification. Tropomyosin, actin and myosin subfragment-1 (S1) were prepared by the methods described in Hichcock-DeGregori *et al.*, (1985), Spudich and Watt (1971) and Weeds and Taylor (1975), respectively.

Digestion of troponin

Troponin in 0.1 M NaCl, 5 mM $MgCl_2$, 1 mM dithiothreitol, 20 mM Tris-HCl and either 1 mM $CaCl_2$ or 1 mM EGTA, pH 8.0 at a concentration of about 5 mg/ml was digested with 1/2000 weight ratio of TLCK-treated α-chymotrypsin (Sigma, type VII) at 37°C for period 5 min and 2 h. The presence $CaCl_2$ plus $MgCl_2$ and $MgCl_2$ plus EGTA, respectively, mimic the activated and the resting state of muscle. The reaction was terminated by the addition of phenylmethansulfonyl fluoride in isopropanol to give a final concentration of 1 mM.

Isolation of digested fragments

Digested troponin was applied to an 1.5×10 cm column of Q-sepharose fast flow (Pharmacia) equilibrated with 0.1 M NaCl, 0.1 mM $CaCl_2$, and 20 mM Tris-HCl, pH 8.0 (the starting solution) and was eluted with a linear gradient of 0.1 M-0.5 M NaCl in the starting solution at 4°C. The fractions containing TnT2-TnC-TnI fragment ternary complex were identified by size exclusion column (TSKgel $G3000SW_{XL}$, Toso, Japan) and SDS gel electrophoresis. Further purification of each component is described in part II.

Reconstitution of ternary and binary complexes

Equimolar amount of troponin components or troponin fragments were combined in a solution containing 6 M urea, 1 M NaCl, 1 mM 0.1 mM $CaCl_2$, 1 mM dithiothreitol and 20 mM Tris-HCl, pH 8.0. The mixture was then dialyzed consecutively against NaCl solution of 1 M, 0.5 M, 0.3 M and 0.1 M, each containing 1 mM $CaCl_2$, 1 mM dithiothreitol and 20 mM Tris-HCl, pH 8.0. After dialysis, the protein solutions were clarified by centrifugation and then applied to a Mono-Q HR 5/5 column (Pharmacia) equilibrated with 0.1 M NaCl, 0.1 mM $CaCl_2$ and 20 mM Tris-HCl, pH 8.0. Ternary or binary complexes were eluted with a linear gradient of 0.1-0.5 M NaCl in the same solution. The fractions containing pure complex were identified by SDS gel electrophoresis.

Acto-S1 ATPase activity measurements

The reconstituted Tn complexes were dialyzed against 20 mM KCl, 3.5 mM $MgCl_2$, 0.5 mM EGTA, 1 mM dithiothreitol, and 20 mM MOPS, pH 7.0. Actin and tropomyosin were mixed in a 6:1 molar ratio and dialyzed against the same solution. Actin (6 μM), tropomyosin (1 μM), reconstituted troponin (0-10 μM) and myosin (0.23 μM) were mixed. In the case of assay measurements in the presence of Ca^{2+}, 0.6 mM $CaCl_2$ was added to give a free calcium concentration of 0.1 mM. The samples were preincubated at 25 °C for 30 min and reactions were initiated by adding 2 mM ATP (pH 7.0). The ATPase activity was determined from the time cause of Pi liberation for 5 min. Every 1 min, 50 μl of aliquot was removed and were the reaction was terminated by adding 450 μl of 0.2 M perchloric acid. The amount of released phosphate was determined by the malachite green method as described in Onishi *et al.*, (1995).

Binding experiments

The binding ability of the reconstituted Tn complexes to F-actin-tropomyosin was tested by the sedimentation experiments. Experimental conditions were the same as for the ATPase activity measurements. The mixtures of proteins were centrifuged at 180,000 × *g* at 4 °C for 40 min. The resulting pellets and supernatants were analyzed by SDS gel electrophoresis.

Estimation of protein concentrations

The following extinction coefficients (mg/ml) were used: myosin S1, 0.75 at 280 nm; G-actin, 0.63 at 290 nm; tropomyosin, 0.24 at 277 nm (Lehrer and Morris, 1982). The concentration of reconstituted troponin complexes were determined according to the amino acid compositions of the proteins (Gill and von Hippel, 1989).

Mass spectrometry

Protein samples for mass spectrometry were further purified by reversed-phase HPLC using an Aquapore Buthyl column (Brownlee). Mass spectra of purified proteins were obtained using liquid chromatography/electrospray mass spectrometry as described previously (Taniguchi *et al.*, 1994).

RESULTS

The purification and identification of Tn fragments

The time course of chymotryptic digestion of Tn complex are shown in Fig. 1-1. When digestion was undertaken at 25 °C, (A), almost all TnT was cleaved into TnT1 and TnT2 within 30 min, as described previously (Ohtsuki, 1979; Morris and Lehrer, 1984). Until 30 min, no difference in appeared bands were detected between the two conditions: in the presence of $CaCl_2$ and $MgCl_2$ and in the presence of $MgCl_2$ and EGTA (data not shown). When digestion was undertaken at 37°C, after 30 min, new bands with slightly higher mobility than TnC appeared in the presence of $CaCl_2$ (B). In the presence of $MgCl_2$ and EGTA, after 30 min, new components also appeared. These bands showed different mobility, therefore different apparent molecular weight, from those appeared in the presence of Ca^{2+}. Concomitantly TnI disappeared, while TnC, TnT1 and TnT2 remain, suggesting that the newly appeared components result from proteolysis of TnI. In the present study, the new TnI fragments yielded in the presence of Ca^{2+} and Mg^{2+} are refereed to as $TnI_{Ca\text{-}frag}$ and $TnI_{Mg\text{-}frag}$, respectively. For longer period of reaction, $TnI_{Ca\text{-}frag}$ and $TnI_{Mg\text{-}frag}$ fragments were accumulated, while TnT2 was cleaved into small fragment, TnT2β, which was first described by Tanokura *et al.* (1982). While different peptides of TnC were produced by tryptic digestion, depending on its Ca^{2+}-occupancy (Grabarek *et al.*, 1981), no cleavage of TnC by chymotriptic digestion of whole Tn complex were observed in the present study. Fig. 1-2 and Fig. 1-3 represent the purification steps of the Tn ternary complexes which contain the TnI fragments. The fractions containing ternary complex from an anion exchange column were applied on a size exclusion column. As shown in Fig. 1-2 (B, C) and Fig. 1-3 (B), the Tn complexes eluted as a single peak from a size exclusion column, suggesting that each complex contains TnT2, TnC and either $TnI_{Ca\text{-}frag}$ or $TnI_{Mg\text{-}frag}$.

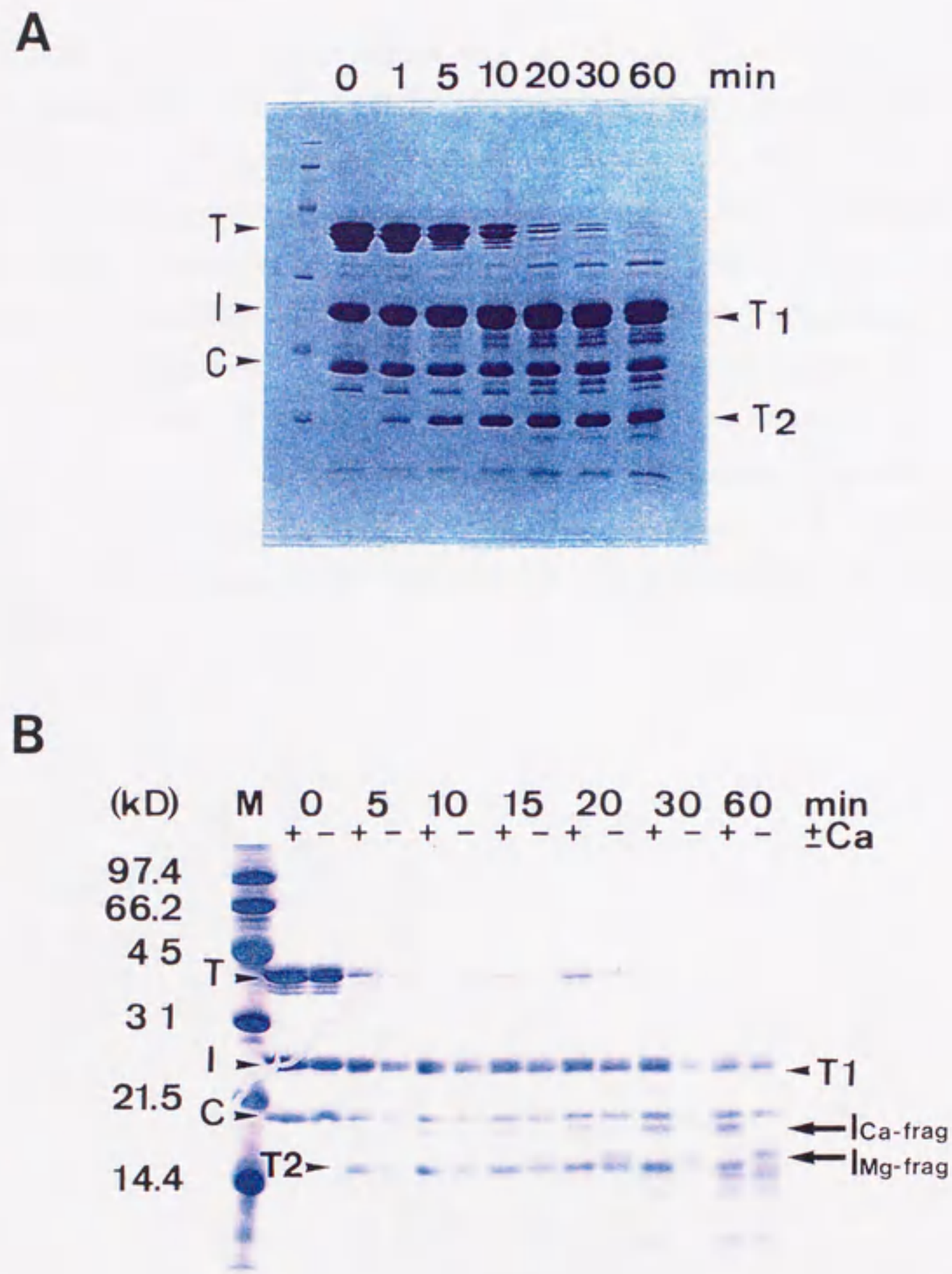

Figure 1-1. Time course of Tn digestion by chymotrypsin visualized on SDS-PAGE. Digestion of Tn was performed as described under "EXPERIMENTAL PROCEDURES" in the presence of either 1 mM $CaCl_2$ (+Ca) or 1 mM EGTA (-Ca) at either 25°C (A) or 37°C (B). The bands corresponding to TnT (T), TnT1 (T1), TnT2 (T2), TnC (C), TnI (I), $TnI_{Ca\text{-}frag}$ ($I_{Ca\text{-}frag}$) and $TnI_{Mg\text{-}frag}$ ($I_{Mg\text{-}frag}$) are indicated.

In order to identify the cleavage sites of TnT and TnI, the peak fractions from a size exclusion column (Fig. 1-2 (C) and Fig. 1-3 (B)) were applied on a reversed-phase HPLC (Fig. 1-4 (A, B)) and major fractions were subjected to mass spectrometry analysis. The major fragments identified by the mass spectrometry are summarized in Table 1-1. Major TnT fragments identified in the present study are found to be identical to TnT2α, TnT2α^s and TnTβ1 which are described by Tanokura *et al.* (1982). Major species of TnI fragments were identified as residues 1-134 and 1-140 for $TnI_{Ca\text{-}frag}$ and residues 1-116 for $TnI_{Mg\text{-}frag}$, respectively. Minor species corresponding to residues 1-122, 1-125, 1-134 and 1-140 were also observed in $TnI_{Mg\text{-}frag}$. No fragments of TnC was obtained. The same results were obtained when the TnI fragments were isolated by the different procedure as described in part II (Table 1-2). In order to clarify the N-terminus and C-terminus of these TnI fragments, digestion products of TnI fragments with lysyl endopeptidase were further analyzed by LC/MS method.

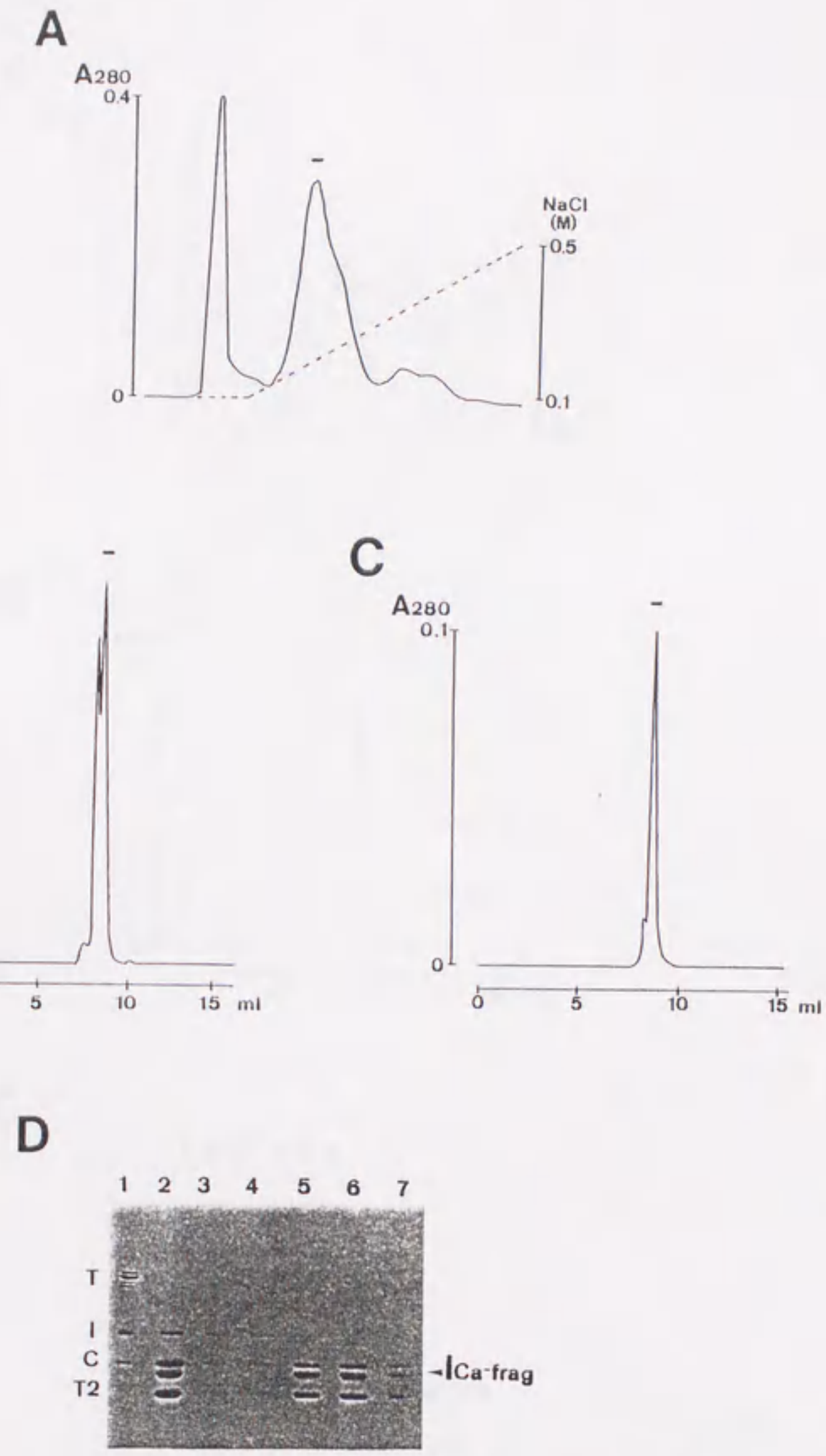

Figure 1-2. Isolation of the ternary Tn complex containing $TnI_{Ca\text{-}frag}$ fragment. Tn was digested in the presence of 1 mM $CaCl_2$ and 5 mM $MgCl_2$ at 37°C for 20 min with 1/2000 weight ratio of TLCK-treated α-chymotrypsin as described under "EXPERIMENTAL PROCEDURES". (A) The separation of the digestion products by Q-sepharose fast flow column. The fractions indicated by a bar were loaded on TSKgel $G3000SW_{XL}$ column. The fractions indicated by a bar were further separated by a TSKgel $G3000SW_{XL}$ column as shown in (C). (D) SDS-PAGE pattern of the fractions. In SDS-PAGE, lane 1, Tn; lane 2, digestion products of Tn; lane 3, the sample that applied on the column; lane 4-9, the fractions indicated by a bar in C, which is divided in 6 portions.

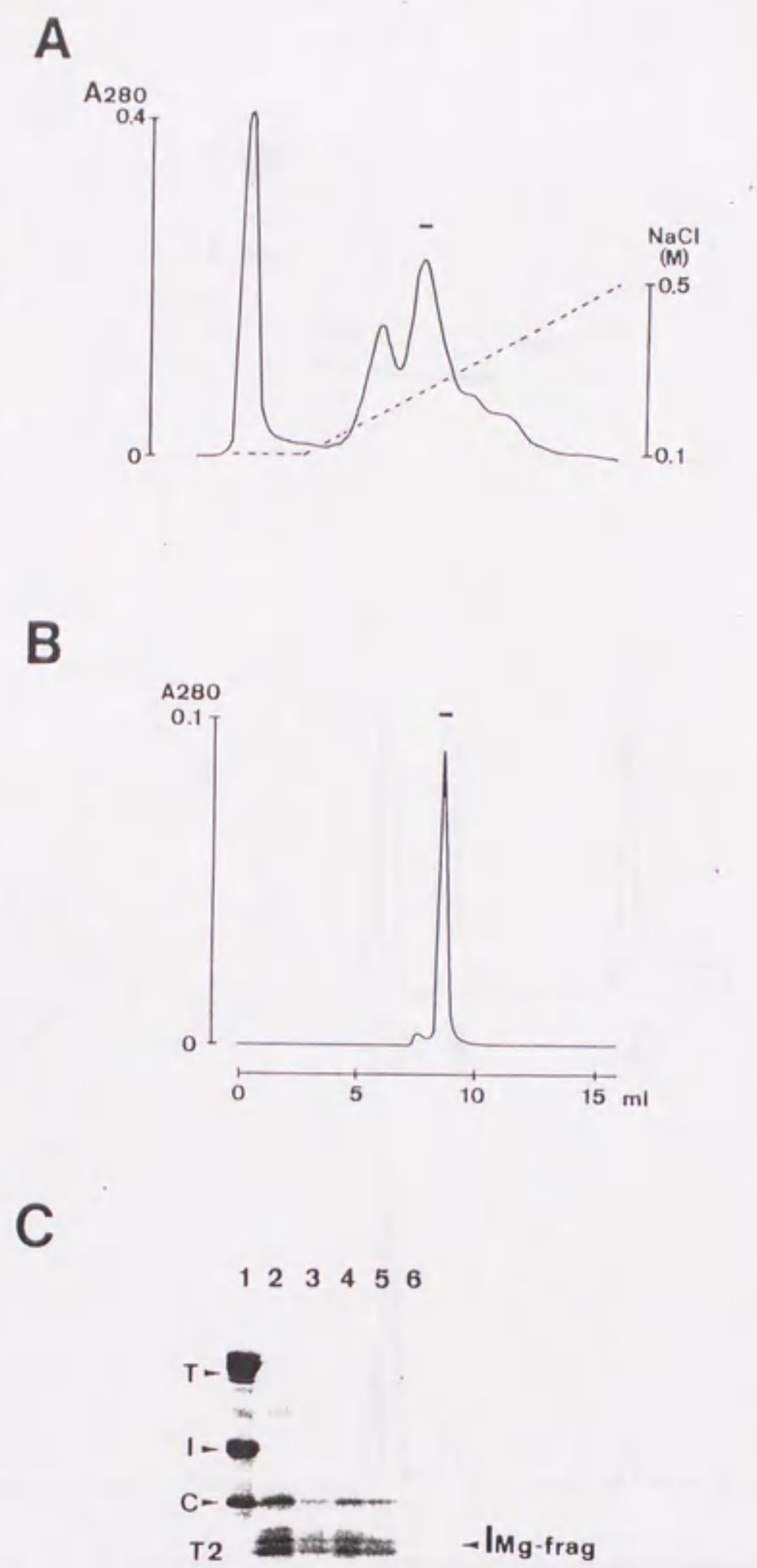

Figure 1-3. Isolation of the ternary Tn complex containing $TnI_{Mg\text{-}frag}$ fragment. Tn was digested in the presence of 1 mM EGTA and 5 mM $MgCl_2$ at 37°C for 20 min with 1/2000 weight ratio of TLCK-treated α-chymotrypsin as described under "EXPERIMENTAL PROCEDURES". (A) The separation of the digestion products by Q-sepharose fast flow column. The fractions indicated by a bar were loaded on TSKgel $G3000SW_{XL}$ column (B). (C) SDS-PAGE pattern of the fractions. In SDS-PAGE, lane 1, Tn; lane 2, the sample before applying; lane 3-6, the fractions indicated by a bar in B, which is divided in 4 portions.

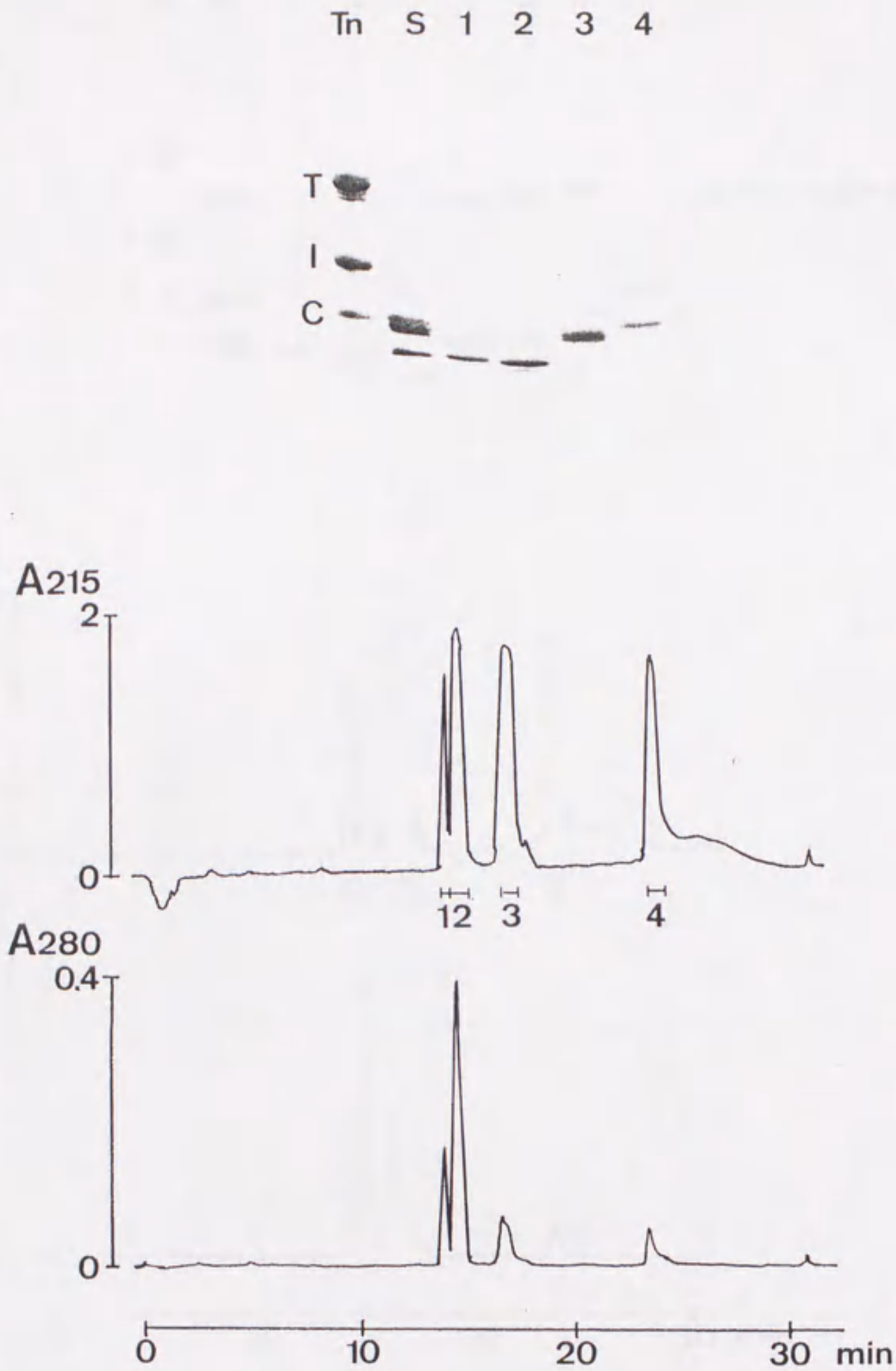

Figure 1-4A. Isolation of the components in the ternary Tn complex containing $TnI_{Ca\text{-}frag}$ fragment. Ternary Tn complex which contains $TnI_{Ca\text{-}frag}$ fragment (Fig. 1-2C) was further applied to a reversed-phase HPLC column as described under "EXPERIMENTAL PROCEDURES". The elution was monitored both at 215 nm and at 280 nm in order to examine both the purity of each peak and the stoichiometry of each component in the ternary complex. Fraction 1, 2 , 3, and 4 predominantly contained TnT2αs, TnT2α, $TnI_{Ca\text{-}frag}$, and TnC, respectively. Note that, each of troponin components, *i. e.* TnT, TnI, TnC and their fragments, exists in the equimolar ratio as intact troponin complex. (The molar ratio was calculated from the molecular extinction coefficient of the each component and the area under each peak at 280 nm.)

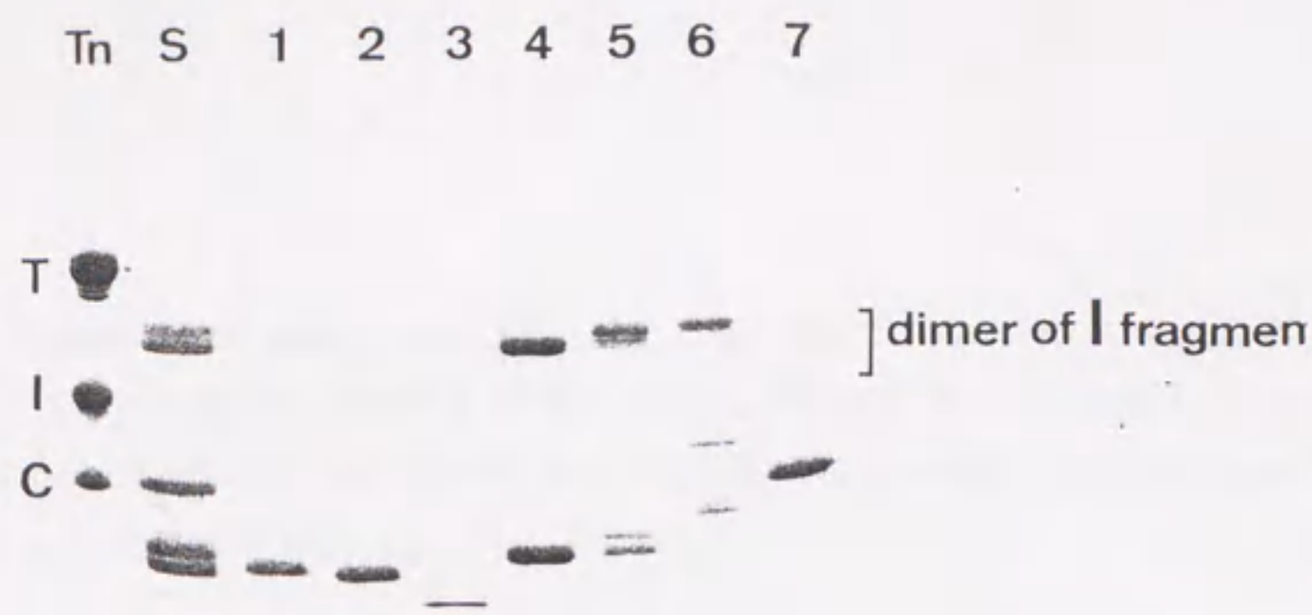

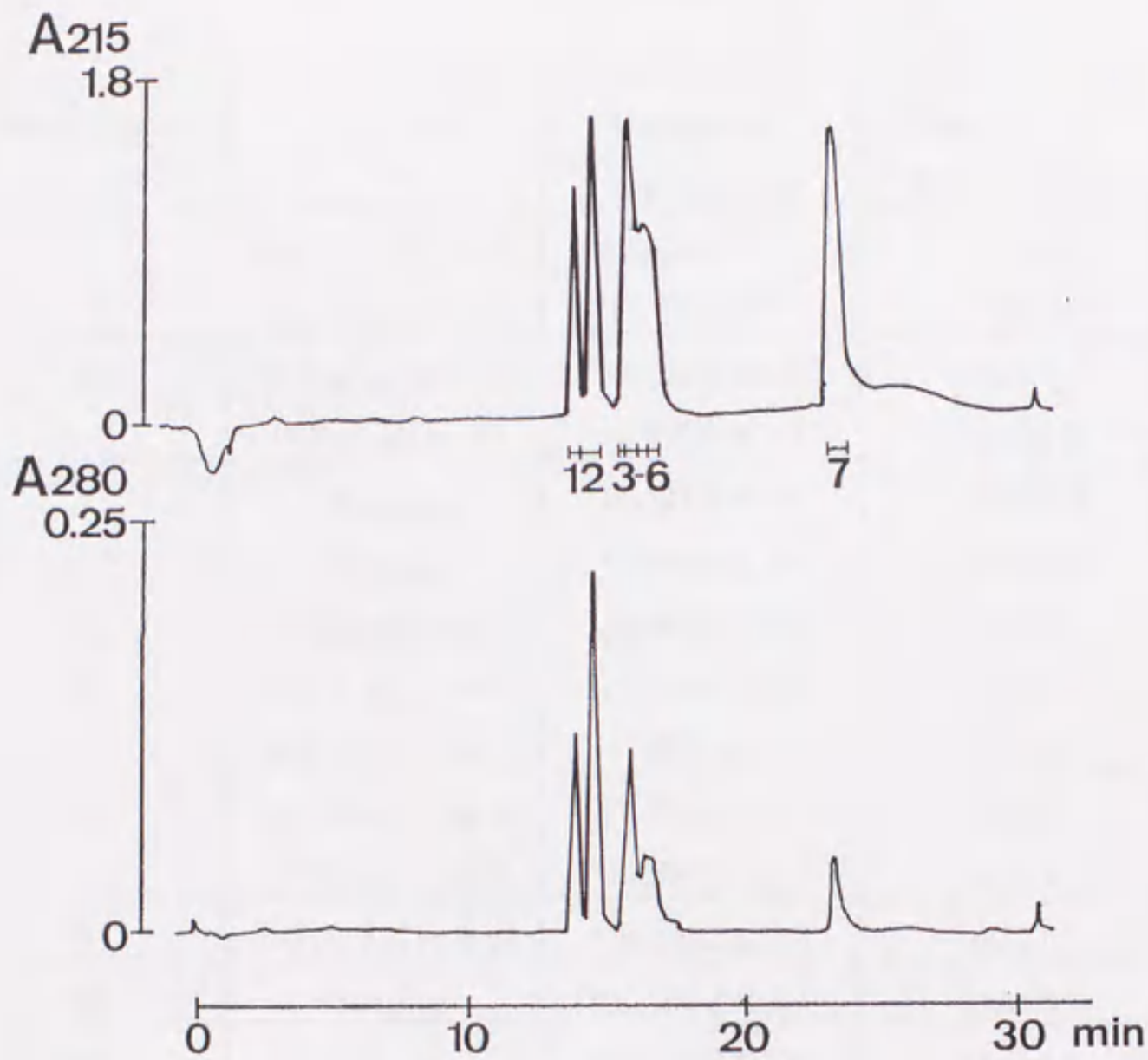

Figure 1-4B. Isolation of the components in the ternary Tn complex containing $TnI_{Mg\text{-}frag}$ fragment. Ternary Tn complex which contains $TnI_{Mg\text{-}frag}$ fragment (Fig. 1-3B) were further applied to reversed-phase HPLC as described under "EXPERIMENTAL PROCEDURES". The elution was monitored both at 215 nm and at 280 nm in order to examine both the purity of each peak and the stoichiometry of each component in the ternary complex. Fraction 1, 2 and 3 predominantly contained TnT2 species. Fraction 4, 5, 6 predominantly contained TnI fragments while fraction 7 contained TnC. Note that, each of troponin components, *i. e.* TnT, TnI, TnC and their fragments, exists in the equimolar ratio as intact troponin complex. (The molar ratio was calculated from the molecular extinction coefficient of the each component and the area of the each peak at 280 nm.)

The major peptides observed were summarized in Fig. 1-5 and Table 1-3 and 1-4. Although N-terminal peptide (Ac-GDEEK) was not observed, both C-terminal peptides (K14a and K17a) were assigned. These results also confirmed that Met-134 and Leu-140 were the major cleavage sites of $TnI_{Ca\text{-}frag}$ and Met-116 was cleaved in $TnI_{Mg\text{-}frag}$.

Table 1-1. Assignment of the fragments produced by limited chymotryptic digestion of Tn complex

[1]HPLC peak No.	Assignment	Mass of MH[+] A (observed)	Mass of MH[+] B (calculated[2])	A-B
A1	$TnT_{156\text{-}259}$ (T_2 α s)	12,229.1±2.1	12,231.3	-2.2
	$TnT_{159\text{-}259}$ (T_2 α)	*11,890.1±2.7	11,894.0	-3.9
A2	$TnT_{156\text{-}259}$ (T_2 α s)	12,227.9±1.7	12,231.3	-3.4
	$TnT_{159\text{-}259}$ (T_2 α)	11,890.1±2.7	11,894.0	-3.9
A3	**$TnI_{1\text{-}140}$**	**16,181.0±6.5**	**16,186.9**	**-5.9**
	$TnI_{1\text{-}134}$	**15,498.1±3.4**	**15,504.1**	**-6.0**
A4	TnC (undigested)	18,000.8±2.8	18,008.0	-7.2
B1	$TnT_{156\text{-}259}$ (T_2 α s)	12,229.6±2.6	12,231.3	-1.7
	$TnT_{159\text{-}259}$ (T_2 α)	*11,891.6±2.1	11,894.0	-2.4
B2	$TnT_{156\text{-}259}$ (T_2 α s)	12,226.7±2.4	12,231.3	-4.6
	$TnT_{159\text{-}259}$ (T_2 α)	*11,889.8±2.1	11,894.0	-4.2
B3	$TnT_{159\text{-}242}$ (T_2 β_1)	*10,148.2±2.3	10,151.9	-3.7
B4	**$TnI_{1\text{-}116}$**	***13,613.8±2.1**	**13,618.7**	**-4.9**
B5	$TnI_{1\text{-}125}$	14,512.3±7.6	14,519.8	-7.5
	$TnI_{1\text{-}122}$	14,203.4±4.2	14,207.4	-4.0
	$TnI_{1\text{-}116}$	13,614.2±2.6	13,618.7	-4.5
B6	$TnI_{1\text{-}160}$	18,633.8±5.0	18,643.5	-7.7
	$TnI_{1\text{-}140}$	16,180.6±5.3	16,186.8	-6.2
	$TnI_{1\text{-}134}$	15,497.8±5.7	15,504.1	-6.3
B7	TnC (undigested)	not measured	18,008.0	

[1]A1-B7 correspond to peaks in the Fig. 1-4 A and B. [2]The mass values observed were compared with the theoretical average compound mass values calculated from the known amino acid sequence. * Major species in the measured samples.

Table 1-2. Assignment of the TnI fragments produced by the chymotryptic digestion.

fragments	residues	mass of MH^+	
		observed	calculated
$TnI_{Ca\text{-}frag}$	1-140	16,187.9	16,186.9
	1-134	15,502.6	15,504.0
$TnI_{Mg\text{-}frag}$	1-116	13,618.7	13,618.7

Table 1-3.Assignment of Lys-C peptides from $TnI_{Ca\text{-}frag}$

peptides	residues	mass of MH^+	
		observed	calculated
K2	6 - 18	1621.6	1620.9
K3	19 - 31	1434.1	1433.7
K4	32 - 40	1104.4	1104.2
K5	41 - 65	2760.2	2759.2
K7	71 - 78	904.8	905.0
K8	79 - 84	798.8	798.9
K11	91 - 98	1006.9	1007.1
K12	99 - 101	848.8	849.0
K13/K14	102 - 123	2175.6	2173.7
K14	104 - 123	1898.6	1898.4
K15	124 - 129	588.2	588.7
K17a	132 - 134	352.1	352.5

TnI

1

GDEEK/RNRAI TARRQHLK/SV MLQIAATELE K/EEGRREAEK/

K2 K3 K4

41

QNYLAEHCPP LSLPGSMAEV QELCK/QLHAK/ IDAAEEEK/YD

K5 K7

81

MEIK/VQK/SSK/ ELEDMNQK/LF DLRGK/F K/RPP LRRVRMSADA

K8 K11 K12 K14a

121

MLK/ALLGSK/H K/VCMDLRANL K/QVK/K/EDTEK/ ERDLRDVGDW

K14 K15 K17a

161 **181**

RK/NIEEK/SGM EGRK/K/MFESE S

a peptide identified in the digestion products of $TnI_{Ca\text{-}frag}$

a peptide identified in the digestion products of $TnI_{Mg\text{-}frag}$

Figure 1-5. Assignment of Lys-C peptides of $TnI_{Ca\text{-}frag}$ and $TnI_{Mg\text{-}frag}$. $TnI_{Ca\text{-}frag}$ and $TnI_{Mg\text{-}frag}$ were digested with lysyl endopeptidase (Lys-C), and the resulting peptides were analyzed by LC/MS method described by Taniguchi *et al.* (1994).The peptides identified in the digestion products are represented.

Table 1-4. Assignment of Lys-C peptides from $TnI_{Mg\text{-}frag}$

peptides	residues	mass of MH^+	
		observed	calculated
K2	6 - 18	1621.6	1620.9
K3	19 - 31	1434.1	1433.7
K4	32 - 40	1104.4	1104.2
K5	41 - 65	2760.2	2759.2
K7	71 - 78	904.8	905.0
K8	79 - 84	798.8	798.9
K11	91 - 98	1006.9	1007.1
K12	99 - 101	848.8	849.0
K14a	104 - 116	1182.0	1181.5

The effects various ternary Tn complexes on acto-S1 ATPase activity

Fig. 1-6 shows a typical effect of intact Tn on the acto-S1 ATPase activity in the presence of tropomyosin: Tn activated the ATPase activity in the high concentration of Ca^{2+} and inhibited the ATPase activity in the presence of EGTA. In both case, maximum activities were obtained at 1.5-2 molar ratio of Tn to Tm. $TnT2\text{-}TnC\text{-}TnI_{Ca\text{-}frag}$ acts as an activator or an inhibitor, depending on Ca^{2+} concentration, although higher concentration of the complex (6 μM over 1 μM of tropomyosin) were required for maximal effect. Since the ternary complexes of TnT2-TnC- TnI fragment bound to actin-tropomyosin at 1:1 (Tn:Tm) molar ratio (data not shown), this might be due to the decreasing affinity of ternary complexes to actin-tropomyosin caused by the deletion of TnT1 region and/or the deletion of the C-terminal part of TnI. As described in the following section, the C-terminal part of TnI was involved in actin-tropomyosin binding at least in the presence of EGTA and Mg^{2+}. Contrary to these complexes, $TnT2\text{-}TnC\text{-}TnI_{Mg\text{-}frag}$ complex had no effect on the activation of ATPase activity and inhibited the acto-S1 activity both in the presence and absence of Ca^{2+}, when it was added to an excess amount.

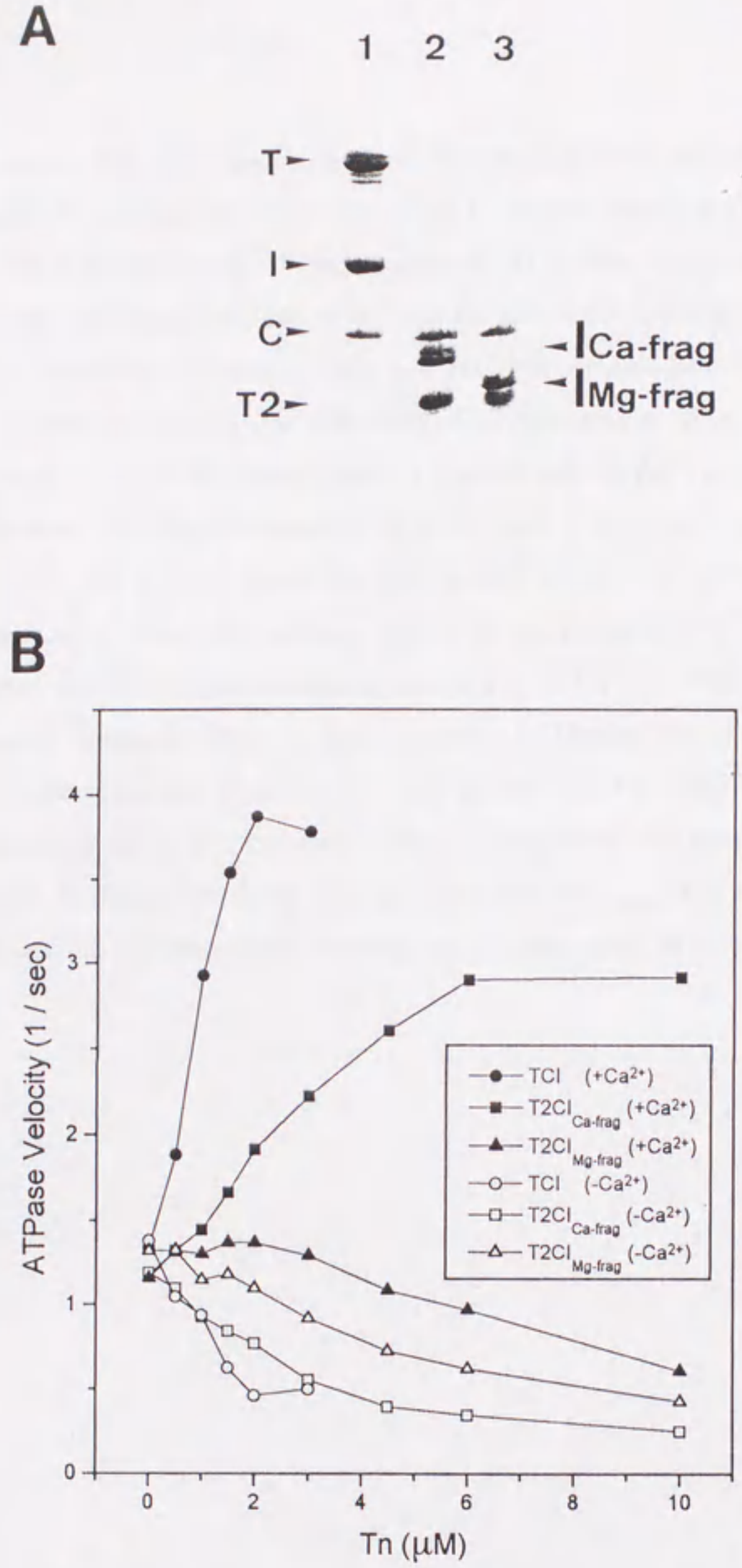

Figure 1-6. The effects of various Tn ternary complexes on the acto-S1 ATPase activity. (A) SDS-PAGE of the reconstituted Tn ternary complexes. Lane 1, the intact Tn complex (TCI); lane 2, TnT2-TnC-$TnI_{Ca\text{-}frag}$ ($T2CI_{Ca\text{-}frag}$); Lane 3, TnT2-TnC-$TnI_{Mg\text{-}frag}$ ($T2CI_{Mg\text{-}frag}$). (B) The effects of the reconstituted Tn ternary complexes on acto-S1 ATPase activity in the presence of either 0.1 mM $CaCl_2$ and 3.5 mM $MgCl_2$ ($+Ca^{2+}$) or 0.5 mM EGTA and 3.5 mM $MgCl_2$ ($-Ca^{2+}$).

The effects of various TnC-TnI binary complexes on acto-S1 ATPase activity

In order to explore the possible functional role of the C-terminal region of TnI, we also studied the effects of TnC-TnI fragment binary complex on the acto-S1 ATPase activity and actin-tropomyosin binding. The binary complexes were chosen because the role of the C-terminal part of TnI would be more prominent without TnT. As shown in Fig. 1-7, TnC-TnI complex inhibited the acto-S1 ATPase activity in Ca^{2+}-dependent manner. The activation of ATPase activity in the presence of Ca^{2+} was not observed. Farah *et al.* (1994) claimed that a 1:1 molar ratio of the TnC-TnI binary complex to actin was required for Ca^{2+}-depend regulation of actomyosin ATPase activity. In the present study, an equimolar ratio of the TnC-TnI binary complex to tropomyosin was sufficient to inhibit acto-S1 ATPase activity in a Ca^{2+}-dependent manner. Neither the binary complexes TnC-$TnI_{Ca\text{-}frag}$ nor TnC-$TnI_{Mg\text{-}frag}$ inhibited acto-S1 ATPase activity in the absence of Ca^{2+}. In order to clarify whether the TnC-TnI fragment complexes bind to actin-tropomyosin filament or not, we carried out co-sedimentation experiments. As shown in Fig. 1-8(A), the TnC-TnI complex co-sedimented with actin-tropomyosin only in the absence of Ca^{2+}, which is consistent with the previous studies (Potter and Gergely, 1974; Hichcock, 1975). On the other hand, TnC-$TnI_{Ca\text{-}frag}$ (Fig. 1-8(B)) and TnC-$TnI_{Mg\text{-}frag}$ (data not shown) did not bind to actin-tropomyosin filaments, even in the absence of Ca^{2+}.

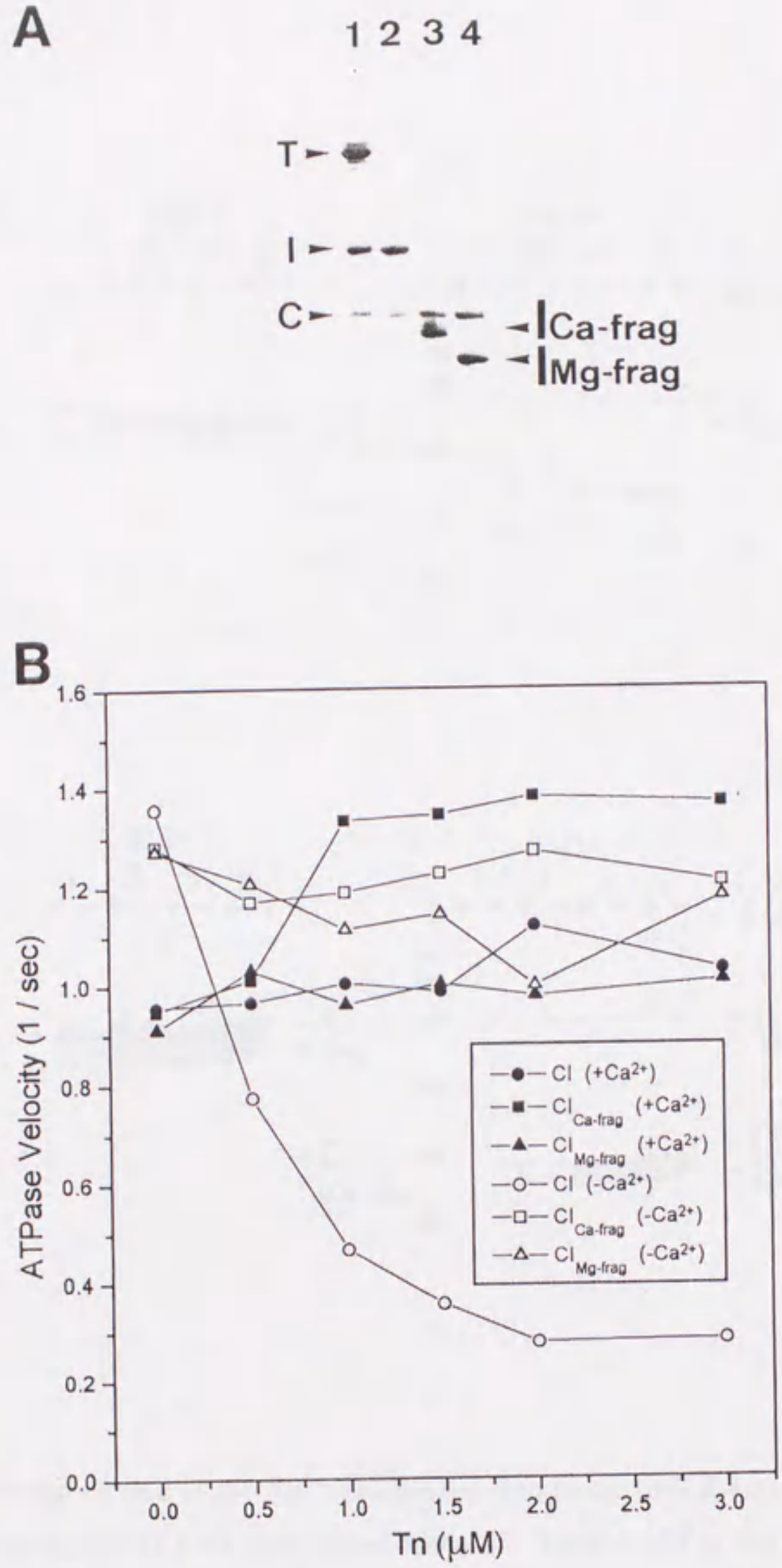

Figure 1-7. The effects of various TnC-TnI binary complexes on the acto-S1 ATPase activity. (A) SDS-PAGE of the reconstituted TnC-TnI binary complexes. Lane 1, the intact Tn complex (TCI); lane 2, TnC-TnI complex (CI); Lane 3, TnC-$TnI_{Ca\text{-}frag}$ complex ($CI_{Ca\text{-}frag}$); lane 4, TnC-$TnI_{Mg\text{-}frag}$ complex ($CI_{Mg\text{-}frag}$). (B) The effects of the reconstituted TnC-TnI binary complexes on acto-S1 ATPase activity in the presence of either 0.1 mM $CaCl_2$ and 3.5 mM $MgCl_2$ ($+Ca^{2+}$) or 0.5 mM EGTA and 3.5 mM $MgCl_2$ ($-Ca^{2+}$).

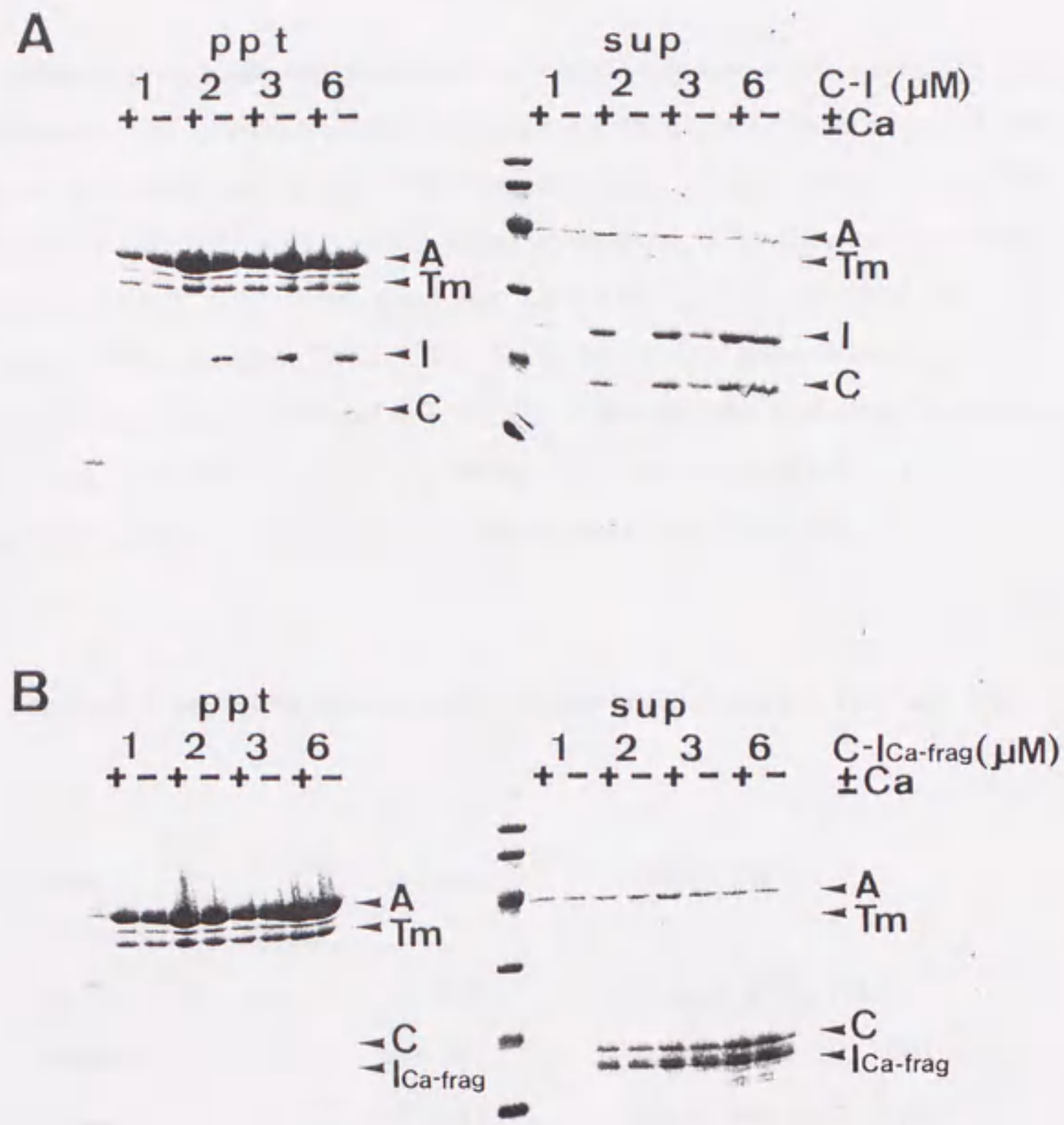

Figure 1-8. The interaction of the TnC-TnI binary complexes with F-actin-tropomyosin. Actin (6 μM) and tropomyosin (1 μM) were mixed with 1, 2, 3 and 6 μM of TnC-TnI complex (A) or TnC-$TnI_{Ca\text{-}frag}$ complex (B). Sedimentation experiments were carried out according to the method described under "EXPERIMENTAL PROCEDURES" in the presence of either 0.1 mM $CaCl_2$ and 3.5 mM $MgCl_2$ ($+Ca^{2+}$) or 0.5 mM EGTA and 3.5 mM $MgCl_2$ ($-Ca^{2+}$). The resulting supernatants (sup) and precipitants (ppt) were analyzed by SDS-PAGE. A, actin; Tm, tropomyosin; C, TnC; I, TnI; $I_{ca\text{-}frag}$, $TnI_{Ca\text{-}frag}$. Note that, in the absence of Ca^{2+}, the binding of the TnC-TnI binary complex to actin-tropomyosin was saturated at 1-2 μM., thus excess TnC-TnI binary complex was seen in supernatants as well as precipitates when the binary complex was added more than 2 μM.

DISCUSSION

In order to understand the molecular mechanism of muscle regulation, it is essentially important to elucidate the structure of Tn complex. While it has been a decade since the crystal structures of TnC were proposed (Herzberg and James, 1985; Sundaralingam *et al.*, 1985), so far, only a low resolution model of TnC-TnI binary complex based on small-angle X-ray and neutron scattering data has been available (Olah *et al.*, 1994; Olah and Trewhella, 1994). The model has proposed that almost all region of TnI interacts with TnC. The results of chemical cross-linking experiments which have supported this idea are summarized in Table 1-5. Taken together with other experiments (Farah *et al.*, 1994; Sheng *et al.*, 1992; Krudy *et al.*, 1994), it has been indicated that TnI interacts with TnC in an antiparallel manner and winds around the full length of TnC (Fig. 1-9).

Table 1-5. The results of cross-linking experiments between TnC and TnI

TnC residues	positions		TnI residues	references
98	in helix E	↔	103-111	Leszyk *et al.*, 1987
89	D/E linker	↔	108-113	Kobayashi *et al.*, 1994
57	in helix C	↔	113-121	Kobayashi *et al.*, 1991
12	N/A loop	↔	132-141	Kobayashi *et al*, 1994
155	in helix H	↔	104	Ngai *et al.*, 1994

The present study clearly showed the C-terminal part of the inhibitory region of the TnI undergoes structural transition upon Ca^{2+}-binding to the regulatory sites of TnC in the TnT-TnC-TnT ternary complex (Fig. 1-10). Chymotrypsin cleaved at residue Met-116 of TnI in the presence of Mg^{2+} and EGTA and residues Met-134 and Leu-140 in the presence of Ca^{2+} (Table 1-2). Previous experiments have indicated several important aspects of this region of TnI on the regulatory mechanism of Tn: (1) the C-terminal part of the inhibitory region of TnI has been known to be close to the N-terminal regulatory domain of TnC (Kobayashi *et al.*, 1991, 1994). (2) Cys-133 of TnI has been shown to move towards Cys-98 of TnC (Wang and Cheung, 1984; Tao *et al.*, 1989) and away from actin upon Ca^{2+}-binding to the regulatory sites of TnC (Tao *et al.*, 1990).

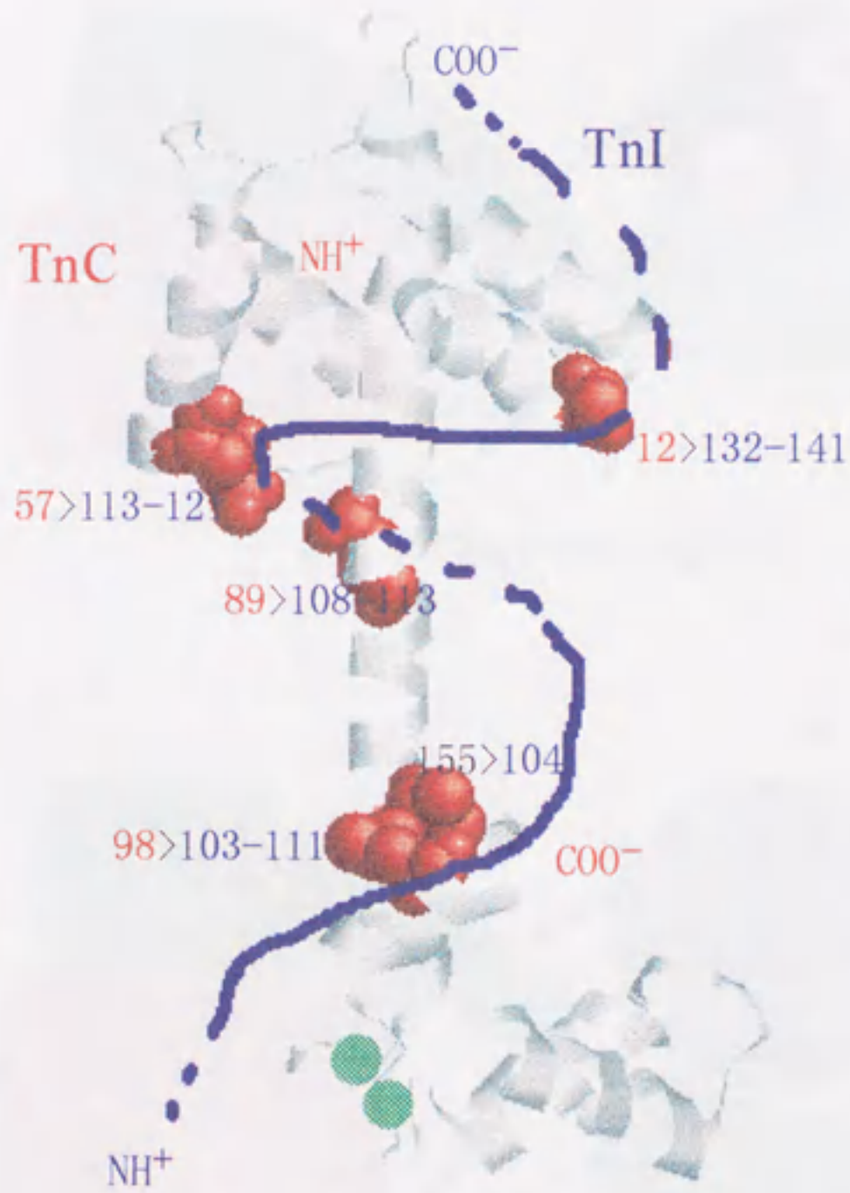

Figure 1-9 TnI and TnC interact with one another in an antiparallel manner. The polypeptide chain of TnC is drown with Ribbon and side chains at the residues, 12, 57, 89, 98 and 155 are shown in red with space-filling model. Two Ca^{2+} ions in the C-terminal domain of TnC are shown as green spheres. Possible arrangement of TnI is represented as blue line.

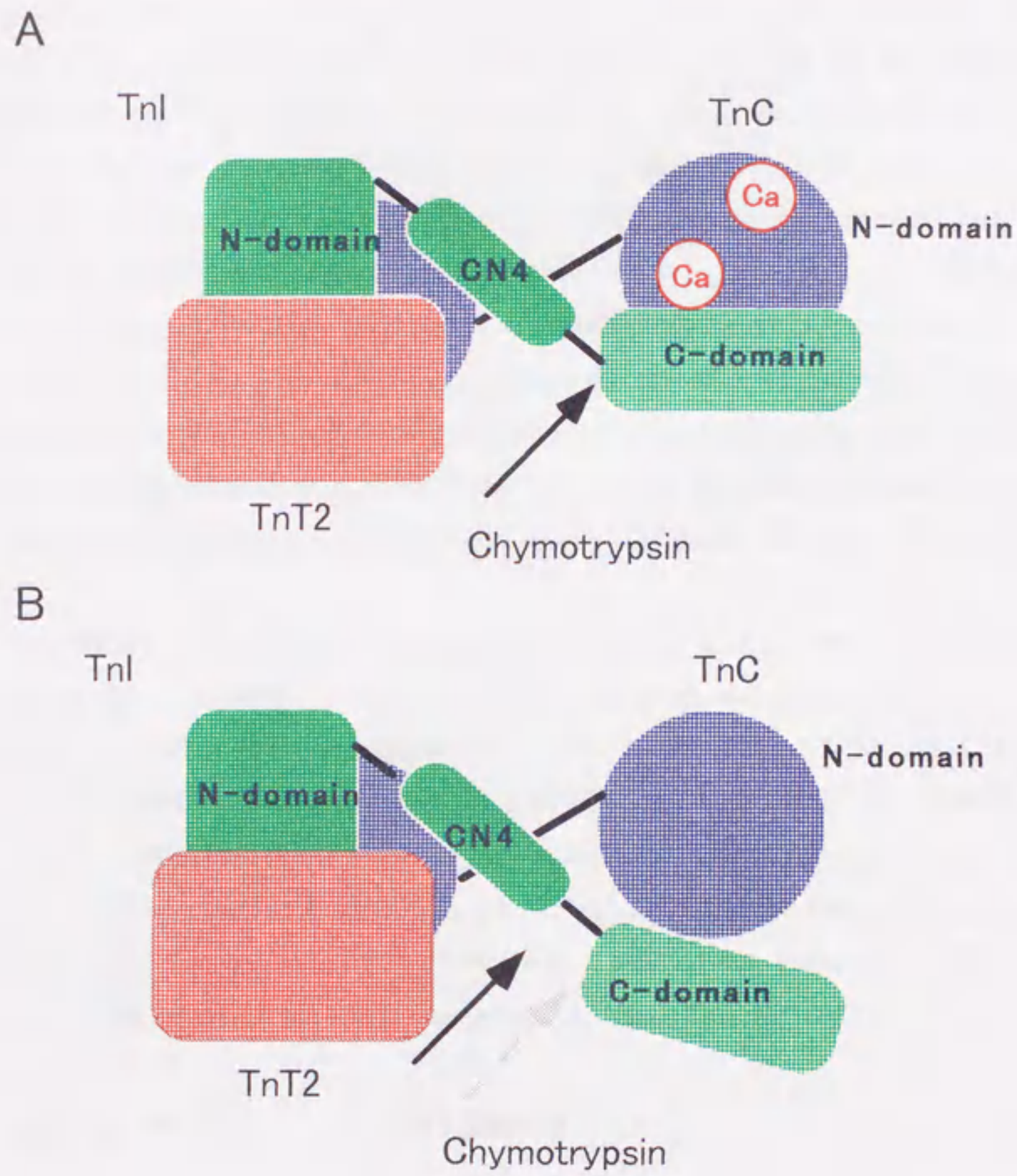

Figure 1-10 Difference in the digestion site by chymotrypsin would reflect the conformational difference of troponin complex. In the presence of high concentration Ca^{2+}, chymotrypsin cleaved at Met-134 (A). On the contrary, in the presence of low concentration of Ca^{2+}, chymotrypsin cleaved at Met-116 (B).

(3) A synthetic peptide corresponding to the residues 1-28 of actin has been shown to bind Tn complex only in the absence of Ca^{2+} not in its presence (Van Eyk *et al.*, 1991). In the present results of the limited digestion of Tn complex in the presence of Mg^{2+} and EGTA, other than TnI fragment resides 1-116, four minor fragments derived from TnI were obtained; TnI (res. 1-122), TnI (res. 1-125), TnI (res. 1-134) and TnI (res.1-140) (Table 1-1). Thus, although Tn complex is rigid in the presence of Mg^{2+} and EGTA comparing with the presence of Ca^{2+} (Zhao *et al.*, 1995), the segment residues 117-134 of TnI in the ternary complex is more susceptible for chymotryptic digestion in the presence of Mg^{2+} and EGTA. This might be explained by the interaction of this region of TnI to TnT and/or the hydrophobic patch on the N-terminal domain of TnC which is exposed upon Ca^{2+}-binding to the regulatory sites (Herzberg *et al.*, 1986; Gagne *et al.*, 1995; Slupsky and Sykes, 1995). On the contrary, this region might be exposed to the solvent enough to bind to actin in the presence of Mg^{2+} and EGTA.

Our results on the effects of TnI fragments on acto-S1 ATPase activity also support the idea that the segment 117-134 or 117-140 interacts with TnT and/or the hydrophobic patch on the N-terminal domain of TnC at high concentration of Ca^{2+}. As shown in Fig. 1-7, TnT2-TnC-$TnI_{Mg\text{-}frag}$ inhibit acto-S1 ATPase activity regardless of Ca^{2+} concentration, while TnT2-TnC-$TnI_{Ca\text{-}frag}$ regulates acto-S1 ATPase activity in a Ca^{2+}-dependent manner. Thus the segment residues 117-134 or 117-140 of TnI is suggested to be responsible for the Ca^{2+}-dependent regulation of ATPase activity. Surprisingly, the residues 117-134 are shown to be less conserved, while the residues 75-95, 99-114, and 135-151 are shown to be highly conserved in various TnIs (Fig. 1-11).

residues 108-115: **RPPLRRVR**

: : • : •

residues 137-144: **RANLKQVK**

Although the homology of the segment residues 137-144 with inhibitory region and with a calmodulin binding domain of phosphorylase kinase have been indicated to have an important role in this segment (for review, see Farah and Reinach, 1995), our results have shown that without this segment, troponin can regulate acto-S1 ATPase in a Ca^{2+}-dependent manner.

```
cray.      ADKAKAAEEAKKKQDDID-RKK-A--EVRKRLEEQSLKKQKKGFMTPERKKKLRLLLRKKAAEELKKEQERKAG    70
bov. ca.   ADRSGGST-AGDTVPAPPPVRRRSSANYRAYATEPHAKKKSK--ISASRKLQLKTLMLQIAKQELEREAEERRG    71
scal. 17K                                                   QKAAEDLANEAKAKAE            71
rab. sk.                                        GDEEKRNRAITARRQHLKSVMLQIAATELEKEEGRREA  38

cray.      ERRKIIDQRCGQPKNLDGANEEQLRAIIKEYFDHTAQIESDKYDVELEIIRKDYEINELNIQVNDLRGKFIXPT   144
bov. ca.   EKGRALSTRC-QPLELAGLGFAELQDLCRQLHARVDKVDEERYDVEAKVTKNITEIADLNQKIFDLRGKFKRPT   144
scal. 17K  AKEKYINDLV-PKFSTDGKDVAALQALCKDFHKRLASLEEDVYDWEAKIRKQDFEINELTLKVNDTKGKFVKPV    89
rab. sk.   EKQNYLAEHC-PPLSLPG-SMAEVQELCKQLHAKIDAAEEEKYDMEIKVQKSSKELEDMNQKLFDLRGKFKRPP   110

cray.      LKKVSKYENKFAKL---QKKAAEF-NFRNQLKTVKKKEFEKE---DDKGATEGDGPAAEEVAAE            201
bov. ca.   LRRVRISADAMMQALLGARAKETL-DLRAHLKQVKKEDTEKEN--REVGDWRKNIDALSGMEGRKKKFEG      211
scal. 17K  LRKVNKTESKLDKI---QRKEAKKSDFRDNLKSSREHEADKE---GGEGENE                        135
rab. sk.   LRRVRMSADAMLKALLGSKHKVCM-DLRANLKQVKKEDTEKERDLRDVGDWRKNIEEKSGMEGRKKMFESES   181
```

↑ Chymotrypsin (Mg^{2+}, EGTA)

↑ Chymotrypsin (Ca^{2+})

Figure 1-11. Alignment of amino acid sequences of various TnIs. Cray., crayfish tail muscle TnI (Kobayashi *et al.*, 1989); rab.sk., rabbit fast skeletal muscle TnI (Wilkinson and Grand, 1978; Sheng *et al.*, 1992; Kluwe *et al.*, 1993); bov.ca., bovine cardiac muscle TnI (Leszyk *et al.*, 1988); scal.17K, C-terminal 17kDa CNBr-fragment of Akazara Scallop TnI (Ojima *et al.*, 1995). The letter X in the sequence of crayfish TnI represents trimethyllysine residue. A dash (-) indicates a deletion introduced to maximize the sequence similarity. Residues identical or conserved in all four TnIs are written in red. Red dashed lines indicate the highly conserved regions. The regions thought to be important for binding of actin or TnC are indicated by a green solid bar (‖ — ‖).

As shown in Fig. 1-8, unlike the TnC-TnI complex, the TnC-TnI fragment binary complex did not bind to actin-tropomyosin even in the absence of Ca^{2+}. The consistent results were obtained by measuring the effects of these binary complexes on acto-S1 ATPase activity (Fig. 1-7). The results indicate that, besides the inhibitory region of TnI, residues 135 to 181 or 141 to 181, takes part in the interaction with actin-tropomyosin in the absence of Ca^{2+} Recently similar results were obtained by the use of TnI deletion mutants (Jha *et al.*, 1996). Thus along the TnI molecule there are two distinct sites that interact with actin-tropomyosin in a Ca^{2+} dependent manner: the inhibitory region and the C-terminal segment, residues 135-181 or 141-181. Although we did not verify which component binds to C-terminal region of TnI, Pearlstone and Smille (1983) reported that TnI weakly binds to immobilized tropomyosin. Thus it is likely that the C-terminal segment of TnI (residues 135 to 181 or 141 to 181) interacts with tropomyosin.

The functions of the segments of TnI proposed in the present study are summarized in Fig. 1-12.

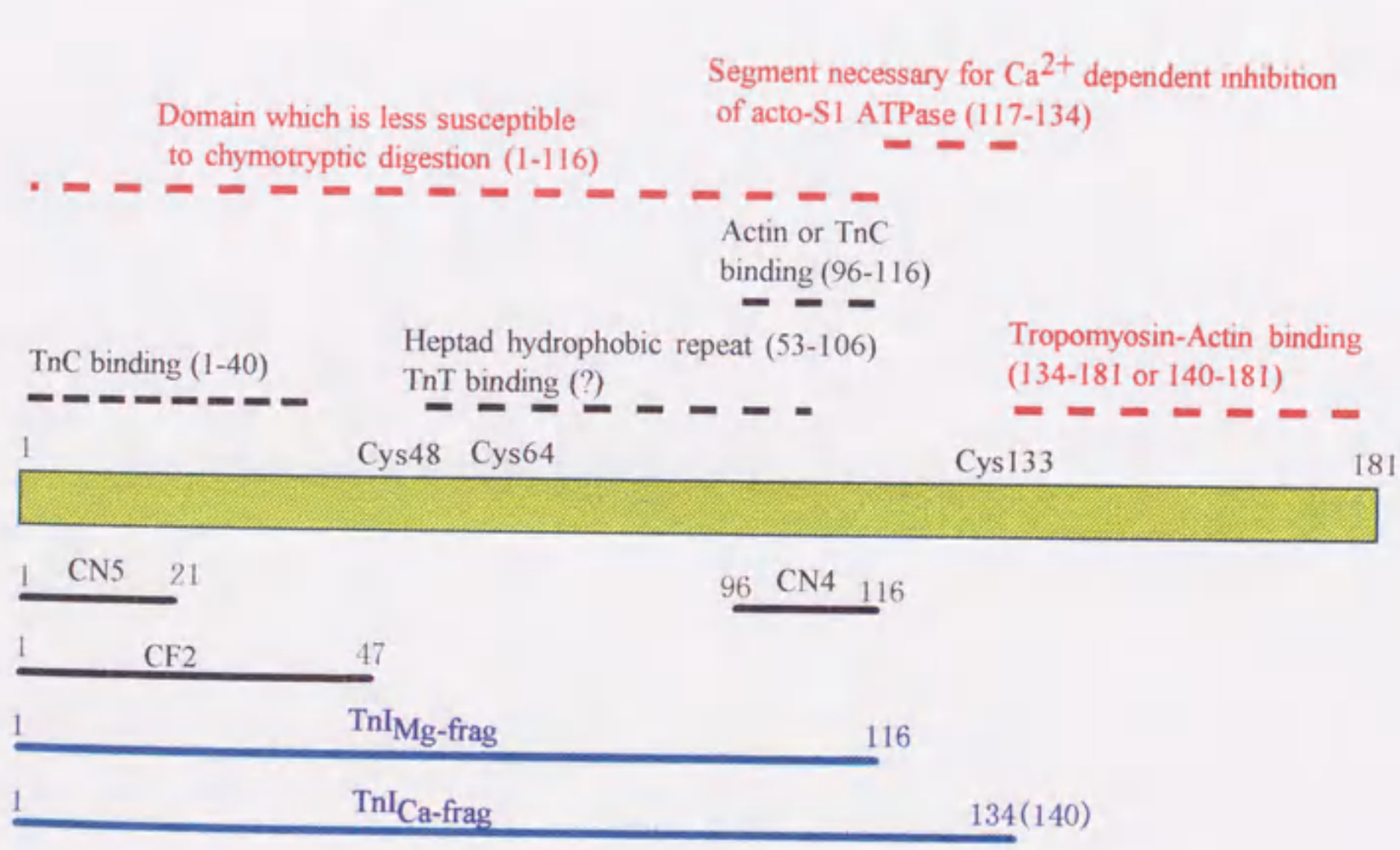

Figure 1-12. Schematic representation of domains of TnI.

【Part II】

Isolation of TnT2 and TnI Fragments

SUMMARY

In this part, optimized purification procedure of $TnI_{Ca\text{-}frag}$, $TnI_{Mg\text{-}frag}$, TnT2 (TnT2α) and TnT2β fragments from chymotryptic digestion products of rabbit skeletal muscle troponin complex are described in detail. The fragments obtained were reconstituted into ternary or binary complexes which were used in ATPase assay and sedimentation experiments which are described in part I, as well as, in crystallization trials. The procedure is also described which was devised in order to isolate the ternary complex consisting of the digestion fragments in large quantities.

EXPERIMENTAL PROCEDURES

Digestion of troponin

The conditions to digest troponin are described in "EXPERIMENTAL PROCEDURES" in part I.

Isolation of digested fragments

Digested troponin was applied on an 1.5×10 cm column of Q-sepharose fast flow (Pharmacia) equilibrated with 0.1 M NaCl, 0.1 mM $CaCl_2$, and 20 mM Tris-HCl, pH 8.0 (the starting buffer) and was eluted with a linear gradient of 0.1 M-0.5 M NaCl in the starting buffer at 4°C. TnT2-TnC-TnIfragment ternary complex containing fractions were identified by SDS-PAGE, pooled and dialyzed against 0.1 M NaCl, 1 mM EDTA, 1 mM dithiothreitol and 20 mM Tris-HCl, pH 8.0. After dialysis, solid urea was added to give a final concentration of 6 M. The protein solution was applied to Q-sepharose fast flow column (1.5×10 cm) equilibrated with 6 M urea, 1 mM EDTA and 20 mM Tris-HCl, pH 8.0. TnC adsorbed to the resin under these conditions was recovered by a linear gradient of salt concentration. The flow through fractions were pooled and loaded onto an SP-sepharose fast flow column (1.5×10 cm) equilibrated with the same buffer and TnT2 and TnI fragments were separated with a linear gradient of 0.1-0.6 M NaCl in the same buffer. Further purification of TnT2 fragments was performed on a gel filtration column chromatography. TnT2 fragments which was eluted from the SP-sepharose column were applied on a 2.5×50 cm column of Sephacryl S-100 (Pharmacia) equilibrated with 0.3 M NaCl and 20 mM Tris-HCl, pH 8.0.

Isolation of digested fragments as ternary complexes

If reconstitution of complexes is not necessary for a purpose of experiments, digested fragments can be recovered as ternary complexes. TnT2-TnC-TnI fragment ternary complex containing fractions from the Q-sepharose fast flow column were pooled and loaded on a hydroxyapatide prepackaged column (HCA A5010G, Koken, Japan) equilibrated with 10 mM potassium/phosphate, pH 6.8 and TnT2-TnC-TnI fragment ternary complex were separated with a linear gradient of 10-500 mM potassium/phosphate, pH 6.8.

RESULTS AND DISCUSSION

Digestion of troponin

Although it has already been described in "EXPERIMENTAL PROCEDURES" in part I, some additional points which are better to mention are described in this part. In order to obtain the $TnI_{Ca\text{-}frag}$ and $TnI_{Mg\text{-}frag}$ fragments in large quantity, it is essential to digest Tn complex for long period to diminish undigested TnI. Because it turned out to be extremely difficult to isolate TnI fragments from undigested TnI by conventional chromatographic techniques, especially in the case of $TnI_{Ca\text{-}frag}$. On the other hand, longer period of digestion causes not only to diminish undigested TnI but also to produce TnT2 subfragments, *i. e.*, TnT2β fragments described by Tanokura *et al.* (1983). Therefore, digestion period was determined by a small scaled experiment. In the present study, it was found that 15 min of digestion with 1/400 weight ratio of chymotrypsin at 37°C is sufficient to diminish undigested TnI, and maximum yield of $TnI_{Ca\text{-}frag}$ and $TnI_{Mg\text{-}frag}$ were achieved under these conditions.

Purification of $TnI_{Ca\text{-}frag}$, $TnI_{Mg\text{-}frag}$, TnT2α, TnT2β and TnC

Fig. 2-1 and Fig. 2-2 represent the purification steps of $TnI_{Ca\text{-}frag}$. Firstly, digestion products were separated by a Q-sepharose fast flow column (Fig. 2-1). And then, the troponin components from the Q-sepharose fast flow column were dissociated by adding 6 M urea and 1 mM EDTA, then further applied to Q-sepharose fast flow column which was connected to an SP-sepharose fast flow column. TnT2α, TnT2β and $TnI_{Ca\text{-}frag}$ which were absorbed to the SP-sepharose fast flow column were separated with a linear gradient of NaCl (Fig. 2-2). Separation of TnT2α and TnT2β were performed on a gel filtration chromatography (Fig. 2-3). TnC which was absorbed to a Q-sepharose fast flow column was eluted with a linear gradient of NaCl (Fig. 2-4).

Purification of $TnI_{Mg\text{-}frag}$

Fig. 2-5 and Fig. 2-6 represent the purification steps of $TnI_{Mg\text{-}frag}$. Firstly, digestion products were separated by a Q-sepharose fast flow column (Fig. 2-5). And then, the troponin components from the Q-sepharose fast flow column were dissociated by adding 6 M urea and 1 mM EDTA, then further applied to a Q-sepharose fast flow column which was connected to an SP-sepharose fast flow column. TnT2α, TnT2β and $TnI_{Mg\text{-}frag}$ which were absorbed to SP-sepharose fast flow column were separated with a linear gradient of NaCl (Fig. 2-6).

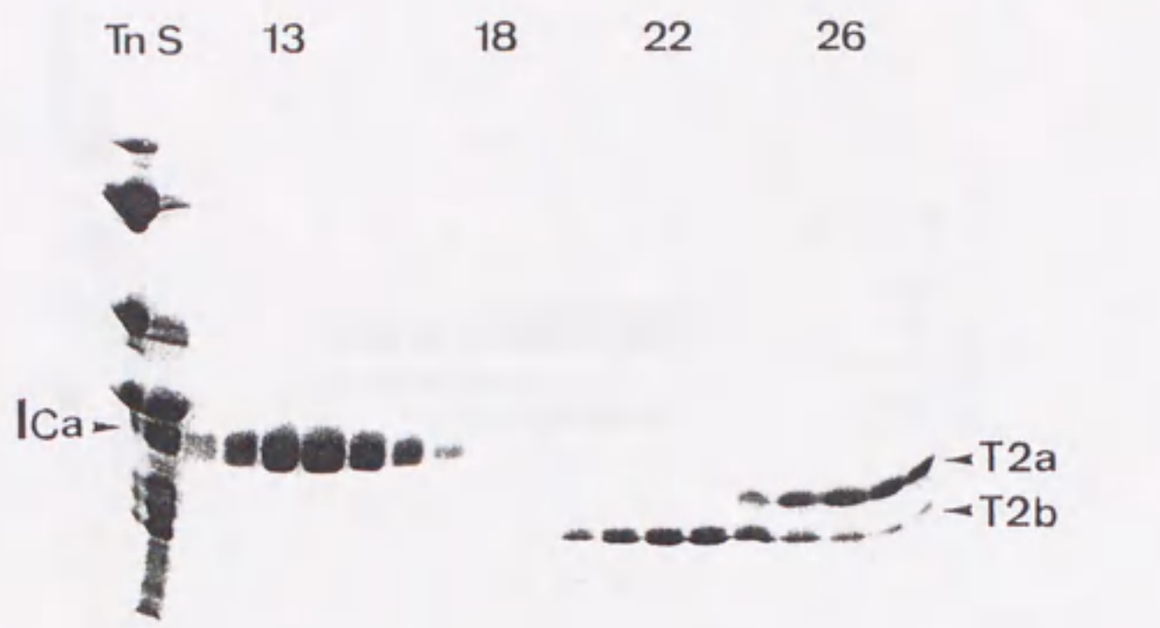

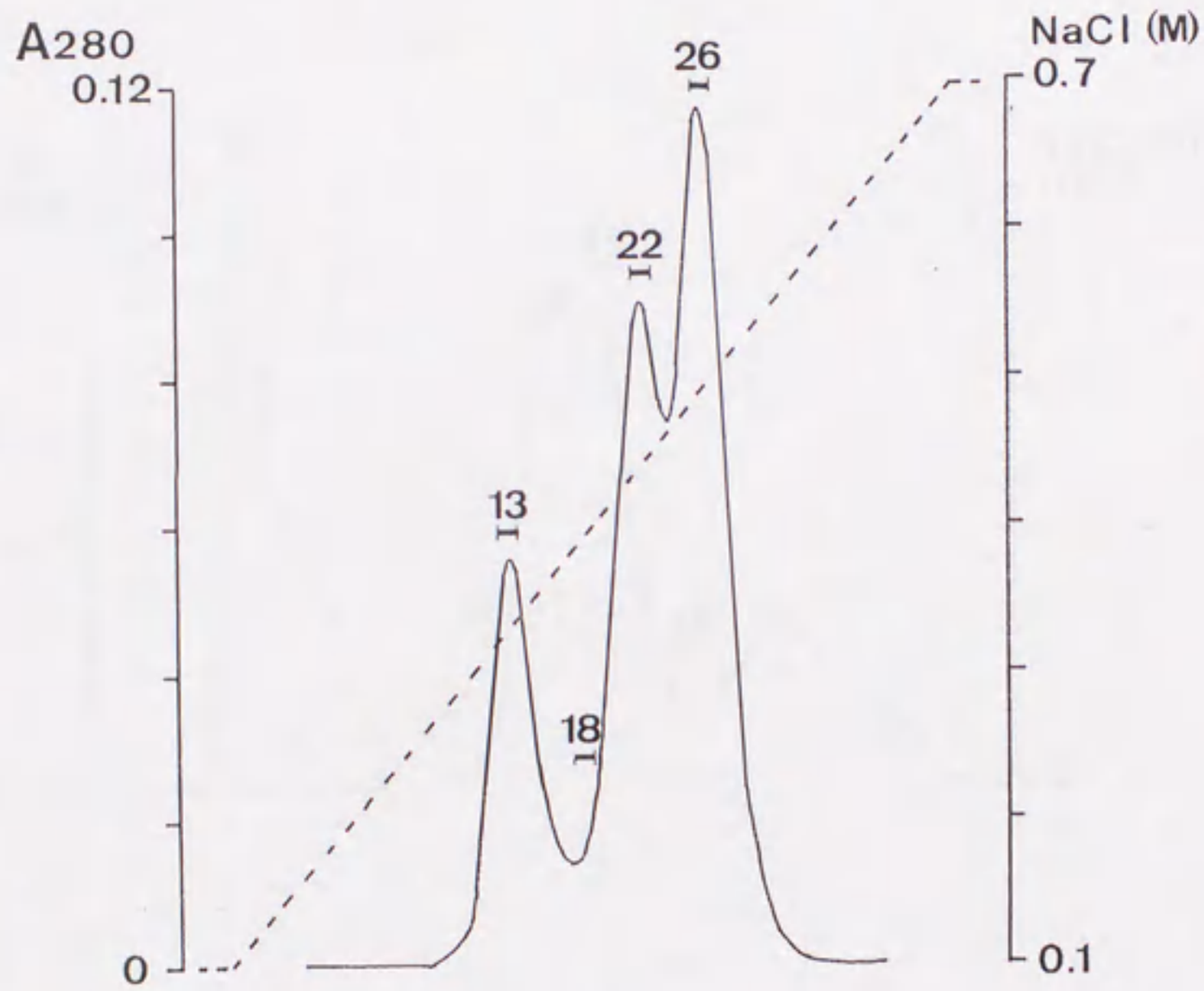

Figure 2-1. Isolation of the ternary Tn complex containing $TnI_{Ca\text{-}frag}$ fragment. Tn was digested in the presence of 1 mM $CaCl_2$ and 5 mM $MgCl_2$ at 37°C for 15 min with 1/400 weight ratio of TLCK-treated α-chymotrypsin as described under "EXPERIMENTAL PROCEDURES". The digestion products were separated by a Q-sepharose fast flow column. TnT1, T1; TnC, C; $TnI_{Ca\text{-}frag}$, I_{Ca}; TnT2α, T2a; TnT2β, T2b.

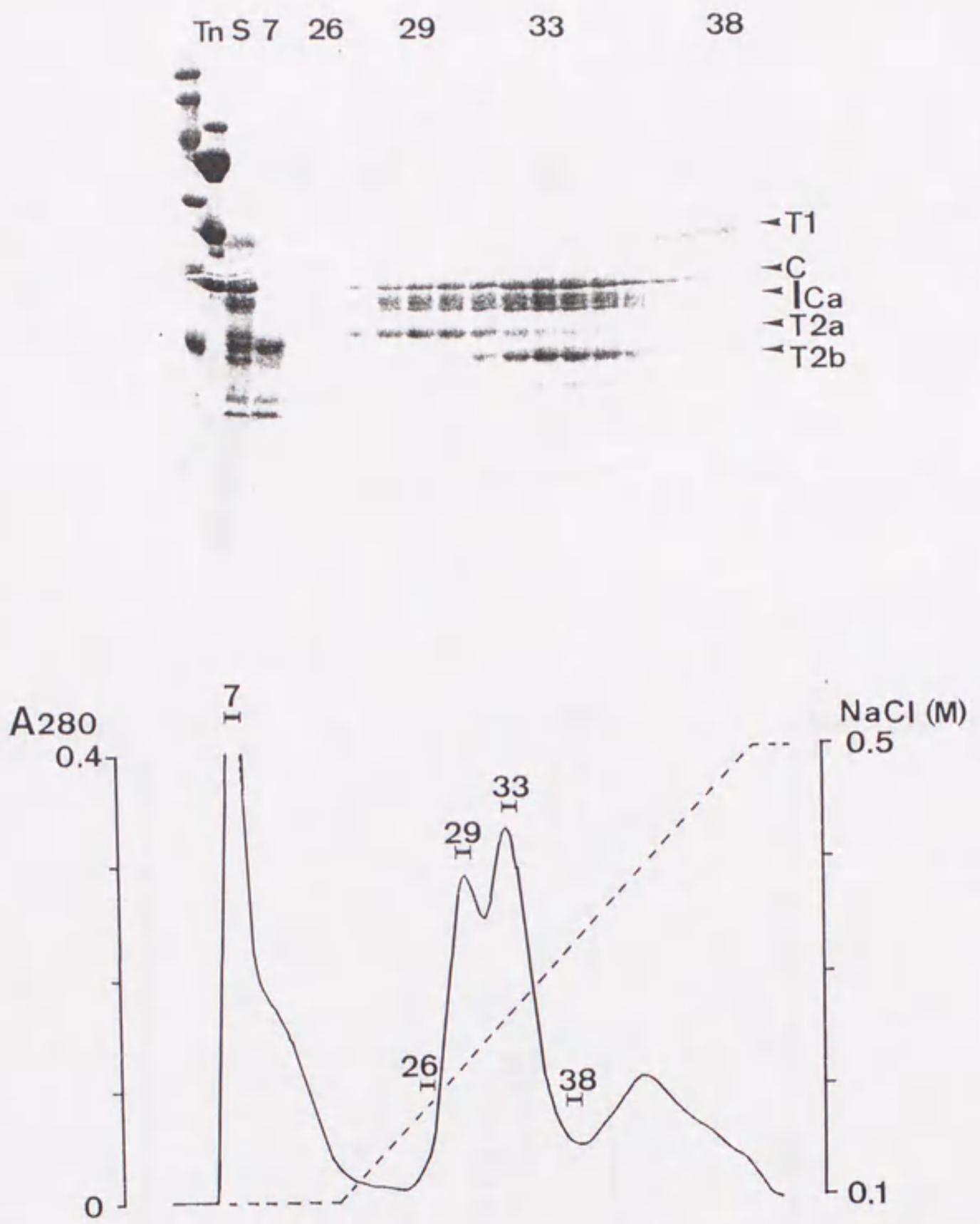

Figure 2-2. Isolation of $TnI_{Ca\text{-}frag}$, TnT2 α and TnT2β by an Sp-sepharose fast flow column. The troponin components from the Q-sepharose fast flow column (Frac. No. 27-35 in Fig. 2-1) were dissociated by adding 6 M urea and 1 mM EGTA, and then applied to a Q-sepharose fast flow column which was connected to an Sp-sepharose fast flow column. $TnI_{Ca\text{-}frag}$, TnT2 α and TnT2β which were absorbed to the Sp-sepharose fast flow column were recovered by a linear gradient of 0.1-0.7 M NaCl. $TnI_{Ca\text{-}frag}$ were $TnI_{Ca\text{-}frag}$, I_{Ca}; TnT2α, T2a; TnT2β, T2b.

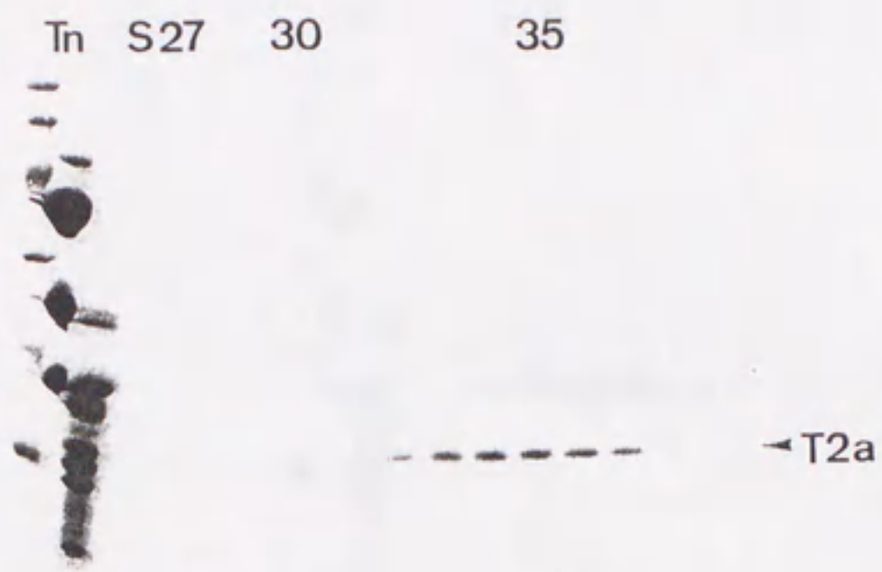

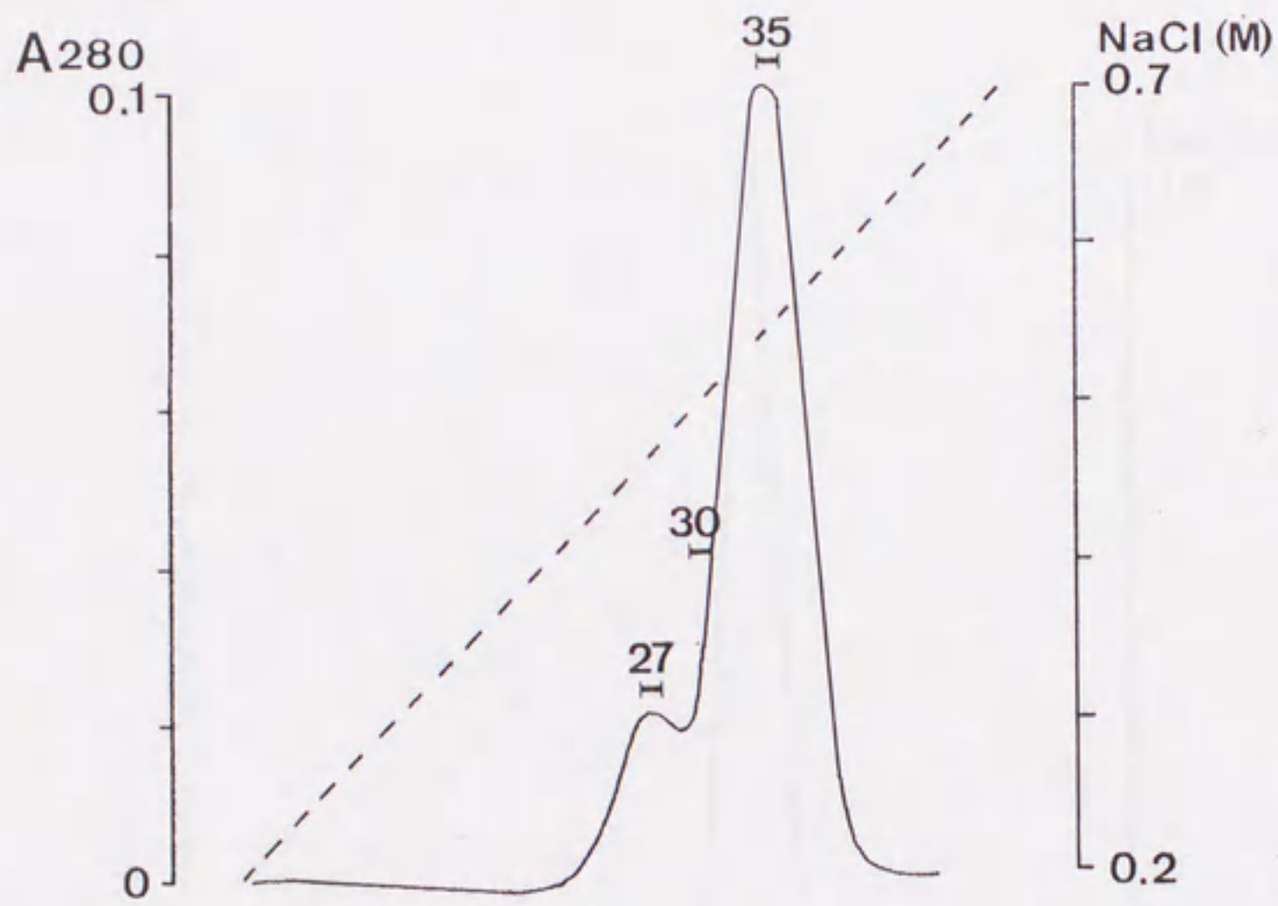

Figure 2-3. Isolation of TnT2α by Sephacryl S-100 column. The fractions containing TnT2α (No. 24–28 in Fig. 2-2) were concentrated and further applied to a Sephacryl S-100 column (2.5×50 cm) equilibrated with 20 mM Tris-HCl, 0.3M NaCl, pH 8.0.

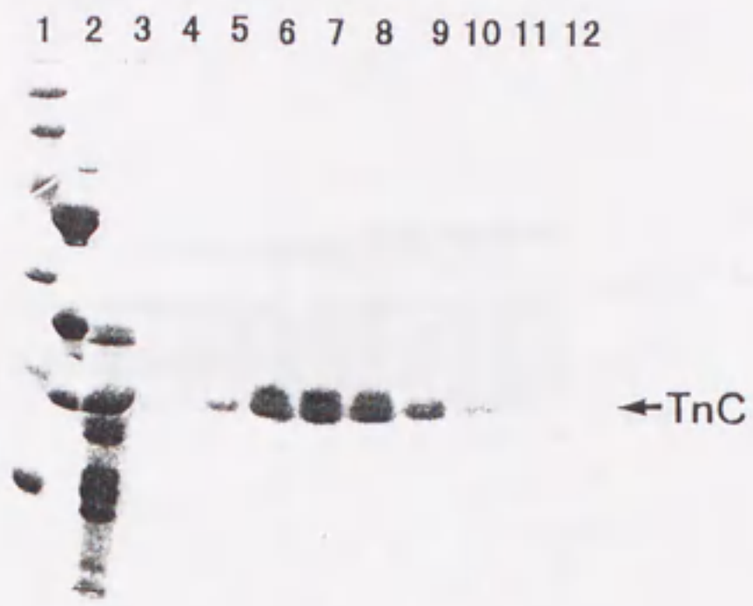

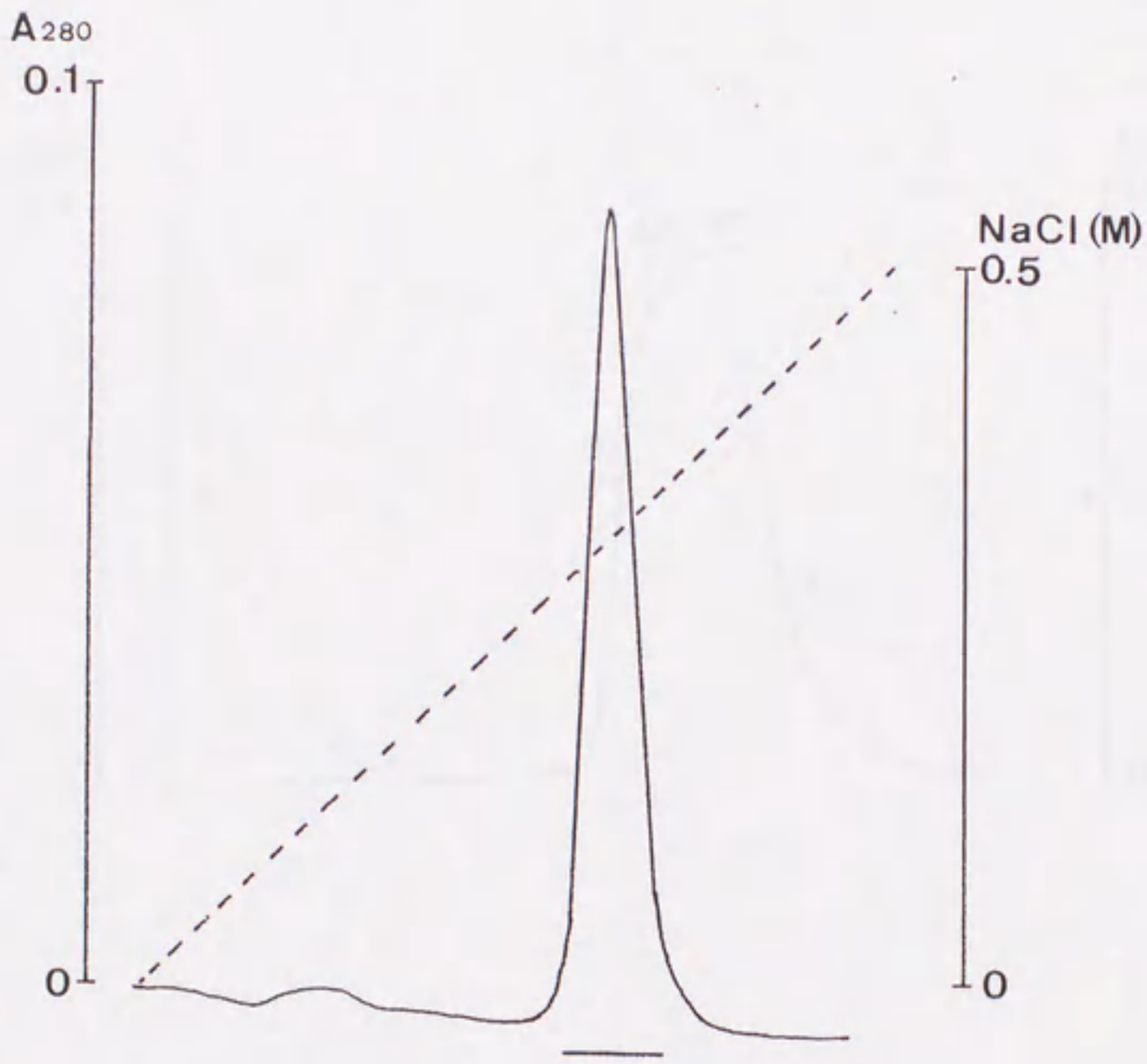

Figure 2-4. Isolation of TnC by a Q-sepharose fast flow column. TnC which was absorbed to the Q-sepharose fast flow column was eluted with a linear gradient of 0.1-0.6 M NaCl in the starting solution, 20 mM Tris-HCl, 1 mM EDTA, 6 M urea, pH 8.0.

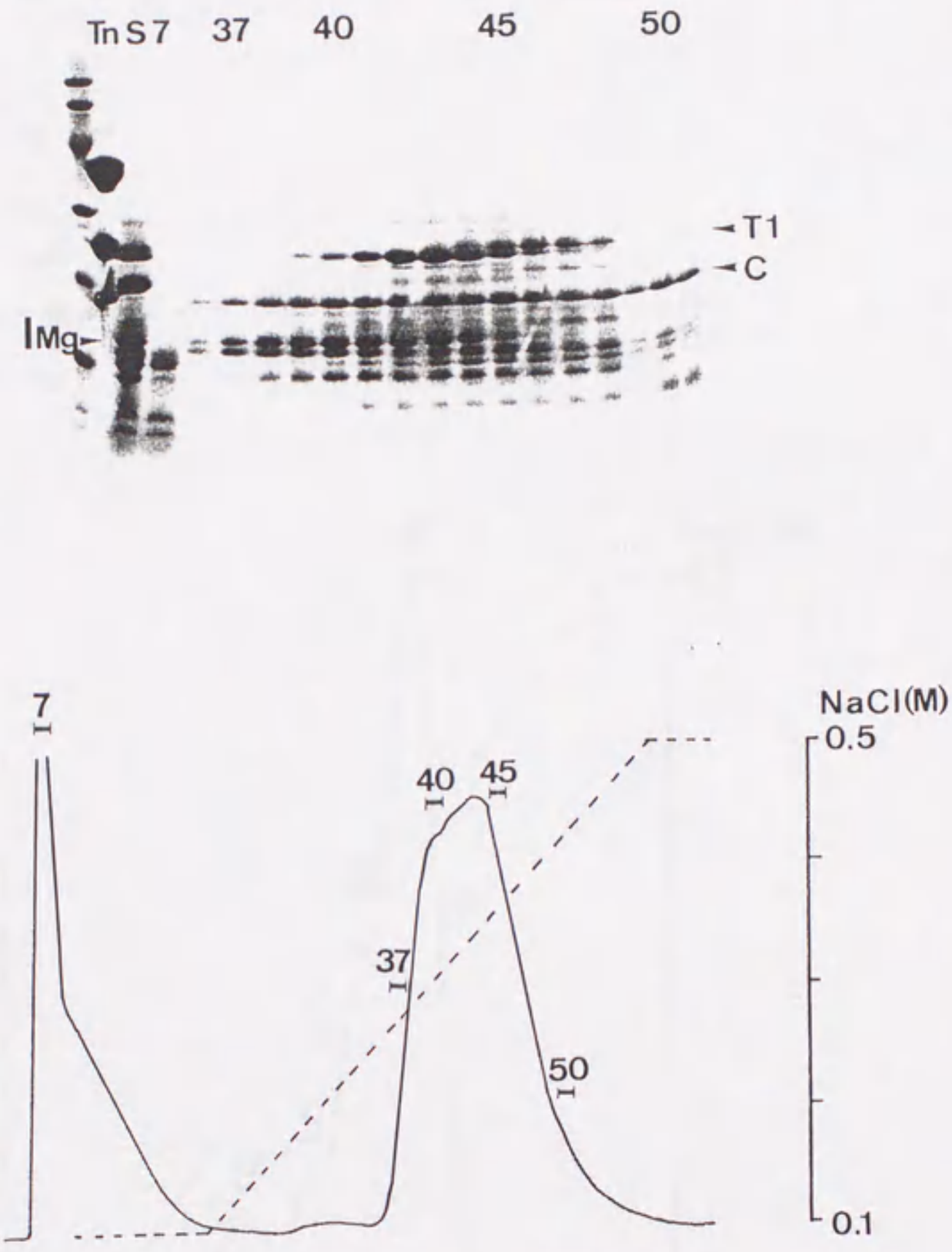

Figure 2-5. Isolation of the ternary Tn complex containing $TnI_{Mg\text{-}frag}$ fragment. Tn was digested in the presence of 1 mM EGTA and 5 mM $MgCl_2$ at 37°C for 15 min with 1/400 weight ratio of TLCK-treated α-chymotrypsin as described under " EXPERIMENTAL PROCEDURES". The digestion products were separated by a Q-sepharose fast flow column. TnT1, T1; TnC, C; $TnI_{Mg\text{-}frag}$, I_{Mg}.

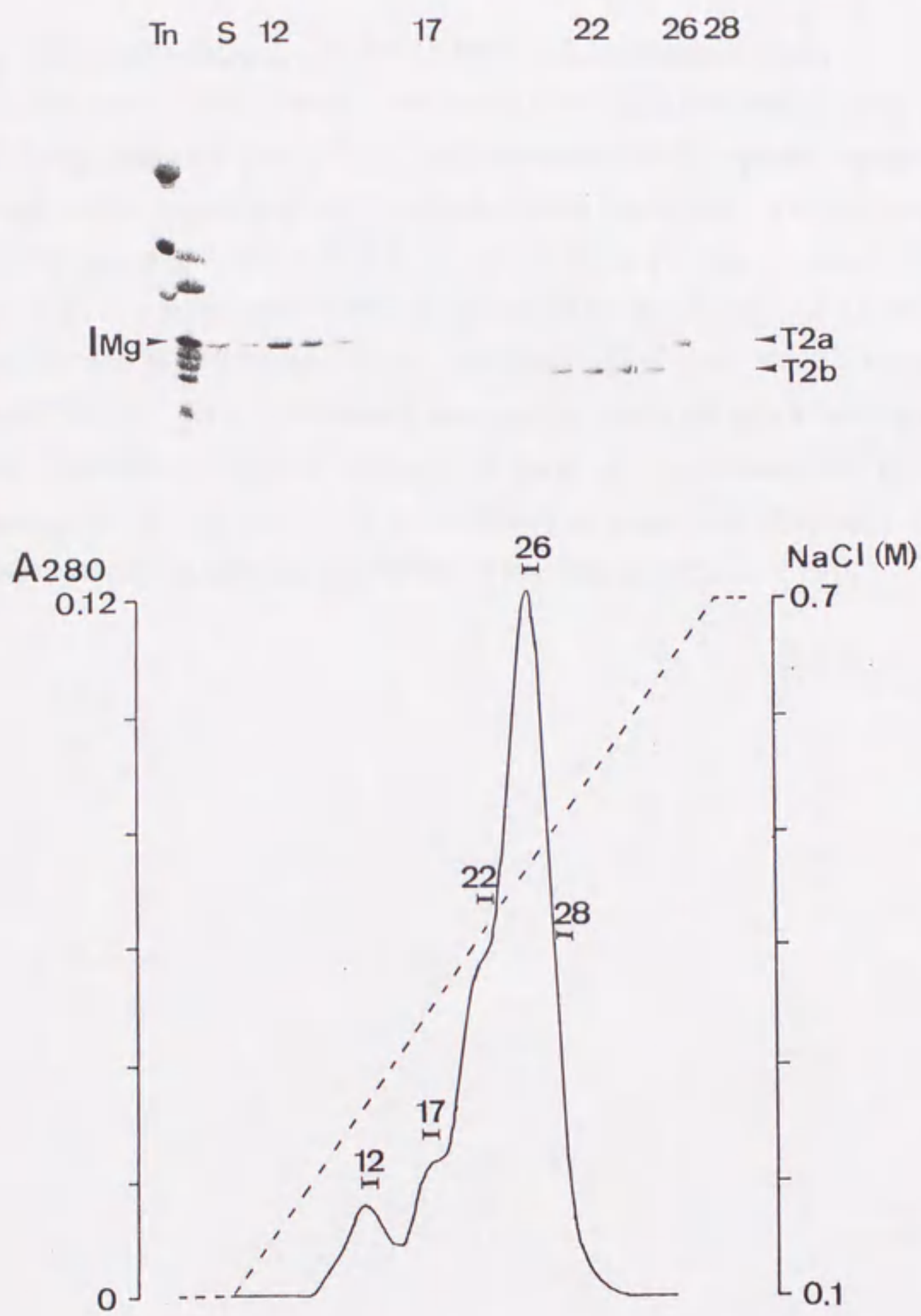

Figure 2-6. Isolation of $TnI_{Mg\text{-}frag}$, TnT2 α and TnT2β by Sp-sepharose fast flow column. The troponin components from the Q-sepharose fast flow column (Frac. No. 37-45 in Fig. 2-5) were dissociated by adding 6 M urea and 1 mM EGTA, and then applied to a Q-sepharose fast flow column which was connected to an Sp-sepharose fast flow column. $TnI_{Mg\text{-}frag}$, TnT2 α and TnT2β which were absorbed to the Sp-sepharose fast flow column were eluted with a linear gradient of 0.1-0.7 M NaCl. $TnI_{Mg\text{-}frag}$ were $TnI_{Mg\text{-}frag}$, I_{Ca}; TnT2α, T2a; TnT2β, T2b.

Isolation of TnT2α-TnC-TnI$_{Ca\text{-}frag}$ and TnT2β-TnC-TnI$_{Ca\text{-}frag}$ ternary complex

Although, size exclusion chromatography was shown to be a powerful tool to purify TnI fragment containing ternary complexes (Fig. 1-2, Fig. 1-3), the amount of the complex which was isolated, was not enough for the purpose such as crystallization trials. By the use of a hydroxyapatide column, TnT2α-TnC-TnI$_{Ca\text{-}frag}$ and TnT2β-TnC-TnI$_{Ca\text{-}frag}$ ternary complex were separated and gave good quantity (Fig. 2-6). Ternary complex containing fractions were dialyzed against 0.1 M NaCl, 10 mM Tris-HCl, pH 8.0 and applied to mono-Q HR 5/5 column equilibrated with 0.1 M NaCl, 0.1 mM $CaCl_2$, 10 mM Tris-HCl, pH 8.0 (the starting solution) and recovered with a linear gradient of 0.1-0.5 M NaCl in the starting solution. Although the purity of ternary complexes without mono-Q column is enough for crystallization trials, it is necessary to remove phosphate ions, which chelates Ca^{2+}, in order to keep the conformational stability of troponin complex.

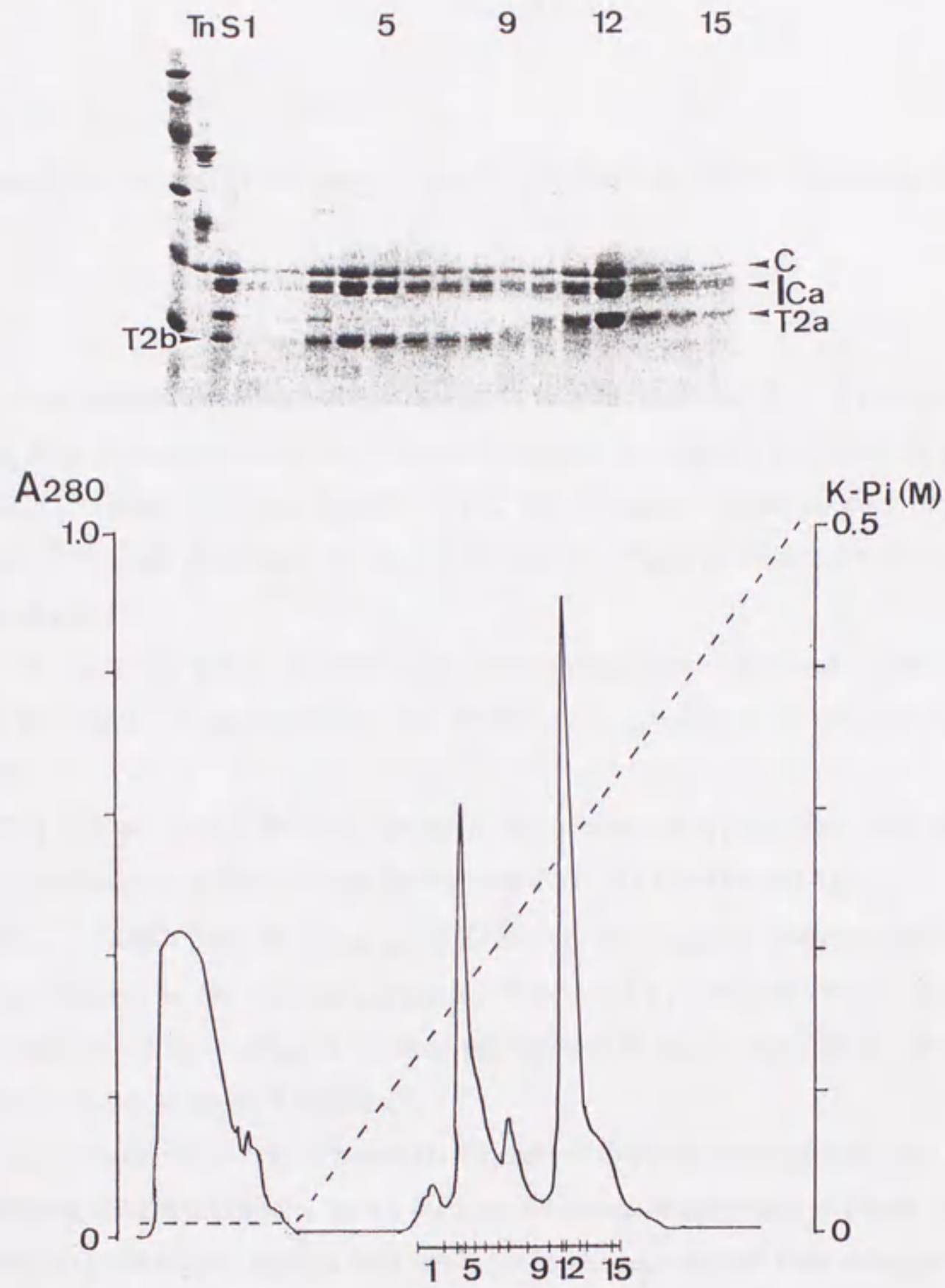

Figure 2-7. Isolation of the ternary Tn complexes containing $TnI_{Ca\text{-}frag}$ by a hydroxylapatide column. $TnI_{Ca\text{-}frag}$ (Frac. No. 27-35 in Fig. 2-1) was applied to a hydroxylapatide column (HCA A5010G, Koken, Japan) equilibrated with 10 mM Potassium phosphate, pH 6.8 (starting solution). The ternary Tn complexes containing $TnI_{Ca\text{-}frag}$ was eluted with a linear gradient of 10-500 mM Potassium phosphate, pH 6.8.

【Part III】

Crystallization and Preliminary Crystallographic Analysis of Troponin Complex

SUMMARY

In order to understand the molecular mechanism of muscle regulation, it is of crucial importance to obtain the three dimensional structure of troponin complex at an atomic resolution. In order to obtain the crystals suitable for X-ray crystallography, We designed several species of complex and optimized purification procedures for high homogeneity. Preparation of each complex protein is described in part IV.

So far, three species of complexes were reproducibly crystallized. In this part, We will describe the results of crystallization and preliminary crystallographic analysis of these three complexes.

(III-1) T2CI complex (TnT2-TnC-TnI complex) - Rhombohedral crystals have been obtained in the solution containing zinc acetate, polyethyleneglycol 4000 and Tris-HCl pH 8.0.

(III-2) $Tm_{141-284}$T25kCI complex ($Tm_{141-284}$-TnT25k-TnC-TnI complex) - Microcrystals up to 20 μm have been obtained in the solution containing 2-methyl-2,4-pentandiol. While X-ray diffraction patterns have not yet been obtained, electron micrographs of thin sections of the crystals indicated that they were really made up of proteins.

(III-3) CI_{1-47} complex (TnC-TnI_{1-47} complex) - Crystals of different morphologies have been obtained under different solvent conditions. In the presence of high concentrations of citrate or tartrate ions, rombohedron or rod-shaped crystals with hexagonal cross-sections has been obtained. On the other hand, in the presence of several kinds of organic solvent or polymers, crystals with a regular octahedral morphology have been obtained. These two different crystal forms were characterized.

EXPERIMENTAL PROCEDURES

Vapor diffusion method with hanging drops

In order to screen the wide array of crystallization conditions, vapor diffusion method were carried out following the procedure according to the description by MacPhason (1990). The method relies on the transport of either water or some volatile agent between a microdrop of mother liquor, which contains protein and is generally 2-20 μl volume, and a much larger reservoir solution of 0.5-1 ml volume. Through the vapor phase, the droplet and reservoir come to equilibrium, and because the reservoir is of much larger volume, the final equilibration conditions are essentially those of the initial reservoir state. This method has the advantage that it requires only small amount of material and is ideal for screening a large number of conditions. A variety of devices which are designed for hanging drop or sitting drop method have been available. In the present study, hanging drop method was carried out using tissue culture multi-well plates (Linbro). The wells on the plastic plate were filled with 0.5-1 ml of reservoir solution. On a silicon coated cover slip, 1-5 μl of protein and 1-5 μl of the reservoir solution were mixed and then the cover slip with the drop hanging from the slip was placed over the well which was filled with reservoir solution. Between the cover slip and the edge of the well was sealed with silicon grease. The plates were allowed to keep at 4°C, 16°C or room temperature. The process of the crystal growth was observed under an optical microscope.

Protein solutions

The purification procedure for samples for crystallization are described in part IV. Fig. 3-0-1 shows the SDS-PAGE patterns of the troponin complexes used for crystallization trials (B), and schematic representation of these troponin complexes (A). Before crystallization, each protein sample was allowed to be concentrated by centriprep-10 or centricon-10 (Amicon) to give a final concentration of 10-30 mg protein/ml. The protein concentration of each protein solution was determined according to their amino acid compositions (Gill and von Hippel, 1989).

Reservoir solutions

Generally each reservoir solution contains three different components; (1) a precipitating agent (or agents) which creates the supersaturated state of protein, (2) a buffer which keeps the pH during the crystallization process, (3) some additives such as salts, chelating agents, detergents, reducing agents, etc. And combinations of these compounds, wide array of crystallization conditions were screened.

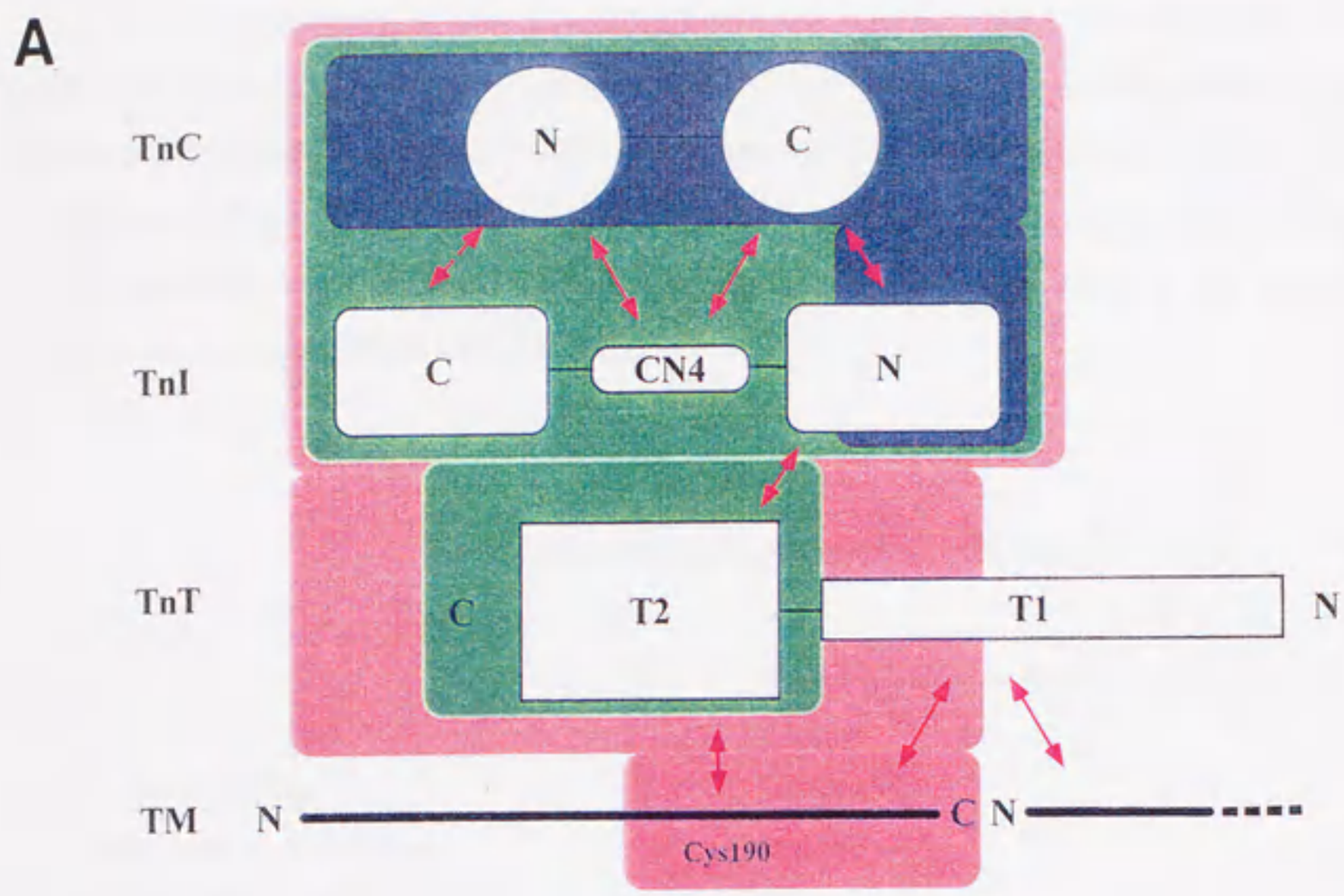

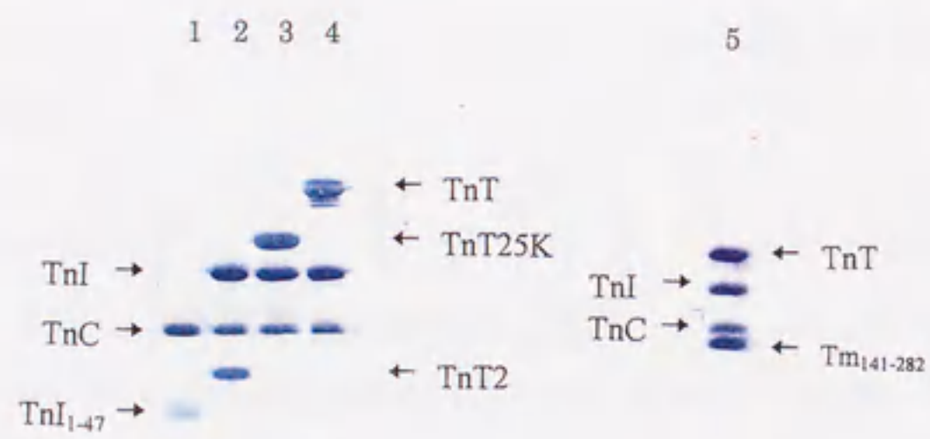

Figure 3-0-1. Schematic representation of the interactions among troponin subunits and tropomyosin (A), and SDS-PAGE of the troponin complexes used for crystallization (B). Lane 1, CI_{1-47} complex; lane 2, T2CI complex; lane 3, T25kCI complex; lane 4, intact troponin complex isolated from rabbit skeletal muscle; lane 5, $Tm_{141-284}$-T25kCI complex.

(1) Precipitating agents: Protein precipitants fall into four broad categories: (a) salts, (b) organic solvents, (c) long-chain polymers and (d) low-molecular-mass polymers and non-volatile organic compounds. The first two classes are typified by ammonium sulfate and ethanol, respectively, and higher polymers such as PEG 4000 are characteristic of the third. MPD (2-methyl-2, 4-pentanediol) is one of the most popular precipitants in the fourth category. The precipitants used in this study are summarized in Table 3-0-1.

Table 3-0-1. Precipitants used in this study

Salts	*Organic solvents (volatile)*
Ammonium/Sodium sulfate	Ethanol
Lithium sulfate/chloride	Isopropanpl
Ammonium/Sodium citrate/tertrate	Dioxane
Sodium/Potassium/Ammonium chloride	Aceton
Sodium/Ammonium acetate	Dimethyl sulfoxide
Calcium/Magnecium sulfate	

Organic solvents (non-volatile)	*Polymers*
2-Methyl-2, 4-penthanediol (MPD)	Polyethyleneglycol 1000/4000/8000/20000
Polyethyleneglycol 200/400/600	

(2) Buffers: Because protein crystals are stabilized by a relatively small number of favorable interactions between molecules, including Van der Waals interactions, hydrogen bonds, salt bridges which are formed between neighboring molecules at the lattice contacts, a small change in pH may affect the crystal packing. Also proteins always vary in solubility as with pH. Various pH buffers which were used in the present study are summarized in Table 3-0-2.

Table 3-0-2. Buffers used in this study

Acetate/NaOH	pH 4.6	HEPES/NaOH	pH 7.5/8.0
Cacodylate/NaOH	pH 5.2	Tris-HCl	pH 7.5/8.0/8.5
MES/NaOH	pH 6.0	Borate/NaOH	pH 9.0
PIPES/NaOH	pH 6.5/7.0		

(3) Additives: Troponin complex changes its conformation dependent on external Ca^{2+} concentration, $CaCl_2$ or $MgCl_2$ plus EGTA are added to the reservoir solution to give final concentrations, 5 mM, 10 mM and 1 mM, respectively, in order to keep the structural homogeneity. In some cases, metal ions such as, Cd^{2+}, Mn^{2+}, Zn^{2+} and Cu^{2+} which act as electrostatic crosslinking agents, were used as additives.

In other cases, commercially available crystallization screening kits, such as Crystal Screen and Crystal Screen II (Hampton Research) were used in a primary screening.

X-ray diffraction

Most of X-ray diffraction photographs were recorded using an R-AXIS imaging system mounted on a Rigaku FR rotating anode X-ray generator, and some were recorded at BL-6B, Photon Factory, Tsukuba.

Preparation of thin-sectioned crystals

Preparation of thin-sectioned crystals was performed according to the procedure described by Winkelman *et al.* (1985, 1991) with modification. Small crystals of $Tm_{141-284}$T25kCl complex were washed with reservoir solution and then fixed using 2.5 % (vol./vol.) glutaradehyde in reservoir solution for 30 min. They were then washed three times with distilled water for 5 min, and prestained with 1 % (wt/vol.) osmium tetroxide in 0.1 M potassium/phosphate, pH 7.0 for 1 hour at 0°C. The samples were washed two times with distilled water, then dehydrated by transferring them through increasing concentration steps (50 %, 70 %, 90 %, 99 % and 100 % (vol./vol.), 5 min per step) of ethanol in water. Then, the sample were infiltrated by transferring them through increasing concentration steps (0 %, 50 % and 100 % (vol./vol.), 2 hour per step) of the epon-araldite resin (mixture of 11.3 g of Araldite M, 24 g of DDSA, 12.1 g of Epon 812, and 0.66-0.88 g of DMP 30) in propylene oxide. The samples were polymerized at 60°C for 48 hours. The blocks were cut using a glass knife on ultramicrotome. Sections of ~800 Å thickness, based on interface colors, were picked up on carbon-coated copper grids. The sections were post-stained with 2 % (wt/vol.) aqueous uranyl acetate for 20 min.

RESULTS AND DISCUSSION

(III-1) T2CI complex

Design of the sample for crystallization

T2CI complex (TnT2-TnC-TnI complex) was chosen as one of the first protein samples to be crystallized because it is widely accepted not only that the major function of troponin complex is retained in this portion but also T2CI is likely more globular than intact troponin complex.

Previously, T2 fragment was obtained by a limited chymotryptic digestion of TnT (Ohtsuki, 1979) or Tn complex (Morris and Lehrer, 1984). In this study, an alternative method has been introduced. Rabbit skeletal muscle TnT has two types of isoforms, *i. e.*, α and β, which differ in amino acid sequences near the C-terminus (Fig. 3-1-1). These isoforms arise from alternative splicing of a primary transcript of the TnT gene and are expressed in a tissue-specific and developmentally regulated manner (Medford *et al.*, 1984). Binding affinities for tropomyosin and Ca^{2+} affinity of Ca^{2+}-specific sites of TnC have been shown to be different between α and β isoforms (Pan and Potter, 1992). Notably, β -TnT has only 3 methionine residues, at 70, 151 and 175, in its primary sequence. A mutant β -TnT was prepared in which methionine at 175 is substituted with leucine. By cleaving this mutant TnT with cyanogen bromide T2 fragment (res. 152-259) was obtained. Fig. 3-1-2 summarizes this procedure. Detailed purification procedures will be described in part IV-2. The TnT2 preparations thus prepared are of higher purity than those prepared by the previous methods.

Mutant TnI with three cysteine residues substituted (C48A, C64A, C133S) was also used in this study in order to prevent inter- and/or intramolecular cross-linking (Kluwe *et al.*, 1993). These three cysteine residues may need to be reduced to maintain activity in reconstituted complex (Horwitz *et al.*, 1979). Such an approach to substitute cysteine residues to others have been succeeded in the crystallization of the hepatitis A virus 3C protease (Chernais, *et al.*, 1993).

1 11 21 31 41

SDEEVEHVEE EAQEEAPSPA EVHEPAPEHV VPEEVHEEEK PRPKLTAPKI

|→ 26K

51 61 71 81 91

PEGEKVDFDD IQKKRQNKDL **M**ELQALIDSH FEARKKEEEE LVALKERIEK

||→ 25K

101 111 121 131 141

RRAERAEQQR IRAEKERERQ NRLAEEKARR EEEDAKRRAE EDLKKKKALS

151 161 171 181 191

S**M**GANYSSYL AKADQKRGKK QTARE**M**KKKI LAERRKPLNI DHLSDEKLRD

201 211 221 231 241

(α) I **M**NVRARVE**M**L AKF

KAKELWDTLY QLETDKFEFG EKLKRQKYD SKKAGTT

(β) I TNLRSRIDQA QKH

251

AKGKVGGRWK

Figure 3-1-1. Amino acid sequences of α– and β– TnT. The sequence of the β-type is from Fujita *et al.* (1991). The sequence of the α-type is from Pearlstone *et al.* (1977). 26K denotes a 26kDa fragment of α-TnT described by Ohtsuki *et al.* (1984), while 25K denotes β-TnT(N'-208) (Fujita *et al.*, 1992) used in this study. Methionine residues are underlined.

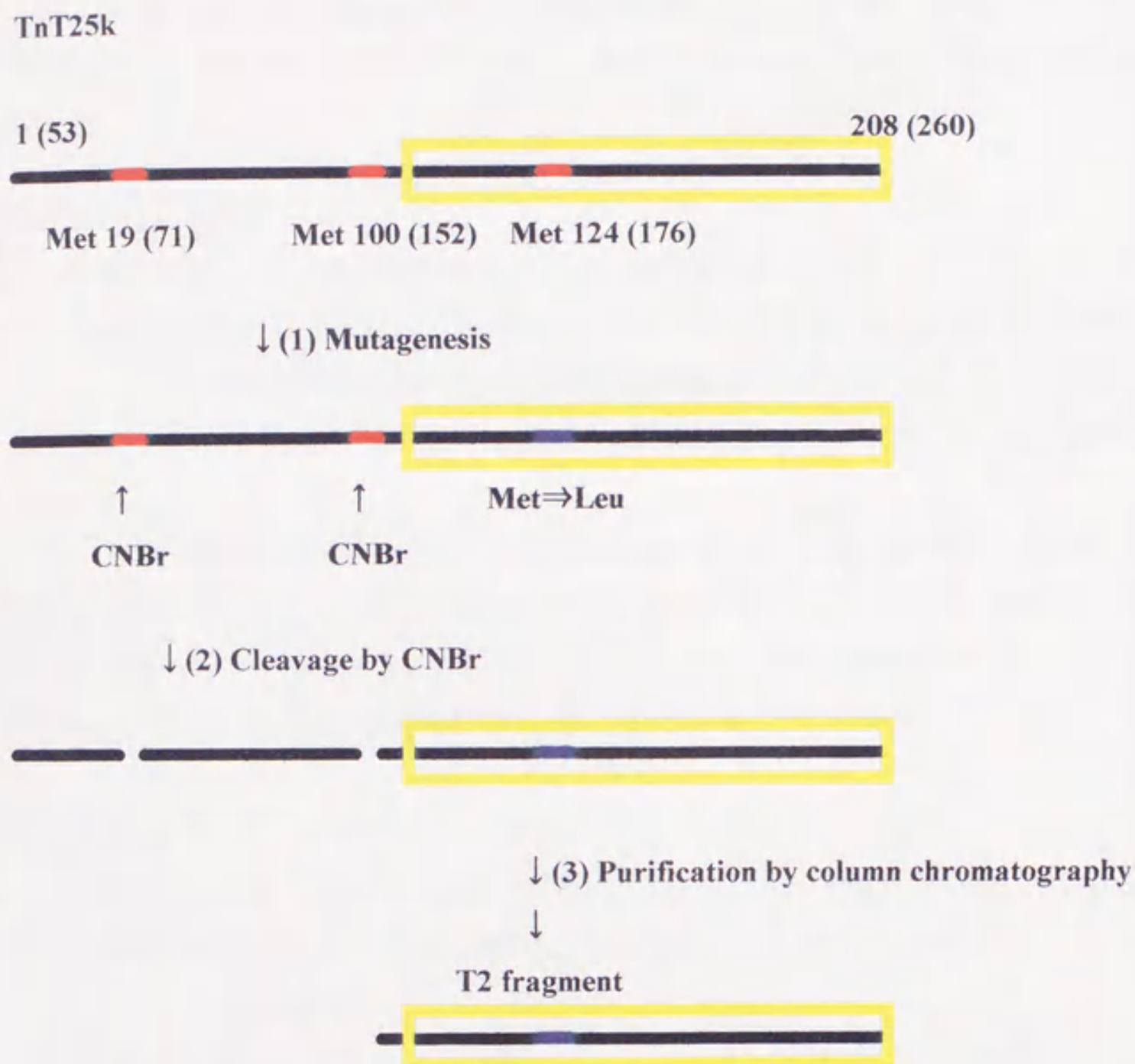

Figure 3-1-2. A schematic description of procedures for obtaining the T2 fragment. The positions of methionine residues are indicated by red segments. TnT2 segment (indicated by a yellow box) was isolated by the following procedures. (1) Methionine residue at 124 of TnT25k was substituted by leucine. (2) This mutant TnT25k was treated with CNBr to cleave at methionine residues. (3) T2 fragment was isolated by column chromatography.

Crystallization of T2CI complex

T2CI complex, which was prepared according to the method described in part IV-2 and was dialyzed against 0.1 M NaCl, was used for primary screening for crystallization conditions. Only in one drop, numbered A09-16, out of 1780 drops, protein crystals appeared. The conditions of A09-16 were as follows.

Conditions of A09-16

Protein solution -13 mg/ml protein in 0.1 M NaCl without buffer

Reservoir solution -0.5 ml of 10 mM Tris-HCl, 10 % polyethylenglycol 4000, 10 mM $MgCl_2$, 1 mM EGTA and 10 mM zinc acetate, pH 8.5.

Drop consists of 1.5 μl of protein solution and 1.5 μl of reservoir solution: Incubated at 16°C

Subsequent investigations have elucidated to know the essential factors that affect crystallization of T2CI complex under these conditions. Eventually, it was found that EGTA and $MgCl_2$ were not necessary for crystallization. The crystals with the identical morphology as the first ones were obtained in the drop, numbered T3-19. The conditions were as follows.

Conditions of T3-19

Protein solution - 15 mg/ml protein in 10 mM Tris-HCl, pH 8.0, 0.1 M NaCl and 1 mM $CaCl_2$.

Reservoir solution - 0.6 ml of 10 mM Tris-HCl, 6 % polyethylenglycol 4000, and 10 mM zinc acetate, pH 8.5.

Drop consists of 2 μl of protein solution and 2 μl of reservoir solution: Incubated at 16°C

As already mentioned, the concentration of calcium ion is an essential factor for crystallization of troponin complex. In the presence of excess amount of zinc ions over EGTA, EGTA in the mother liquor must be saturated with zinc ions. And Ca^{2+} in the protein solution used in A09-16 was just removed by dialyzing the protein solution against the solution without Ca^{2+}. Thus ,the free calcium ions, which were added in the protein solution, must be sufficient to saturate all the four Ca^{2+}-binding sites of troponin complex in the crystals in A09-16. So we concluded that the crystals appeared in both A09-16 and T3-19 are identical. The conditions of the both reservoir solutions and protein solutions which gave a good yield of crystals are summarized as follows.

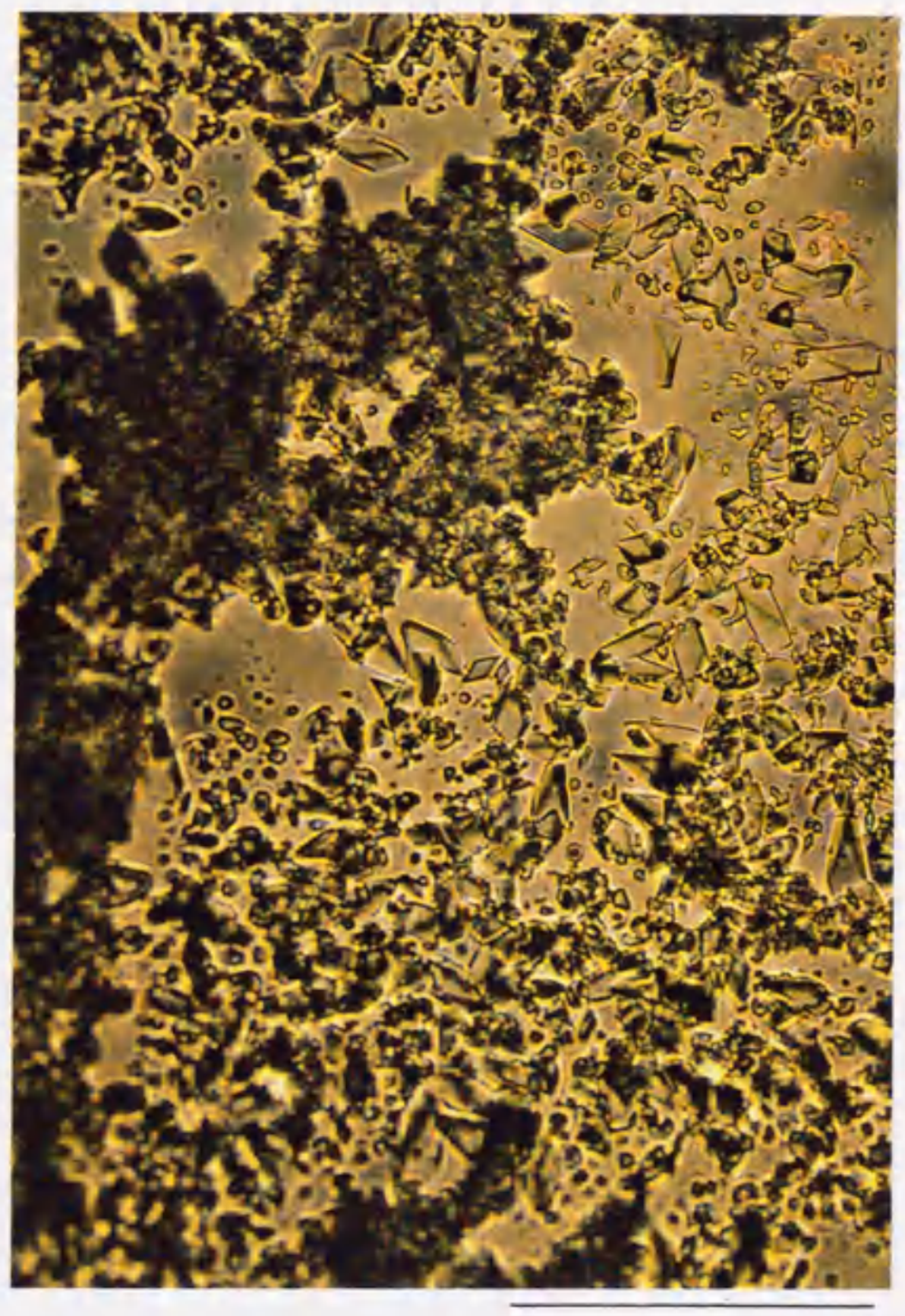

Figure 3-1-3. Gallery of crystals of T2CI complex. Bars are 200 μm.

Optimized conditions

Protein solution - 13-20 mg/ml protein in 0.1 M NaCl, 10 mM Tris-HCl, 1 mM $CaCl_2$, pH 8.0

Reservoir solution - 10 mM Tris-HCl, pH 8.5 containing 2.5-14% polyethleneglycol 4000, 2-10 mM zinc acetate

Drop consists of 2 ml of protein solution and 2 ml of reservoir solution: Incubated at 16°C

Fig. 3-1-3 shows micrographs of T2CI complex crystals obtained under the conditions described above.

The stability of the protein sample was turned out to be crucial for crystallization of T2CI complex. All the protein samples which give rise to crystals were shown to be stable for a long period of storage, whereas, the samples which never produce crystals were shown to be degraded into smaller fragments during a long period of storage (Fig. 3-1-4). As shown in Fig. 3-1-3, degradation obviously occurred in TnI. And comparing the mobility of a newly appeared band in the degraded T2CI complex sample and that of $TnI_{Ca\text{-}frag}$ described in part 1, it was indicated that complexes which were similar to $T2CI_{Ca\text{-}frag}$ complex were accumulated during a long period of storage. Moreover,TnT2 was partly degraded into smaller species, TnT2β1 and TnT2β3. In order to prevent proteolysis, we paid much attention for TnC preparations because proteolytic activity might be associated with TnC preparations. Degraded samples were never crystallized, therefore we checked the integrity of samples before crystallization. Prior to crystallization, we incubated aliquot of samples at 37°C for 2 days, and analyzed them by SDS-PAGE. If the samples still kept their integrity, we used them for crystallization, if not, we did not. We think that this is the best way to avoid waste of time. It was also found that, in a few cases, crystals with different morphology were obtained under almost the same conditions (Fig. 3-1-5). But this form of crystals have not been characterized by X-ray.

Although nearly one thousand of drops were set up under the optimized conditions described above, only in 33 drops (~3 % of the total drops) we got crystals and only in 2 drops (~0.2 % of the total drops) relatively large size of crystals (150-500 μm) were grown. It turned out to be vary difficult to improve this situation. Because protein crystals always grow in supersaturated solutions, it is obviously important to known the phase diagram of the protein in the solution. Although we have paid a lot of efforts to obtain the relationship between the concentrations of the precipitants (in this case, polyethyleneglycol 4000 and zinc acetate) and the solubility of T2CI complex, we have not yet found out any relationship. Independent to concentrations of polyethyleneglycoly 4000 (2.5-14%) and zinc acetate (0.1-10 mM), some drops gave rise to crystals and the other drops formed amorphous precipitant (Fig. 3-1-6).

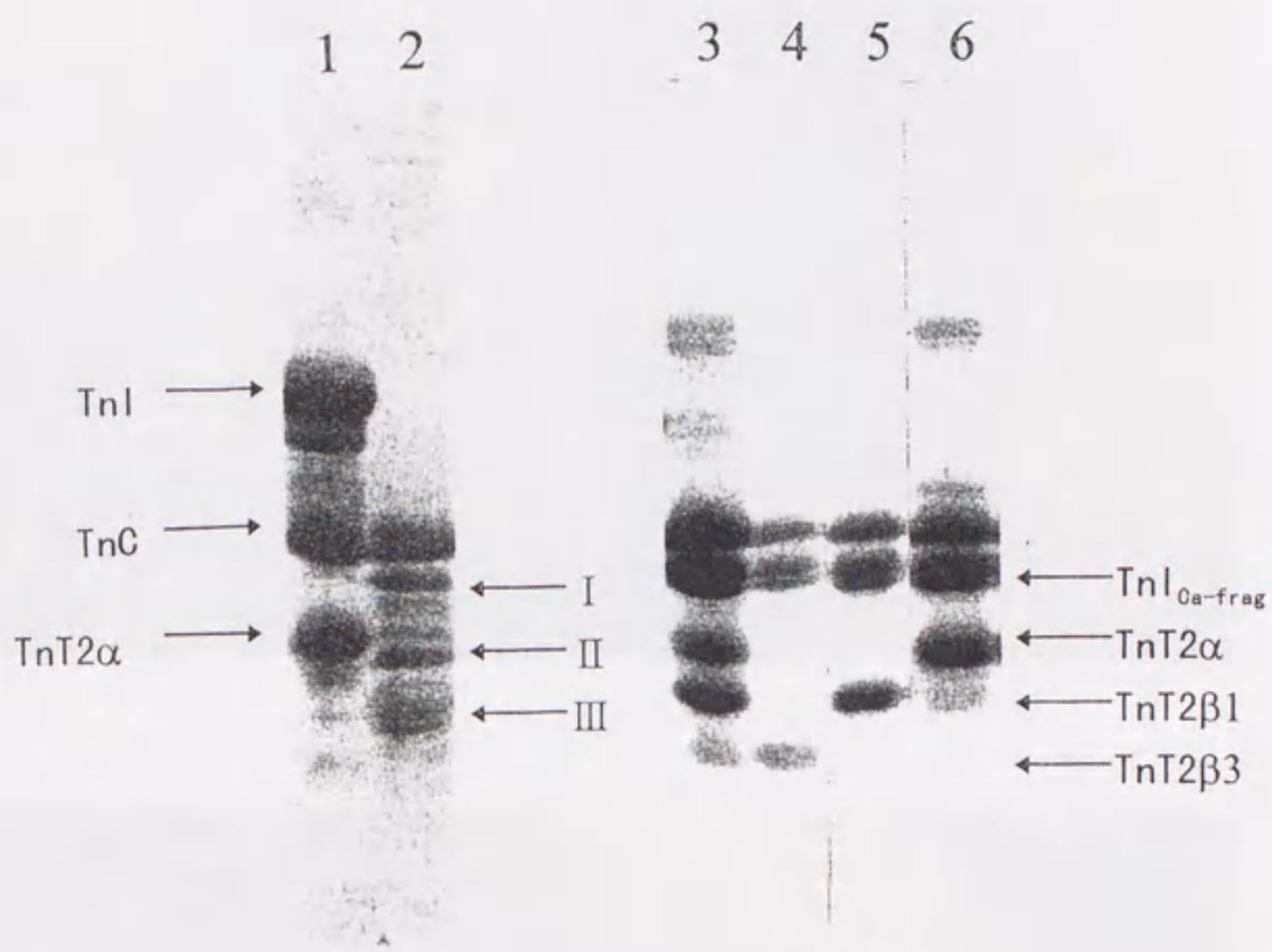

Figure 3-1-4. Degradation of T2CI complex during a long period of storage. Stability of samples that were used in crystallization trials were analyzed by SDS-PAGE after ~10 months storage at 4°C. Lane 1, a protein sample that gave rise to crystals. Lane 2, a protein sample that did not produce crystals. Newly appeared bands (I~III in lane 2) were compared with the bands which were produced by a limited chymotryptic digestion of T2CI complex. A mixture of digestion products (Lane 3) were separated into major three species by Mono-Q column (Lane 4~6). Note that, band I shows almost the same mobility as that of $TnI_{Ca\text{-}frag}$, while band II and III show similar mobilities as those of TnT2β1 and TnT2β3, respectively.

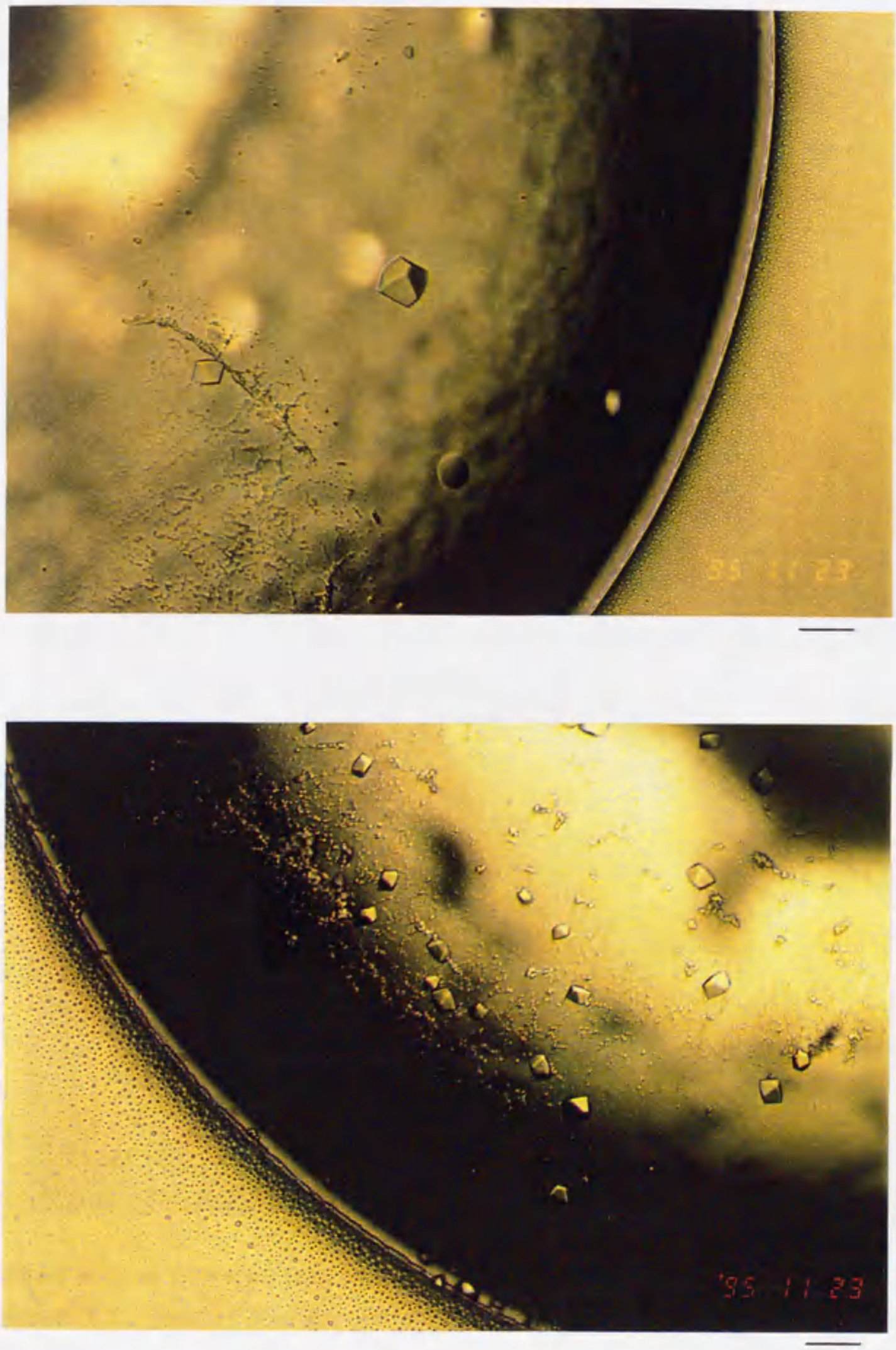

Figure 3-1-5. Crystals of T2CI complex with different morphology. These crystals were obtained under almost the identical conditions as those represented in Fig. 3-1-3. Bars are 100 μm.

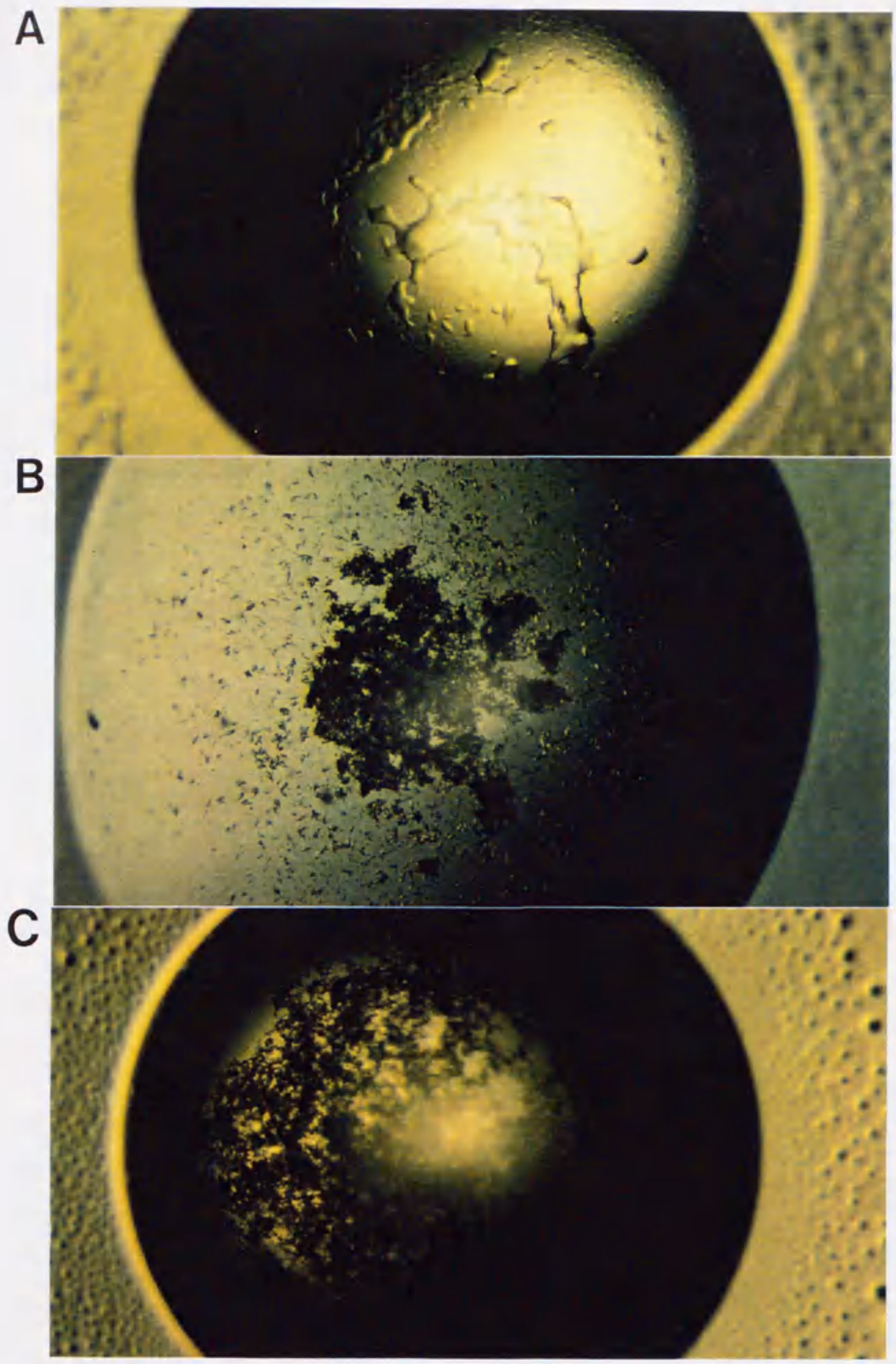

Figure 3-1-6. Some are crystallized and some are amorphously precipitated under the identical conditions. T2CI complex was allowed to be crystallized under the conditions as follows. The protein solution, 13 mg/ml T2CI complex in 0.1 M NaCl, 10 mM Tris-HCl, 1 mM $CaCl_2$, pH 8.0. Reservoir solution, 10 mM Tris-HCl, pH 8.5, 4 % polyethyleneglycol 4000, 2 mM zinc acetate. Under these conditions, protein in a drop precipitated in one of three different ways typified in A~C. A, C, amorphous precipitants. B, small crystals. Bars are 0.5 mm.

X-ray diffraction pattern of T2CI complex crystals

Crystals from independent two drops were used for diffraction analysis. In a drop, numbered T29-14, crystals nearly 0.5 mm long were obtained. These crystals appeared in 1 week after setting up, and continued to grow to its maximum size in 1 month (Fig. 3-1-7A, B). Although they had regular faces and sharp edges and their size might be sufficient for diffraction analysis, when they were exposed to X-ray, all of them showed only poor diffraction patterns (data not shown). We do not know if the crystals were poorly ordered from the beginning, damaged by handling, or damaged by exposure to the X-ray beam. In another drop, numbered T8-1, crystals 150 μm long were obtained. These crystals appeared in 5 days after setting up, and continued to grow to their maximum size in 1 month (Fig. 3-1-7 C, D). Compared to the crystals in T29-14, the crystals in T8-1 had neither sharp edges nor regular faces. Nevertheless, the X-ray diffraction pattern from one of these crystals was obtained by using the synchrotron radiation (Fig. 3-1-8). A preliminary analysis indicated that the crystal belongs to the trigonal space group $P3_112/P3_212$ with cell dimensions a=b=54 Å, c=250 Å. Diffraction was extended to about 8 Å resolution.

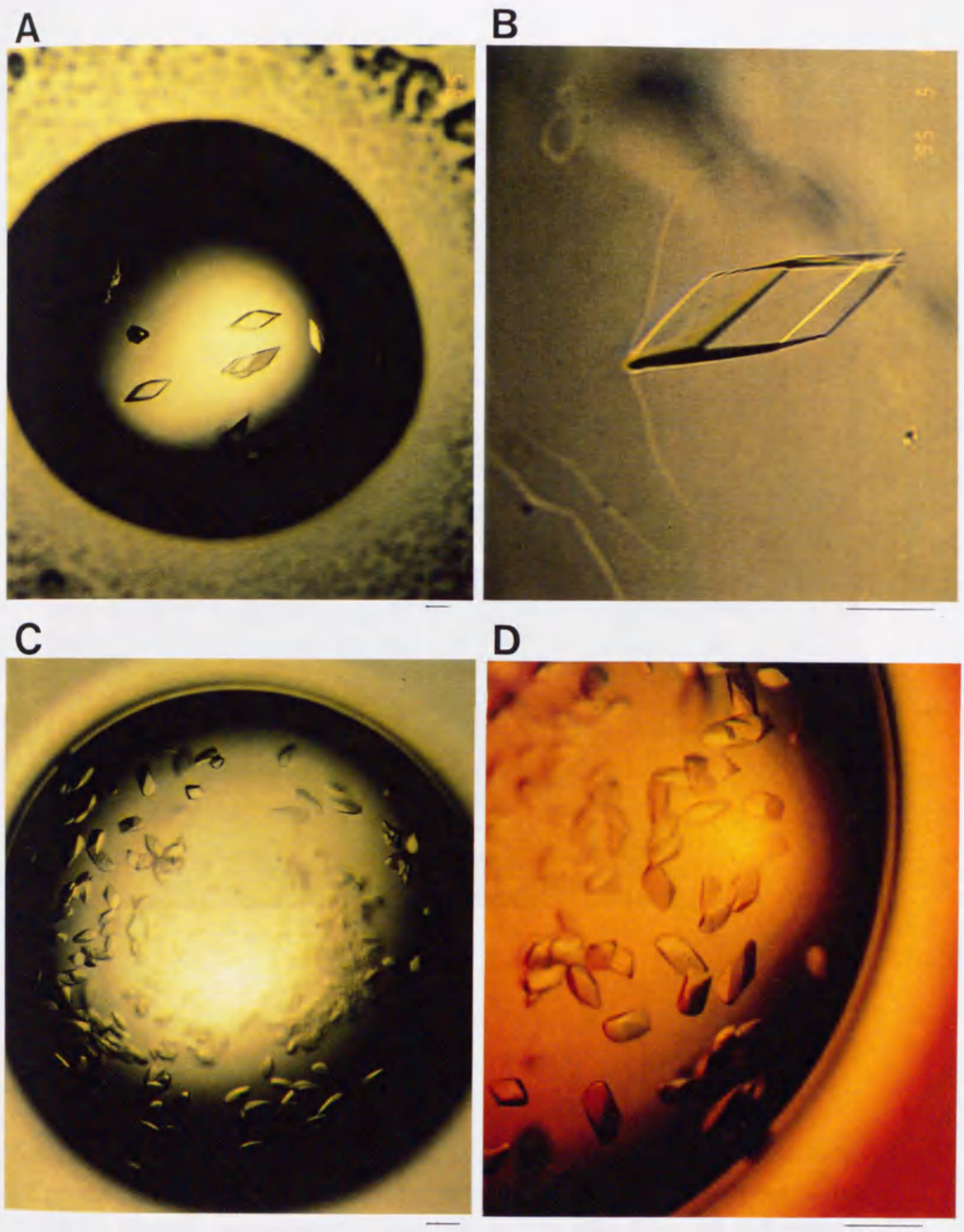

Figure 3-1-7. Crystals used for diffraction analysis. Crystals grown in the independent two drops were shown (AB and CD). Bars are 200 μm.

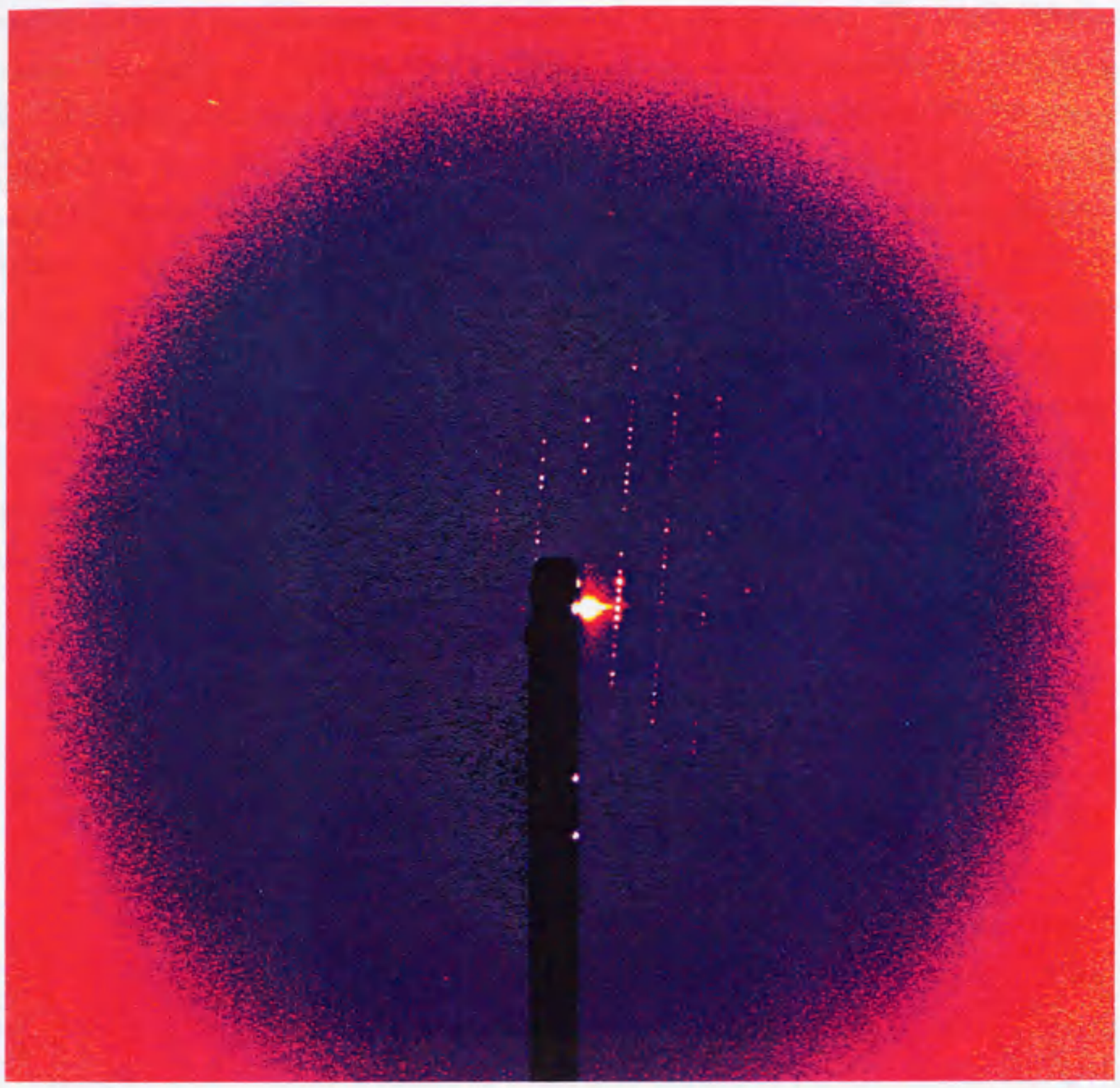

Figure 3-1-8. An oscillation photographs of the crystal of T2CI complex. A crystal shown in Fig. 3-1-7 A was used for diffraction analysis. The photograph was taken at BL-6A (Photon Factory, Tsukuba). Diffraction spots are observed beyond 8 Å resolution along c*-axis, and 10 Å resolution perpendicular to the c*-axis. Oscillation angle, 6.5 deg. Exposure time for 260 sec. The crystal to detector distance was 430 mm. $\lambda = 1$ Å.

Further possibilities

Poor diffraction would be improved by optimizing the crystallization conditions, employing cryocrystallography, *etc*. In the case of TnC-TnI_{1-47} complex crystals (described in part III-3), we could succeed in improving the diffraction quality in the consequence of such attempts. Zinc ions are indispensable for crystallization of T2CI complex, indicating zinc ions might act as electrostatic cross-linker within the crystal lattice. Different divalent cations in the mother liquor give rise to different crystal forms of LIVBP-leucine complex protein (Trakhanov *et al.*, 1995). The addition of different divalent cations to T2CI complex might give rise to better crystals. To change protein source sometimes results in producing better crystals. For example, crystals of TnC from rabbit skeletal muscle diffracted only to 8-10Å resolution and were unstable under X-ray irradiation (Mercola *et al.*, 1975), while those from chicken and turkey diffracted beyond 2.5 Å resolution and stable for X-ray irradiation (Strasburg *et al.*, 1980; Herzberg *et al.*, 1984). So T2CI complex from other sources may give rise to better crystals. There are many things remain to be tried.

⟨III-2⟩ $Tm_{141-284}$T25kCI complex

Design of the sample for crystallization

Native tropomyosin (Ebashi and Endo, 1968), *i. e.*, the complex of troponin and tropomyosin, must retain more physiological significance than the isolated troponin complex. Although the atomic structure of native tropomyosin is highly desirable, and crystals of native tropomyosin have been reported for more than two decades (Higashi and Ooi, 1968), high resolution analysis has not been succeeded yet. The physico-chemical properties, especially high viscosity of native tropomyosin itself pose serious problem in crystallization. Therefore $Tm_{141-284}$T25kCI complex has been designed in order to improve the likelihood of obtaining crystals of native tropomyosin. Unlike native tropomyosin, this complex can not polymerize because of the lack of the N-C overlap of tropomyosin.

Firstly, A troponin complex was designed which is suitable for co-crystallization with tropomyosin. It has been shown that 26kD fragment of TnT, which is produced by endogenous protease in muscle, retains physiologically essential properties of TnT (Ohtsuki *et al.*, 1984). Moreover, it was shown that this TnT fragment more strongly binds to immobilized tropomyosin both in the presence and in the absence of other Tn components (Pan *et al.*, 1991). It is also suggested that the first 45 residues of TnT are not essential for anchoring the troponin complex to the thin filament and do not play an essential role in the cooperative response of regulated acto-S1 ATPase to Ca^{2+} (Pan *et al.*, 1991). In the present study, *E. coli* expressed 25kD fragment of TnT (T25k), which has shown to have almost the same properties as 26kD fragment (Fujita *et al.*, 1992), has been used in the place of TnT to reconstitute a ternary troponin complex.

Secondly, a truncated tropomyosin was designed based on previous findings as follows. Although there have not yet been obtained clear evidences that show where troponin binds on the tropomyosin strand under the physiological conditions, it has been suggested that N-terminus of TnT spans the head-to-tail joint of the tropomyosin filament, and the globular "head" region of the whole troponin complex binds ~200Å away near residues 150-180 of the tropomyosin molecule (White *et al.*, 1987). Previously, a variety of large fragments of tropomyosin have been prepared either by limited proteolysis or by chemical cleavage procedures at the methionine residues and at the single cysteine residue to investigate the interactions between troponin and tropomyosin. The experiments indicated that all fragments encompassing residues 190-284 showed interaction with TnT on the affinity column (Pato *et al.*, 1981). Although these results would reflect some part of physiological significance, they should be treated with caution because fragments very often show different properties from the native molecules (Ohtsuki *et al.*, 1986). Although we prepared several kinds of tropomyosin fragments, encompassing residues 190-284, as described by Pato *et al.* (1981), none of

obtained fragments were pure enough for crystallization. So we decided to express the fragment in *E.coli*. Eventually, It was found that the tropomyosin expressed in *E. coli* (Kluwe *et al.*, 1995) contains a smaller fragment which turned out to be an internal-start product of translation, corresponding to residues 142-284. By constructing an expression vector, $Tm_{141-284}$ fragment was obtained in good quantity and high purity. The fragment can be too long for troponin binding, but at least, it must contain the entire part of the troponin binding site.

It has been shown that these troponin and tropomyosin components can make a complex which is suitable for crystallization trials (for preparations, see part IV-4).

Crystallization of $Tm_{141-284}$T25kCI complex

In the case of $Tm_{141-284}$T25kCI complex, 330 different crystallization conditions were tested as primary screening. In 10 drops (~3% of the total drops), crystals which had almost identical morphology were appeared (Fig. 3-2-1). The conditions of 6 drops were summarized as follows;

Protein solution - 10 mg/ml protein in 10 mM Tris-HCl, 5 mM $MgCl_2$, 1 mM EGTA, pH 8.0
Reservoir solution - 0.5 ml of 20-30% MPD, 50 mM either of Good buffers (PIPES/NaOH, pH 6.5-7.0, Hepes/NaOH, pH 7.5, Tris-HCl, pH 8.0), 10 mM $CaCl_2$
Each drop consists of 1.5 µl of protein solution and 1.5 µl of reservoir solution: Incubated at 16°C

The conditions of other 4 drops were as follows;

Protein solution - 10 mg/ml protein in 10 mM Tris-HCl, 5 mM $MgCl_2$, 1 mM EGTA, pH 8.0
Reservoir solution - 0.5 ml of 20-30% MPD, 50 mM either of Good buffers (Mes/NaOH, pH 6.0, PIPES/NaOH, pH 6.5-7.0, Hepes/NaOH, pH 7.5)
Each drop consists of 1.5 µl of protein solution and 1.5 µl of reservoir solution: Incubated at 16°C

These two sets of conditions are almost identical except for the following two points; (1) In the former condition, 10 mM $CaCl_2$ was added in the reservoir solution. (2) In the former condition, pH was adjusted between 6.0 and 7.0, whereas in the latter condition, pH was between 6.5 and 7.5. The concentration of Ca^{2+} in the drop must affect the conformational state of $Tm_{141-284}$T25kCI complex. Therefore the conformation of the complex within the crystal is likely dependent on the Ca^{2+} concentrations. Moreover pH, by itself and by altering the affinity of troponin complex for Ca^{2+}, would alter the conformation of the complex. Although, we do not know the conformation of the molecule until the structure itself is solved.

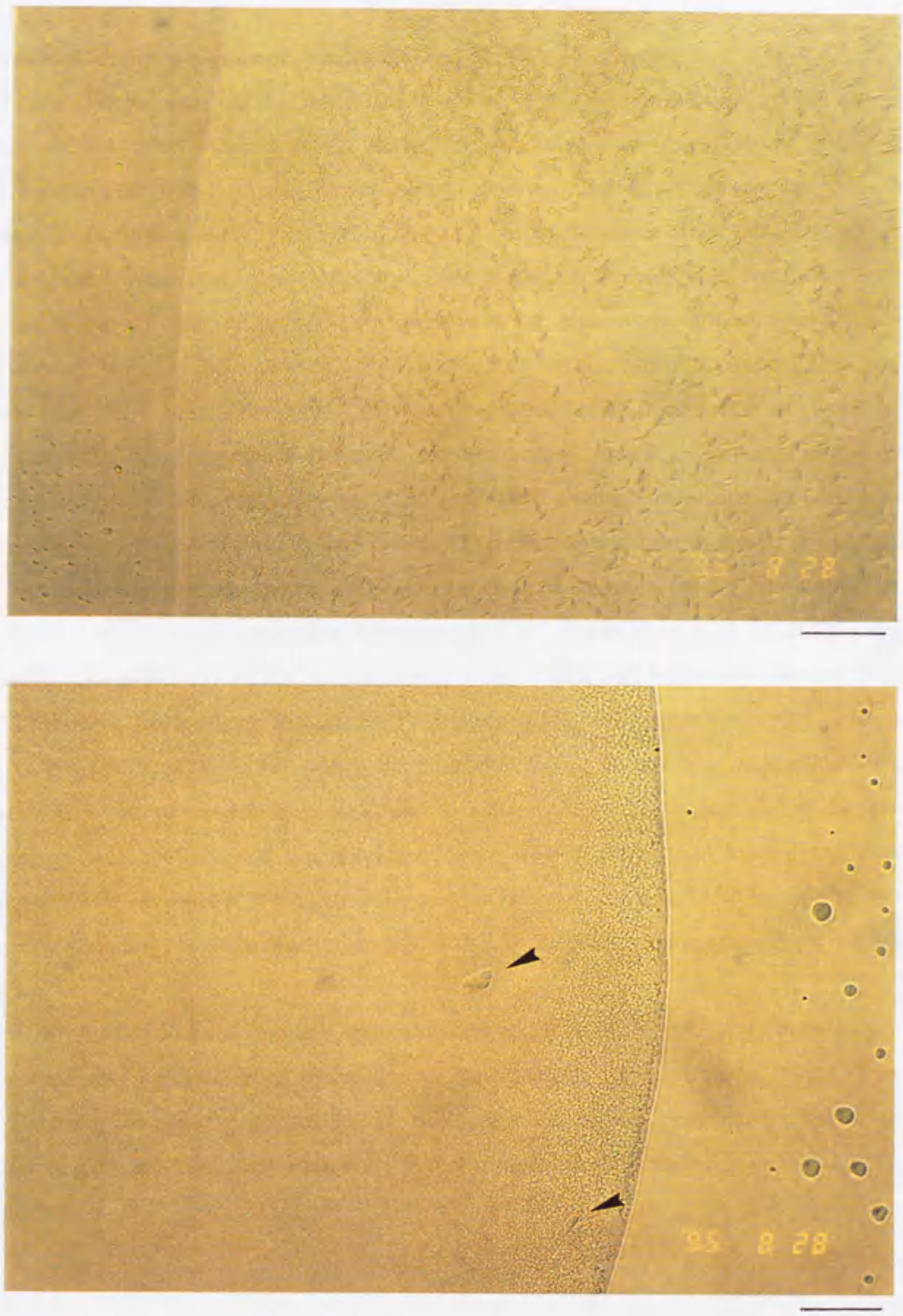

Figure 3-2-1. Crystals of $Tm_{141-284}$T25kCI complex. The conditions for obtaining the crystals were as follows. The wells contained 0.5 ml solution of 30 % MPD (2-methyl-2, 4-pentanediol) in a mixture of 10 mM $CaCl_2$ and 50 mM Tris-HCl, pH 8.0. The drop on the coverslip suspended over the well was made by mixing 1.5 μl of 10 mg/ml of the protein solution and 1.5 μl of the solution in the well. Bars are 30 μm.

EM observation of thin-sectioned crystals of $Tm_{141-284}$T25kCI complex

Because the crystals were not large enough for X-ray analysis, thin-sections of the crystals were made for electron microscopic analysis. Image analysis of electron micrographs of thin-sectioned myosin subfragment-1 (S1) crystals were used to determine the shape of myosin head at ~25 Å resolution (Winkelmann *et al.*, 1991) before an atomic model was obtained (Rayment *et al.*, 1993). In that case, the crystals was large enough for X-ray diffraction analysis, but poor diffraction (~4.5 Å resolution in the still photographs) was an obstacle for high resolution analysis (Rayment and Winkelmann, 1984). We have adopted a similar approach for analysis of crystals of $Tm_{141-284}$T25kCI complex. Fig. 3-2-2 represents typical electron micrographs of thin-section of $Tm_{141-284}$T25kCI complex crystals. A micrograph image of a macromolecular crystal is composed of the individual images of many crystallographically identical unit cells arranged in a specific two dimensional periodic array and projected onto a single plane. By further application of digital or optical filtering techniques to micrographs of crystals, shape and structure of the molecule can be obtained as with an X-ray study at a comparable resolution. Although we have tried to apply such techniques to obtained EM images, it was found that the obtained images were not good enough for further analysis. An optical diffraction pattern from the one of the images in Fig. 3-2-2 represents only poor resolution (~100 Å). It might be possible that during the process of fixing, embedding, sectioning, and staining, the packing of the molecules was destroyed to some extent. Especially, during the process of sectioning it was obvious that the specimens were little bit deformed toward the direction of sectioning. While attempts of structural analysis of crystals of $Tm_{141-284}$T25kCI complex by electron microscopy and image analysis was unsuccessful, it was revealed that the crystals are really made up proteins.

So far this form of crystal has never exceeded 20 mm in size, trials to grow larger crystals suitable for X-ray analysis being unsuccessful. Nevertheless, there are many things remain to be tried. Because structural information of this complex would give us important clues for understanding the mechanism of regulation, farther efforts should be spend to grow larger crystals of this complex.

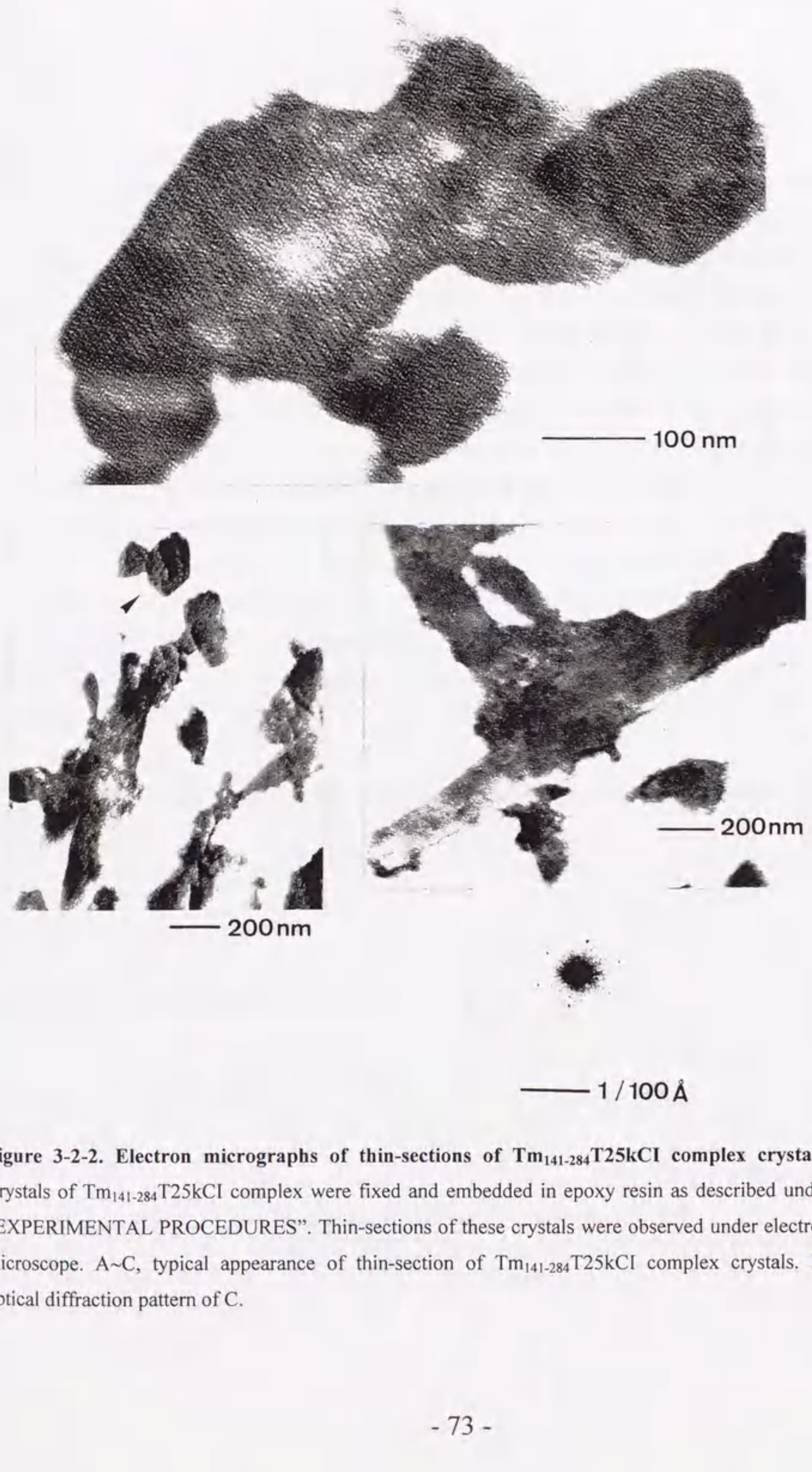

Figure 3-2-2. Electron micrographs of thin-sections of $Tm_{141-284}$T25kCI complex crystals. Crystals of $Tm_{141-284}$T25kCI complex were fixed and embedded in epoxy resin as described under "EXPERIMENTAL PROCEDURES". Thin-sections of these crystals were observed under electron microscope. A~C, typical appearance of thin-section of $Tm_{141-284}$T25kCI complex crystals. D, optical diffraction pattern of C.

⟨III-3⟩ CI_{1-47} complex

Design of the sample for crystallization

It has been shown that N-terminal region of TnI interacts with C-terminal domain of TnC. Krudy *et al.* (1994) described that cardiac TnI was cleaved into smaller fragments during the NMR measurement of TnC-TnI complex. They assigned the fragment bound to TnC as residues 33-80 that was almost corresponding to N-terminal residues 1-47 of skeletal TnI. Their result suggests that N-terminal region of TnI is resistant to proteolytic digestion, forming structural core domain within the TnC-TnI binary complex. We also noticed that some preparations of TnI-TnC binary complex, which were used for crystallization trials, were degraded into smaller complexes after a long period of storage ("aged" preparation), and this smaller complexes consist of TnC and N-terminal fragment of TnI (Fig. 3-3-1, Table 3-3-1). Moreover, it was also found that the complexes of TnC and the N-terminal fragment of TnI is produced by prolonged chymotryptic digestion of Tn complex (Fig. 3-3-1, Table 3-3-1). The results obtained from experiments using synthetic peptide (Ngai and Hodges, 1992) and deletion mutant TnI (Sheng *et al.*, 1992; Potter *et al.*, 1995) are also consistent with the suggestion. Later, properties of these TnI fragments will be described in detail. Because a stable complex often gives rise to good crystals, this complex was chosen as a target complex to be crystallized.

Table 3-3-1. N-terminal fragments of TnI produced upon different conditions

	Residues	Mass of MH[+] observed	calculated
Fragments produced by prolonged chymotryptic digestion of Tn complex			
	Ac-1 - 43	5126.7	5126.1
	Ac-1 - 44	5239.9	5239.1
Fragments produced in the crystallization sample after long period of storage			
	1 - 40	4679.3	4677.8
	1 - 41	4807.4	4908.3
	1 - 42	4921.5	4922.0
Fragments produced by chemical cleavage of mutant TnI at single cystaine residue			
	1-47	5535.2	5533.5
	1-48	5638.3	5636.8

Troponin I

Cleavage with NTCB

↓

1

GDEEKRNRA ITARRQHLKSV MLQIAATELE KEEGRREAEK QNYLAEHCPP

- -

1 **40 41 42**

— - - — - - — - - — - - — - - — - - — - - — - - — - -

1 **43 44**

———

1 **47 48**

51

LSLPGSMAEV QELCKQLHAK IDAAEEEKYD MEIKVQKSSK ELEDMNQKLF

→A

101

DLRGKFKRPP LRRVRMSADA MLKALLGSKH KVCMDLRANL KQVKKEDTEK

→S

151

ERDLRDVGDW RKNIEEKSGM EGRKKMFESE S

- - - - - - - Fragments produced in the "aged" TnC-TnI complex

— - — - — Fragments produced by prolonged chymotryptic digestion of Tn ternary complex

——————— Fragments produced by chemical cleavage of mutant TnI at a single Cys-48

Figure 3-3-1. N-terminal fragments of Troponin I produced under different conditions.

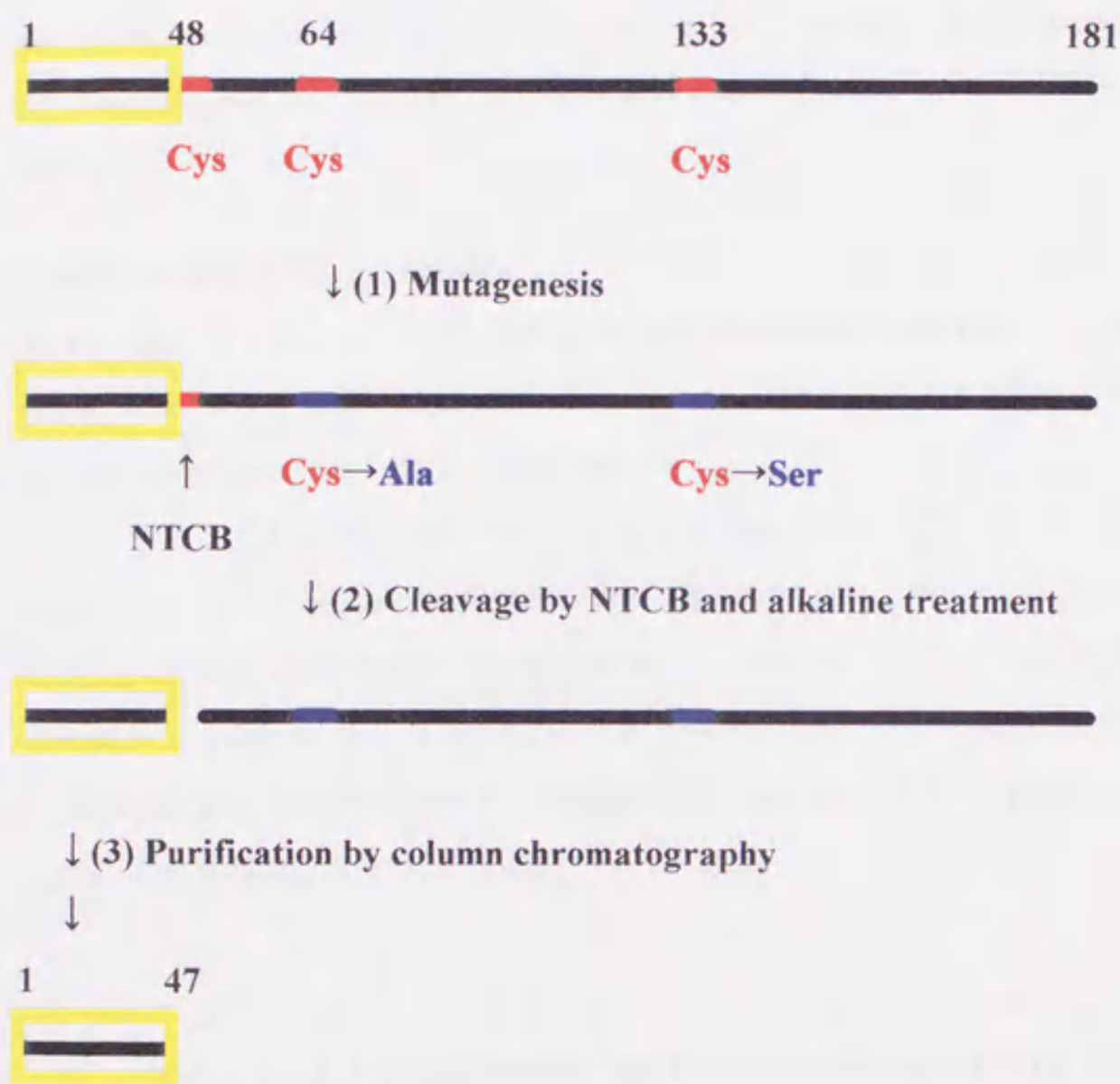

Figure 3-3-2. Summary of isolation procedure for TnI_{1-47} fragment. Amino acid sequence of rabbit skeletal muscle TnI was schematically represented. The positions of cysteine residues are indicated by red segments. TnI_{1-47} segment (indicated by a yellow box) was isolated as following procedure. (1) Cysteine residues at 64 and 133 of TnI were substituted by alanine and serine, respectively. (2) This mutant TnI was treated with NTCB to cleave at the cysteine residue. (3) TnI_{1-47} fragment was isolated by column chromatography.

In order to obtain the homologous preparation of N-terminal fragment of TnI, a mutant TnI which has a single cystaine residue at 48 was used. By chemically cleaving this mutant TnI with NTCB, N-terminal 1-47 fragment could be obtained (the procedure is summarized in Fig. 3-3-2, and details of preparation procedure were described in part IV-3). On the contrary to my prediction, two species of fragments (res. 1-47 and res. 1-48) were produced under this condition (Table 3-3-1) and we could not isolate one species from each other. Therefore our preparation of CI_{1-47} complex was not homogenous. Nevertheless crystal were obtained under several different conditions as described below.

Crystallization of CI_{1-47} complex

In the case of CI_{1-47} complex, 260 different conditions were tested as a primary screening. It was found that two groups of precipitating agents effectively crystallized CI_{1-47} complex. These two groups are typified by sodium citrate and MPD.

1.2-1.4 M Sodium citrate which is buffered at pH 7-8 crystallized CI_{1-47} complex. The crystals of different morphologies were obtained under almost identical conditions (Fig. 3-3-1). Other salts such as sodium or potassium tertrate, potassium or ammonium citrate also crystallized the complex in a similar way. Under these conditions, rombohedral crystals or rod-shaped crystals with a hexagonal cross-section were most abundantly obtained. In most cases, crystals appeared within 1-2 week after hanging drop was made.

Table 3-3-2. Organic solvents or polymers effectively crystallized CI_{1-47} complex

Precipitants	Effective conc.	pH	Morphology of crystals
MPD/2, 5-Hexandiol	18-30 %	6-8	rhombic plate at low conc.
			regular octahedron at high conc.
PEG4000/8000	6-15 %	5-6	needle
		6-8	rhombic plate
PEG200/400	10-25 %	7-8	regular octahedron
Ethanol	16-20 %	8	rhombic plate
DMSO	25-40 %	8	rhombic plate at low conc.
			regular octahedron at high conc.

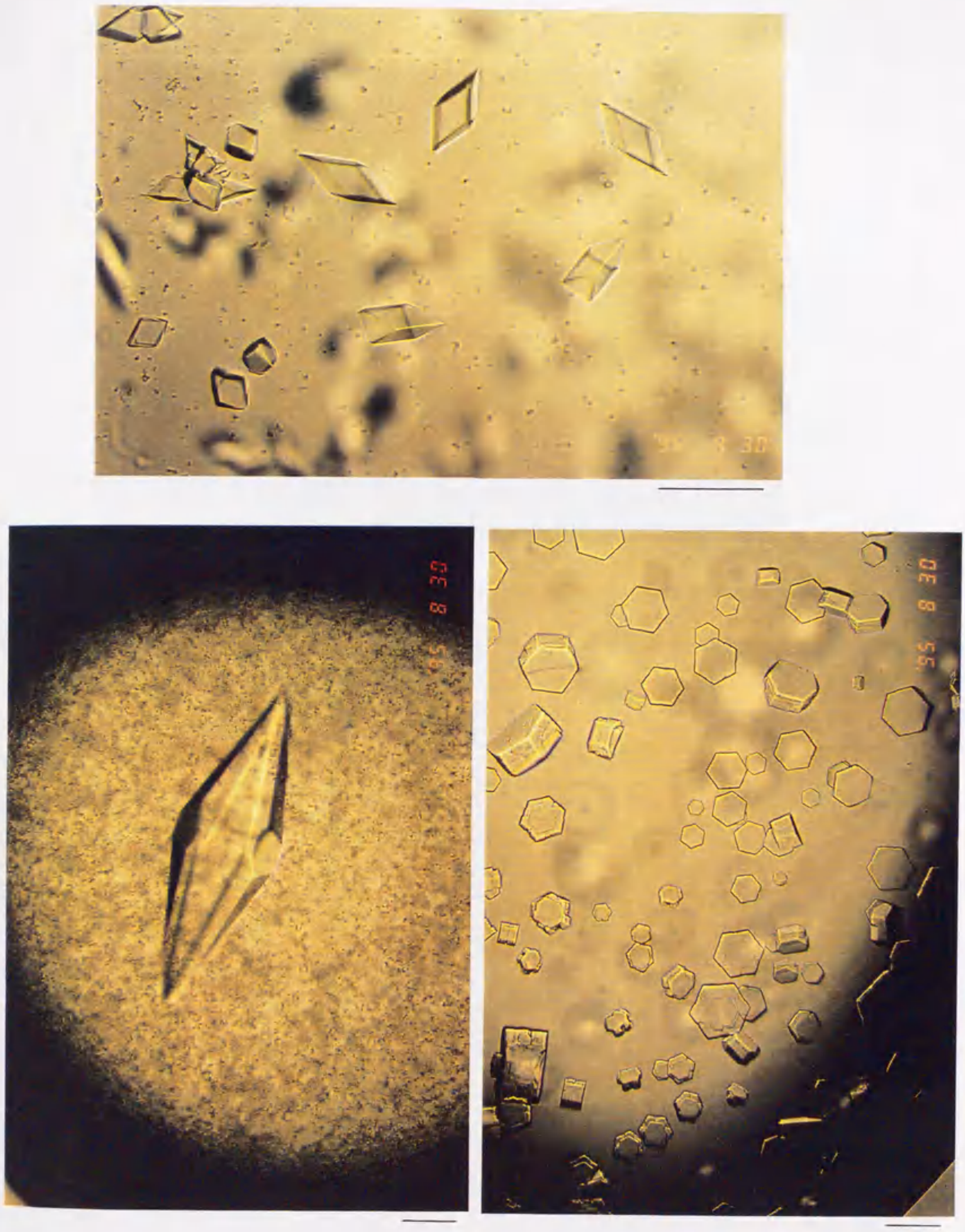

Figure 3-3-3. Gallery of photographs of crystals from CI_{1-47} complex grown in the presence of 1.4 M sodium citrate and 0.1 M Tris-HCl, pH 8.0. Bars are 200 μm.

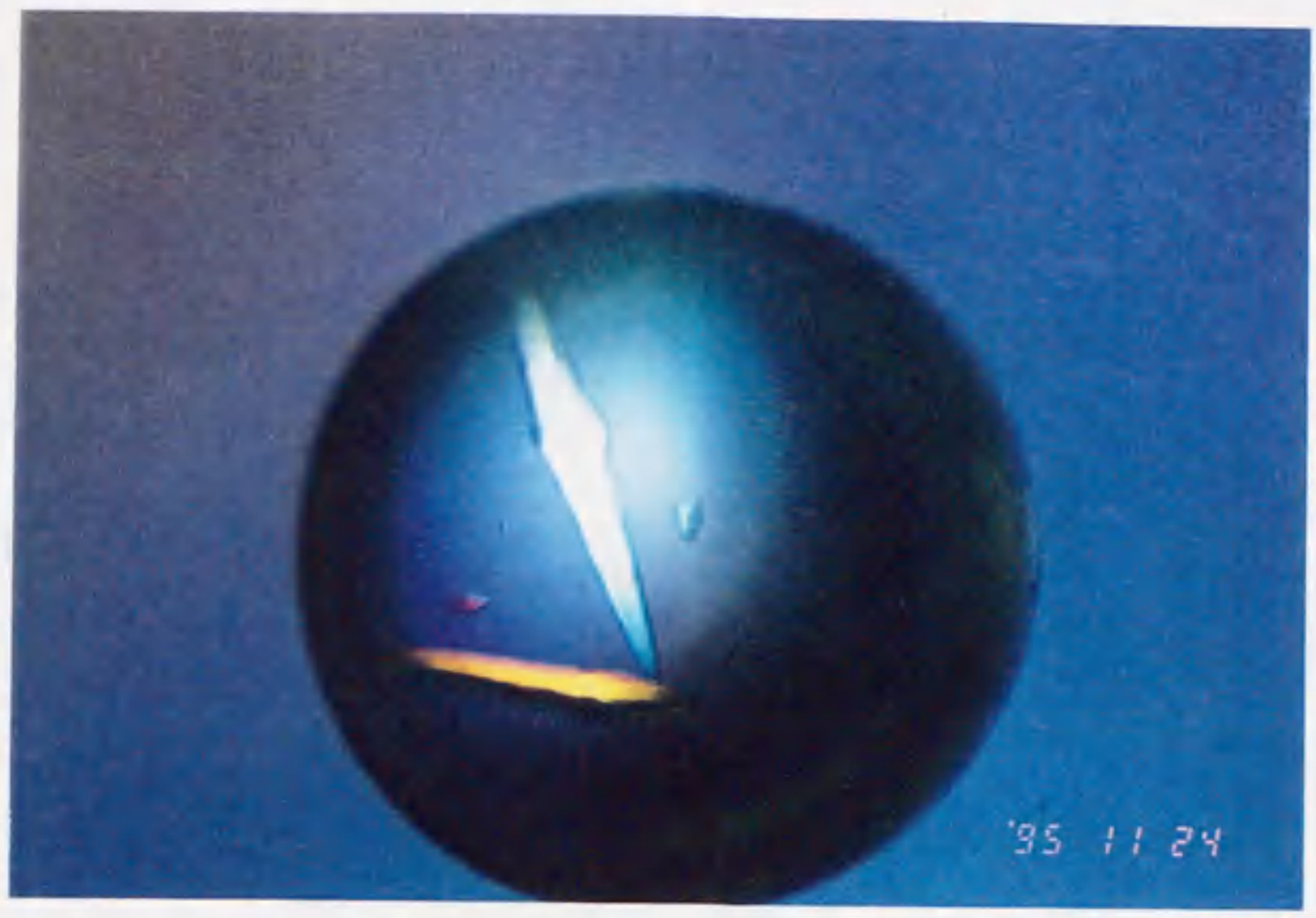

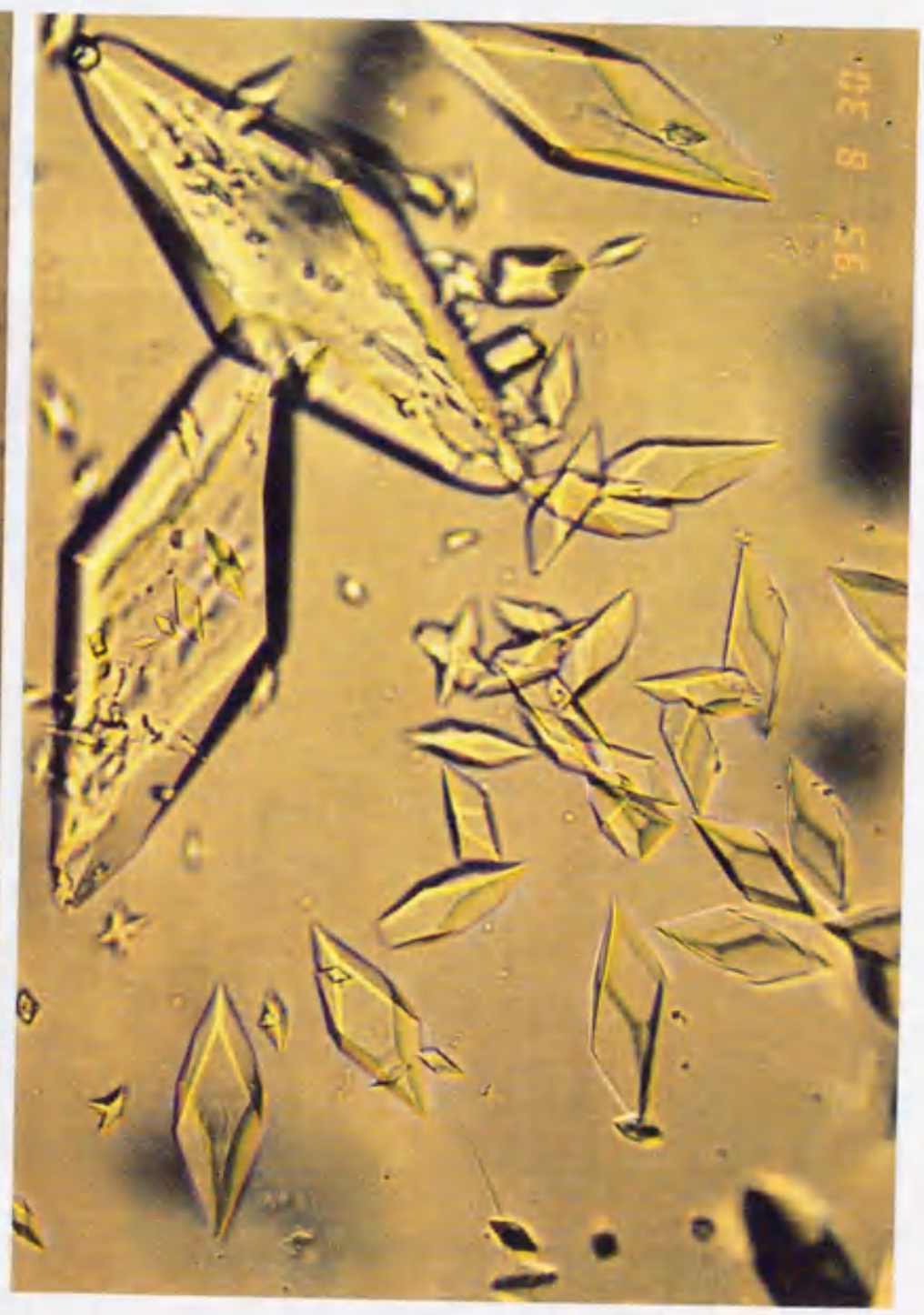

Figure 3-3-3. Continued.

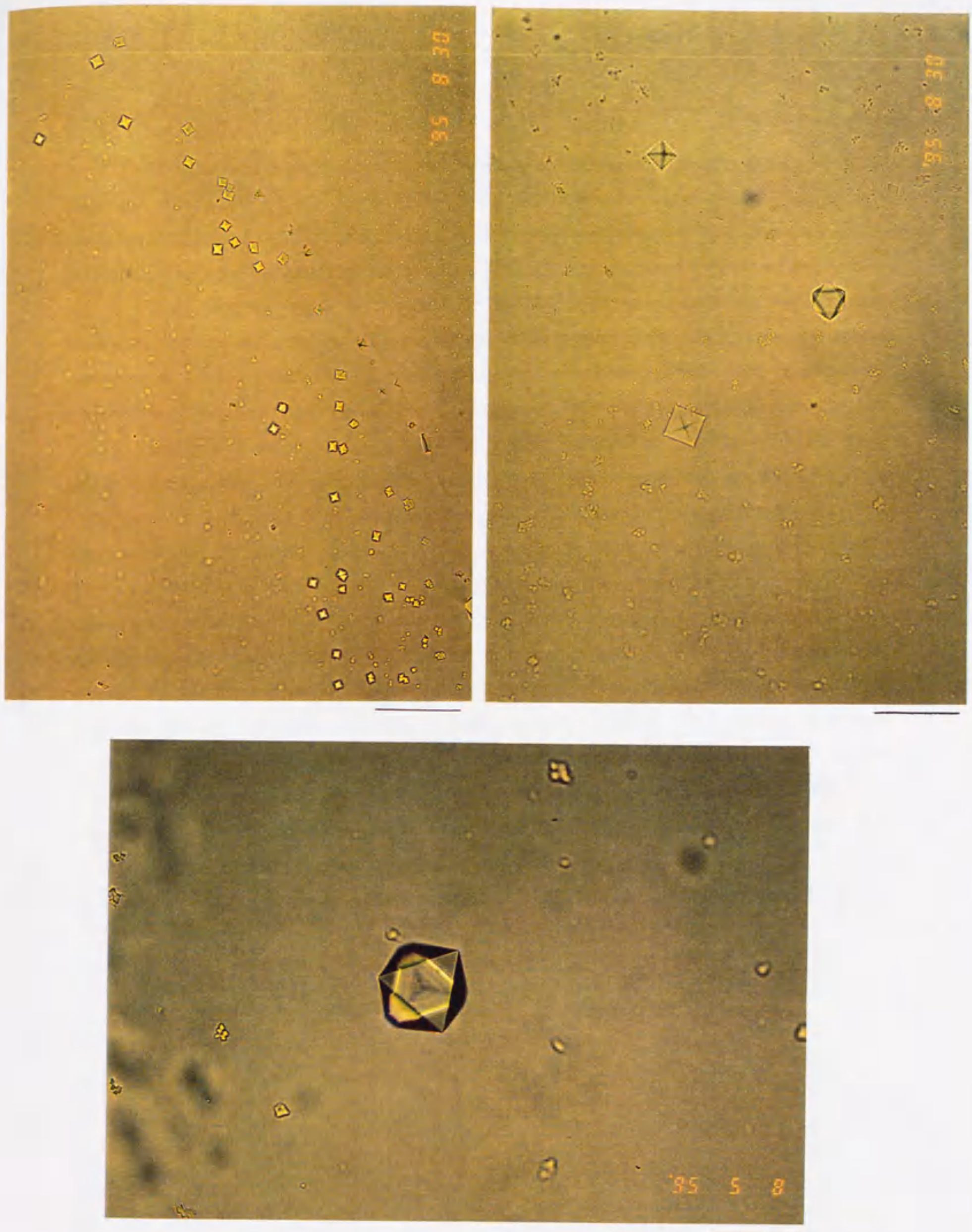

Figure 3-3-4. Gallery of photographs of crystals from CI_{1-47} complex obtained in the presence of 20 % MPD (2-methyl-2, 4-penthanediol), 5 mM $CaCl_2$ and 10 mM Tris-HCl, pH 8.0. Bars are 100 μm

Some organic solvents or polymers effectively crystallized this complex (Table 3-3-2). In each case, at least 5 mM $CaCl_2$ was contained in the drop, and without adding $CaCl_2$, few crystals were obtained. Among organic solvents tested, MPD was the most effective agent to crystallize CI_{1-47} complex. Fig. 3-3-4 represents typical crystals of CI_{1-47} complex grown in a MPD solution.

Comparing two types of crystals, *i. e.*, typified by citrate-crystals and MPD-crystals, interesting features are noted as follows. Firstly, citrate-crystals were rather easily crystallized compared to MPD-crystals. Out of more than 10 protein samples which were independently prepared, only two gave rise to crystals in the presence of MPD, while all samples except only one readily crystallized by sodium citrate. It would be possible that MPD-crystals requires higher purity and/or better structural homogeneity of the protein sample than citrate-crystals do. Secondly, CI_{1-47} complex was also prepared from TnI_{1-47} fragment and TnC extracted from the rabbit muscle. Here, for convenience, the complex containing *E. coli* expressed TnC and the complex containing rabbit TnC are referred to as R-CI_{1-47} and E-CI_{1-47} complex, respectively. It was found that only E-CI_{1-47} complex was crystallized by MPD (or other compound in this group). On the contrary, both R-CI_{1-47} complex and E-CI_{1-47} complex in the presence of sodium citrate gave rise to indistinguishable crystals. A possible explanation of the different behavior of two species of complexes is the acetylation of the N-terminus residues. In TnC prepared from the rabbit muscle, N-terminal theronine is 100 % acetylated by post-translational modification. In TnC expressed in *E. coli*, the mass spectrometry analysis of our own indicated a partial (almost half) acetylation of the molecules, as summarized in Table 3-3-3. These results were somewhat surprising, we expected less acetylation of the *E. coli* expressed proteins (Lischwe *et al.*, 1993; Tsunazawa, 1995). Only the complex containing TnC which has non-acetylated N-terminus would form crystals in the presence of MPD.

Table 3-3-3. Mass spectrometry of TnC from different sources

specimens	N-terminus acetylation	mass of MH^+ observed	calculated
TnC (rabbit muscle)	+	18,002.6	18,008.0
TnC (E. coli expressed)	+	18,003.5	18,008.0
	–	17,964.8	17,965.9

X-ray diffraction patterns of CI_{1-47} complex crystals

Citrate-crystals were thought to belong to trigonal or hexagonal space group from their appearance. Fig. 3-3-5 shows precession photographs of a citrate-crystal. BC and DE represent the h0l plane and the plane perpendicular to the h0l plane, respectively. The lattice is trigonal with unit cell dimensions, a=b=49 Å, c=163.8 Å. In both photographs, on the l-axis (c*-axis), only refraction with 3n (n: any integer) are visible, and mirror symmetry is observed in D and E, suggesting this crystal seems to belong to space group $P3_121$ or $P3_221$. Comparing to these precession photographs, rather good diffraction patterns were obtained by both still and rotation photographs. Fig. 3-3-6 represents one of the rotation photographs which were taken with rotation around c-axis. It is shown that diffraction extends over 3.0 Å along the c-axis and 3.5 Å along a direction perpendicular to the c-axis. It is obvious that diffraction is always further extended in the direction along the c-axis than in the other direction perpendicular to the c-axis. The reason has not been clarified, but this tendency would reflect the crystallinity of the crystals. As already mentioned, citrate-crystals show different morphology on the identical conditions. Although the diffraction patterns shown in both Fig. 3-3-5 and Fig. 3-3-6 were obtained from the crystals with rhombohedral appearance, diffraction patterns which were obtained from the other crystals with rod-shape appearance were shown to be almost identical (data not shown). And also it is notable that, as is the case with crystals of T2CI complex, good appearance is not always associated with good diffraction. As shown in Fig. 3-3-3, rod-shaped crystals, which usually have neither regular faces nor sharp edges, sometimes gave good diffraction. On the contrary, rhombohedral crystals, even with both sharp edges and regular faces, sometimes gave poor diffraction. Crystals are rather easily obtained, but unfortunately, resolution and quality of the diffraction of these crystals are not enough for a structural analysis at an atomic resolution. So still it is necessary to improve the crystallization conditions. Later, we will describe what we have done so far to improve the quality of the crystals of this type.

A

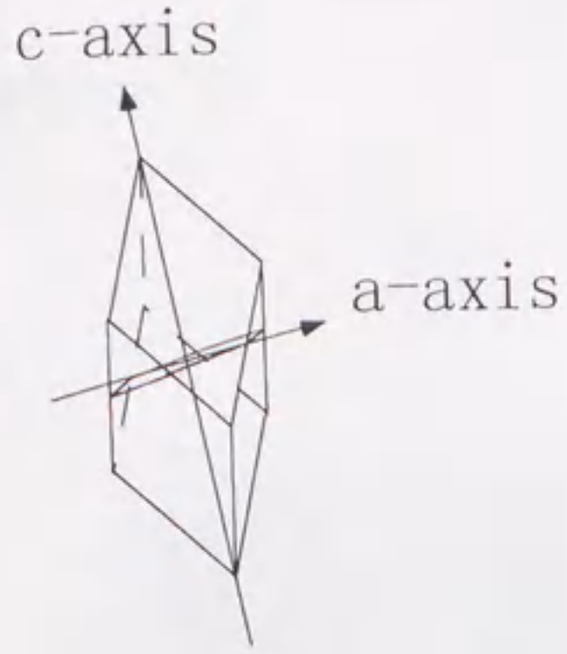

B

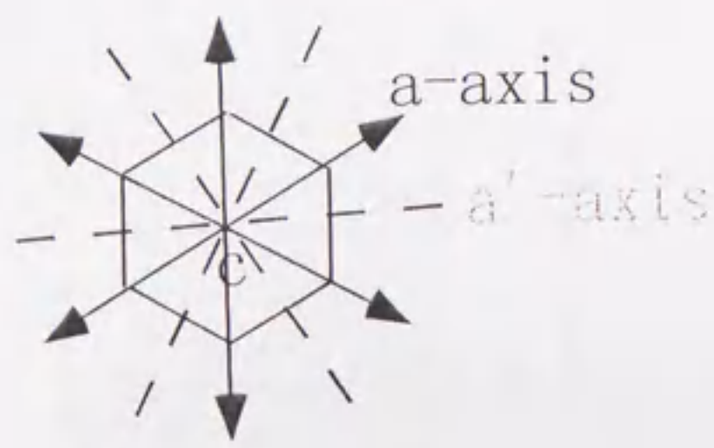

C

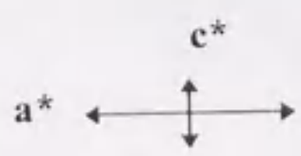

D

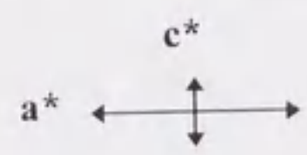

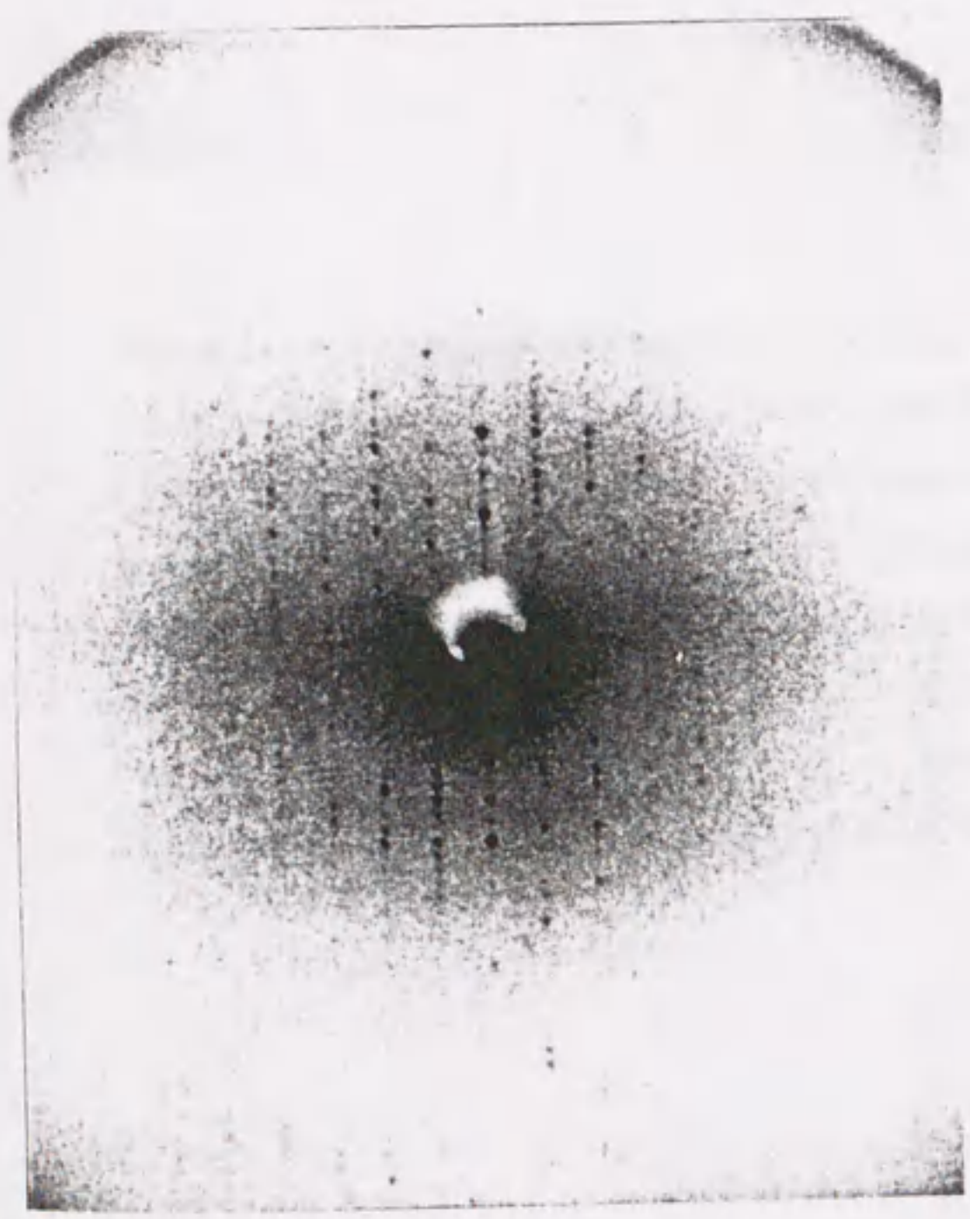

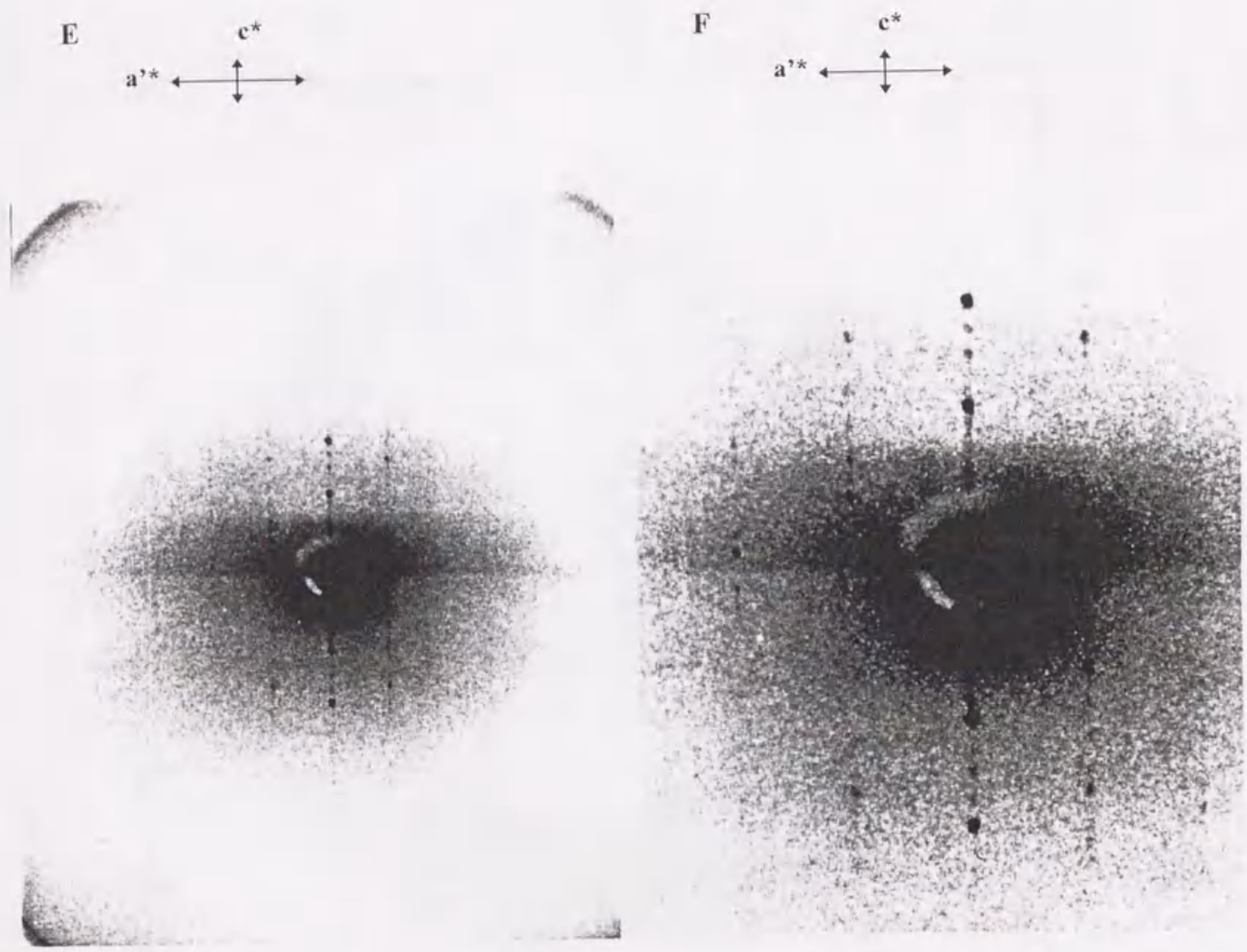

Figure 3-3-5. Precession photographs of a CI_{1-47} complex crystal obtained in the presence of 1.4 M sodium citrate and 0.1 M Tris-HCl, pH 8.0. A and B represent a relationship between crystal morphology and crystal axes. C, a precession photograph of the plane h0l (including the c*-axis and a*-axis). C, a magnification of the central part of C. E, a precession photograph of the plane perpendicular to the plane h0l (including the c*-axis and a'*-axis). F, a magnification of the central part of E. RU-200 X-ray generator (Rigaku) with precession camera was used. Camera length, 75 mm. μ= 15.0. Exposure time, 67 min for A, and 90 min for B. Note that, in both precession photographs, on the l-axis (c* axis), only refraction with 3n (n: any integer) are visible.

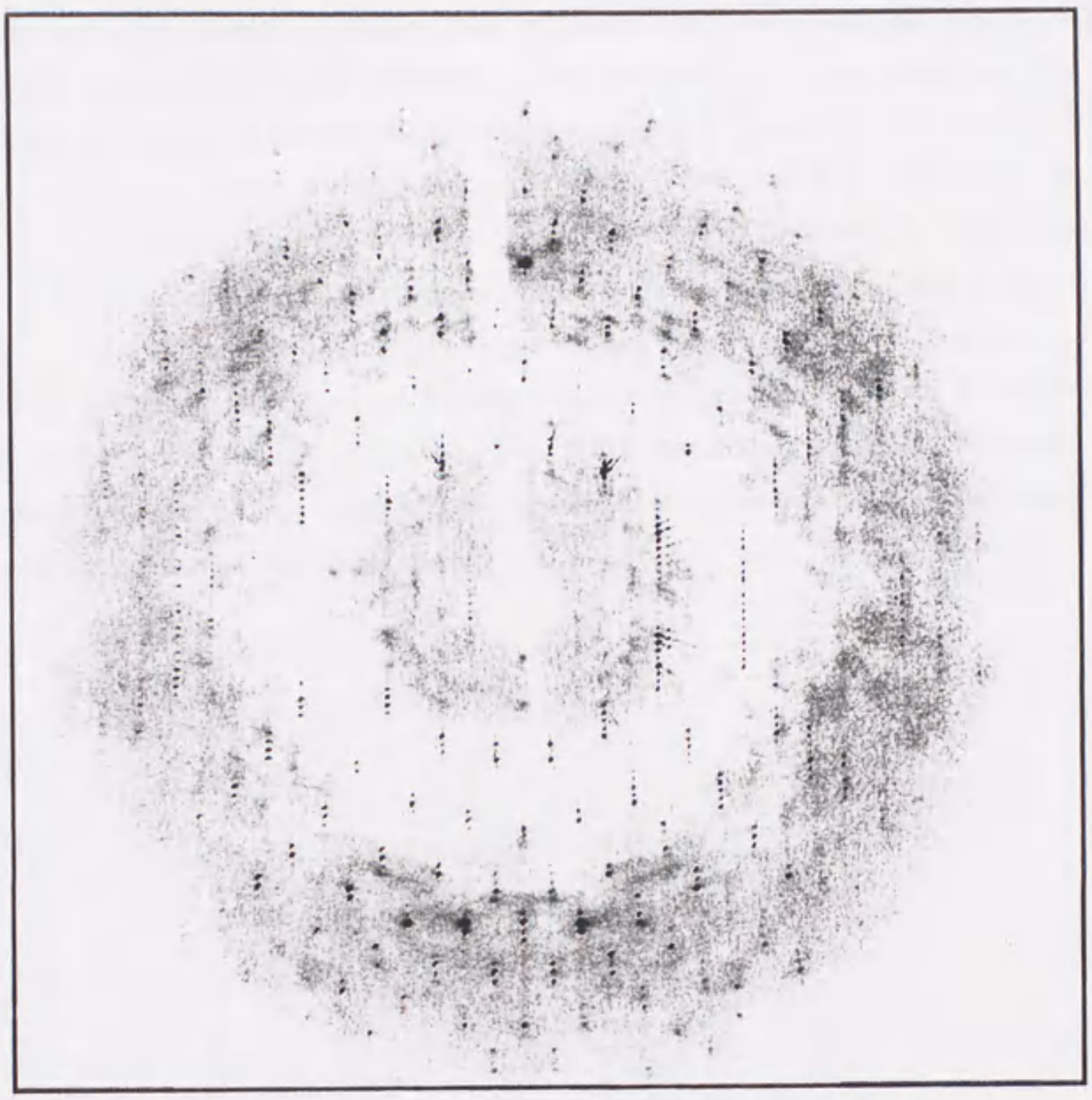

Figure 3-3-6. A rotation photograph of a CI_{1-47} complex crystal grown in the presence of 1.4 M sodium citrate and 0.1 M Tris-HCl, pH 8.0. Diffraction spots are observed beyond 3.0 Å resolution along c*-axis, while up to 3.5 Å perpendicular to c*-axis. Rotation angle, 0.5 deg. Exposure time for 45 min. The crystal to detector distance was 157 mm.

X-ray diffraction patterns has also been obtained from the crystals grown in the presence of MPD at a concentration of higher than 18% and 5mM $CaCl_2$ and has regular octahedron appearance. Since we have rarely obtained this form of crystals with a size larger than 100 μm, we used synchrotron radiation for analysis of the crystals. Fig. 3-3-7 represents a oscillation photograph of a MPD-crystal which was recorded by the use of synchrotron radiation. As shown in the figure, the crystal with a size of 80 μm diffracts to better than 3.2 Å in all directions. MPD-crystal would have a cubic lattice judging from its appearance. A protein crystal with a cubic lattice has a high degree of symmetry, because it has at least 4 triad axes of symmetry along the diagonals of the cube. Among the diffraction spots, some are forming regular triangles, also suggesting that the crystal has a cubic system. On the contrary to citrate-crystals, MPD-crystals have not well characterized because of the limited number of large crystals. Improvements in the preparation of the proteins are required for reproducible production of larger crystals.

Figure 3-3-7. An oscillation photograph of a CI_{1-47} complex crystal grown in the presence of MPD. Crystal was obtained in the presence of 20 % MPD (2-methyl-2, 4-penthanediol), 5 mM $CaCl_2$ and 10 mM Tris-HCl, pH 8.0. The photograph was taken at room temperature at BL-6A (Photon Factory, Tsukuba). Diffraction spots are observed beyond 3.2 Å resolution in all direction. Oscillation angle, 2 deg. Exposure time for 120 sec. The crystal to detector distance was 430 mm. λ = 1 Å. The diffraction pattern was recorded at room temperature.

Attempts to improve quality of crystals

Higher resolution of diffraction are required for the structural analysis of TnC-TnI_{1-47} complex crystals at an atomic resolution. Therefore, we have undertaken three different approaches for improving the quality of crystals.

Firstly, we re-examined the methods for isolation of the TnC-TnI_{1-47} complex for possible improvements. Isolation of the TnC-TnI_{1-47} was performed by a gel filtration column with a low ionic strength buffer consisting of 10 mM Tris-HCl, 5 mM $CaCl_2$ (Fig.4-4-2, part IV). Therefore, non-specific binding of small molecules to the complex could occurred and the small molecules could be carried over to the final preparations. In order to examine this, we applied thus purified sample to an analytical gel filtration column (TSKgel G3000SW_{XL}, Toso, Japan) equilibrated with 10 mM Tris-HCl, 0.1 M NaCl and 5 mM $CaCl_2$ (Fig. 3-3-8). TnC-TnI_{1-47} complex was eluted in the main peak (fractions 1 and 2 indicated in the chromatogram), being followed by minor peaks (fractions, 3-5). These peaks were identified by absorption at 280 nm while we could not see any bands on a SDS-PAGE gel (top of Fig. 3-3-8). These minor peaks might contain small molecules which bound to the TnC-TnI_{1-47} complex by ionic interactions. It was shown that some small inorganic compounds, such as H_2SO_4 or H_3PO_4, could bind to proteins, and affected on the crystallization conditions (Kautt and Ducruix, 1994). Although we could not characterize these components, we decided to change the methods to isolate TnC-TnI_{1-47} complex. After a search for materials and conditions suitable for chromatography of this complex, we found that the interaction between TnC and TnI_{1-47} fragment is strong enough to isolate this complex by anion exchange chromatography. The complex, reconstituted in the same methods as before, was applied to a Mono-Q column (HR 5/5, Pharmasia) equilibrated with 10 mM Tris-HCl, 0.1 M NaCl, 5 mM $CaCl_2$. Figure 3-3-9 shows the elution profile of the TnC-TnI_{1-47} complex from this column. Excess TnI_{1-47} fragment was eluted in the flow through fractions (fraction, 10 and 16). TnC-TnI_{1-47} complex was eluted at about 0.35 M NaCl (fraction, 33-38) with a linear gradient of NaCl at 0.1-0.7 M. TnC-TnI_{1-47} complex thus purified consisting of equimolar amounts of TnC and TnI (data not shown), was dialyzed against 10 mM Tris-HCl, 5 mM $CaCl_2$, pH 8.0 and used for further experiments. Preparations isolated by this alternative method would be good effect on the crystallization of TnC-TnI_{1-47} complex both under the citrate conditions and under the MPD conditions. The samples thus prepared gave rise to indistinguishable crystals previously obtained. Later we will discuss the effect of this change on crystallization of this complex.

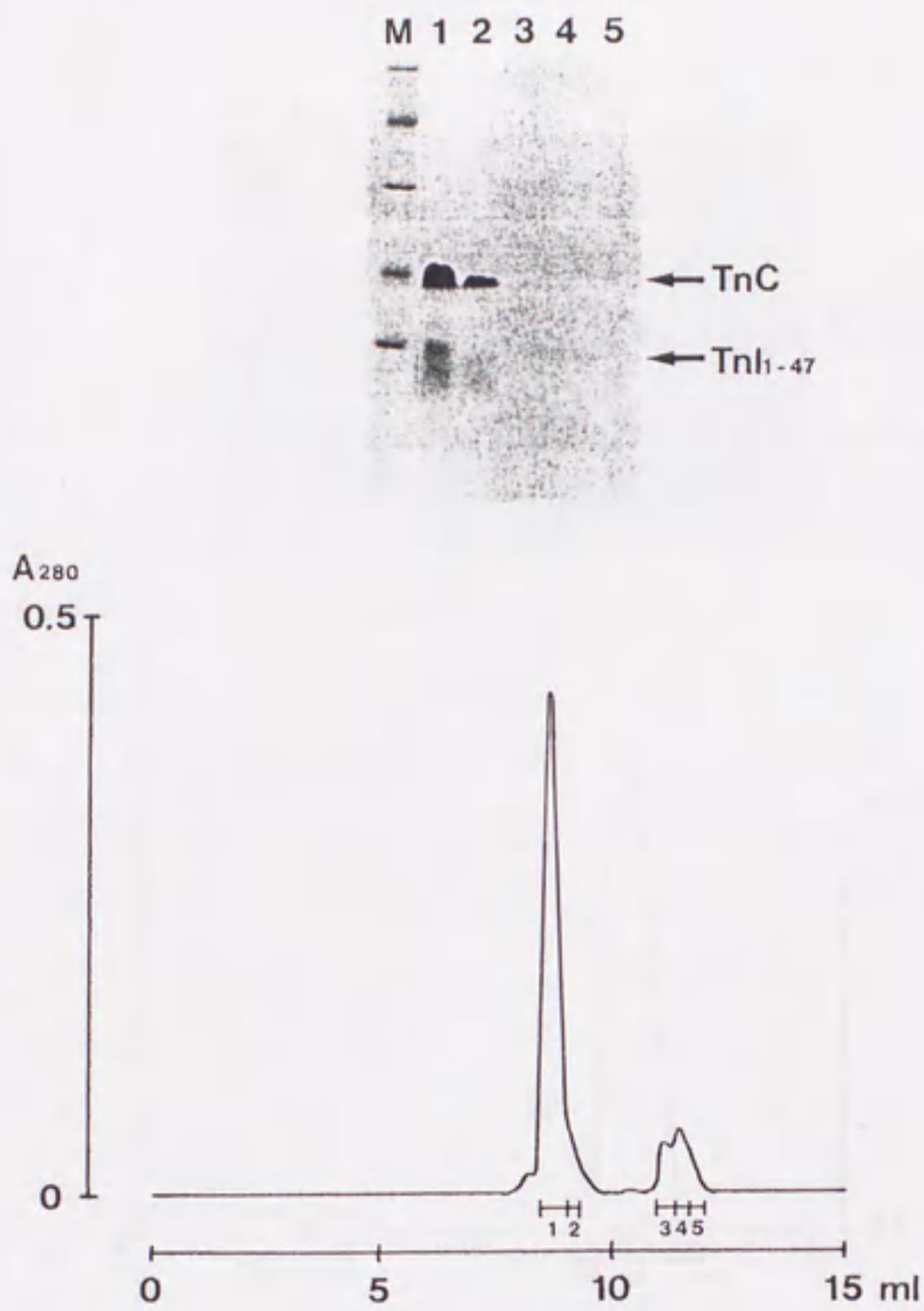

Figure 3-3-8. Analysis of the components consisting TnC-TnI$_{1-47}$ complex at an ionic strength of 0.1 M NaCl. TnC-TnI$_{1-47}$ complex isolated by a gel filtration column as described in part IV-3 are loaded on a TSK3000SW$_{XL}$ column equilibrated with 10 mM Tris-HCl, 0.1 M NaCl, 5 mM $CaCl_2$, pH 8.0. The components consisting fractions 1-5 were identified by SDS-PAGE. The bands corresponding to TnC and TnI$_{1-47}$ are indicated by arrows.

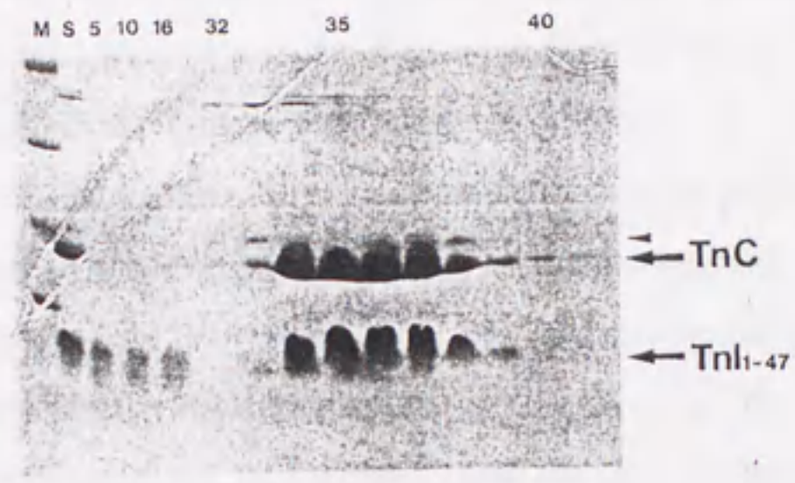

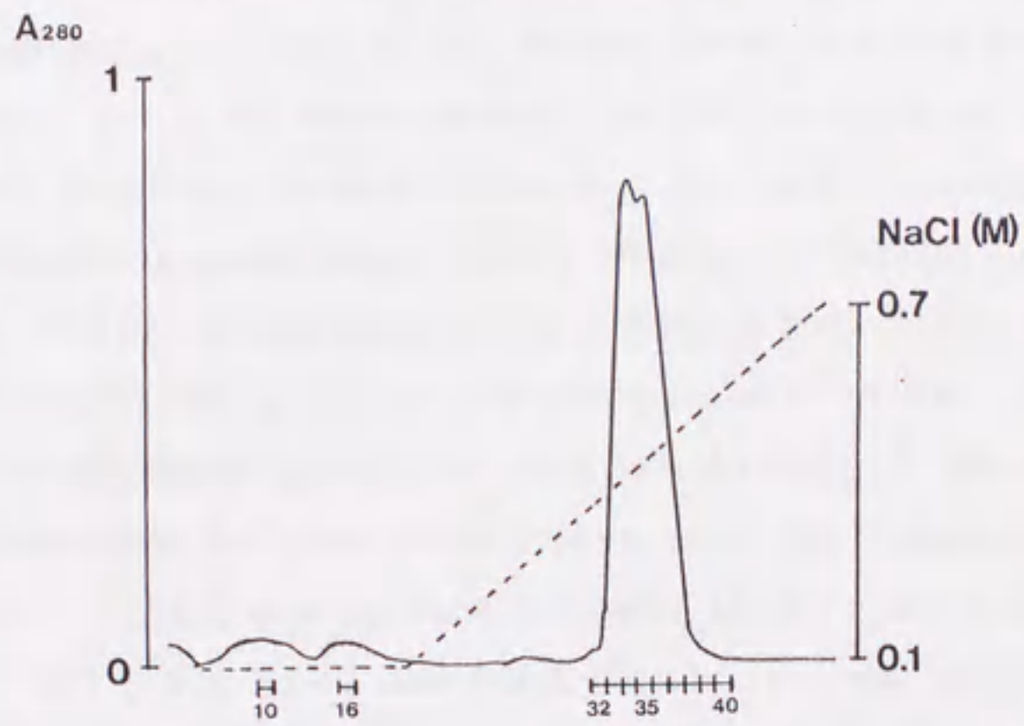

Figure 3-3-9. Isolation of TnC-TnI$_{1-47}$ complex by Mono-Q column. TnC-TnI$_{1-47}$ complex reconstituted as described in part IV-3 were applied to a Mono-Q HR 5/5 column equilibrated with 10 mM Tris-HCl, 0.1 M NaCl, 5 mM $CaCl_2$, pH 8.0 (starting solution). TnC-TnI$_{1-47}$ complex was eluted with a linear gradient of 0.1-0.7 M NaCl in the starting solution. The components contained in each fraction were identified by SDS-PAGE. The bands corresponding to TnC and TnI$_{1-47}$ were indicated by arrows. The band which has a slightly lower mobility (indicated by an arrow head) is also identified as TnC. The fractions 35-38 were pooled and used for further experiments.

Secondly, we re-examined the methods for isolation of the N-terminal fragment of TnI. Biological significance of this fragment was originally characterized by Syska *et al.* (1974). They prepared a dozen of fragments of TnI by chemically cleaving the TnI molecule either at cysteine or methionine residues, or by tryptic cleavage. They found that two fragments CF2 (res. 1-47) and CN4 (res. 96-117) interacted with TnC. Further study by Ngai and Hodges (1994) showed the fragments consisting residues either 1-20 or 20-40 of TnI were less effective than the longer fragment (res. 1-40) on the ability to release the inhibition of acto-S1 ATPase caused by TnI or TnI inhibitory peptide (res. 96-105). These results suggested that in TnI there are a couple of regions which specially interact to TnC. However these results did not give us any information about the structure of the interacting regions. More over, in these experiments, the segments studied were obtained not by cleavage of the peptide according to the boundaries of structural domains but by arbitral cleavage or synthesis. Therefore we were not sure if the interaction of TnI_{1-47} to TnC was not an artifact associated with particular peptide segments, and if TnI_{1-47} was the best choice among the N-terminal segments of TnI interacting specifically to TnC. We analyzed the proteolytic products of the ternary complex of troponin and of the binary complex TnI-TnC, and subjected these complexes to crystallization trials. As already described in "*Design of the sample for crystallization*", prolonged chymotryptic digestion of troponin ternary complex produced the complex consisting of TnC and TnI fragment. Fig. 3-3-10 shows the elution profile of digestion products thus prepared. Comparing this elution profile with that in Fig. 2-2, the peak corresponding to fraction No. 15 in Fig. 3-3-10 is not seen in the chromatogram in Fig. 2-2. (The peaks are wider in Fig. 2-2 than those in Fig. 3-3-10, because of the difference in the quality of the columns used. The fractions of the peak appeared around fraction 45 in Fig. 2-2, mostly consisted of TnT1. On the contrary, no peaks which were corresponding to TnT1 in Fig. 3-3-10 were found, because TnT1 was already removed from the sample solution before further digestion.). The components contained in fraction No. 15 were turned out to be TnC and a smaller fragment which has a apparent molecular weight of 10 K on the SDS-PAGE gel (upper in Fig. 3-3-10). These components were further characterized by reversed-phase HPLC (the results will be discussed later).

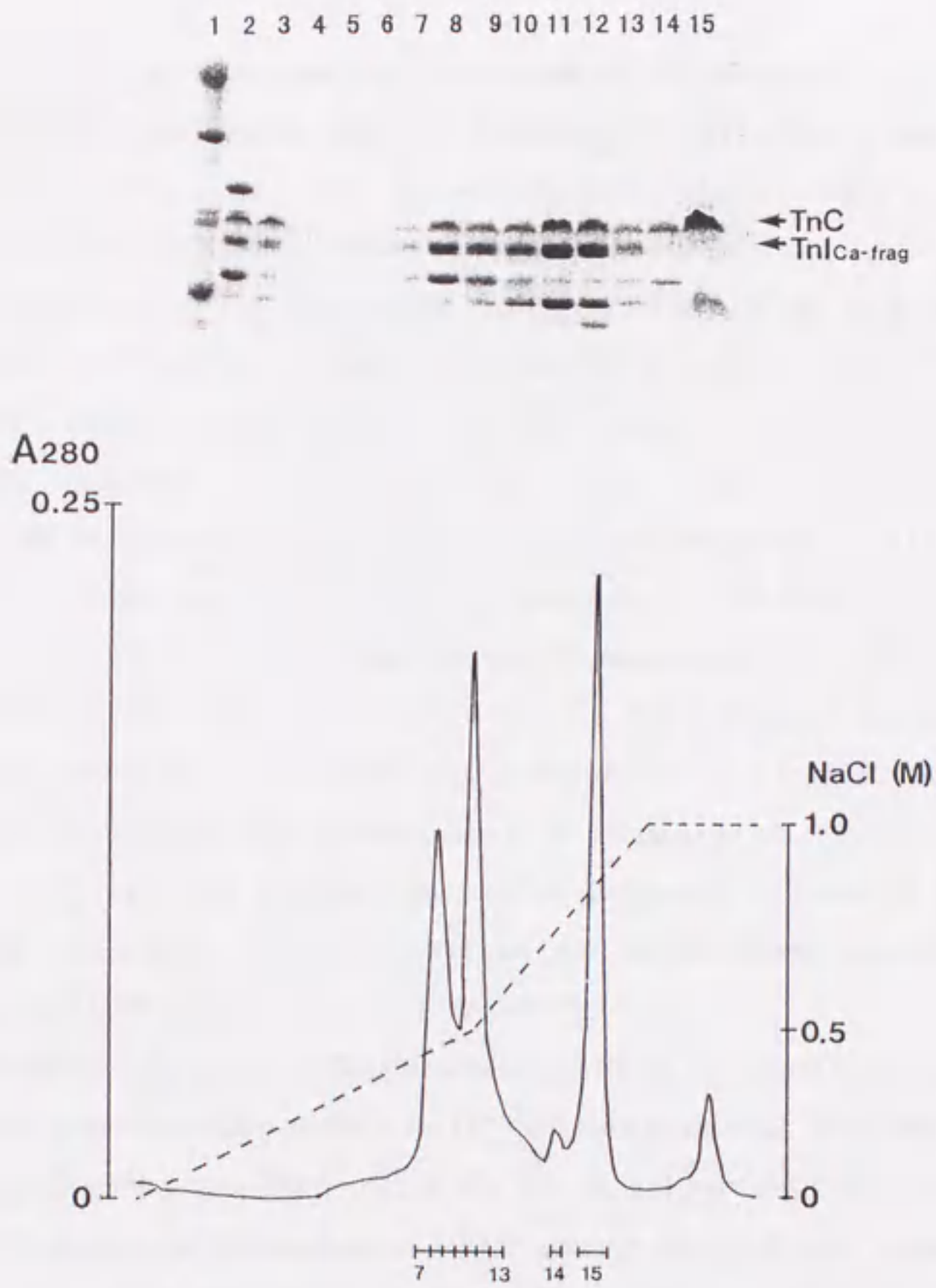

Figure 3-3-10. Elution profile of the prolonged chymotryptic digestion products of troponin ternary complex on a Mono-Q HR 5/5 column. Tn was predigested in the presence of 1 mM $CaCl_2$ and 5 mM $MgCl_2$ at 37°C for 20 min with 1/2000 weight ratio of TLCK-treated α-chymotrypsin as described under "EXPERIMENTAL PROCEDURES" in part I, then TnC containing fractions were isolated as shown in Fig. 1-2. These fractions were pooled and dialyzed against 10 mM Tris-HCl, 0.1 M NaCl, 1 mM $CaCl_2$, 5 mM $MgCl_2$, pH 8.0. After dialysis, the protein sample (lane 2) was further digested at 37°C for 60 min with 1/200 weight ratio of TLCK-treated α-chymotrypsin. The digestion products (lane 3) were applied to a Mono-Q HR 5/5 column equilibrated with 10 mM Tris-HCl, 0.1 M NaCl, 1 mM $CaCl_2$, 5 mM $MgCl_2$, pH 8.0. The components which were adsorbed to the column were separated with a gradient of 0.1-1.0 M NaCl. The components in each fraction was identified by SDS-PAGE (Top). The bands corresponding to TnC and $TnI_{Ca\text{-}frag}$ (see, part I) were indicated by arrows.

On the other hand, we also found that TnI is sometimes degraded into smaller fragments in the protein preparation for crystallization, especially in the case of TnC-TnI binary complexes during a long period of storage. Fig. 3-3-11 shows the elution profile of one of the "aged" TnC-TnI complex preparations from a gel filtration column (TSKgel G3000SW$_{XL}$, Toso, Japan). Fractions 4-7, contained TnC and fragments of TnI. TnI must be degraded first to give rise to a larger fragment (with an apparent molecular weight of 10K) which is contained in fractions 4 and 5. This larger be further degraded into a smaller fragment which is found in fractions 6 and 7. The complex consisting TnC and this larger fragment of TnI (fractions 4 and 5) was stable for further ion exchange chromatography, while the complex consisting TnC and the smaller fragment of TnI (fractions 6 and 7) was not. Indicating, some part of interacting regions might be lost in the smaller fragment. Fractions 4 and 5 were pooled and further analyzed by reversed-phase HPLC (the results will be discussed later). These results indicated that TnI, within the TnC-TnI binary complex, is highly susceptible to proteolytic enzymes. This finding was also confirmed by a further experiment. TnC-TnI binary complex was digested with chymotrypsin in a similar way as described in part I. As shown in Fig. 3-3-12, TnI was cleaved into smaller fragments independent of Ca^{2+} ion concentrations while TnC was not. The newly appeared band showed almost identical mobility as that of the TnI fragments both shown in Fig. 3-3-10 and in Fig. 3-3-11.

These results strongly indicated that the small segment of TnI would form stable core with TnC, either within the troponin ternary complex or TnC-TnI binary complex. In order to characterize the components consisting the peaks (fraction 15 in Fig. 3-3-10, and fractions 4 and 5 in Fig. 3-3-11), we applied these fractions to a reversed-phase HPLC column (4.6×100 mm, Aquapore buthyl, Brownlee). Fig. 3-3-13 shows the elution profiles of three different preparations of TnC-TnI fragment complex; A, fraction No. 15 in Fig. 3-3-10; B, fractions 4 and 5 in Fig. 3-3-11; C, TnC-TnI$_{1-47}$ complex prepared as described in Fig. 3-3-9. Each of the elution was monitored at three different wave length of 215 nm, 280 and 300, which are indicative of peptide bonds, tryptophan plus tyrosine residues, and tryptophan residues, respectively. Arrow heads in each chromatogram indicate the peaks corresponding to TnI fragments, and the peaks corresponding to TnC are indicated by arrows. The three chromatograms resemble each other, except for two points. Firstly, no absorption of TnI fragment at 280 nm was observed in B, indicating no tyrosine residues in this fragment. Secondly, two peaks of TnC were observed in B and C, while single peak of that was observed in A. The reason was already described above (provably, as a consequence of heterogeneous post-translational modification of *E. coli* expressed TnC). For further characterizations, each peak was applied to liquid chromatography/Mass spectrometry (LC/MS).

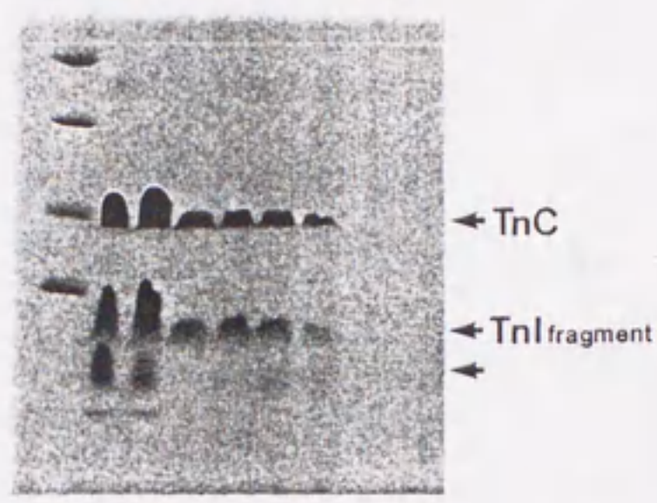

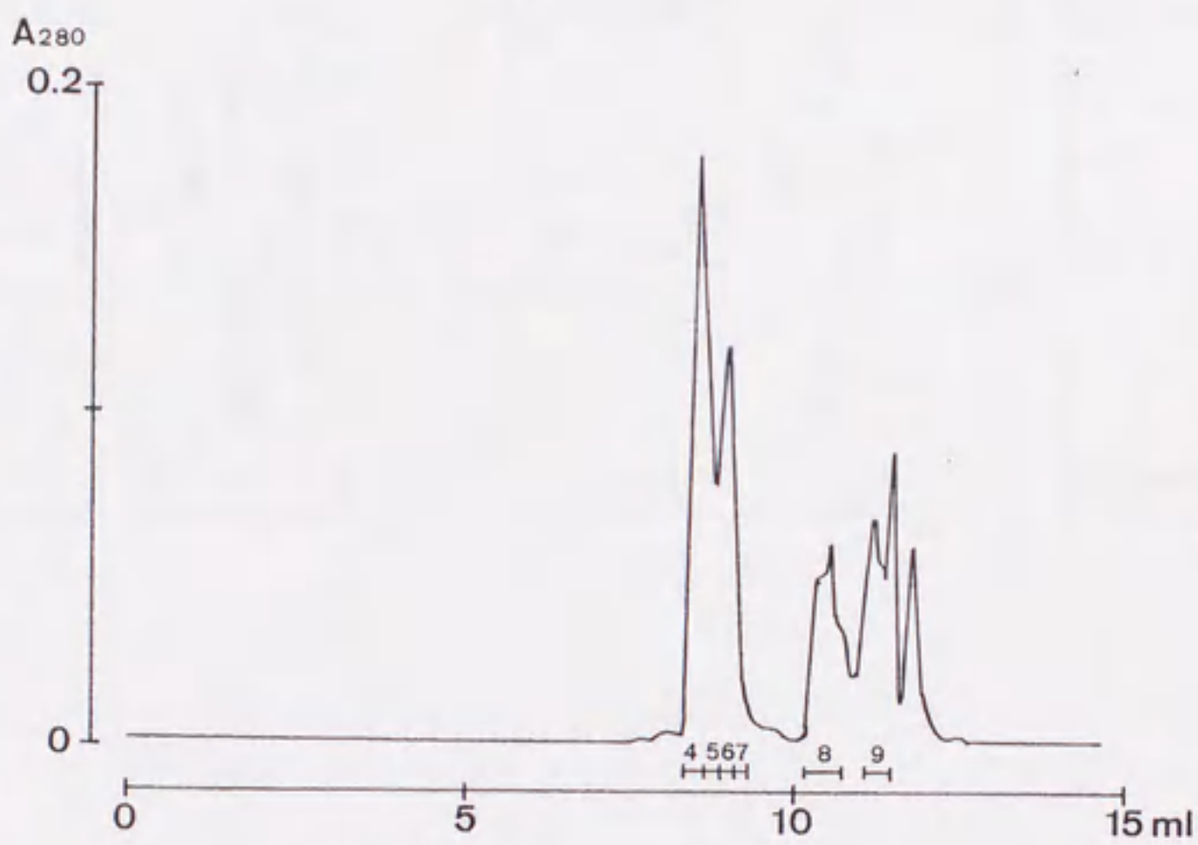

Figure 3-3-11. Elution profile of an "aged" TnC-TnI complex preparation on a TSKgel G3000SW$_{XL}$ column. A TnC-TnI complex preparation after a long period of storage ("aged" preparation, lane 2and 3) was applied to a TSKgel G3000SW$_{XL}$ column equilibrated with 10 mM Tris-HCl, 0.1 M NaCl, 5 mM $CaCl_2$, pH 7.5. The fractions indicated by bars were analyzed by SDS-PAGE (Top). The bands corresponding to TnC and the fragments of TnI are indicated by arrows.

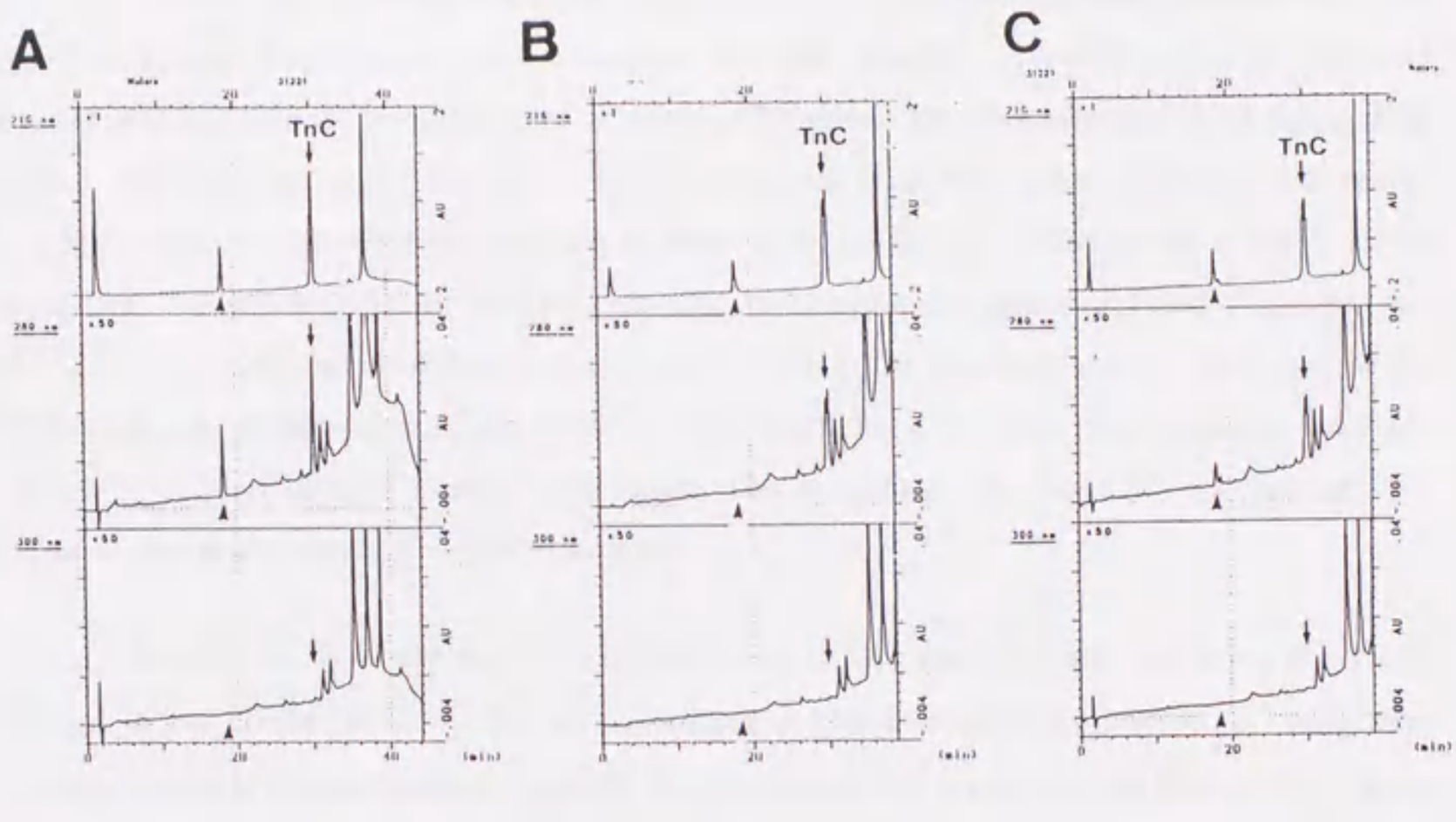

Figure 3-3-12. Analysis of various TnC and TnI fragment complexes on a reversed-phase HPLC column. TnC and TnI fragment complexes from different preparations were applied to a reversed-phase HPLC column (4.6×100 mm, Aquapore buthyl, brownlee) equilibrated with 0.1 % TFA and eluted with a linear gradient of 0-54 % acetonitrile in 0.1 % TFA at a flow rate of 1 ml/min (the gradient of acetonitrile concentration: 0.9 %/min). The elution was monitored at three different wavelength (215 nm, 280nm and 300 nm, from top to bottom). A, The complex from a prolonged chymotryptic digestion of the troponin ternary complex (fraction 15 in Fig. 3-3-10); B, The complex from an "aged" TnC-TnI complex preparation (fraction 4 and 5 in Fig. 3-3-11); C, TnC-TnI_{1-47} complex preparation used for crystallization. The peaks corresponding to TnC are indicated by arrows, and the peaks corresponding to TnI fragments are indicated by arrow heads.

Assignments of each fragment of TnI are shown in Table 3-3-1. From molecular extinction coefficients for each fragment, each TnI fragments binds to TnC in an equimolar ratio. Each of TnI component, found in these three different preparations, contained one dominant species of complex. Although, each was not completely homogeneous, we subjected each preparation to crystallization trials. We hoped for a better crystal form, on the ground that these preparations are produced by proteolysis, presumably being cleaved at the domain boundaries.

Each of TnC-TnI fragment complexes (fraction 15 in Fig. 3-3-10, and fractions 4 and 5 in Fig. 3-3-11) was pooled and dialyzed against 10 mM Tris-HCl, 5 mM $CaCl_2$, pH 8.0, and concentrated to give a protein concentration of about 20 mg/ml. For crystallization, the hanging drop method was employed under the almost identical conditions as for crystallization of TnC-TnI_{1-47} complex. So far, we have not obtained any crystals in the presence of either citrate or MPD as the precipitant. The results indicated the importance of the C-terminal residues of TnI_{1-47} fragment (res. 44-47) in the crystallization of TnC-TnI_{1-47} complex both in the sodium-citrate solutions and in the MPD solutions. Moreover, residues 44-47 of TnI might be within the protein-protein interface between adjacent complexes in the crystal lattice. This is because TnC alone did not form crystals neither in the citrate solutions nor MPD solutions.

Thirdly, we have searched for additives which extend the diffraction resolution of crystals obtained in the citrate solutions. For crystallization, a protein preparation should be "pure" and "homogeneous". It is usually stated explicitly that this means that the protein has been purified away from other cellular proteins. Other sources of structural heterogeneity, isoform heterogeneity, heterogeneity in the state of posttranslational modifications, the presence of proteolyzed species, and heterogeneity in the state of the protein's sulfhydryl groups, may also be mentioned. Established purification procedures, including bacterial expression of cloned proteins and sited directed mutagenesis, and chromatographic methods, are adequate for obtaining such "pure" and "homogeneous" preparations. On the other hand, the dynamic conformational flexibility of the protein itself may be considered to be another source of structural heterogeneity. In solution a protein molecules may exist as a number of interchanging conformers. These conformers may display the same overall fold, but may exhibit flexible surface-exposed loops, disordered termini, *etc.* When a protein is restricted in a crystal lattice, its conformational flexibility may be markedly restrained relative to its solution state (Zhu *et al.*, 1992). The number of protein conformers which can be accommodated in an amorphous precipitate is expected to be greater than those which can be accommodated in a crystal. Thus increasing conformational flexibility in a protein will increasingly favor amorphous precipitation over crystallization. It would, therefore, be useful for crystallizing proteins to identify agents which generally would help suppress conformational flexibility and stabilize protein against denaturation.

Glucose, sorbitol, sucrose, glycerol, and a number of other polyols have been shown to increase protein thermal denaturation temperatures. Also, polyols have been commonly used to stabilize protein structures. For example, tubulin, which is very labile after purification, becomes much more stable for a storage without loss of activity upon addition of glycerol or sucrose. Increasing evidences suggest that these agents can not only stabilize protein structure, but can also suppress protein conformational flexibility, making protein less "floppy" (for review, see Sousa, 1995). Thus, these agents are expected to be effective for improving the quality of crystals. Recent progress of cryo-crystallography is throwing a light on the effects of these agents. Previously, investigator have used cryoprotective agents to depress the freezing points and to improve flash freezing of crystals (Hope, 1990; Teng, 1990; Ray *et al.*, 1991). Many have noted an improvement in the diffraction resolution and an increase in the crystal lifetime. It is commonly believed that the improvement in resolution is due solely to the stabilizing effect of lower temperature and to the ability to record the short-lived diffraction pattern at higher resolution. Recently, Schick and Jurnak (1994) demonstrated that extension of the diffraction resolution of their crystals of the guanine nucleotide-exchange factor complex, EF-Tu-Ts, was achieved solely by the addition of cryoprotective agents at room temperatures. Although it is still obscure whether the effectiveness of polyols to improve diffraction quality is a general case or not, we tried this strategy for improving our TnC-TnI_{1-47} complex crystals.

Table 3-3-4. Additives tried for improving the quality of citrate-crystals of TnC-TnI_{1-47} complex

Additives	*Concentrations*	
glycerol	5-30%	(5% steps)
sorbitol	2.5-15%	(2.5% steps)
sucrose	2.5-15%	(2.5% steps)
1,2,3,-heptanetriol	0.01, 0.1, 0.5 %	
polyethyleneglycol 4000	2, 4%	

A

B

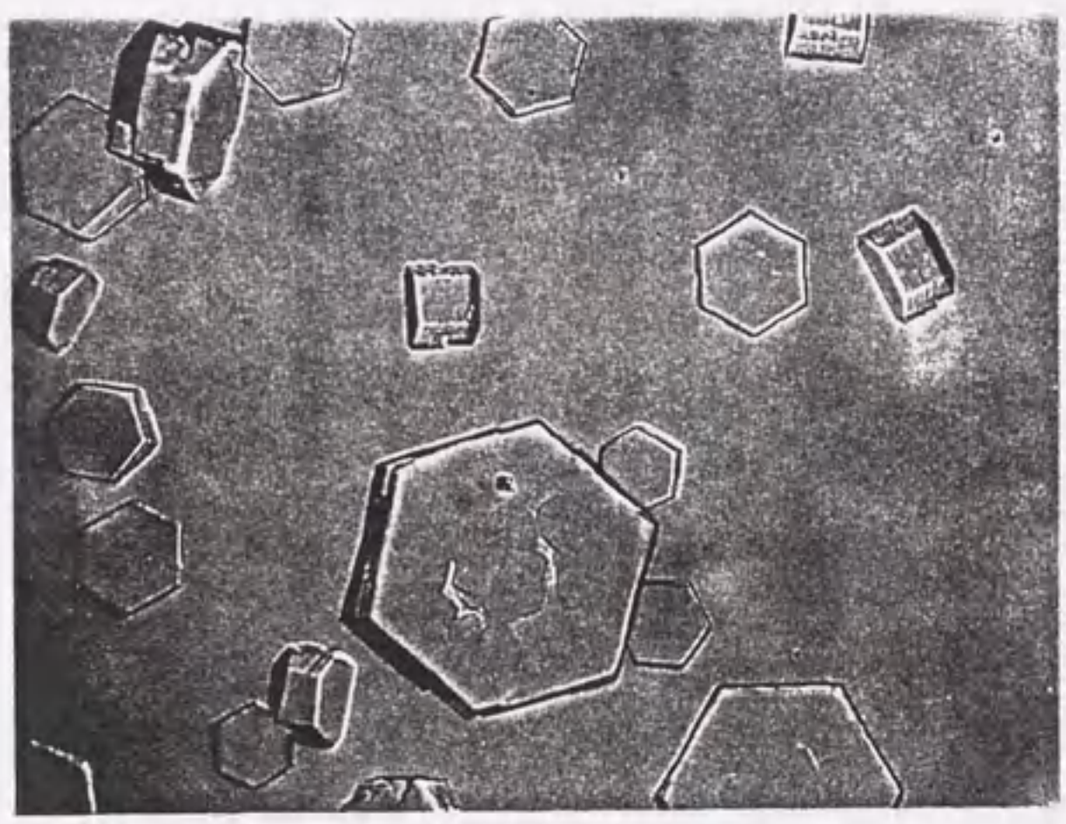

Figure 3-3-13. Photos of TnC-TnI_{1-47} complex crystals obtained from either 1.5 M sodium citrate plus 2.5% sorbitol (A) and in 1.5 M sodium citrate plus 2.5 % sucrose (B).

For screening effective additives, we undertook following experiments. Several kinds of polyols which were used as additives in the present study, are listed in Table 3-3-4. These compounds were mixed with the reservoir solutions containing 1.3, 1.4, or 1.5 M sodium citrate buffered with 0.1 M Tris-HCl, pH 8.0, and the hanging drop method was employed as in the previous experiments.

Among these compounds, sorbitol (2.5% in 1.5 M sodium citrate), sucrose (2.5% in 1.5 M sodium citrate) and 1, 2, 3-heptantriol (0.1% in 1.5M sodium citrate) have shown visible effects on the crystallization of TnC-TnI_{1-47} complex. Fig. 3-3-14 shows micrographs of the crystals obtained under above conditions. Similar crystals with hexagonal cross-section were sometimes obtained without these additives (Fig. 3-3-3), while in the presence of either sorbitol, sucrose or 1,2,3-heptanetriol, such crystals were predominantly obtained. Unfortunately, these crystals diffracted only to 8-10 Å resolution (data not shown). In the presence of either glycerol or polyethyleneglycol 4000, no crystals were obtained. On the contrary to our expectation, quality of the crystals could not be improved by using these compounds.

Although the strategy which we had undertaken to improve the quality seemed to have failed, recently my collaborators have succeeded in extending diffraction limit of citrate-crystals beyond 2.3 Å by extended the search along the same line. We will describe the recent progress in the following page.

Supplement to III-3

After the trials described above, my collaborators extended the work along the same line. In addition to both the changes in the preparation methods and the screening of effective additives, a strong X-ray source from synchrotron (ESRF) with cryocrystallography have been employed for extending the diffraction resolution of citrate-crystals. For freezing crystals, cryoprotectants are indispensable to avoid crystalline ice formation which exerts an evil influence on a structural analysis. For this purpose, a survey for effective cryoprotectants were also undertaken. Among various compounds tried, trehalose, the compound which has been used for EM specimen preparations to protect the labile proteins against both freezing and dehydration stress, has been shown not only to prevent ice formation but also to extend diffraction resolution. In fact, using a laboratory X-ray source, the diffraction resolution was extended from 3.0 Å to 2.6 Å, when the crystals grown in the presence of trehalose were compared with those grown in its absence (data not shown). We do not know whether the treharose or lower temperature or different preparation methods, or both of them, are responsible for the extension of the diffraction resolution. Similar observation was reported by Rould *et al.* (1991). Cooling the crystals of glutaminyl-tRNA synthetase to -8°C in the presence of 20% glycerol extended the diffraction resolution beyond 2.5 Å, and increased the order of the two β-barrel domains interacting with the anticodon which were not clearly resolved in the previous electron density maps from the crystals obtained in the absence of glycerol. The extended diffraction resolution of the TnC-TnI_{1-47} complex crystals, grown in the presence of 15% trehalose and 1.5 M sodium citrate, was associated with a shrinkage of the unit lattice; a=b=48.2 Å, c=163.8 Å in the absence of trehalose, while a=b=48.2 Å, c=161.9 Å in its presence. Interestingly, upon PCMBS (p-chloromercuricbenzenefonate) labeling, the lattice further shrank (7.5% in terms of the volume) and diffraction patterns were further improved. Correlation between the extension of the diffraction resolution and the shrinkage of the unit cell were also reported on the crystals of EF-Tu-Ts complex (Shick and Jurnak, 1994). These results may indicate the general applicability of cryoprotective agents to the systematic extension of the diffraction resolution of other macromolecular crystals.

We now have crystals gave rise to reflections up to 2.3 Å resolution (Fig. 3-3-15), with completeness of 84-91% and Rmerge=6.2-6.8%, and also have the crystals of PCMPS-derivative which must be suitable for crystallography using MAD method. The analysis is now under way.

Figure 3-3-15. (A) Photo of a crystal obtained in 15 % trehalose plus 1.5 M sodium citrate and (B) the diffraction pattern from the crystal.

【Part IV】

Purification of Recombinant Tn Components and Reconstitution of Tn Complexes

SUMMARY

Preparations of the proteins used in the crystallization trials given in part 3 are described in detail. This part is divided into following 4 sections.

⟨IV-1⟩ Isolation of TnT25k, TnI and TnC from *E. coli. cells.*

⟨IV-2⟩ Isolation of TnT2 fragment and reconstitution of T2CI complex.

⟨IV-3⟩ Isolation of TnI_{1-47} fragment and reconstitution of CI_{1-47} complex.

⟨IV-4⟩ Isolation of $Tm_{141-242}$ and reconstitution of $Tm_{141-242}$T25kCI complex.

(IV-1) Purification of TnT25k, TnI and TnC from E. coli. cells.

EXPERIMENTAL PROCEDURES

Preparation of TnT25k and TnI

Expression of TnT25k and TnI were previously described (Fujita-Becker, *et al.*, 1993; Kluwe *et al*, 1993). Expressed TnT25k and TnI went into the insoluble fraction so-called "inclusion body" in the bacterial cell. The proteins were extracted from the inclusion bodies according to the description by Babbitt *et al.* (1990). Cells were suspended in STET solution which contains 50 mM Tris-HCl, 8 % Sucrose, 5 % Triton X-100 and 5 mM EDTA, pH 8.0 at a ratio of 5 ml/g wet weight cells. Lysozyme was added to give a final concentration of 0.5 mg/ml. The suspension was incubated at room temperatures for 1 hour, then sonicated to break the cells. Pellets were collected by centrifugation at 30,000 × *g* for 20 min and resuspended in STET. The sonication procedure was repeated three times in STET and once in 50 mM Tris-HCl, 1 mM EDTA, pH 8.0. The pellets were resuspended in 6 M urea, 20 mM Tris-HCl, 0.1 M NaCl, 1 mM EDTA (solution A), and clarified by centrifugation at 30,000 × *g* for 20 min. The supernatant was applied to a DE 52 column (Whatman, 5.0×10 cm) equilibrated with solution A. The flow through fraction was then applied to SP-sepharose fast flow column (Pharmacia, 2.5×10 cm) equilibrated with solution A. TnT25k and TnI were eluted with a linear gradient of 0.1-0.4 M NaCl in solution A. And further purification was performed by reversed-phase HPLC (10×30 cm, Aquapore Butyl, Brownlee). A linear gradient of 32-35 % acetonitrile in 0.1 % TFA (35-45 % solution B in 0.1% TFA; solution B, 0.1% TFA and 90 % acetonitrile) was used for isolating either TnI or TnT25k. The Tn component containing fractions were pooled and lyophilized by centrifugal concentrator. The proteins thus purified were stored at -20°C.

Preparation of TnC

Expression of TnC was previously described (Fujita-Becker *et al.*, 1993). The bacterial cells which expressed TnC were suspended in a solution containing 20 mM Tris-HCl, 20 % Sucrose, 1 mM EDTA, pH 8.0 at a ratio of 5 ml/g wet weight cells. Lysozyme was added to give a final concentration of 0.5 mg/ml. The suspension was incubated at room temperatures for 1 hour, then sonicated to break the cells and centrifuged at 30,000 × *g* for 20 min. The supernatant of 35 % in saturated ammonium sulfate was applied to a phenyl-sepharose CL-4B column (5.0×10 cm, Pharmacia) equilibrated with 50 mM Tris-HCl, 50 mM NaCl, 5 mM $CaCl_2$, 1 mM $MgCl_2$, 1 mM dithiothreitol, pH 8.0 (the starting solution). The column was washed with the starting solution, then with 50 mM Tris-HCl, 1 M NaCl, 0.1 mM $CaCl_2$, 1 mM dithiothreitol, pH 8.0 (solution A). The

crude TnC was eluted with 50 mM Tris-HCl, 1 mM EDTA, 1 mM dithiothreitol, pH 8.0 (solution B). The TnC containing fraction were combined and dialyzed against 10 mM Tris-HCl, 1 mM EDTA, 1 mM dithiothreitol, pH 8.0, then solid urea was added to protein solution to give a final concentration of 6 M. The protein solution was applied to a Q-sepharose fast flow column (2.5×10 cm) equilibrated with 6 M urea, 20 mM Tris-HCl, 0.1 M NaCl, 1 mM EDTA, 1 mM dithiothreitol, pH 8.0 (the starting solution). TnC was eluted with a linear gradient of 0.1-0.5 M NaCl in the starting solution. TnC was further purified by reversed-phase HPLC (10×30 cm, Aquapore Butyl column, Brownlee). A linear gradient of 40-58.5 % acetonitrile in 0.1 % TFA (45-65 % solution B in 0.1% TFA; solution B, 0.1% TFA and 90 % acetonitrile) was used for isolating TnC. The TnC containing fractions were pooled and lyophilized by centrifugal concentrator. TnC thus purified was stored at -20°C.

RESULTS

Isolation of TnI

The elution profile from an SP-sepharose fast flow column was shown in Fig. 4-1-1. From 6 liter bacterial culture, almost 150 mg of crude TnI was recovered after SP-sepharose fast flow column chromatography. The fractions indicated by a bar were pooled and further purified by reversed-phase HPLC (Fig. 4-1-2). From about 15 mg of crude fractions from the SP-sepharose column, 12 mg of TnI was recovered from the HPLC column. TnI thus purified was lyophilized and stored at -20°C. The yield of TnI after HPLC was about 120 mg from 6 liter bacterial culture.

Isolation of TnT25k

The elution profile from the SP-sepharose fast flow column was shown in Fig. 4-1-3. From 6 liter bacterial culture, almost 350 mg of crude TnT25k was recovered after SP-sepharose fast flow chromatography. The fractions indicated by a bar were pooled and further purified by reversed-phase HPLC (data not shown). From about 15 mg of crude fractions form the SP-sepharose column, 10 mg of TnT25k was recovered from the HPLC column. TnT25k thus purified was lyophilized and stored at -20°C. The yield of TnT25k after HPLC was about 240 mg from 6 liter bacterial culture.

Isolation of TnC

The elution profiles from the phenyl sepharose CL-4B column, from the Q-sepharose fast flow column and from the reversed-phase HPLC column are shown in Fig. 4-1-4, Fig. 4-1-5 and Fig. 4-1-6, respectively. TnC thus purified was lyophilized and stored at -20°C. The yield of TnC after HPLC was about 90 mg from 6 liter culture.

Note that without purifying TnC by reversed-phase HPLC, we could not remove proteolytic activity which is associated with TnC containing fractions from the Q-sepharose fast flow column. When we reconstituted TnC, which was not purified by reversed-phase HPLC, with other Tn components, the other Tn components degraded into smaller fragments by the proteolytic enzyme which must be associated with TnC.

The yields of each troponin component from bacterial cells are summarized in Table 4-1-1.

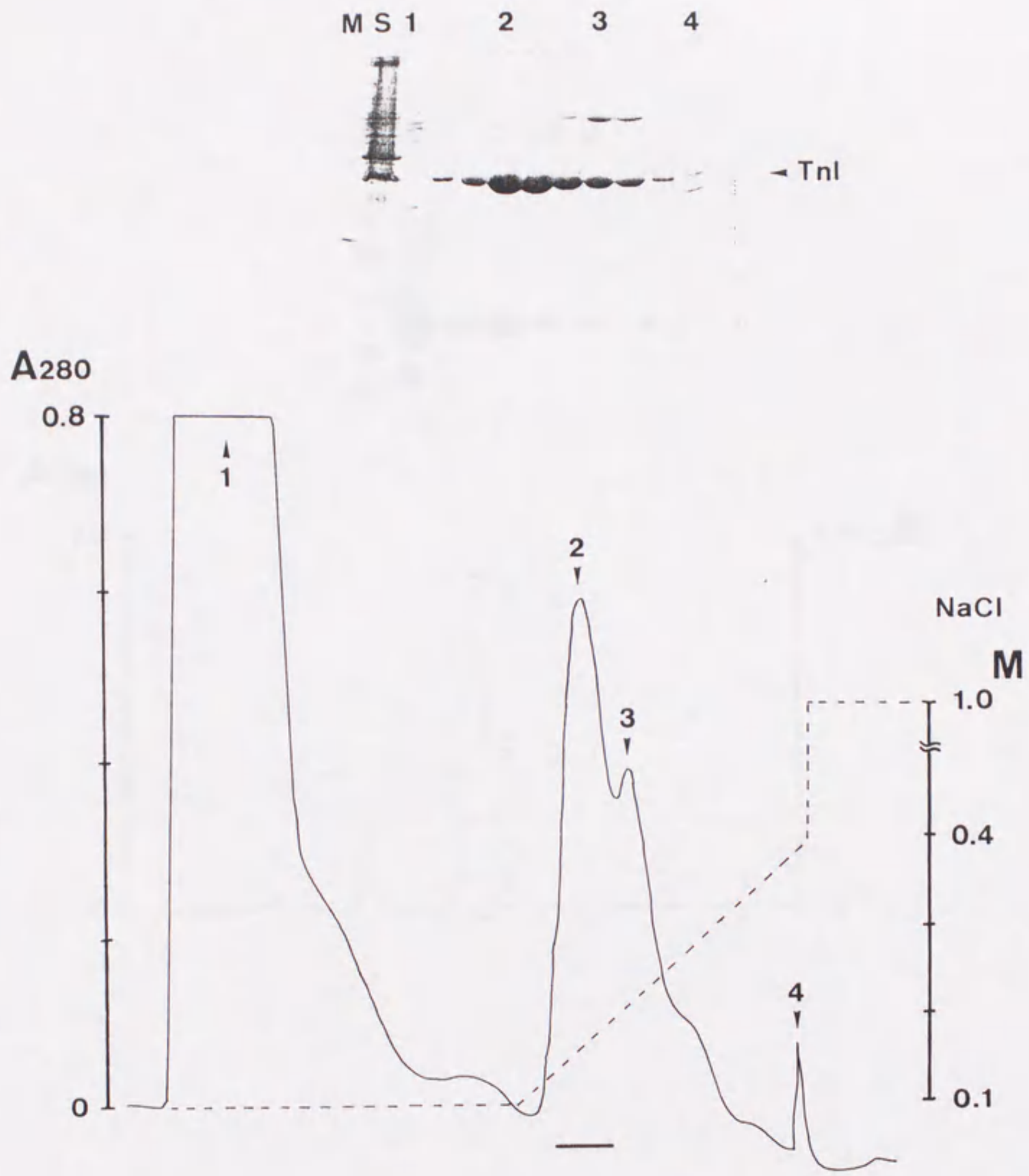

Figure 4-1-1. Chromatography of *E. coli* expressed TnI on a SP-sepharose fast flow column. Inclusion body was extracted as described under "EXPERIMENTAL PROCEDURES" and applied to a DE 52 column. The flow through fractions from the DE 52 column were applied to an Sp-sepharose column equilibrated with 50 mM Tris-HCl, 1 mM EDTA, 6 M urea, pH 8.0. The TnI containing fractions were eluted with a linear gradient of 0.1-0.4 M NaCl in the starting solution. The fractions indicated by a bar were applied to reversed-phase HPLC for further purification.

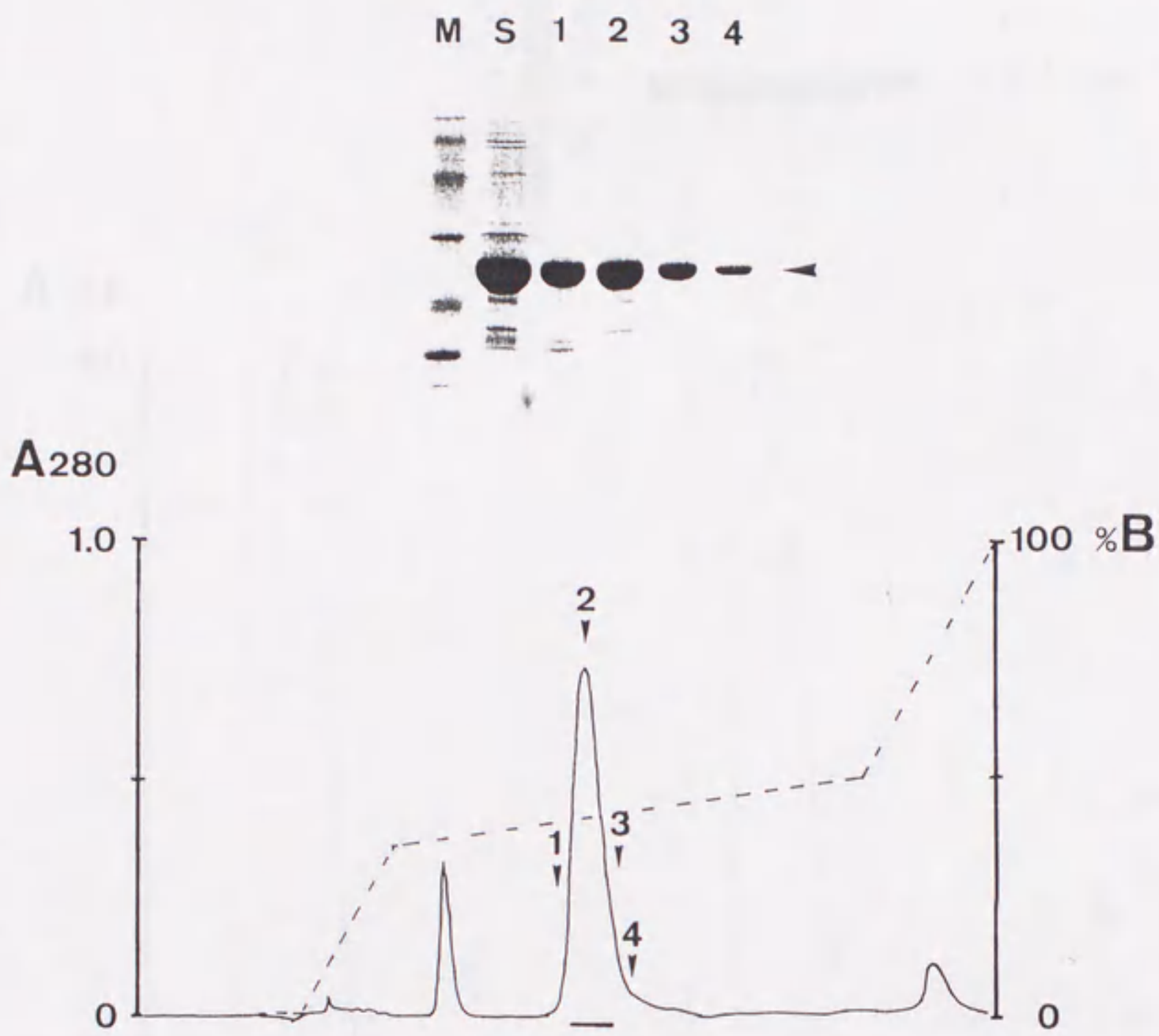

Figure 4-1-2. Final purification of *E. coli* expressed TnI by a reversed-phase HPLC column.
The TnI containing fractions eluted from an SP-sepharose fast flow column were applied to a reversed-phase HPLC column (Aquapore butyl, Brownlee) equilibrated with 0.1 % TFA. TnI was eluted with a linear gradient of 32-45 % acetonitrile in 0.1 % TFA. The fractions containing TnI indicated by a bar were used for reconstitution of Tn complex. From each run on the HPLC, about 10 mg of TnI could be recovered under these conditions.

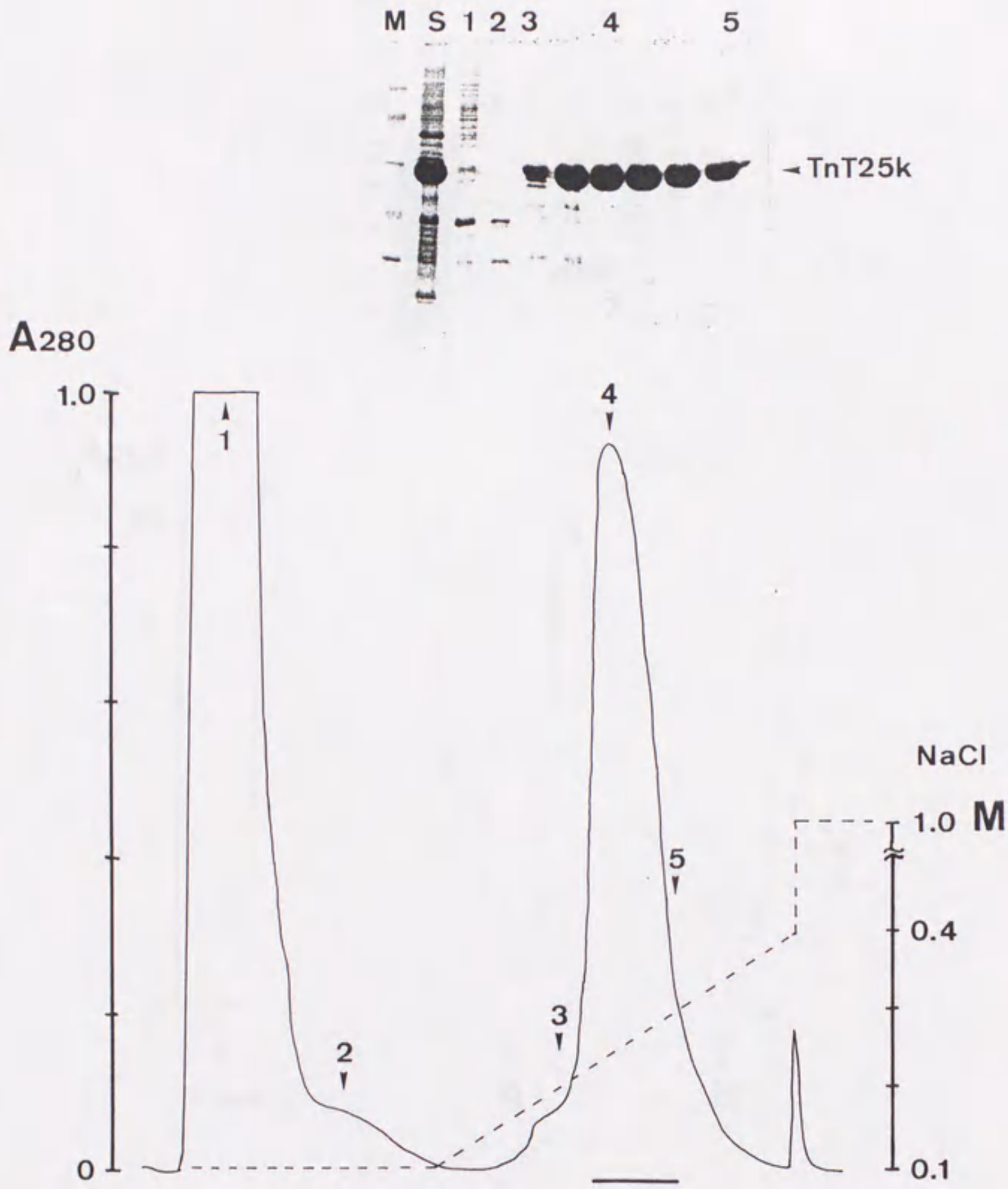

Figure 4-1-3. Chromatography of *E. coli* expressed TnT25k on an SP-sepharose fast flow column. Inclusion body was extracted as described under "EXPERIMENTAL PROCEDURES" and applied to a DE 52 column. The flow through fractions from the DE 52 column were applied to an Sp-sepharose column equilibrated with 50 mM Tris-HCl, 1 mM EDTA, 6 M urea, pH 8.0. The TnI containing fractions were eluted with a linear gradient of 0.1-0.4 M NaCl in the starting solution. The fractions indicated by a bar were applied to reversed-phase HPLC for further purification.

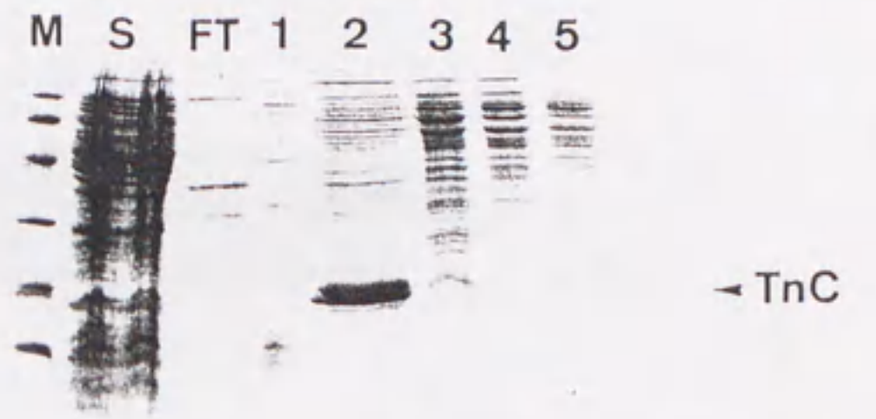

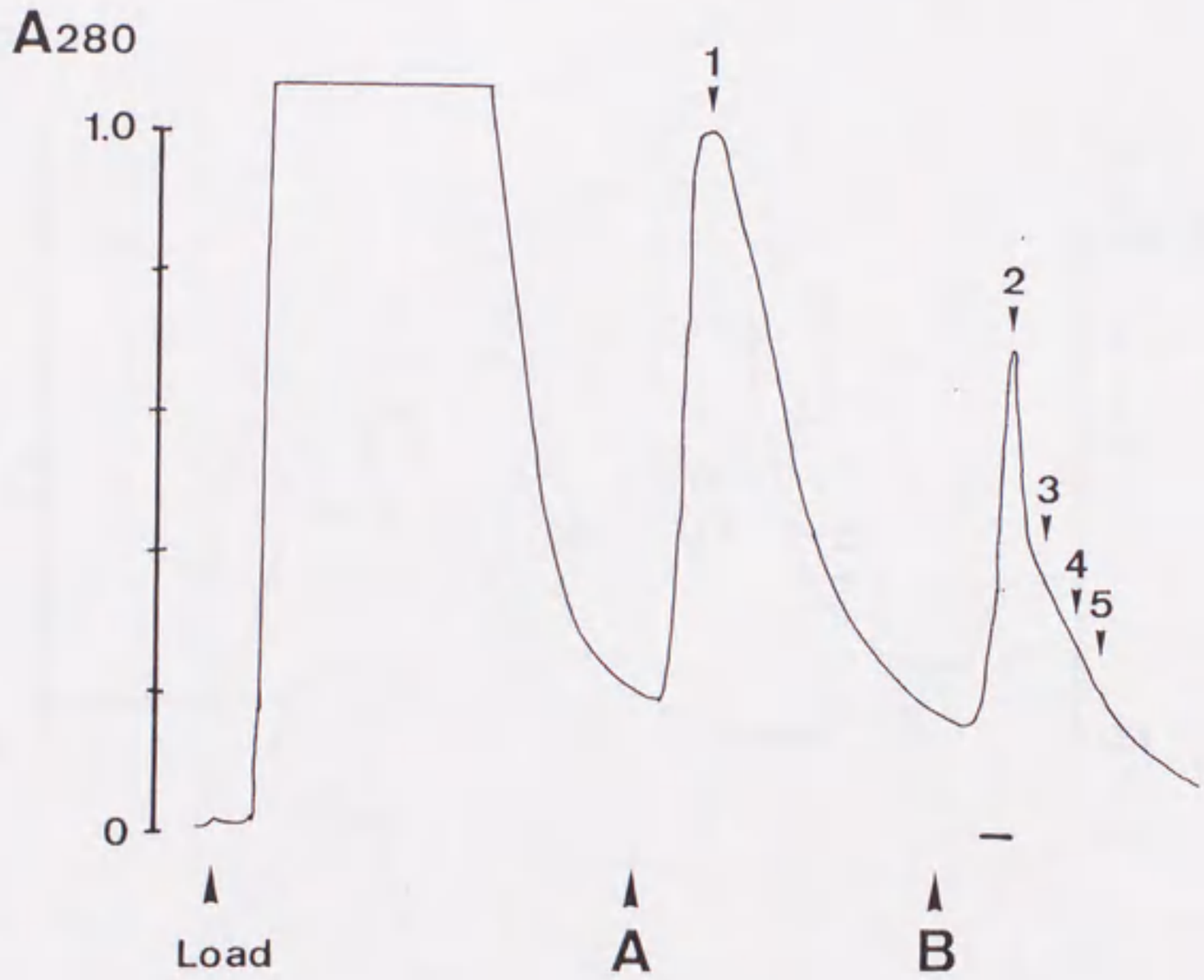

Figure 4-1-4. Chromatography of *E. coli* expressed TnC on a Phenyl-sepharose CL-4B column. The supernatant of the cell lysate in 35 % saturated ammonium sulfate was applied to a phenyl-sepharose CL-4B column. After loading the sample, the column was washed with solution A (50 mM Tris-HCl, 1 M NaCl, 0.1 mM $CaCl_2$, 1 mM dithiothreitol, pH 8.0). Then the fractions containing TnC were eluted with solution B (50 mM Tris-HCl, 1 mM EDTA, 1 mM dithiothreitol, pH 8.0). The fractions indicated by a bar were further purified by a Q-sepharose fast flow column.

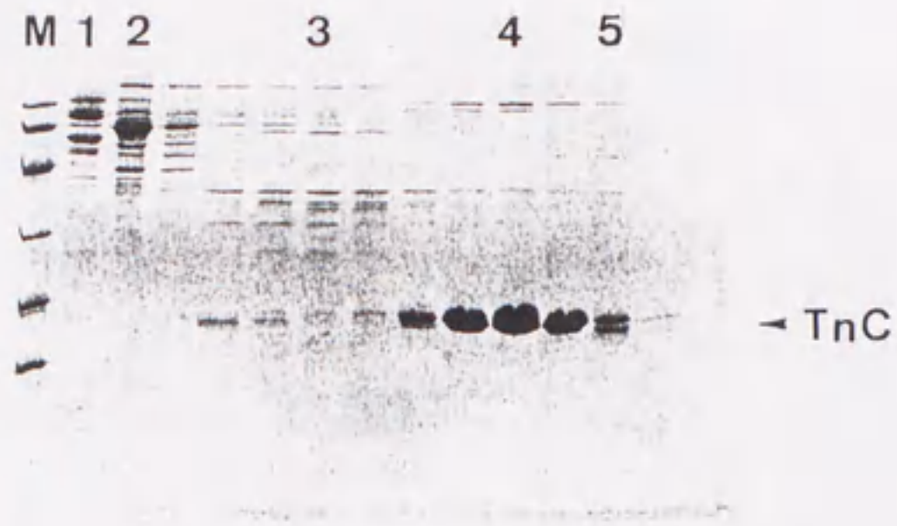

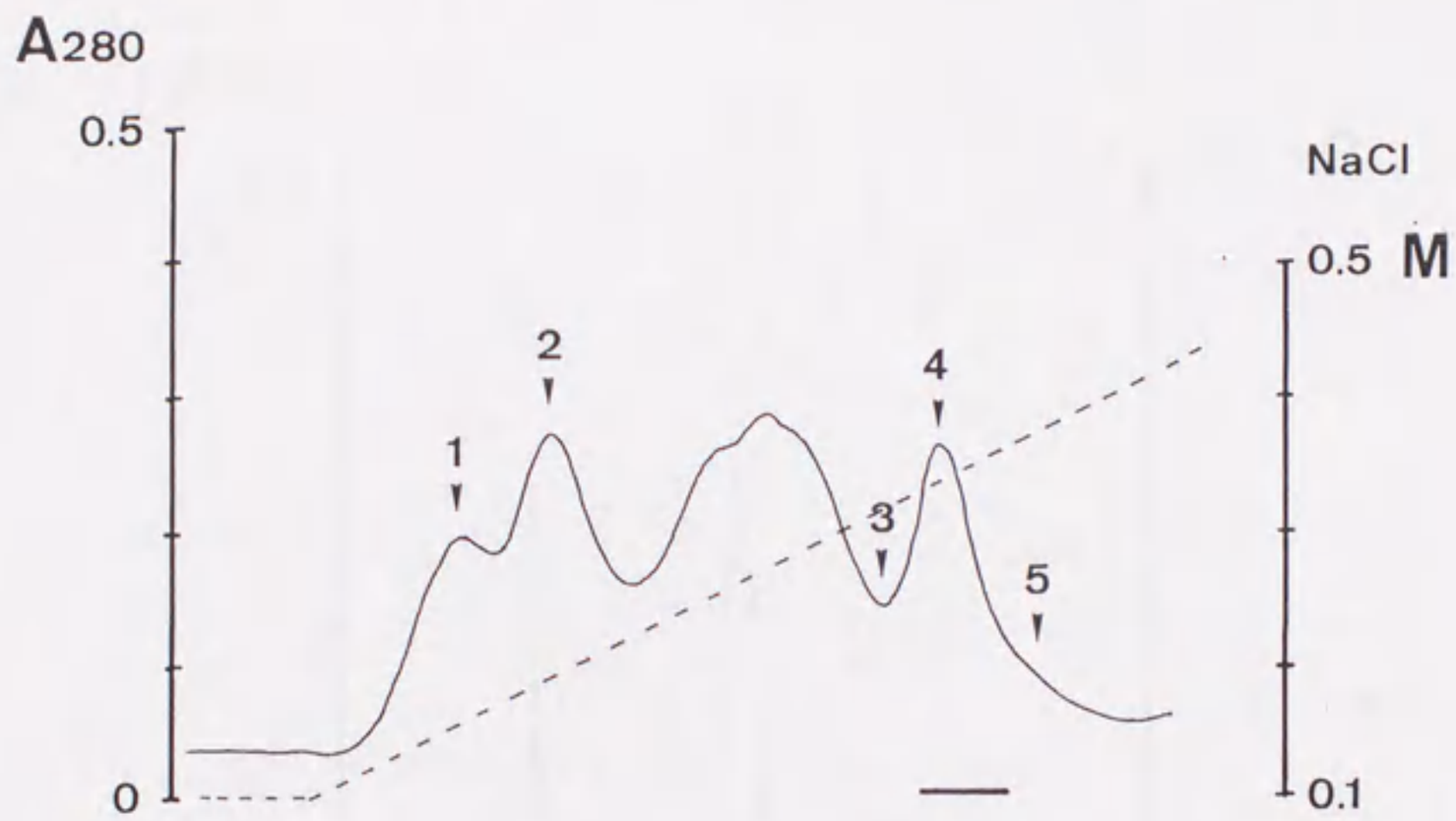

Figure 4-1-5. Chromatography of *E. coli* expressed TnC on a Q-sepharose fast flow column. The fractions containing TnC which were eluted from the phenyl sepharose CL-4B column (Fig. 4-1-4) were dialyzed against 50 mM Tris-HCl, 0.1 M NaCl, 1 mM EDTA and 1 mM dithiothreitol, pH 8.0, then solid urea was added to the protein solution to give a final concentration of 6 M, and applied to a Q-sepharose fast flow column equilibrated with 50 mM Tris-HCl, 0.1 M NaCl, 1 mM EDTA and 1 mM dithiothreitol, pH 8.0 (the starting solution). TnC was eluted with a linear gradient of 0.1-0.5 M NaCl in the starting solution. The fractions indicated by a bar were further purified by reversed-phase HPLC.

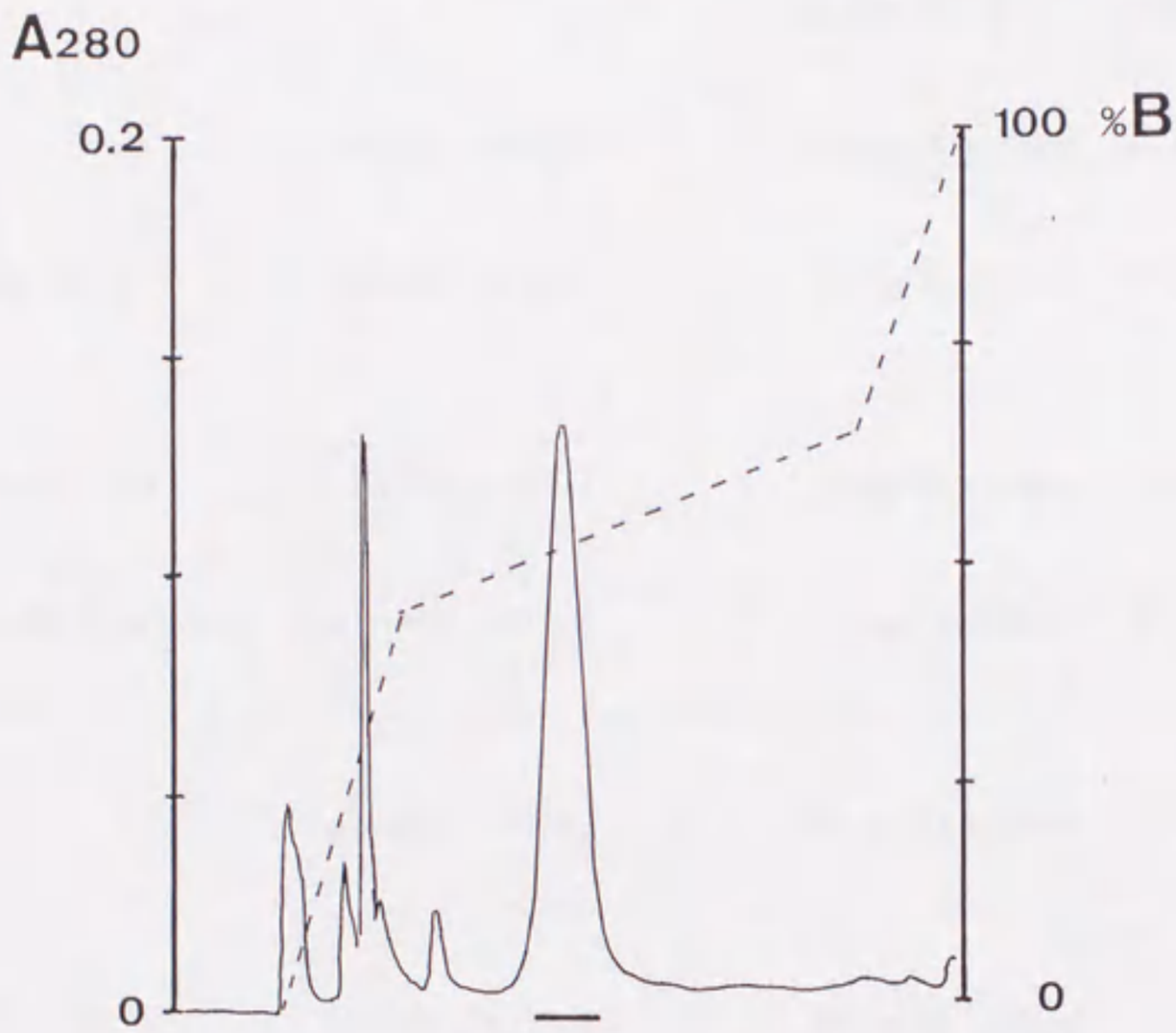

Figure 4-1-6. Chromatography of *E. coli* expressed TnC on a reversed-phase HPLC column. The fractions containing TnC which were eluted from the Q-sepharose fast flow column were loaded on a reversed-phase HPLC column (Aquapore butyl, Brownlee) equilibrated with 0.1 % TFA. TnC was eluted with a linear gradient of 40-58.5 % acetonitrile in 0.1 % TFA. The fractions marked by a bar predominantly containing TnC, indicated by the SDS-PAGE pattern on the top, were pooled and used for reconstitution of Tn complex. From each run on the HPLC, about 10 mg of TnC could be recovered under these conditions.

Table 4-1-1. Summary of the yield of Tn subunits and $Tm_{141-284}$ expressed in and purified from *E. coil*.

subunit	plasmid, host cell	Yield	
		before HPLC	after HPLC
TnT25k	pTrc99c, AD202	60 mg/1L culture	40 mg/1L culture
TnT25k (M124L)	pTrc99c, AD202	60 mg/1L culture	40 mg/1L culture
TnI (C64A/C133S)	pTrc99c, AD202	30 mg/1L culture	20 mg/1L culture
TnI (C48A/C64A/C133S)	pTrc99c, AD202	30 mg/1L culture	20 mg/1L culture
TnC	pTrc99c, AD202	20 mg/1L culture	15 mg/1L culture
$Tm_{141-284}$	pTrc99c, AD202	40 mg/1L culture	

(IV-2) Isolation of TnT2 fragment and reconstitution of T2CI complex.

EXPERIMENTAL PROCEDURES

Cleavage of TnT25k and isolation of T2 fragment

The mutant TnT, TnT25k (M124L), in which methionine at 124 was replaced by leucine was purified by the same procedure as for TnT25k without mutation. The protein was dissolved in 70 % formic acid, and excess amount of cyanogen bromide was added. The reaction was allowed to proceed for 10-20 hours. The protein solution was then lyophilized and dissolved in a solution containing 6 M urea, 20 mM Tris-HCl, 0.1 M NaCl, pH 8.0 (the starting solution) and was applied to a SP-sepharose fast flow column. TnT2 was eluted with a linear gradient of 0.1-0.4 M NaCl in the starting solution. The TnT2 containing fractions were concentrated by a centricon-10 (Amicon), and further purified by a Sephacryl S-100 (2.5×50 cm) column equilibrated with 20 mM Tris-HCl, 0.3 M NaCl, pH 8.0.

Reconstitution of T2CI complex

Equimolar amounts of T2, TnC and TnI were combined in a solution containing 6 M urea, 1 M NaCl, 20 mM Tris-HCl, 0.1 mM $CaCl_2$ and 1 mM dithiothreitol, pH 8.0. The mixture was then dialyzed consecutively against NaCl solution of 1 M, 0.5 M, 0.3 M and 0.1 M, each containing 20 mM Tris-HCl, 0.1 mM $CaCl_2$ and 1 mM dithiothreitol, pH 8.0. After dialysis, the protein solution was clarified by centrifugation and applied to a Q-sepharose fast flow column (1.5×10 cm) equilibrated with 0.1 M NaCl, 20 mM Tris-HCl, 0.1 mM $CaCl_2$ and 1 mM dithiothreitol, pH 8.0. T2CI complex was eluted with a linear gradient of 0.1-0.5 M NaCl in the same solution. Fractions containing predominantly T2CI ternary complex were identified by SDS gel electrophoresis.

RESULTS

Cleavage of TnT25k (M124L) and isolation of T2 fragment

The amino acid sequence of rabbit skeletal β-TnT25k is shown in Fig. 3-1-1. Fig. 4-2-1 and Fig. 4-2-2 represent purification steps of T2 fragment. T2 fragment was eluted together with uncleaved TnT25k and partially cleaved species (about 23K) on a SP-sepharose fast flow column (Fig. 4-2-1). The longer reaction of CNBr did not give rise to increase the yield of T2 fragment. The incomplete cyanogen bromide cleavage of the Met-Glu bond between residues 71 and 71 could possibly be related to the extra negatively charge at this position (Pearlstone *et al.*, 1976; Pato *et al.*, 1981), while incomplete cleavage of the Met-Gly bond between residues 152 and 153 is obscure. T2 fragment was further purified by a gel filtration column (Fig. 4-2-2). By other chromatography tested, T2 was not isolated from other two components, *i. e.* TnT25k and a partially cleaved product (23k), because the net charges of these three components are almost the same. The yield of purified T2 fragment was about 30 % of the starting material.

Reconstitution of T2CI complex

Elution profile of T2CI complex on a Q-sepharose fast flow column is shown in Fig. 4-2-4. And the purity of reconstituted T2CI complex was checked by SDS-PAGE. The stoichiometry of each component within the T2CI complex was further examined on a reversed-phase HPLC column. The elution profile (Fig. 4-2-5) indicated that each component exists in the equimolar ratio in the complex. The T2CI complex thus purified (indicated by a bar) was pooled and dialyzed against 10mM Tris-HCl, 0.1 M NaCl, pH 8.0. After dialysis, the protein solution was concentrated by a centriprep concentrator (Amicon) to give a concentration of 10-20 mg/ml, and used for crystallization.

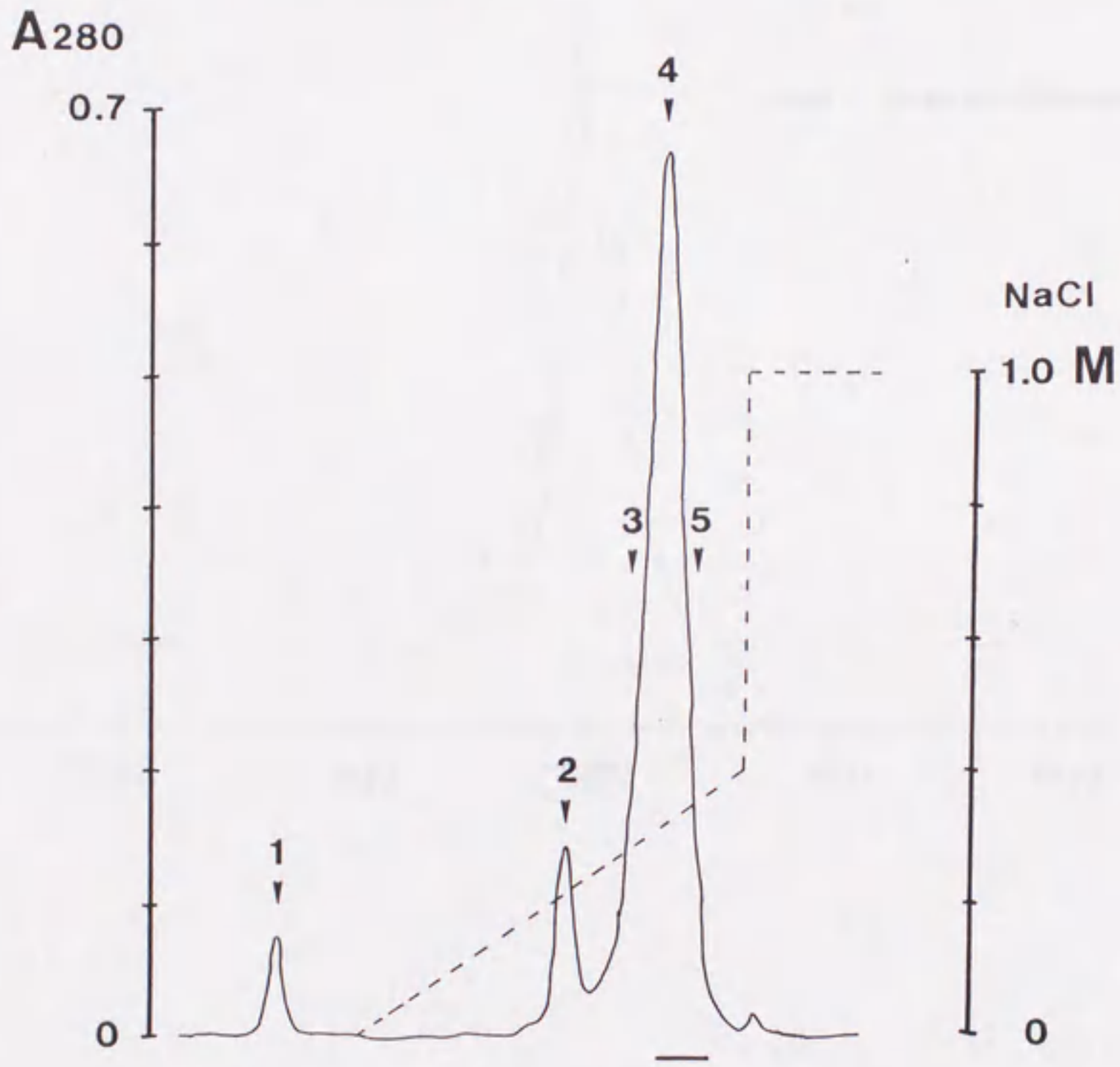

Figure 4-2-1. Chromatography of CNBr-treated products of TnT25k on an SP-sepharose fast flow column. The CNBr-treated product of TnT25k was lyophilized and dissolved in solution A (6 M urea, 50 mM Tris-HCl and 0.1 M NaCl, pH 8.0) and applied to an SP-sepharose fast flow column equilibrated with solution A. T2 fragment was eluted with a linear gradient of 0.1-0.4 M NaCl in solution A. The fractions containing TnT2 fragment, indicated by a bar in the chromatogram were further purified by a gel filtration column.

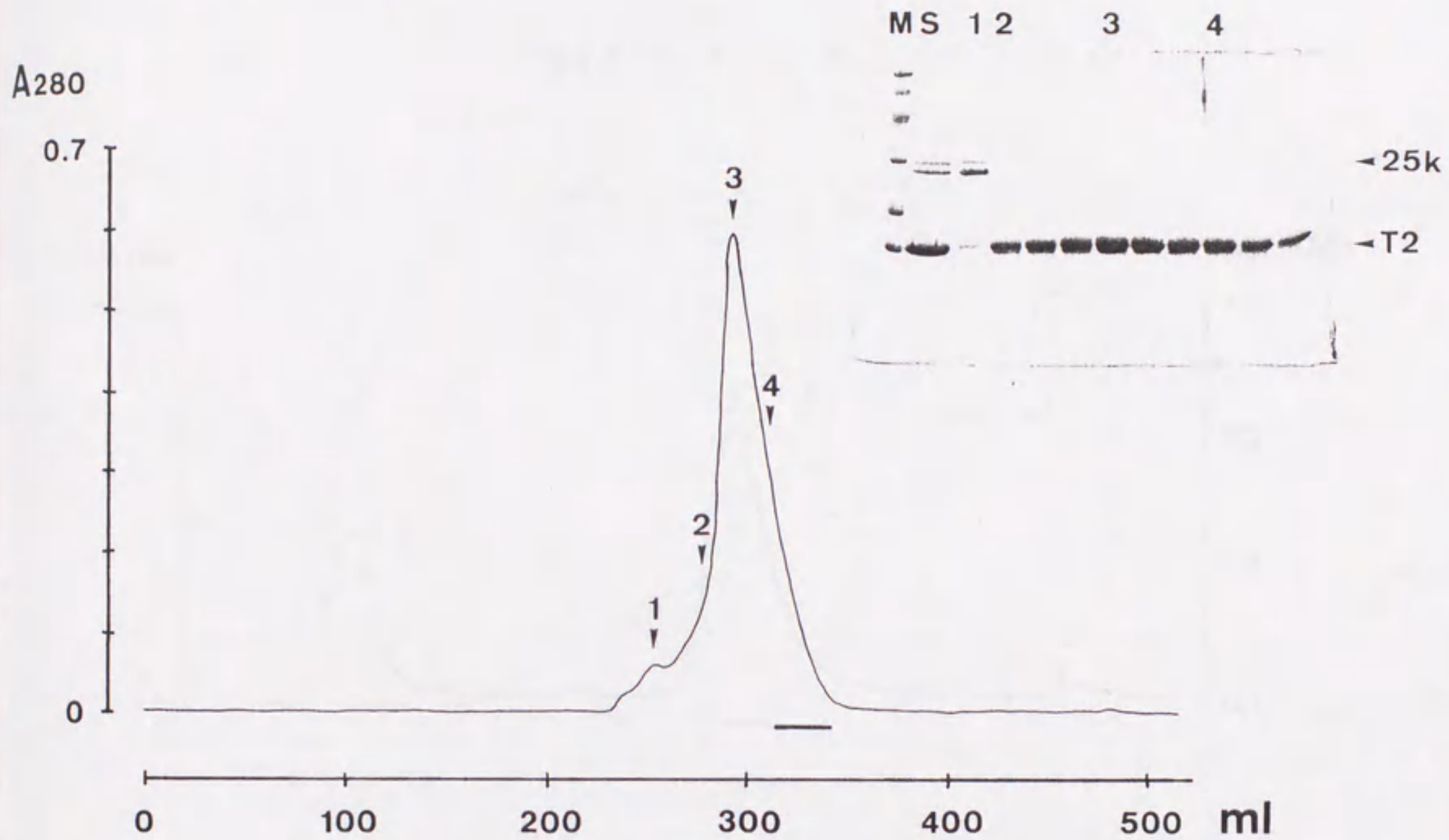

Figure 4-2-2. Purification of TnT2 fragment by a Sephacryl S-100 column. The fractions containing TnT2 fragment, indicated by a bar in Fig. 4-2-1, were concentrated by a centripep concentrator (Amicon) to ~2 ml and loaded on a sephacryl S-100 column (2.5×100 cm) equilibrated with 50 mM Tris-HCl and 0.3 M NaCl, pH 8.0. The fractions containing pure TnT2 fragment indicated by a bar were used for reconstitution of Tn complex.

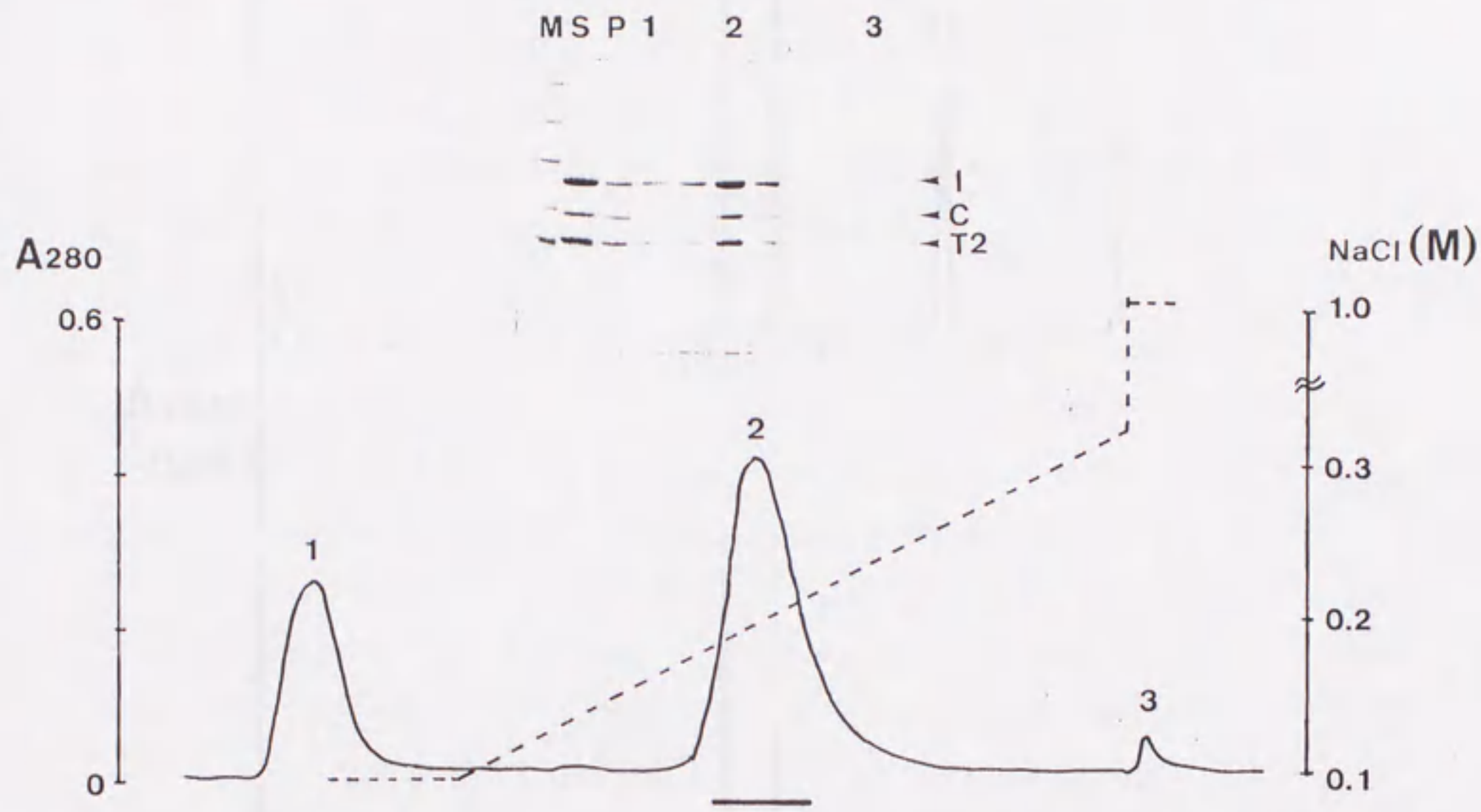

Figure 4-2-4. Isolation of TnT2-TnC-TnI ternary complex by a Q-sepharose fast flow column. TnT2-TnC-TnI ternary complex which was reconstituted as described under "EXPERIMENTAL PROCEDURES" was applied to a Q-sepharose fast flow column equilibrated with 10 mM Tris-HCl, 0.1 M NaCl and 0.1 mM $CaCl_2$, pH 8.0 (the starting solution). TnT2-TnC-TnI ternary complex was eluted with a linear gradient of 0.1-0.3 M NaCl in the starting solution. The fractions indicated by a bar contained predominantly TnT2, TnC and TnI at a ratio of roughly 1:1:1 as indicated by the SDS-PAGE pattern on the top.

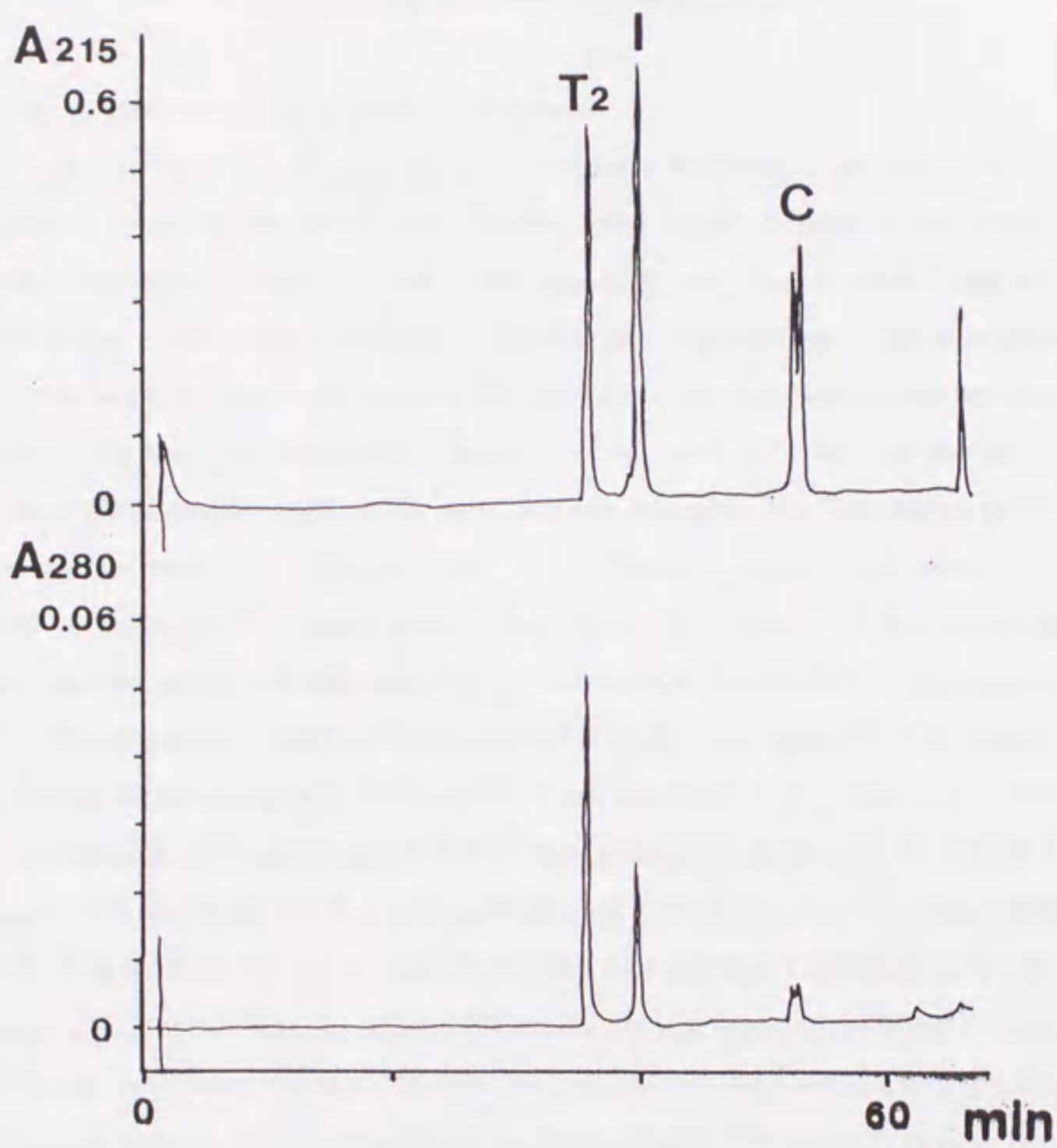

Figure 4-2-5. The stoichiometry of components of TnT2-TnC-TnI ternary complex analyzed by a reversed-phase HPLC column (4.6×100 mm, Aquapore butyl, Brownlee). The purified TnT2-TnC-TnI ternary complex was applied to a reversed-phase HPLC column (equilibrated with 0.1 % TFA) and eluted with a linear gradient of 0-54 % acetonitrile in 0.1 % TFA at a flow rate of 1 ml/min (the gradient of acetonitrile concentration: 0.9 %/min).The effluent was monitored at both 215 nm and 280 nm. Note that, the molar ratio of TnT, TnI and TnC is almost 1:1:1 (The molar ratio was calculated from the molecular extinction coefficient of the each troponin component and the area under each peak at 280 nm).

(IV-3) Isolation of TnI_{1-47} fragment and reconstitution of CI_{1-47} complex.

EXPERIMENTAL PROCEDURES

Cleavage of TnI and isolation of TnI_{1-47} fragment

The property of the TnI_{1-47} fragment was first reported by Syska *et al.* (1975). They produced this fragment by treating TnI, which was isolated from rabbit skeletal muscle, with DTNB (5.5'-dithiobis-2-nitrobenzoic acid) and following with KCN, with the procedure originally described by Jacobson *et al.* (1973). Since the rabbit skeletal muscle TnI has three cysteine residues in its amino acid sequence (Wilkinson and Grand, 1978) and incomplete cleavages would be occurred, the yield of TnI_{1-47} fragment by this method should not be satisfactory for our purpose. Therefore we developed the alternative method for obtaining this fragment. The TnI mutant (C64A, C133S), in which cysteine residues at 48 and at 133 were replaced by alanine and serine, respectively, was purified according to the method already described. This mutant TnI was chemically cleaved at unique cysteine residue at 48, according to the method described by Swenson and Fredrickson (1992), by using 2-nitro-5-thiocyanobenzoic acid (NTCB). This method is more convenient than that described by Jacobson *et al.*(1973) because it is not necessary to use toxic agent, KCN. The protein, at a concentration of 5 mg/ml, was dissolved in a solution containing 0.2 M Tris-HCl, pH 8.0, 4 M guanidine hydrochloride, and 0.2 mM dithiothreitol. NTCB (Sigma) was added to 10-fold excess over the total sulfhydryl groups contained in the buffer and TnI, and the mixture was incubated for 20 min at 37°C; at this time, by adding NaOH, the pH was increased to 9 and the cleavage reaction was allowed to proceed for 6 h. The reaction mixture was then applied to a gel filtration column (Sephacryl S-100, 2.5×50 cm, Pharmacia) equilibrated with 0.3 M NaCl, 10 mM Tris-HCl, pH 8.0. TnI_{1-47} fragment which was eluted with the same solution was further purified by a reverse phase column (10×30 cm, Aquapore Butyl column, Brownlee). TnI_{1-47} fragment thus purified was lyophilized and stored at -20°C.

Reconstitution of CI_{1-47} complex

TnI_{1-47} fragment was mixed with TnC in a molar excess of TnI_{1-47} over TnC in the solution containing 6 M urea, 20 mM Tris-HCl, 5 mM $CaCl_2$, 1 mM dithiothreitol, pH 8.0. Excess amount of TnI_{1-47} fragment over TnC should be mixed in order to avoid an incomplete complex formation. The mixture was then dialyzed consecutively against NaCl solution of 1 M, 0.5 M, 0.3 M, 0.1 M, 0 M each containing 5 mM $CaCl_2$, 10 mM Tris-HCl, 1 mM dithiothreitol, pH 8.0. After dialysis, the protein solution was clarified by centrifugation and then applied to a Sephacryl S-100 (2.5×110 cm) column equilibrated with 10 mM Tris-HCl, 5 mM $CaCl_2$, pH 8.0. The fractions containing CI_{1-47}

complex were identified by SDS-PAGE and the stoichiometry was confirmed on a reversed-phase HPLC. Column.

RESULTS

Isolation of TnI_{1-47} fragment

Fig. 4-3-1 represents an elution profile of chemically cleaved products of TnI (C64A, C133S) from a Sephacryl S-100 column. The former bigger peak contained uncleaved TnI and the C-terminal fragment, while the latter peak contained N-terminal TnI_{1-47} fragment. The fractions containing TnI_{1-47} fragment was further purified by reversed-phase HPLC (data not shown). The yield of TnI_{1-47} fragment after reversed-phase HPLC is about 60 % of the starting material.

Reconstitution of CI_{1-47} complex

Fig. 4-3-2 represents a elution profile of CI_{1-47} complex on a Sephacryl S-100. Fractions containing CI_{1-47} complex (which are indicated by the bar in Fig. 4-3-2) were pooled and concentrated by a centriprep concentrator (Amicon), and used for crystallization. The purity of the preparation was checked by a reversed-phase HPLC column (Fig. 4-4-3). From the extinction coefficients for TnC and TnI, two components existed in the equimolar ratio in the complex.

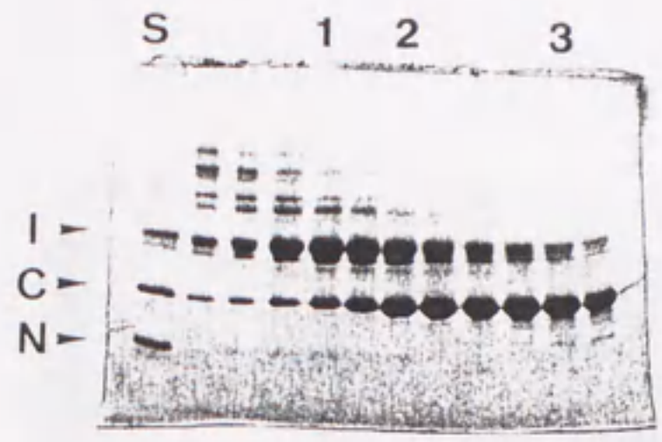

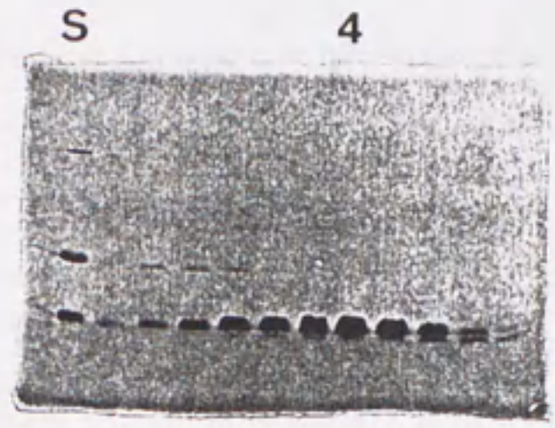

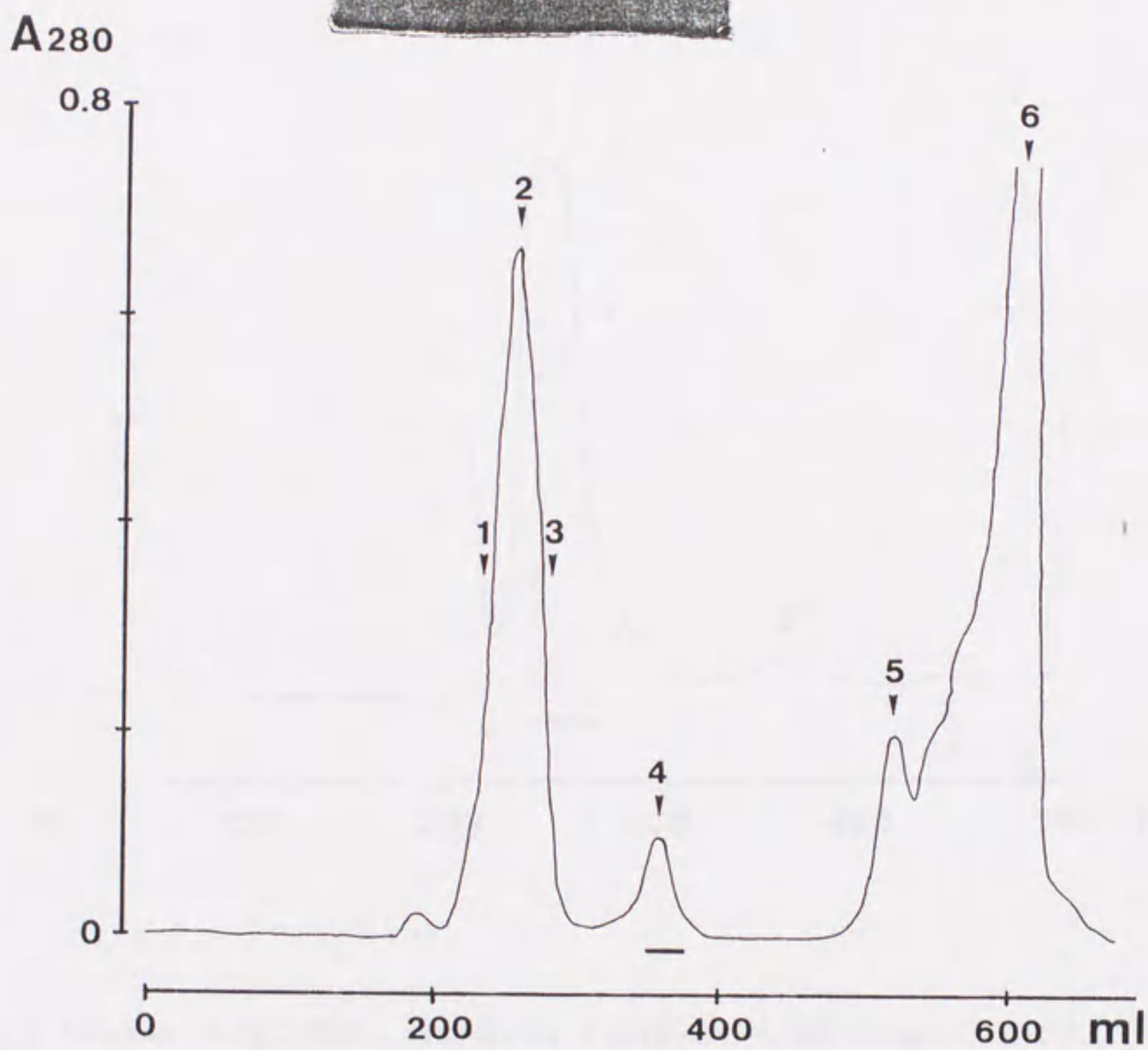

Figure 4-3-1. Purification of TnI_{1-47} fragment by a Sephacryl S-100 column. The NTCB-treated product of TnI (C64A, C133S) was loaded on a Sephacryl S-100 column (2.5×100 cm) equilibrated with 10 mM Tris-HCl, 0.3 M NaCl, pH8.0. The fractions indicated by a bar were further purified by a reversed-phase HPLC column.

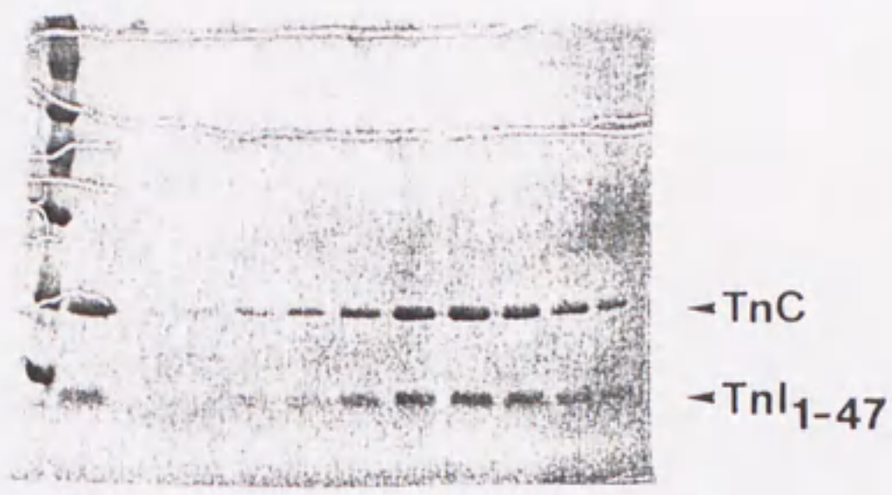

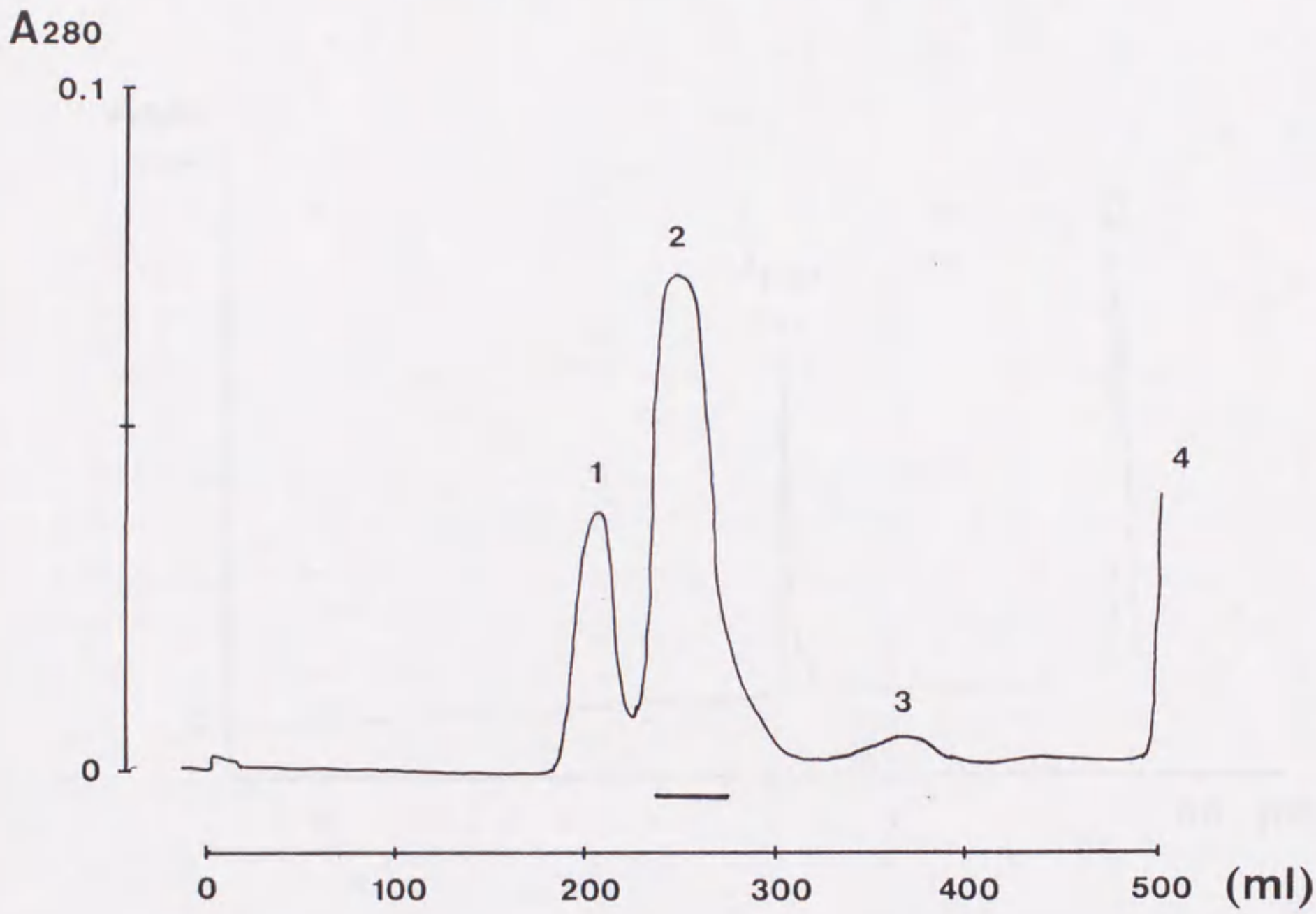

Figure 4-3-2. Isolation of TnC-TnI$_{1-47}$ complex by a Sephacryl S-100 column. TnC-TnI$_{1-47}$ complex which was reconstituted as described under "EXPERIMENTAL PROCEDURES" was applied to a Sephacryl S-100 column (2.5×100 cm) equilibrated with 10 mM Tris-HCl, 5 mM $CaCl_2$, pH 8.0. The fractions indicated by a bar, containing predominantly TnC and TnI$_{1-47}$ at a ratio of 1:1 (see Fig. 4-3-3), were pooled and concentrated by a centripep (Amicon) and used for crystallization trials.

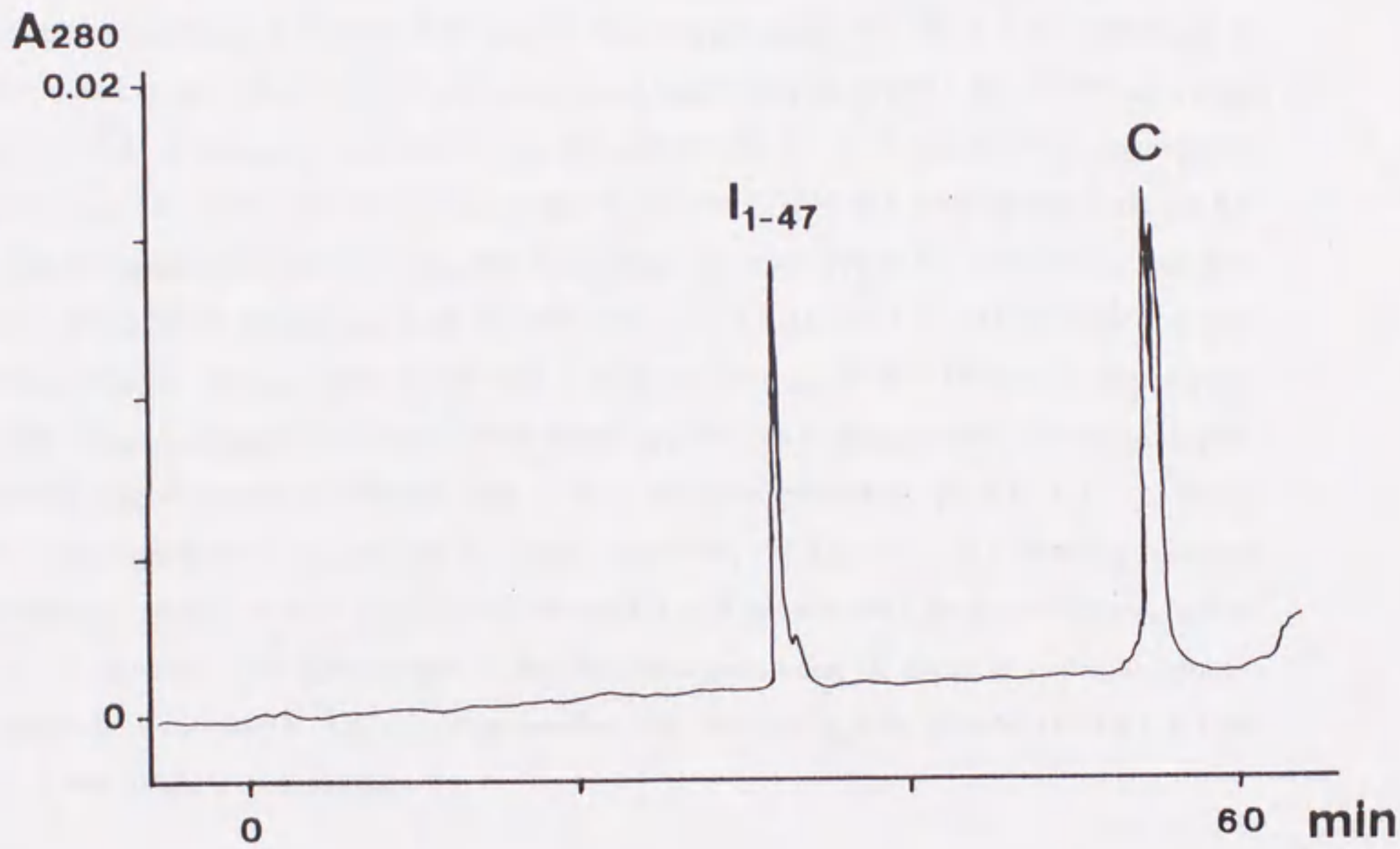

Figure 4-3-3. The stoichiometry of the components in the TnC-TnI$_{1-47}$ complex, examined on a reversed-phase HPLC column (4.6×100 mm, Aquapore butyl, Brownlee). TnC-TnI$_{1-47}$ complex was applied to a reversed-phase HPLC column (equilibrated with 0.1 % TFA) and eluted with a linear gradient of 0-54 % acetonitrile in 0.1 % TFA at a flow rate of 1 ml/min (the gradient of acetonitrile concentration: 0.9 %/min).The effluent was monitored at both 215 nm and 280 nm. Note that, the molar ratio of TnI$_{1-47}$ and TnC is one to one. (Molar ratio was calculated form the molecular extinction coefficient of each troponin component and the area of each peak at 280 nm).

(IV-4) Isolation of $Tm_{141-242}$ and reconstitution of $Tm_{141-242}$T25kCI complex .

EXPERIMENTAL PROCEDURES

Preparation of $Tm_{141-242}$

$Tm_{141-242}$ expressed in bacterial cells was extracted and purified as follows. The cells were suspended in 20 mM Tris-HCl, 25 % sucrose, 1 mM EDTA, 1 mM dithiothreitol, pH 8.0 at a ratio of 5 ml/g wet weight of cells. Lysozyme was added to give a final concentration of 0.5 mg/ml and incubated at room temperatures, until the suspension became viscous. The mixture was sonicated for 5 min, then centrifuged at 30,000 × g for 20 min. Ammonium sulfate was added to the supernatant to 35 % saturation. After centrifugation, the supernatant was heated up to 70°C. The supernatant, after removing heat denatured components, was brought to pH 4.5 to precipitate the fragment of tropomyosin. The pellet obtained was suspended in 20 mM Tris-HCl, 1 mM dithiothreitol, pH 8.0 and dialyzed against the same solution. The preparation was then applied to a Q-sepharose fast flow column (Pharmacia) equilibrated with 20 mM Tris-HCl, 0.1 M NaCl, 1 mM dithiothreitol (the starting solution). $Tm_{141-242}$ was eluted with a linear gradient of 0.1-0.5 M NaCl in the starting solution. $Tm_{141-242}$ containing fractions were further applied to a hydroxylapatide column (Gigapite, Seikagaku-kogyo, Japan) equilibrated with 10 mM potassium/phosphate, pH 6.8. $Tm_{141-242}$ eluted with a linear gradient of 10-300 mM potassium phosphate, pH 6.8. $Tm_{141-242}$ containing fractions were dialyzed against 20 mM Tris-HCl, 0.1 M NaCl, 1 mM dithiothreitol, then re-chromatographed on the Q-sepharose fast flow column under the same conditions as above in order to remove phosphate ions completely. $Tm_{141-242}$ thus purified was dialyzed against 10 mM Tris-HCl, 0.1 M NaCl, 1 mM dithiothreitol, pH 8.0.

Reconstitution and isolation of $Tm_{141-242}$T25kCI

Firstly, troponin ternary complex which contains TnT25k, TnI (C48A; C64A; C133S) and TnC was prepared by the same methods as described for T2CI complex. T25kCI complex was then mixed with $Tm_{141-242}$ in a molar excess of T25kCI complex over $Tm_{141-284}$ in the solution containing 10 mM Tris-HCl, 0.1 M NaCl, 5 mM $MgCl_2$, 1 mM EGTA, 1 mM dithiothreitol, pH 8.0, and dialyzed against 10 mM Tris-HCl, 5 mM $MgCl_2$, 1 mM EGTA, 1 mM dithiothreitol, pH 8.0. The protein solution was clarified by a centrifugation. Glycerol was added to the supernatant to give a final concentration of 20 % to give protein solution a higher density than that of a buffer used in the following chromatography. Then the protein solution was loaded onto a gel filtration column (Sephacryl S-200, 2.5×110 cm, Pharmacia) equilibrated with 10 mM Tris-HCl, 5 mM $MgCl_2$, 1 mM EGTA, pH 8.0. $Tm_{141-242}$T25kCI containing fractions were identified by reversed-phase HPLC

(4.6×100 mm, Aquapore Butyl, Brownlee) and SDS gel electrophoresis.

RESULTS

Preparation of $Tm_{141-242}$

Fig. 4-4-1 represents an elution profile of $Tm_{141-242}$ from a Q-sepharose fast flow column. The $Tm_{141-242}$ containing fractions (indicated by the bar in Fig. 4-4-1) were further loaded on a hydroxylapatide column (Fig. 4-4-2). Resultant purified $Tm_{141-242}$ after re-chromatographed on a Q-sepharose fast flow column were used to reconstitute $Tm_{141-242}$T25kCI complex.

Reconstitution of $Tm_{141-242}$T25kCI

Fig. 4-4-3 represents a elution profile of $Tm_{141-242}$T25kCI complex on Sephacryl S-200 column. $Tm_{141-242}$T25kCI complex containing fractions (indicated by the bar in Fig. 4-4-3) were used for crystallization trials. The components in the complex were analyzed by reversed-phase HPLC (Fig. 4-4-4). From extinction coefficients for these components, $Tm_{141-242}$T25kCI complex had the same stoichiometry (TnT:TnI:TnC:$Tm_{141-242}$ =1:1:1:2; mole peptide/mole complex) of the components as in the muscle filaments.

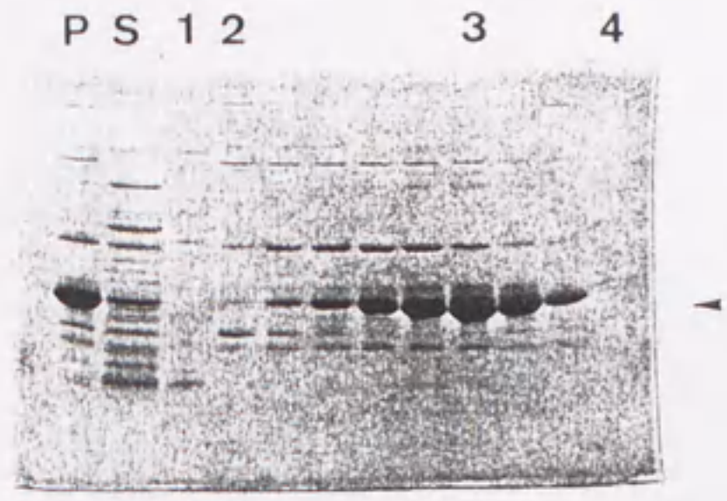

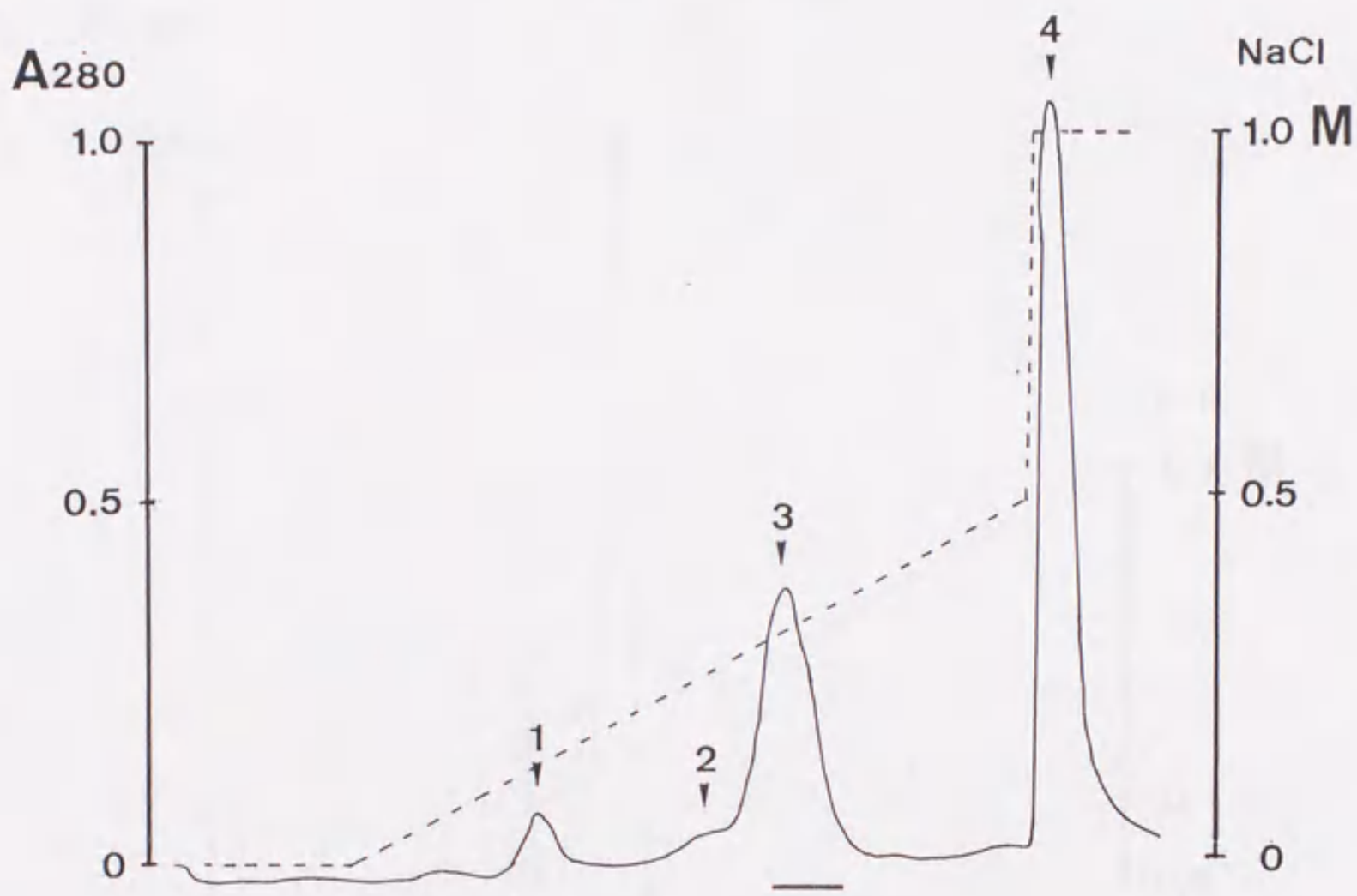

Figure 4-4-1. Chromatography of $Tm_{141-284}$ on a Q-sepharose fast flow column. The precipitant and the supernatant of the protein solution of $Tm_{141-284}$ after isoelectric precipitation are shown in the SDS-PAGE, as P and S, respectively. The precipitant was dissolved in 10 mM Tris-HCl, 0.1 M NaCl, and 0.1 mM $CaCl_2$, pH 8.0 (the starting solution) and was applied to a Q-sepharose fast flow column (1.5×10 cm) equilibrated with the starting solution. $Tm_{141-284}$ was eluted with a linear gradient of 0.1-0.5 M NaCl in the starting solution. The fractions indicated by a bar were further applied to a hydroxylapatite column.

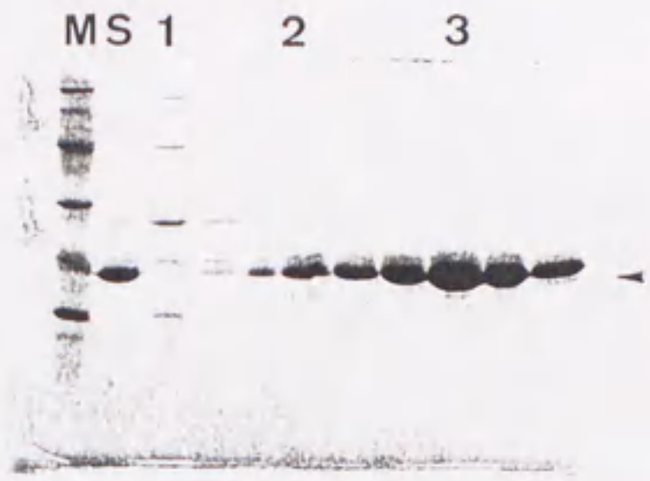

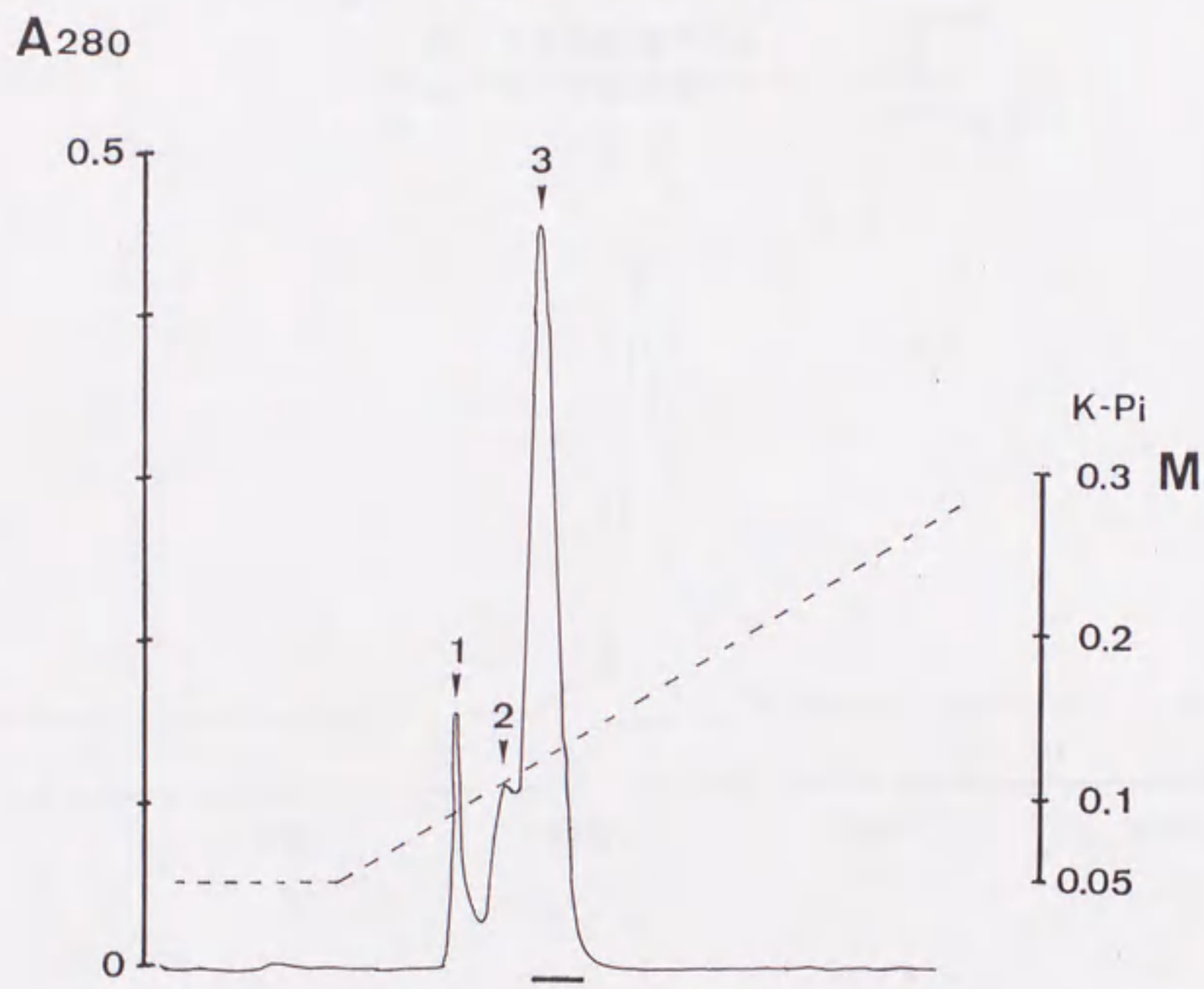

Figure 4-4-2. Chromatography of $Tm_{141-284}$ on a hydroxylapatite column. The fractions containing $Tm_{141-284}$ eluted from the Q-sepharose fast flow column were loaded on a hydroxylapatite column equilibrated with 10 mM potassium phosphate, pH 6.8. $Tm_{141-284}$ was eluted with a linear gradient of 10-300 mM potassium phosphate, pH 6.8. The fractions indicated by a bar were pooled and dialyzed against 20 mM Tris-HCl, 0.1 M NaCl, 1 mM dithiothreitol, then chromatographed on the Q-sepharose fast flow column under the identical conditions described under the legend of Fig. 4-3-3. $Tm_{141-284}$ eluted from the Q-sepharose was used for reconstituting $Tm_{141-284}$T25kCl complex.

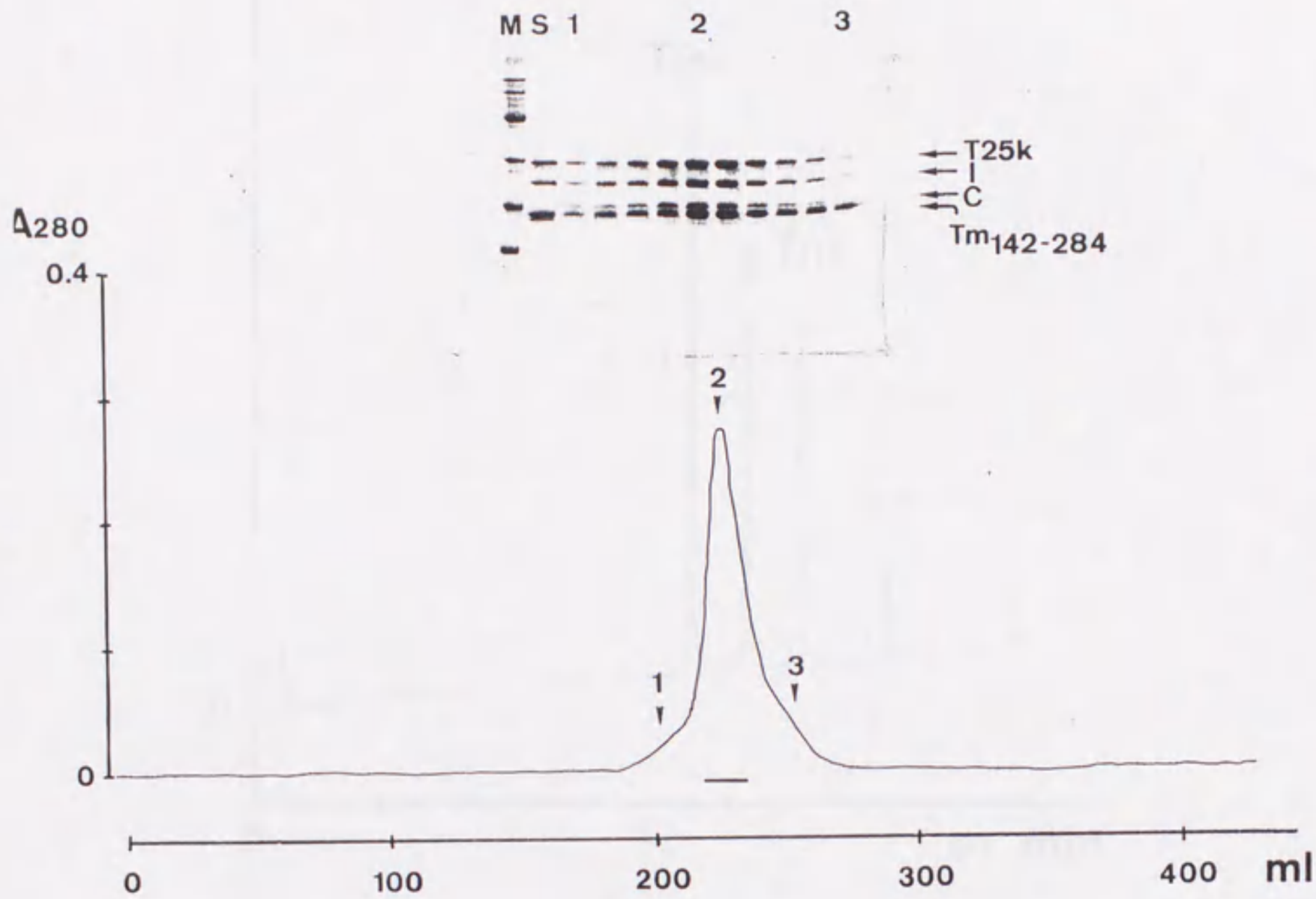

Figure 4-4-3. Isolation of $Tm_{141-284}$T25kCI complex by a Sephacryl S-200 column. $Tm_{141-284}$T25kCI complex which was reconstituted as described under "EXPERIMENTAL PROCEDURES" was applied to a Sephacryl S-200 column (2.5×100 cm) equilibrated with 10 mM Tris-HCl, 1 mM EGTA, and 5 mM $MgCl_2$, pH 8.0. Fractions containing $Tm_{141-284}$T25kCI complex consisting of components at as appropriate stoichiometry were identified by SDS-PAGE. The fractions indicated by a bar were pooled and concentrated by a centripep (Amicon) and used for crystallization trials.

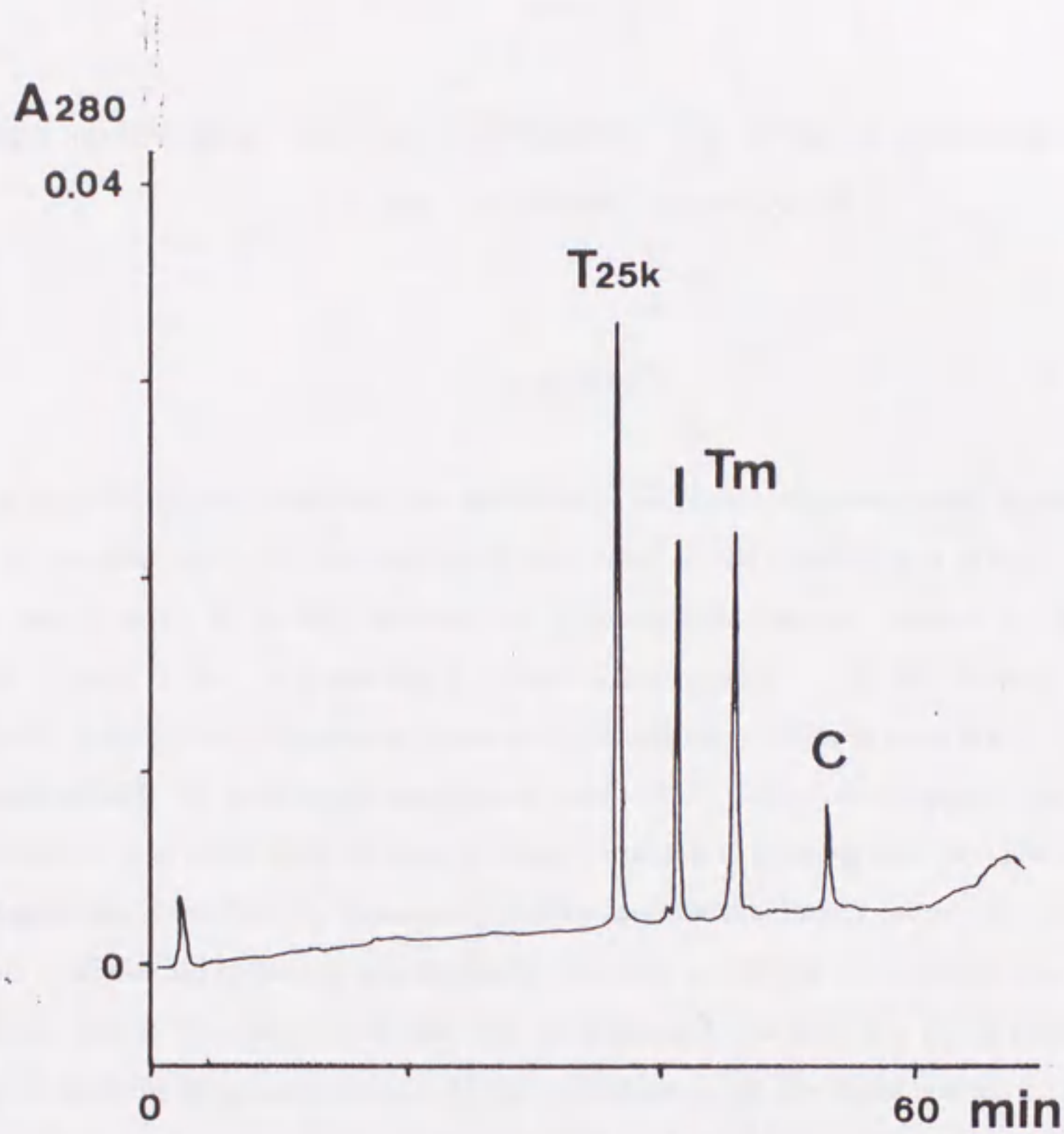

Figure 4-4-4. The stoichiometry of the components of $Tm_{141-284}$T25kCI complex analyzed by a reversed-phase HPLC column (4.6×100 mm, Aquapore butyl, Brownlee). The purified $Tm_{141-284}$T25kCI complex was applied to a reversed-phase HPLC column (equilibrated with 0.1 % TFA) and eluted with a linear gradient of 0-54 % acetonitrile in 0.1 % TFA at a flow rate of 1 ml/min (the gradient of acetonitrile concentration: 0.9 %/min). The effluent was monitored at both 215 nm and 280 nm. Note that, each of troponin and tropomyosin components exists in the equimolar ratio. (The molar ratio was calculated form the molecular extinction coefficient of the each component and the area of the each peak at 280 nm).

【Part V】

Protein Engineering for Structure Determination: Two Different Approaches to Improve A Chance to Obtain Protein Crystals

SUMMARY

Protein engineering has opened up new possibilities for protein crystallography in several different ways; in preparing homogeneous proteins, in improving crystal qualities, and in phasing reflections. In the present study, we have undertaken two different approaches to improve a chance to obtain protein crystals. Firstly, we employed reductive methylation of lysine residues for troponin complexes. Reductive methylation of lysine residues was successfully applied myosin S1 giving rise to crystals suitable for X-ray analysis (Rayment *et al.*, 1993). Their finding suggests the applicability of this method to crystallization of other proteins. First step to examine this, we optimized reductive methylation procedure both for monomeric proteins and for multimeric complexes, using lysozyme, troponin subunits and its complexes. Secondly, we made an attempt to crystallize troponin complex as a fusion protein. Fusion proteins, featuring the combined characteristics of the parental products, have been used for numerous purposes. In the present study, we expressed and purified TnT2 which was fused to maltose binding protein (MBP-TnT2), and reconstituted it into MBP-TnT2-TnC-TnI ternary complex, and tried to crystallize the complex.

So far we have not obtained any crystal of the troponin complex along this line, general applicability of this approach is discussed.

⟨V-1⟩ Reductive methylation of proteins

EXPERIMENTAL PROCEDURES

Reductive methylation of lysine residues

The procedure for reductive methylation employed in the present study is based on the procedures described by Rypniewski *et al.* (1993) and by Rayment *et al.* (1993). A 1 M stock solution of sodium borohydride ($NaBH_4$) was prepared in 200 mM sodium borate buffer, pH 9.0, immediately prior to use. Formaldehyde, purchased as a 20 % solution from Wako, was diluted with 100 mM sodium borate buffer, pH 9.0, to form a 1 M stock solution immediately before use. The protein, at 10 mg/ml was dialyzed against 200 mM sodium borate, pH 9.0 (plus either 0.1 M NaCl for the troponin complex or 0.3 M NaCl for TnT25k and TnI) prior to modification. The protein solution (1 ml) was reductively methylated at 4°C by the sequential addition of 6 μl of the $NaBH_4$ solution and 30 μl of the formaldehyde solution with rapid mixing. The mixture was kept on ice for 10 min, then 6 μl of the $NaBH_4$ solution was added to the mixture. The reaction was allowed to proceed for 20 min on ice. This process was repeated several times until all lysine residues were completely modified. Then, the reaction was quenched by the addition of solid ammonium sulfate to give a final concentration of 75 % saturation, and the resulting precipitant was dialyzed either against 10 mM Tris-HCl, pH 8.0 (for lysozyme and for TnC) or against 10 mM Tris-HCl, 150 mM NaCl, pH 8.0 (for TnT25k, TnI, and for the Tn ternary complex). The modified proteins thus prepared were used for crystallization trials.

Measurements of the extent of labeling of lysine residues

After each cycle of the process, 10 μl of the mixture was applied to a reversed-phase HPLC column (4.6×100 mm, Aquapore buthyl, Brownlee) equilibrated with 0.1 % TFA. The modified protein was eluted with a linear gradient of acetonitrile in 0.1 % TFA. Each of the elusion was monitored at 280 nm, and main peaks of each elusion were collected and lyophilized. Each of the lyophilized proteins was dissolved in 50 mM Tris-HCl, 2 M urea, pH 9.0, then was digested with 1/5000 weight ratio of lysyl endopeptidase (Wako).for 4 hours at 37°C. This protease does not cleave at the modified lysine residues. The reaction was terminated by applying the reaction mixture to a reversed-phase HPLC column (4.6×100 mm, Aquapore buthyl, Brownlee) equilibrated with 0.1 % TFA. The digestion products were eluted from the column with a linear gradient of 0-54 % acetonitrile in 0.1 % TFA.

RESULTS AND DISCUSSION

Reductive methylation of lysine residues

Crystallization of myosin head portion was first reported by Rayment and Winkelmann (1984), however, obtained crystals did not diffract to give an atomic resolution. Therefore, they undertook an alternative approach to the usual ways of obtaining crystals suitable for X-ray crystallography. The protein was subjected to mild chemical modification of amino group of lysine side chains by reductive methylation. This method had been used as a gentle way to introduce a radioactive label into a protein. They optimized procedure for modifying the protein. Furthermore, they evaluated the effects of modification on its functions and the structure in parallel studies both on S1 and on hen egg white lisozyme (White and Rayment, 1993; Rypniewski *et al.*, 1993). Under the conditions, which they employed, almost all lysine residues were converted rapidly to dimethyllysine without detectable modification of other amino acid side chains. The protocol for reductive methylation that we employed was entirely based on what was optimized by them, except for the process of measuring the extent of labeling of lysine residues.

Measurements of the degree of labeling of the lysine residues

To measure the degree of labeling of the lysine residues, Rypniewski *et al.* (1993) employed the calorimetric assay using specific modificators of ε-amino group of lysine side chains. We have developed an alternative method. Firstly, we also chosen hen egg white lysozyme for this investigation. After each cycle of the process, aliquot of the reaction mixture was applied to reversed-phase HPLC. Fig. 5-1-1 A, B, and C shows the elution profiles of modified products after 0, 1, and 2 cycles of modification procedures, respectively. The retention time for each peak (indicated by an arrow) was increased according to the modification cycles. The delay in the retention time was almost saturated after 2 modification cycles. These results indicated that almost all lysine residues were modified after 2 cycles. To confirm this, each peak was collected and further digested with lysyl endopeptidase. After digestion, protein solutions were applied to a reversed-phase HPLC column (Fig. 5-1-2). Although hen egg white lysozyme has 6 lysine residues in its sequence, there were more than 7 components eluted from the column when unmodified lysozyme was applied to the column (A), indicating the digestion was not completed. After 2 cycles, one component became predominant (C). The concentration of acetonitrile to elute this component was identical to that of the protein before digestion (Fig. 5-1-1 C) suggesting this component was not cleaved by lysyl endopeptidase, in other words, the lysine residues of protein was fully modified. The fully modified lysozyme thus prepared was used for crystallization trials.

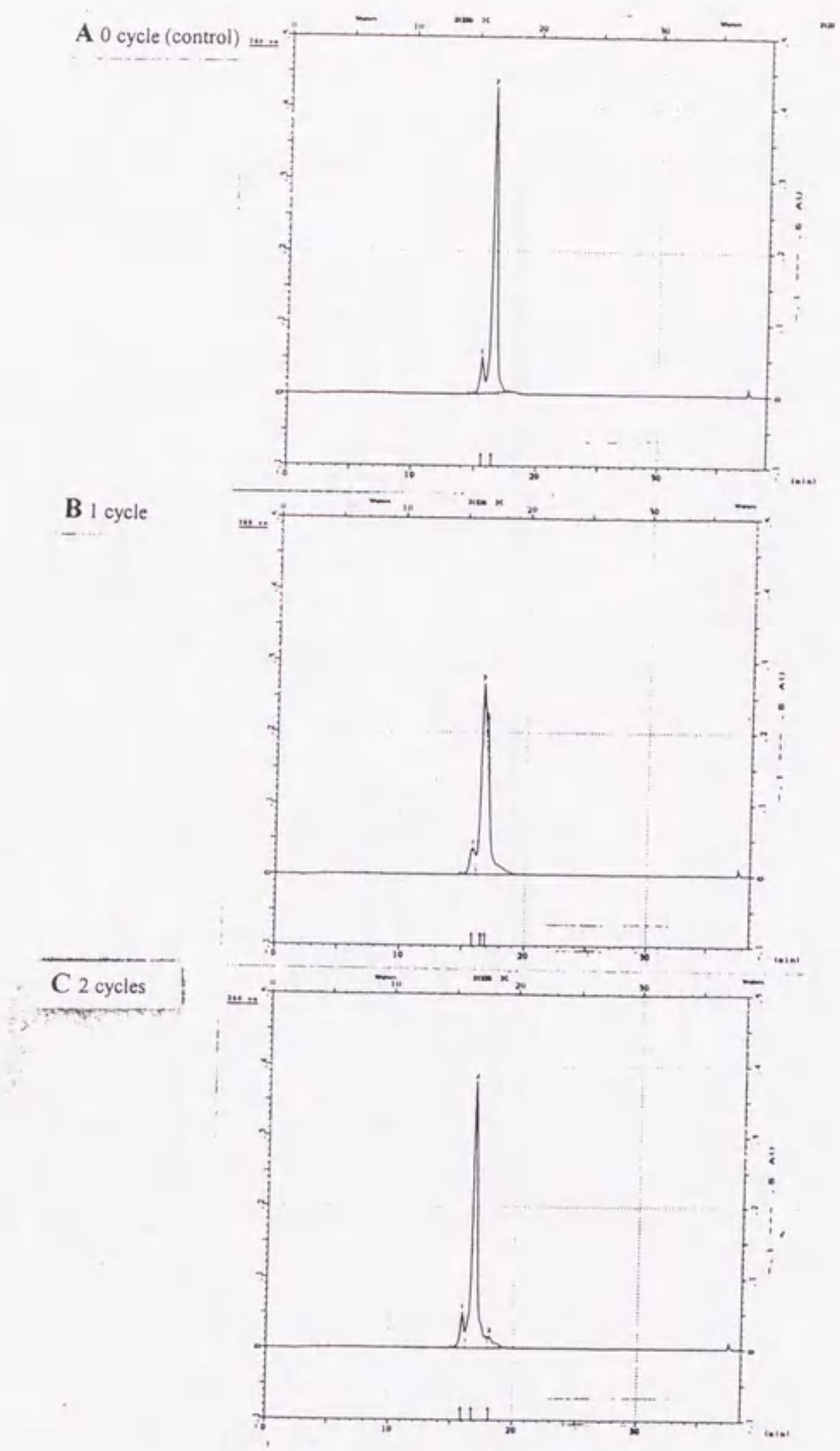

Figure 5-1-1. Elution profiles of reductive methylated hen egg white lysozyme from a reversed-phase HPLC column (4.6×100 mm, Aquapore, C18, Brownlee). Hen egg white lysozyme was reductively methylated according to the method described under "EXPERIMENTAL PROCEDURES", and 10 μl of reaction mixture was applied to reversed-phase HPLC after 0 (A), 1 (B), and 2 cycles (C) of the procedures. The protein was eluted with a linear gradient of acetonitrile in 0.1 % TFA.

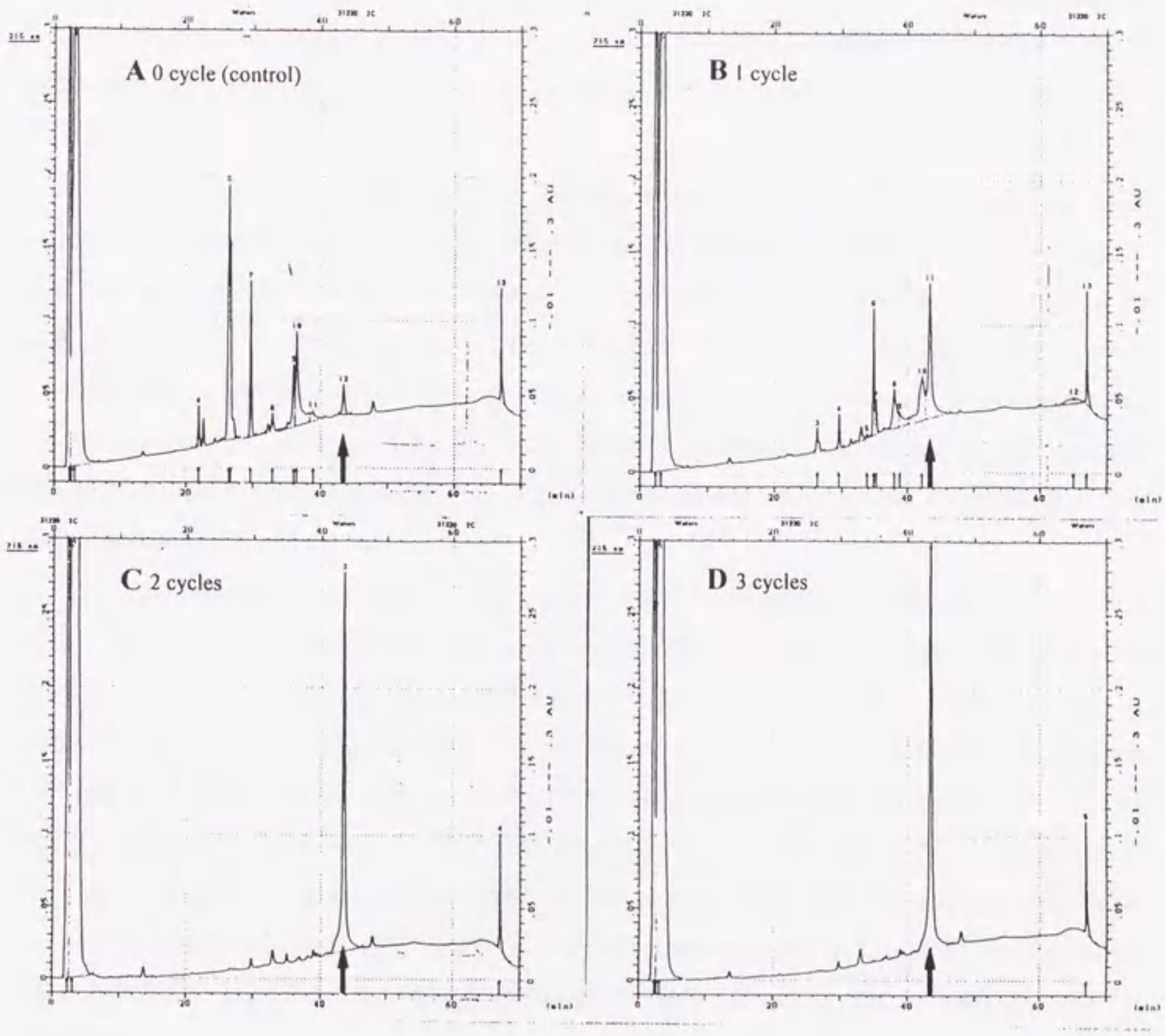

Figure 5-1-2. Elution profiles of Lys-C digestion products of reductive methylated lysozyme. Each of the peak components eluted from the HPLC column (shown in Fig. 5-1-1) was pooled and lyophilized, and digested with lysyl endopeptidase as described under "EXPERIMENTAL PROCEDURES". The digestion products were analyzed on a reversed-phase HPLC column (C18, 4.6×100 mm, Browlee): A, control; B, 1 cycle; C, 2 cycles; D, 3 cycles. The arrowheads indicate the retention time for the molecules without Lys-C digestion.

Crystallization of methylated hen egg white lysozyme

Crystals of hen egg white lysozyme can be grown easily from approximately 1 M sodium chloride, buffered with sodium acetate at pH 4.7. Under these conditions, the protein crystallizes with the lattice belonging to space group of $P4_32_12$ and with the unit cell dimensions of a=b=79.1 Å, c=37.9 Å, $\alpha=\beta=\gamma=90^\circ$.

Rypniewski *et al.* (1993) reported that the methylated lysozyme never crystallized under the conditions described above, while crystallized from the solution containing 2.2 M $MgSO_4$ and 50 mM Tris-HCl at pH 8.0. The protein crystallizes with the lattice belonging to space group of $P2_12_12_1$ with the unit cell dimensions of a=30.6 Å, b=56.3 Å and c=73.2 Å. From the structural analysis, it became apparent why the methylated protein did not crystallize in the same space group. Because in the space group $P4_32_12$, Lys116, which has low temperature factors, was packed near a symmetry related molecule, the amino acid residues in this region can not accommodate the addition of two methyl groups to Nζ of Lys116.

We repeated the experiment. For crystallization, the hanging-drop method was employed at 16°C by mixing the protein solution, either the methylated lysozyme (5 mg/ml in 10 mM Tris-HCl, pH 8.0) or the native molecule (7 mg/ml in distilled water), with the reservoir solution containing either 1.0-2.0 M NaCl or 1.0-1.8 M $MgCl_2$, and either 0.1 M sodium acetate (pH 4.6) or 0.1 M Tris-HCl (pH 8.0). Clusters of rod-shaped crystals of the methylated lysozyme were grown form 1.8 M $MgSO_4$ solutions buffered with 0.1 M Tris-HCl, pH 8.0, while no crystals of the native molecule were obtained under these conditions. These crystals showed very similar appearance with those reported by Rypniewski *et al.* (1993). On the contrary, in the presence of 1.0-2.0 M NaCl buffered either with 0.1 M Tris-HCl or 0.1 M sodium acetate, the native lysozyme was crystallized, while the methylated molecule did not give crystals with a visible size. Although tiny crystals of the methylated lysozyme were identified in the drop containing 2 M NaCl and 0.1 M sodium acetate at pH 4.6, under a polarizing microscope, they never grew any larger. Rod-shaped crystals of the methylated lysozyme grown form 1.8 M $MgSO_4$ were further examined by X-ray (data not shown). Diffraction patterns obtained in the present study were indistinguishable from those obtained by Rypniewski *et al.* (1993).

Reductive methylation of lysine residues in the troponin complex

We employed this procedure for the troponin complex, hoping that a better crystal form is obtained from the protein.

A

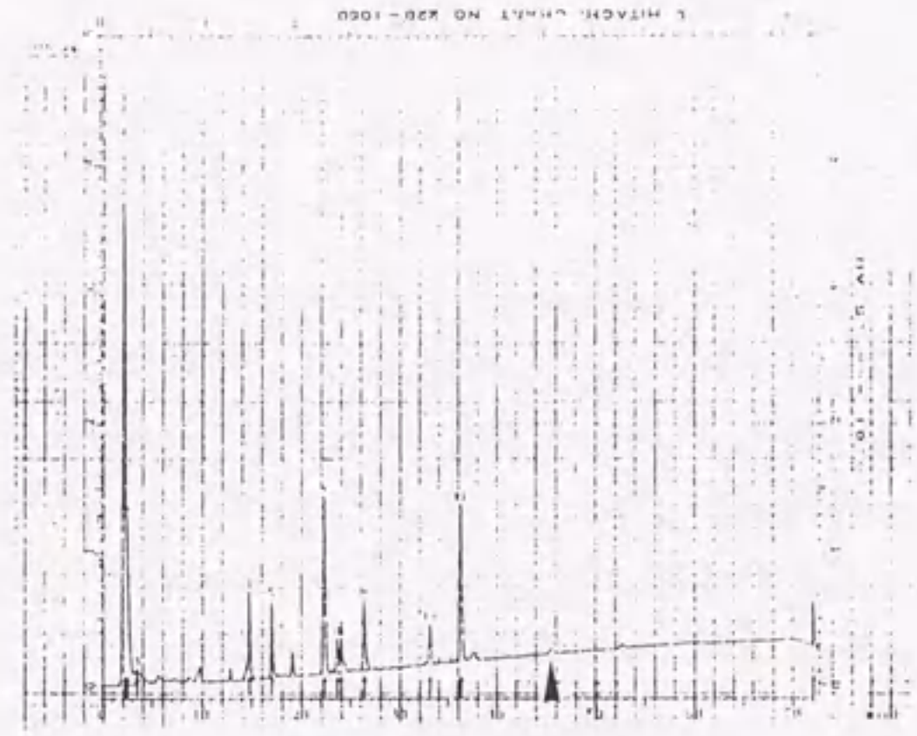

B

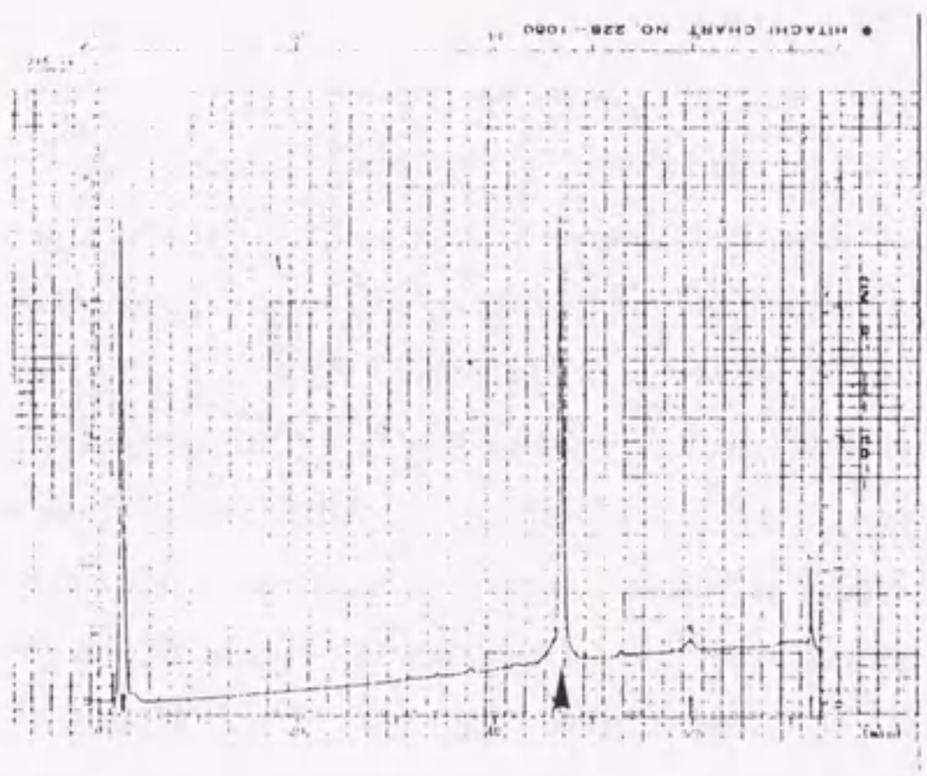

Figure 5-1-3. Elution profiles of Lys-C digestion products of reductive methylated TnI. TnI was reductively methylated, and 10 μl of the reaction mixture was applied to a reversed-phase HPLC column (Aquapore C18, 4.6×100 mm, Brownlee) after 0-5 cycles of the modification procedures. Fractions under each peak were pooled, lyophilized, and digested with lysyl endopeptidase as described under "EXPERIMENTAL PROCEDURES". The digestion products were analyzed on reversed-phase HPLC: A and B show the elusion profiles of the digestion products of the unmodified TnI and those of methylated TnI after 3 cycles. The arrowheads indicate the retention time for the molecules before Lys-C digestion.

Firstly, we modified each of troponin subunits in the absence of other troponin components. After 3 cycles of the procedure, lysine residues in TnI was shown to be fully modified (Fig. 5-1-3). Each of TnC and TnT25k was also shown to be fully modified after 5 and 3 cycles of the procedure, respectively (data not shown).

Secondly, we performed modification procedure on the troponin ternary complex. TnT25k-TnC-TnI complex, of which each subunit was expressed in *E. coli* (see part IV), was used in this study. Fig. 5-1-4 represents the elusion profiles of either troponin components (A, C) or Lys-C digestion products of troponin components (B, D) from a reversed-phase HPLC column. Each component of modified protein eluted from the column with longer retention times (C) than those of unmodified protein (A). Lys-C digestion of unmodified troponin complex resulted in numerous peaks on the chromatogram (B) because the troponin complex contains 70 lysine residues in total (TnT25k, TnI and TnC contain 37, 24 and 9 lysine residues, respectively). On the other hand, Lys-C digestion of the methylated troponin complex gave rise to only four major peaks (D). Comparing C and D, three of the major peaks in D were identified as fully methylated TnT25k, TnI and TnC. The results indicating that almost all lysine residues within the troponin complex were accessible for formaldehyde, in other words, exposed to the solvent. The component eluted from the column just before the fully methylated TnC, seems to be one of the digestion products of partially methylated TnC. When the peak corresponding to the methylated TnC in the chromatogram C was isolated and digested with Lys-C, identical two peaks were observed, which showed the retention time of approximately 60 min, being close to that of undigested TnC (data not shown). Additional several cycles of the procedure did not result in full modification of TnC. We do not know the reason why TnC could not be fully modified. There are nine lysine residues in rabbit skeletal TnC. Three of them form a cluster in the central helix (Lys-84, 88, 90) and the remaining six are equally distributed between the N-terminal (Lys-20, 37, 52) and the C-terminal (Lys-136, 140, 153) domain. Two lysines, Lys-37 in the N-domain and Lys-140 in the C-domain, respectively, are located in the Ca^{2+}-binding loops. We have not identified which residues are not modified, although the apparent molecular weight of these two peaks on the SDS-PAGE gel indicated that the unmodified lysine residue(s) might be near N- or C-terminus. Myosin S1 was crystallized in spite of incomplete methylation (four unmodified lysine residues were identified in the crystallization sample), so we tried to crystallize methylated troponin complex thus prepared. Unfortunately, just after starting crystallization experiments, we noticed that this protein sample, methylated TnT25k-TnC-TnI complex, degraded into smaller complexes, mostly into TnT2-TnC-TnI complex. Because we could not remove the proteolytic activity, which was associated with this preparation, by the use of proteolytic inhibitors, we gave up the search for crystallization conditions.

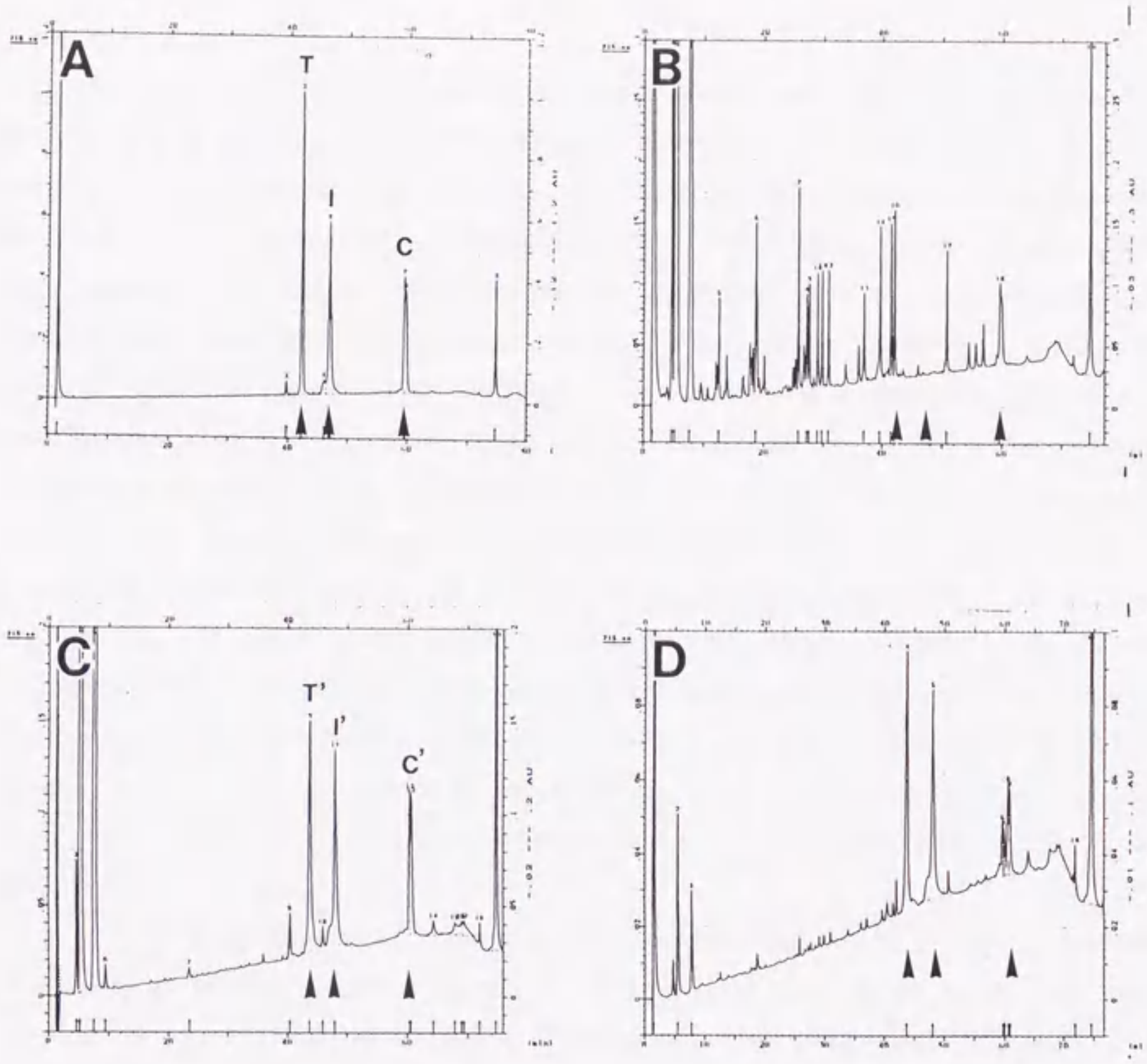

Figure 5-1-4. Elusion profiles of Lys-C digestion products of reductive methylated troponin ternary complex (TnT25k-TnC-TnI) from a reversed-phased HPLC column. Troponin complex was reductively methylated, and 10 μl of reaction mixture was applied to a reversed-phase HPLC column (Aquapore C18, 4.6×100 mm, Brownlee) before (A) and after 5 cycles of the procedures (C). And another 10 μl of reaction mixture, taken before and after 5 cycles of the modification procedures, was digested with lysyl endopeptidase as described under "EXPERIMENTAL PROCEDURES". The digestion products were analyzed on reversed-phase HPLC: B and D show the elusion profiles of the digestion products of the unmodified TnI and those of methylated troponin complex after 5 cycles, respectively. The arrowheads indicate the retention time for the molecules before Lys-C digestion.

Further possibility

Most of chemical modification experiments that have been performed have focused on the changes produced in local areas of a protein such as active site of an enzyme with the goal of understanding a catalytic mechanism rather than observing the global changes in the molecule as a whole. Moreover, chemical modifications have not been adopted to solve a crystallization problem except that they have been used to introduce the heavy atoms into the crystals. This chemical modification approach, reductive methylation of lysine residues, produces limited changes in the overall enzymatic properties (White and Rayment, 1993) and results in little three-dimensional structural alternation as well (Rypniewski *et al.*, 1993). These results indicated the general applicability of this method to change the crystal forms and/or to improve the quality of the crystals. The changes in the surface property of the proteins might result in making new contacts which allows the protein to be crystallized. Amino acid substitutions also can change the surface properties of the proteins, unfortunately, it is very difficult to predict which amino acid residues to change by site directed mutagenesis. Therefore, reductive methylation might be useful for the proteins of which the three-dimensional structure have not been solved. So far we have not yet obtained crystals of methylated troponin complex, other proteins might be crystallized along this line. We have not yet tried modification of T2C1 complex, it might be possible to improve the quality of the crystals by this method.

Specific modification of lysine side chain would also be useful for obtaining structural information of the protein. The measurements of the relative reactivity of lysines with acetic anhydride were used to study the interactions of the troponin subunits (Hichcock, 1981; Hichcock *et al*, 1981; Hichcock-DeGregori, 1982). In those studies, relative reactivity was elucidated from the differential labeling of proteins with isotopically different acetic anhydride, *i. e.*, ^{14}C-labeled and ^{3}H-labeled molecules. The analysis was too complicated to map the interaction sites precisely. We propose here an alternative method to study the interaction sites of multimeric proteins. As described above, modified lysines would be detected by proteolysis. Controlling the degree of labeling, we expect different protelytic peptides would be obtained by this procedure. The peptides thus obtained would be assigned directly by applying them to a liquid chromatography/electrospray massspectrometory apparatus. From the assignments of the peptide, we would calculate the relative reactivity of the lysine residues. The acetylated lysines by acetic anhydride would also be detected by this method. Comparing two modification methods, reductive methylation would be milder than acetylation by acetic anhydride. Because acetylation by acetic anhydride converts positively charged lysine side chains to uncharged products, the modification itself might affect the protein structure. The information about the interfaces of the multimeric protein would be useful for understanding the interactions of each subunits, thus this approach would be useful for other protein systems.

⟨V-2⟩ Crystallization of troponin complex as a fusion protein

EXPERIMENTAL PROCEDURES

Expression and purification of MBP-TnT2

An expression plasmid pTrc-MBP-TnT2, which is constructed by my collaborator, was used in this study. *E. coli* AD202 was transfected with expression plasmid pTrc-MBP-TnT2 and cells were grown in LB medium containing 50 μg/ml of ampicillin at 37°C. At a cell density of OD_{600}=0.4, IPTG (isopropyl-1-thio-β-D-galactopyranoside) was added to give a concentration of 0.4 mM, and the cells were allowed to grow for additional 18 hours. Expressed MBP-TnT2 went into soluble fraction in the bacterial cells. Cells were washed twice with the solution containing 50 mM Tris-HCl, 5 mM EDTA, pH 7.3, and then suspended in the same solution at a ratio of 5 ml/g wet weight cells. Lysozyme was added to give a final concentration of 0.5 mg/ml. The suspension was incubated at room temperatures for 1 hour, then sonicated to break the cells. The suspension was then centrifuged at 30,000 × *g* for 20 min, and the resultant supernatant was loaded on an amylose resin column (2.5×10 cm, amylose resin, Biolabs, New Zealand) equilibrated with 20 mM Tris-HCl, 0.2 M NaCl, 1 mM dithiothreitol, pH 7.3 (solution A). The column was washed with 5 column volume of solution A, then MBP-TnT2 was eluted with solution A plus 10 mM maltose. The protein thus isolated was dialyzed against 10 mM Tris-HCl, pH 8.0 and stored at -20°C until use.

Reconstitution of MBP-TnT2-TnC-TnI ternary complex

Reconstitution of MBP-TnT2-TnC-TnI ternary complex is performed as follows. MPB-TnT, which is prepared as described above, was mixed with TnC-TnI binary complex, which is prepared as described in part I, in a molar excess of MBP-TnT2 over TnC-TnI complex in the solution containing 6 M urea, 1 M NaCl, 20 mM Tris-HCl (pH 8.0), 5 mM $CaCl_2$, 1 mM dithiothreitol. The mixture was then dialyzed consecutively against NaCl solution of 1M, 0.7 M, 0.5 M, 0.3 M, and 0.1 M each containing 5 mM $CaCl_2$, 20 mM Tris-HCl (pH 8.0), 1 mM dithiothreitol. After dialysis, the protein solution was clarified by the centrifugation and then applied to a Q-sepharose fast flow column (1.5×10 cm) equilibrated with the same solution. MBP-TnT2-TnC-TnI ternary complex was eluted by a gradient of NaCl from 0.1 to 0.3 M. The fractions containing MBP-TnT2-TnC-TnI ternary complex were pooled and dialyzed against 10 mM Tris-HCl, pH 8.0 for 24 hours, then dialyzed against distilled water for 24 hours. The preparation was concentrated to about 20 mg/ml, and then used for crystallization. The complex was identified by SDS-PAGE and the stoichiometry was confirmed on reversed-phase HPLC.

RESULTS

Isolation of MBP-TnT2

Fig. 5-2-1 shows the elution profile of MBP-TnT2 on an amylose column. The MBP-TnT2 containing fractions (indicated by a bar) were pooled and used for reconstituting ternary troponin complex. After purification by an amylose column, more than 50 mg of protein was obtained from 1 liter bacterial culture.

Reconstitution of MBP-TnT2-TnC-TnI ternary complex

Fig. 5-2-2 shows the elution profile of MBP-TnT2-TnC-TnI ternary complex on a Q-sepharose fast flow column (1.5×10 cm). Excess MBP-TnT2 was eluted in the flow through fraction, while MBP-TnT2-TnC-TnI ternary complex was adsorbed to the column and eluted with by a gradient of NaCl from 0.1 to 0.3 M. The fractions containing MBP-TnT2-TnC-TnI ternary complex (indicated by a bar) were pooled and used for crystallization. MBP-TnT2-TnC-TnI ternary complex thus purified still possessed the ability to bind to amylose column (data not shown), suggesting the procedure of denature-renature did not result in the deformation of the molecule. Therefore we thought the preparation would be structurally homogeneous enough for crystallization.

Crystallization of MBP-TnT2-TnC-TnI ternary complex

MBP-TnT2-TnC-TnI ternary complex showed increased solubility. TnT2-TnC-TnI complex, isolated by a procedure as described in part IV-2, can be solved in 0.1 M NaCl without buffers, while precipitated without adding 0.1 M NaCl. On the contrary, MBP-TnT2-TnC-TnI was even soluble after dialysis against distilled water. The increased solubility, which would be solely due to MBP portion, would be an advantage in searching for crystallization conditions because of simplicity of protein solution.

Although search for the crystallization condition was performed as described under "EXPERIMENTAL PROCEDURES" in part III, so far we have not yet obtained any crystal from MBP-TnT2-TnC-TnI complex.

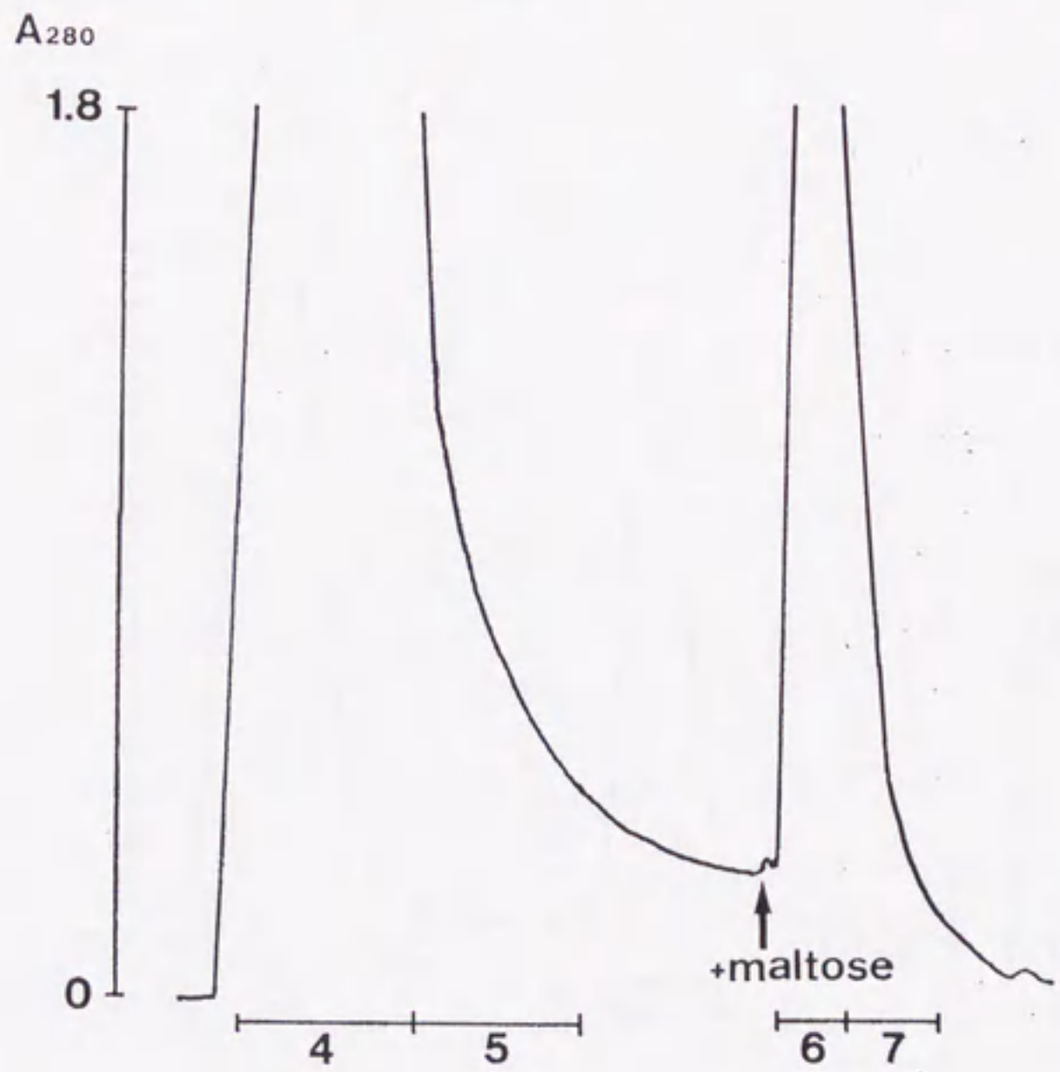

Figure 5-2-1. Isolation of MBP-TnT2 by an amylose column. Soluble fraction of the cell lysate was extracted and applied to an amylose column as described under "EXPERIMENTAL PROCEDURES". Lane 1, molecular weight markers; lane 2 and 3, cell lysate; 4-5, the fractions indicated by bars in the chromatogram. Fractions 6 and 7 were pooled and used for further experiments.

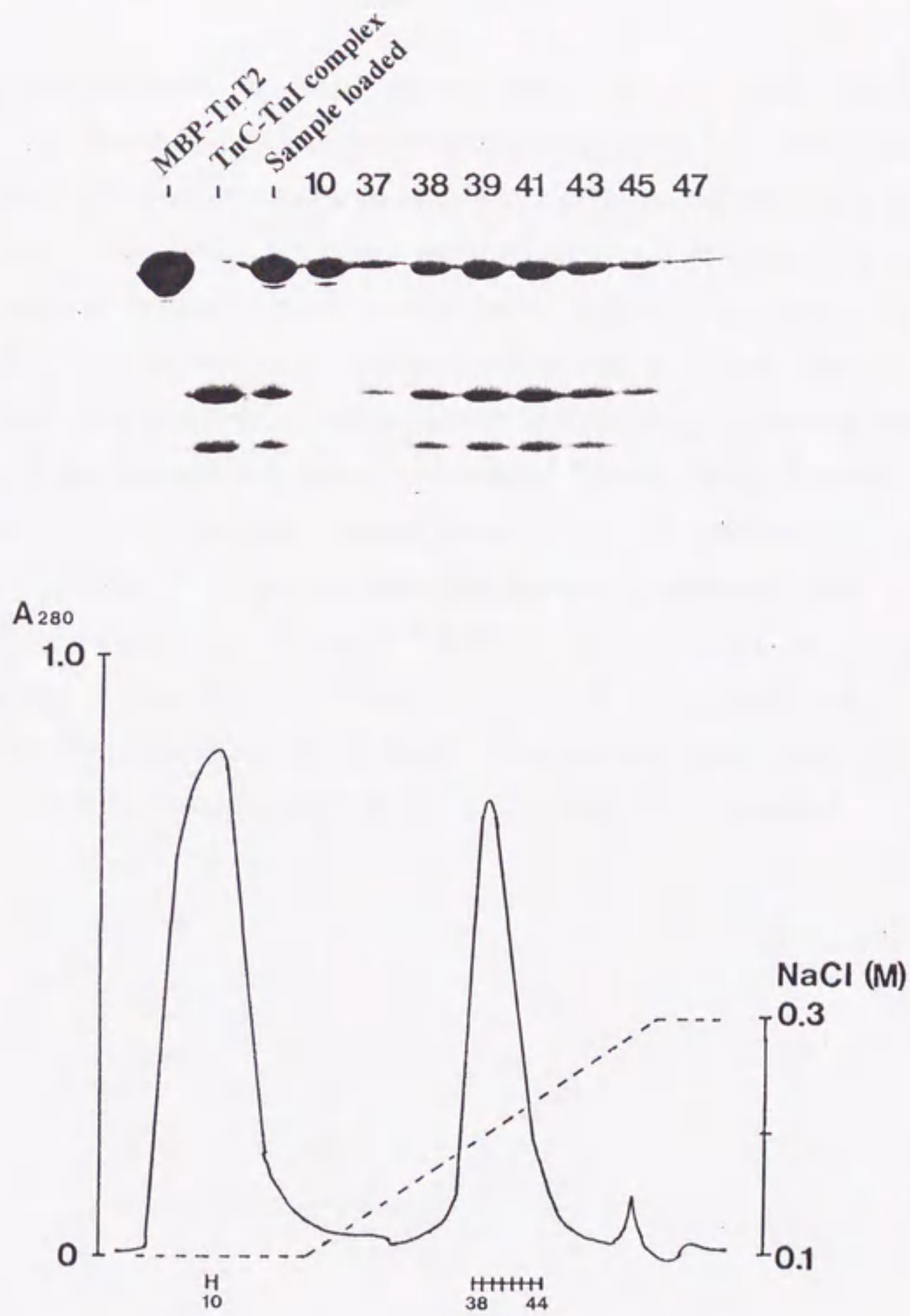

Figure 5-2-2. Isolation of MBP-TnT2-TnC-TnI ternary complex by a Q-sepharose fast flow column. MBP-TnT2-TnC-TnI complex which was reconstituted as described under "EXPERIMENTAL PROCEDURES" was applied to a Q-sepharose fast flow column (1.5×10 cm) equilibrated with 10 mM Tris-HCl, 0.1 M NaCl, 5 mM $CaCl_2$, pH 8.0 (the starting buffer). MBP-TnT2-TnC-TnI ternary complex was eluted with a linear gradient of 0.1-0.3 M NaCl in the starting buffer. Fractions 38-45 were pooled and used for further experiments.

DISCUSSION

Gene fusion techniques allow the production of recombinant proteins featuring the combined characteristics of the parental products. These techniques are not only used to facilitate the recovery of the proteins but also used to enhance the solubility and/or the stability of the molecules (for review, see Nilsson *et al*, 1992). We started the study using a fusion protein in the hope of a universal structural determination domain, which can be engineered onto the cloned proteins to promote solubility in expression systems, allow rapid affinity purification, add possible lattice contacts for crystal growth, and bind a heavy metal with high specificity and avidity for isomorphous replacement or anomalous scattering phase determination. Similar approach has been made in the structural determination of cytochrome c oxidase (Iwata *et al.*, 1995; Ostermeier *et al.*, 1995). They attempted to co-crystallize cytochrome c oxydase with antibody F_v fragment in order to improve the likelihood for obtaining crystals. Binding of antibody fragment could not only allow rapid purification but also increase polar surface which is involved in the crystal contact of membrane proteins. Although the methodology undertaken by them are substantially different from that of fusion proteins, both aim at the same goal to find such a "crystallographer's stone"

CONCLUDING REMARK

In the field of muscle research, it is remarkable that principle actors in the contractile apparatus, actin and myosin have been analyzed at an atomic resolution. On the contrary, high resolution models of the regulatory system have not been available for nearly 30 years since its discovery. The goal of the present study is to elucidate the three-dimensional structure of troponin complex by the use of X-ray crystallography in order to understand the mechanism of regulation at molecular level. Crystallization of proteins is still the "bottle neck" in the structure determination. To overcome this obstacle, I have designed several kinds of troponin complex based on biochemical data, prepared them using protein engineering techniques and attempted to crystallize them. As a consequence of these attempts, three species of complexes were reproducibly crystallized. Diffraction of the crystals of TnC-TnI_{1-47} complex, grown in the presence of sodium-citrate, has improved to 2.3 Å resolution, and structural analysis is now under way.

We have also made another attempts to elucidate the domains of troponin complex by the use of limited proteolytic digestion. We found that the complex consisting of TnT2, TnC and $TnI_{Ca-frag}$ (TnI residues 1-134), which was produced by limited chymotryptic digestion of Tn complex in the presence of Ca^{2+} and Mg^{2+}, retained the function of Ca^{2+}-dependent regulation on acto-S1 ATPase activity. We think this catalytic core domain is suitable for crystallization experiments because this domain not only retains the function of Ca^{2+} regulation but also has a higher stability for enzymatic digestion. Now we are trying to crystallize this complex.

To improve the crystallizability of troponin complex, we have undertaken two different approaches: reductive methylation of lysine residues and crystallization as a fusion protein. These new methodology have been developed to improve the diffraction quality and the crystallizability of proteins.

Now, not only crystallographers but also biochemists have much desire for the common strategies and the methodologies to obtain crystals suitable for X-ray crystallography in view of central importance of for understanding the molecular basis of cellular phenomena. I hope the approaches which we have taken in the present study, designing the crystallization samples and preparing the samples by the use of protein engineering techniques, would be useful for crystallizing other proteins.

謝辞

名古屋大学臨海実験所所長、林　博司教授には私が初めて研究の道に足を踏み入れて以来 5 年余りの間、研究の面白さと厳しさを教えて頂きました。そして研究上だけでなく人生の先輩として、多くの事を学ばさせて頂きました。後期課程での私の学外での研究活動を快く認めて頂いたことを非常に感謝いたします。

松下電器国際研究所所長、前田雄一郎博士には、本研究を行う機会を与えて下さった上、必要なもの全てを提供して頂き、何不自由を感じることなく研究を進める事が出来ましたことを非常に感謝いたします。本研究の指針を示して頂き、また本学位論文執筆にあたっては数多くの有意義な議論と本文の詳細な推敲をして頂きました。

松下電器国際研究所、前田佳代博士には本研究で用いた蛋白質の発現系、および変異体を作成して頂きました。小林智芳博士には、生化学実験の手ほどき、非常に多くの有意義な議論、論文の作成と多大な技術の伝授とご指導を頂きました。西條由見子研究員には、蛋白の精製、結晶化等多くの技術的補助をして頂きました。また、今田勝巳博士、光岡薫博士、小田俊郎博士、広瀬恵子博士、山本和弘研究員、佐野健一研究員、牧野浩司氏には研究を進める上で有意義な助言を頂きました。

マックスプランク研究所 Mrs. Anna Scherer, Miss Andrea Migel には結晶化の技術指導をして頂きました。

九州大学医学部臨床薬理学講座、大槻磐男教授には超薄切片の作成のための実験環境を提供して頂いたのみならず、文献では得られないトロポニンに関する多くの知見を頂き、有意義な議論をして頂きました。九州大学医学部第三解剖学講座、小坂俊夫教授、樋田一徳博士には結晶の固定・包埋・超薄切片の作成・電顕観察に関わる技術の指導と、実験設備の提供をして頂きました。

藤田保健衛生大学総合医科学研究所、谷口寿章博士には本研究で用いた様々な試料の質量分析機による一次構造の同定をして頂きました。

高エネルギー物理学研究所放射光施設の使用とデータ収集においては、坂部知平教授、鈴木守博士に協力して頂きました。

難波啓一博士、藤吉義則博士(現京都大学)、大沢芳夫博士、山下一郎主任研究員、その他松下国際研究所所員の皆様、NEDO 研究員伊藤光二博士、荒木聡彦博士、佐藤真則氏、松村貴晴氏、その他名古屋大学臨海実験所所員の皆様、OB の皆様には、常に励ましを頂きました。

以上のこの研究に従事する機会を与え、協力して頂いた方々に深く感謝いたします。

最後に、長い間見守っていてくれた両親と、かつては恋人として現在は妻として常に心の支えである広子に心より感謝したいとと思います。

REFERENCES

Books

The preparation and analysis of protein crystals. (1982) by McPharson, A. John Wiley and Sons, New York.

Crystallization of nucleic acid and proteins: a practical approach.(1992), Edited by Ducruix, A and Giegé, R., Oxford Univ. Press.

Diffraction methods for biological macromolecules, Method in Enzymology Vol. 114, 115.(1985), Edited by Wyckoff, H. W., Hirs, C. H. W., and Timasheff, S. N., Academic Press.

Reviews

Berrige, M. J. (1993) Inositol triphosphate and calcium signaling. *Nature* **361**, 315-325.

Chalovich, J. M. (1992) Actin mediated regulation of muscle contraction. *Pharmacology and Therapeutics* **55**, 95-148

Claphan, D. E. (1995) Calcium signaling. *Cell* **80**, 259-268.

Collins, J. H. (1991) Myosin light chains and troponin C: structural and evolutionary relationships revealed by amino acid sequence comparisons. *J. Muscle Res. Cell Motil.* **12**, 3-25.

Ebashi, S., and Endo, M. (1968) Calcium ion and muscle contraction. *Prog. Biophys. Mol. Biol.* **18**, 125-183

El-Saleh, S. C., Warber, K. D., and Potter, J. D. (1986) The role of troponin-tropomyosin in the regulation of skeletal muscle contraction. *J. Muscle Res. Cell Motil.* **7**, 387-404.

Farah, C. S., and Reinach, F. C. (1995) The troponin complex and regulation of muscle contraction.*FASEB J.* **9**, 755-767

Forest, K. and Schutt, C. (1992) Protein engineering for structure determination. *Current Opinion in Struct.l Biol.* **2**, 576-581.

Grabarek, Z., Tao, T., and Gergely, J. (1992) Molecular mechanism of troponin-C function. *J. Muscle Res. Cell Motil.* **13**, 383-393

Leavis, P. C., and Gergely, J. (1984) Thin filament proteins and thin filament-linked regulation of vertebrate muscle contraction. *CRC Crit. Rev. Biochem.* **16,** 235-305

Lehrer, S. S. (1994) The regulatory switch of the muscle thin filament: Ca^{2+} or myosin heads? *J. Muscle Res. Cell Motil.* **15**, 232-236.

Nilsson, B., Forsberg, G., Moks, T., Hartmanis, M., and Uhlén, M. (1992) Fusion proteins in biotechnology and structural biology. *Current Opinion Struc. Biol.* **2**, 569-575.

Ohtsuki, I., Maruyama, K., and Ebashi, S. (1986) Regulatory and cytoskeletal proteins of vertebrate skeletal muscle. *Adv. Protein Chem.* **38**, 1-67.

Pette, D., and Staron, R. S. (1990) Cellular and molecular diversities of mammalian skeletal muscle fibers. *Rev. Physiol. Biochem. Pharmacol.* **116**, 1-76.

Tobacman, L. S. (1996) Thin filament-mediated regulation of cardiac contraction. *Annu. Rev. Physiol.* **58**, 447-481.

Zot, A. S., and Potter, J. D. (1987) Structural aspects of troponin-tropomyosin regulation of skeletal muscle contraction. *Annu. Rev. Biophys. Biophys. Chem.* **16**, 535-559

Troponin and other muscle proteins

Babu, Y. S., Sack, J. S., Greenhough, T. J., Bugg, C. E., Means, A. R., and Cook, W. J. (1985) Three-dimensional structure of calmodulin. *Nature* **203**, 37-40.

Bailey, K. (1948) A new asymmetric protein component of the muscle fibril. *Biochem. J.* **43**, 271-279.

Breitbart, R. E. and Nandal-Ginard, B. (1986) Complete nucleotide sequence of the first skeletal troponin T gene. Alternative spliced exons exhibit unusual interspecies divergence. *J. Mol. Biol.* **188**, 313-324.

Campbell, A. P., and Sykes, B. D. (1991) Interaction of Troponin I and Troponin C. Use of the two-dimensional nuclear magnetic resonance transferred nuclear Overhauser effects to determine the structure of the inhibitory Troponin I peptide when bound to skeletal Troponin C. *J. Mol. Biol.* **222**, 405-421.

Chalovich, J. M., Chock, P. B., and Eisenberg, E. (1981) Mechanism of action of troponin-tropomyosin: inhibition of actomyosin ATPase activity without inhibition of myosin binding to actin. *J. Biol. Chem.* **256**, 575-578.

Chalovich, J. M., and Eisenberg, E. (1982) Inhibition of actomyosin ATPase activity by troponin-tropomyosin without blocking the binding of myosin to actin. *J. Biol. Chem.* **257**, 2432-2437.

Collins, J. H., Greaser, M. L., Potter, J. D., and Horn, M. J. (1977) Determination of the amino acid sequence of troponin C from rabbit skeletal muscle. *J. Biol. Chem.* **242**, 6356-6362.

Ebashi,S. (1963) Third component participating in the superprecipitation of 'natural actomyosin' *Nature* **200**, 1010.

Ebashi, S. and Ebashi, F. (1964) A new protein component participating in the superprecipitation of myosin B. *J. Biochem. (Tokyo)* **55**, 614.

Ebashi, S. and Kodama, A. (1965) A new protein factor promoting aggregation of tropomyosin. *J. Biochem. (Tokyo)* **58**, 107-108.

Ebashi, S., Wakabayashi, T., and Ebashi, F. (1971) Troponin and its components. *J. Biochem. (Tokyo)* **69**, 441-445.

Farah, C. S., Miyamoto, C. A., Ramos, C. H. I., Da Silvia, A. C. R., Quaggio, R. B., Fujimori, K., Smillie, L. B., and Reinach, F. C. (1994) Structural and regulatory functions of the NH_2- and COOH-terminal regions of skeletal muscle troponin I. *J. Biol. Chem.* **269**, 5230-5240.

Fisher, D., Wang, G., and Tobacman, L. S. (1995) NH_2-terminal truncation of skeletal muscle troponin T does not alter the Ca^{2+} sensitivity of thin filament assembly. *J. Biol. Chem.* **270**, 25455-25460.

Flicker, P.F., Phillips Jr, P.F. and Cohen, C. (1982) Troponin and its interactions with tropomyosin. An electron microscopic study. *J. Mol. Biol.* **162**, 495-501.

Fujita-Becker, S., Kluwe, L., Miegel, A., Maeda, K., and Maéda, Y. (1993) Reconstitution of rabbit skeletal muscle troponin from the recombinant subunits all expressed in and purified from *E. coli*. *J. Biochem.* **114**, 438-444.

Fujita, S., Maeda, K. and Maéda, Y. (1991) Complete coding sequences of cDNAs of four variants of rabbit skeletal muscle troponin T. *J. Muscle Res. Cell Motil.* **12**, 560-565.

Fujita, S., Maeda, K. and Maéda, Y. (1992) Expression in *Escherichia coli* and a functional study of a β-troponin T 25kDa fragment of rabbit skeletal muscle. *J. Biochem.* **112**, 306-308.

Gagne, S. M., Tsuda, S., Li, M., Chandra, M., Smillie, L. B., and Sykes, B. D. (1994) Quantification of the calcium-induced secondary structural changes in the regulatory domain of troponin-C. *Protein.Sci.* **3**, 1961-1974.

Grabarek, Z., Drabikowski, W., Vinokurov, L., Lu, R. C. (1981) Digestion of troponin C with trypsin in the presence and absence of Ca^{2+}: identification of cleavage points. *Biochem. Biophys. Acta* **671**, 227-233.

Greaser, M. L. and Gergely, J. (1971) Reconstitution of troponin activity from three protein components. *J. Biol. Chem.* **246**, 4226-4233.

Greaser, M. L. and Gergely, J. (1973) Purification and properties of the components from troponin. *J. Biol. Chem.* **248**, 2125-2133.

Haselgrove, J. C. (1972) X-ray evidence for a conformational change in the actin containing filaments of vertebrate striated muscle. *Cold Spring Harbor Symp. Quant. Biol.* **37**, 341-352.

Herzberg, O., Hayakawa, K., and James, M. N. G. (1984) Crystallographic data for troponin C from turkey skeletal muscle. *J. Mol. Biol.* **172**, 345-346.

Herzberg, O., Moult, J., and James, M.N.G. (1986) A model for the Ca^{2+}-induced conformational transition of troponin C. *J. Biol. Chem.* **261**, 2638-2644.

Herzberg, O., and James, M. N. G. (1985) Structure of the calcium regulatory muscle protein-troponin C at 2.8 Å resolution. *Nature* **313**, 653-659.

Herzberg, O., and James, M. N. G. (1988) Refined crystal structure of troponin C from turkey skeletal muscle at 2.0 Å resolution. *J. Mole. Biol.* **203**, 761-779.

Higashi, S., Ooi, T. (1968) Crystals of tropomyosin and native tropomyosin. *J. Mol. Biol.* **34**, 699-701.

Hill, T. L., Eisenberg, E., and Green, L. E. (1980) Theoretical model for cooperative equilibrium binding of myosin subfragment 1 to the actin-troponin -tropomyosin complex. *Proc. Natl. Acad. Sci. U. S. A.* **80**, 60-64.

Hitchcock, S. E. (1975) Regulation of muscle contraction: Binding of troponin and its components to actin and tropomyosin. *Eur. J. Biochem.* **52**, 255-63

Hitchcock, S. E. (1981) Study of the structure of troponin-C by measuring the relative reactivities of lysines with acetic anhydride. *J. Mol. Biol.* **147**, 153-173

Hitchcock, S. E., Zimmerman, C. J., and Smalley, C. (1981) Study of the structure of troponin-T by measuring the relative reactivities of lysines with acetic anhydride. *J. Mol. Biol.* **147**, 125-151

Hitchcock-DeGregori SE. (1982) Study of the structure of troponin-I by measuring the relative reactivities of lysines with acetic anhydride. *J. Biol. Chem.* **257**, 7372-7380

Hitchcock-DeGregori SE., Lewis, S. F., and Chou, T. M. T. (1985) Tropomyosin lysine reactivities and relationship to coiled coil structure. *Biochemistry* **24**, 3305-3314

Hitchcoch-DeGregori SE., Lewis, S. F., and Mistrik, M. (1988) Lysine reactivities of tropomyosin complexed with troponin. *Arch. Biochem. Biophys.* **264**, 410-416.

Horwitz, J., Bullard, B., and Mercola, D. (1979) Interaction of troponin subunits: the interaction between the inhibitory and tropomyosin-binding subunits. *J. Biol. Chem.* **254**, 350-355.

Huxley, H. E. (1972) Structural changes in the actin and myosin containing filaments during contraction. *Cold Spring Harbor Symp. Quant. Biol.* **37**, 361-376.

Jackson, P., Amphlett, G. W., and Perry, S. V. (1975) The primary structure of troponin T and the interaction with tropomyosin. *Biochem. J.* **151**, 85-97.

Jha, P. K., Mao, C., and Sarkar, S. (1996) Photo-cross-linking of rabbit skeletal troponin I deletion mutants with troponin C and its thiol mutants: the inhibitory region enhances binding of troponin I fragments to troponin C. *Biochemistry* **35**, 11026-11035.

Kabsch, W., Mannerz, H. G., Suck, D., Pai, E. F., and Holmes, K. C. (1990) Atomic structure of the actin: DNase Icomplex. *Nature* **347**, 37-44.

Kluwe, L., Maeda, K., and Maeda, Y. (1993) *E. coil* expression and characterization of a mutant troponin I with the three cysteine residues substituted. *FEBS Lett.* **323**, 83-88.

Kluwe, L., Maeda, K., Miegel, A., Fujita-Becker, S., Maeda, Y., Talbl, G., Houthaeve, T., and Kellner, R. (1995) Rabbit skeletal muscle αα-tropomyosin expressed in baculovirus-infected insect cells possesses the authentic N-terminus structure and functions. *J. Muscle Res. Cell Motil.* **16**, 103-110.

Kobayashi, T., Takagi, T., Konishi, K., and Cox, J. A. (1989) Amino acid sequence of crayfish troponin I. *J. Biol. Chem.* **264**, 1551-1557.

Kobayashi, T., Tao, T., Grabarek, Z., Gergely, J., and Collins, J. H. (1991) Crosslinking of residue 57 in the regulatory domain of a mutant rabbit skeletal muscle troponin C to the inhibitory region of troponin I. *J. Biol. Chem.* **266**, 13746-13751

Kobayashi, T., Tao, T., Gergely, J., and Collins, J. H. (1994) Structure of the troponin complex: implication of photocross-linking of troponin I to troponin C thiol mutants. *J. Biol. Chem.* **269**, 5725-5729

Kobayashi, T., Grabarek, Z., Gergely, J., and Collins, J. H. (1995) Extensive interactions between troponins C and I. Zero-lenght cross-linking of troponin I and acetylated troponin C. *Biochemistry.* **34**, 10946-10952.

Krudy, G. A., Kleercloper, Q., Guo, X., Howarth, J. W., Solaro, R. J., and Rosevear, P. R. (1994) NMR studies delineating spatial relationships within the cardiac troponin I-troponin C complex. *J. Biol. Chem.* **269**, 23731-23735.

Lehman, W., Craig, R., and Vibert, P. (1994) Ca^{2+}-induced tropomyosin movement in *Limulus* thin filaments revealed by three-dimensional reconstitution. *Nature* **368**, 65-67.

Lehrer, S. S., and Morris, E. P. (1982) Dual effects of tropomyosin and troponin-tropomyosin on the actomyosin subfragment 1 ATPase. *J. Biol. Chem.* **257**, 8073-8080

Leszyk, J., Dumaswala, R., Potter, J. D., and Collins, J. H. (1988) Amino acid sequence of bovine cardiac troponin I. *Biochemistry* **27**, 2821-2827.

Leszyk, J., Grabarek, Z., Gergely, J., and Collins, J. H. (1990) Characterization of zero-length cross-links between rabbit skeletal muscle troponin C and troponin I: evidence for a direct interaction between inhibitory region of troponin I and the NH_2-terminal, regulatory domain of troponin C. *Biochemistry* **29**, 299-304.

Mak, A. S., and Smillie, L. B. (1981) Structural interpretation of the two-site binding of troponin on the muscle thin filament. *J. Mol. Biol.* **149**, 541-550.

Malnic, B., and Reinach, F. C. (1994) Assembly of functional skeletal muscle troponin complex in Escherichia coli. *Eur. J. Biochem.* **222**, 49-54.

Medford, R. M., Nguyen, H. T., Destree, A. T., Summers, E., and Nadal-Ginard, B. (1984) A novel mechanism of alternative RNA splicing for the developmentally regulated generation of troponin T isoforms from a single gene. *Cell* **38**, 409-421.

Mercola, D. Bullard, B., and Priest, J. (1975) Crystallization of troponin C. *Nature* **254**, 634-635.

Morris, E. P., and Lehrer, S. S. (1984) Troponin-tropomyosin interactions. Fluorescence studies of the binding of troponin, troponin T, and chymotryptic troponin T fragments to specifically labeled tropomyosin. *Biochemistry* **23**, 2214-2220.

Nagano, K., Miyamoto, S., Matsumura, M., and Ohtsuki, I. (1982) Prediction of a triple-stranded coiled-coil region in tropomyosin-troponin T complex. *J. theor. Biol.* **94**, 743-782.

Nagano, K., Miyamoto, S., Matsumura, M., and Ohtsuki, I. (1980) Possible formation of a triple-stranded coiled-coil region in tropomyosin-troponin T binding complex. *J. Mol. Biol.* **141**, 217-222.

Nakamura, S., Yamamoto, K., Hashimoto, K., and Ohtsuki, I. (1981) Effect of chymotryptic troponin T fragments on the Ca^{2+}-sensitibity of superprecipitation. *J. Biochem.* **89**, 1639-1641.

Ngai, S. M. and Hodges, R. S. (1992) Biologically important interactions between synthetic peptides of the N-terminal region of TnI and TnC. *J. Biol. Chem.* **267**, 15715-15720.

Ngai, S. M, Sonnichsen, F. D., and Hodges, R. S. (1994) Photochemical cross-linking between native rabbit skeletal troponin C and benzoylbenzoyl-troponin I inhibitory peptide, residues 104-115. *J. Biol. Chem.* **269**, 2165-2172.

Nozaki, S., Kobayashi, K., Katayama, E., and Muramatsu, I. (1980) Synthetic studies on troponin I active site. Preparation of a pentadecapeptide with inhibitory activity toward actomyosin adenosine triphosphatase. *Chem. Lett.* **3**, 345.

Ohtstuki, I. (1979) Molecular arrengement of troponin-T in the thin filament. *J Biochem.* **86**, 491-497.

Ohtsuki, I., Siraishi, F., Suenaga, N., Miyata, T., and Tanokura, M. (1984) A 26K fragment of troponin T from rabbit skeletal muscle. *J. Biochem.* **95**, 1337-1342.

Ohtsuki, I., Yamamoto, K. and Hashimoto, K. (1981) Effect of two C-terminal side chymotryptic troponin T subfragments on the Ca^{2+} sensitivity of superprecipitation and ATPase activities of actomyosin. *J. Biochem.* **90**, 259-261

Ohtsuki, I., Onoyama, Y., and Shiraishi, F. (1988) Electron microscopic study of troponin. *J. Biochem.* **103**, 913-919.

Ojima, T., Tanaka, H., and Nishita, K. (1995) Amino acid sequence of C-terminal 17kDa CNBr-fragment of Akazara scallop troponin I. *J. Biochem.* **117**, 158-162.

Olah, G. A., and Trewhella, J. (1994) A model structure of the jmuscle protein complex $4Ca^{2+}$-troponin C-troponin I derived from small-angle scattering data: implication for regulation. *Biochemistry* **33**, 12800-12806

Olah, G. A., Rokop, S. E., Wang, C.-L. A., Blechner, S. L., and Trewhella, J. (1994) Troponin I encompasses as extended troponin C in the Ca^{2+}-bound complex: A small-angle X-ray and neutron scattering study. *Biochemistry* **33**, 8233-8239.

Onishi, H., Maeda, K., Maeda, Y., Inoue, A., and Fujiwara, K. (1995) Functional chicken gizzard heavy meromyosin expression in and purification from baculovirus-infected insect cells. *Proc. Natl. Acad. Sci. U.S.A* **92**, 704-708.

Pan, B. S., Gordon, A. M., and Potter, J. D. (1991) Deletion of the first 45 NH_2-terminal residues of rabbit skeletal troponin T strengthen binding of troponin to immobilized tropomyosin. *J. Biol. Chem.* **266**, 12432-12438.

Pan, B.S., and Potter, J. D. (1992) Two genetically expressed troponin T fragments representing α and β isoforms exhibit functional differences. *J. Biol. Chem.* **267**, 23052-23056.

Parry, D. A. D. and Squire, J. M. (1973) Structural role of tropomyosin in muscle regulation. Analysin of the X-ray diffraction patterns from relaxed and contracting muscles. *J. Mole. Biol.* **75**, 33-55.

Pato, M. D., Mak, A. S., and Smillie, L. B. (1981) Fragments of rabbit striated muscle α-tropomyosin. I. Preparation and

characterization. *J. Biol. Chem.* **256**, 593-601.

Pato, M. D., Mak, A. S., and Smillie, L. B. (1981) Fragments of rabbit striated muscle α-tropomyosin. II. Binding to troponin T. *J. Biol. Chem.* **256**, 602-607.

Pearlstone, J. R., Carpenter, M. R., and Smillie, L. B. (1977) Primary structure of rabbit skeletal muscle troponin-T: purification of cyanogen bromide fragments and the amino acid sequence of fragment CB2. *J. Biol. Chem.* **252**, 971-977.

Pearlstone, J. R., Carpenter, M. R., and Smillie, L. B. (1977) Primary structure of rabbit skeletal muscle troponin-T: sequence determination of four cyanogen bromide fragments, CB4, CB5, CB6, and CB7. *J. Biol. Chem.* **252**, 978-982.

Pearlstone, J. R., Carpenter, M. R., and Smillie, L. B. (1977) Primary structure of rabbit skeletal muscle troponin-T: sequence determination of the NH_2-terminal fragment CB3 and the complete sequence of troponin-T. *J. Biol. Chem.* **252**, 983-989.

Pearlstone, J. R., and Smillie, L. B. (1978) Troponin T fragments: physical properties and binding to troponin C. *Can. J. Biochem.* **56**, 521-

Pearlstone, J. R., and Smillie, L. B. (1982) Binding of troponin-T fragments to several types of tropomyosin. Sensitivity to Ca^{2+} in the presence of troponin-C. *J. Biol. Chem.* **257**, 10587-10592.

Pearlstone, J. R., and Smillie, L. B. (1983) Effects of troponin-I plus -C on the binding of troponin-T and its fragments to α-tropomyosin. *J. Biol. Chem.* **258**, 2534-2542

Potter, J. D., and Gergely, J. (1975) Troponin, tropomyosin, and actin interactions in the Ca^{2+} regulation of muscle contraction. *J. Biol. Chem.* **13**, 2697-2703

Potter, J. D., Sheng, Z., Pan, B. S., and Zhao, J. (1995) A direct regulatory role for troponin T and a dual role for troponin C in the Ca^{2+} regulation of muscle contraction. *J. Biol. Chem.* **270**, 2557-2562.

Rayment, I., Rypniewski, W. R., Schmidt-Base, K., Smith, R., Benning, M. MM., Tomchick, D., Winkelmann, D. A., Wesenberg, G., and Holden, H. M. (1993) Three-dimensional structure of myosin subfragment-1: A molecular motor. *Science* **261**, 50-58.

Rayment, I., and Winkelmann, D. A. (1984) Crystallization of myosin subfragment 1. *Proc. Acad. Sci. U.S.A.* **81**, 4378-4380.

Schulzki, H.-D., Kramer, B., Fleschhauer, J., Mercola, D. A., and Wollmer, A. (1990) Calcium-dependent distance changes in binary and ternary complexes of troponin. *Eur. J. Biochem.* **189**, 683-692.

Sheng, Z., Pan, B. S., Miller, T. E., and Potter, J. D. (1992) Isolation, expression , and mutation of a rabbit skeletal muscle cDNA clone for troponin I. *J. Biol. Chem.* **267**, 25407-25413

Slupsky, C. M., and Sykes, B. D. (1995) NMR solution structure of calcium-saturated skeletal muscle troponin C. *Biochemistry* **34**, 15953-15964

Spudich, J. A., and Watt, S. (1971) The regulation of rabbit skeletal muscle contraction: biochemical studies of the interaction of the tropomyosin-troponin complex with actin and the proteolytic fragments of myosin. *J. Biol. Chem.* **246**, 4866-4871

Strasburg, G. M., Greaser, M. L., and Sundaralingam, M (1980) X-ray diffraction studies of troponin-C crystals from rabbit and chicken skeletal muscles. *J. Biol. Chem.* **255**, 3806-3808.

Sundaralingam, M., Bergstorm, R., Strasburg, G., Rao, S. T., Roychowdhury, P., Greaser, M. L., and Wang, B. C. (1985) Molecular structure of troponin C from chicken skeletal muscle at 3 angstrom resolution. *Science* **227**, 945-948

Sutoh, K. (1980) Direct evidence for the calcium-induced change in the quaternary structure of troponin in situ. Millisecond cross-linking of troponin components by a photosensitive heterobifunctional reagent. *Biochemistry* **19**, 1977-1983.

Syska, J., Wilkinson, M. J., Grand, R. J. A., and Perry, S. V. (1976) The relationship between biological activity and primary structure of troponin I from white skeletal muscle of the rabbit. *Biobem. J.* **153**, 375-387.

Swenson, C. A., and Fredricksen, R. S. (1992) Interaction of troponin C and troponin C fragments with troponin I and the troponin I inhibitory peptide. *Biochemistry* **31**, 3420-3429.

Talbot, J. A., and Hodges, R. S. (1979) Synthesis and biological activity of an icosapeptide analog of the actomyosin ATPase inhibitory region of troponin I. *J. Biol. Chem.* **254**, 3720-3723.

Talbot, J. A., and Hodges, R. S. (1981) Synthetic studies on the inhibitory region of rabbit skeletal troponin I. Relationship of amino acid sequence to biological activity. *J. Biol. Chem.* **256**, 2798-2802.

Talbot, J. A., and Hodges, R. S. (1981) Comparative studies on the inhibitory region of selected species of troponin I. *J. Biol. Chem* **256**, 12374-12378.

Tanokura, M., Tawada, Y., Onoyama, Y., Nakamura, S. and Ohtsuki, I. (1981) Primary structure of chymotryptic subfragments from rabbit skeletal troponin T. *J. Biochem.* **90**, 263-265.

Tanokura, M., Tawada, Y., and Ohtsuki, I (1982) Chymotryptic subfragments of troponin T from rabbit skeletal muscle. I Determination of the primary structure. *J. Biochem.* **91**, 1257-1265.

Tanokura, M., Tawada, Y., Ono, A., and Ohtsuki, I. (1983) Chymotryptic subfragment of troponin T from rabbit skeletal muscle. Interaction with tropomyosin, troponin I and troponin C. *J. Biochem.* **93**, 331-337.

Tao, T., Gowell, E., Strasburg, G. M., Gergely, J., and Leavis, P. C. (1989) Ca^{2+} dependence of the distance between Cys-98 of troponin C and Cys-133 of troponin I in the ternary troponin complex: resonance energy transfer measurements. *Biochemistry* **28**, 5902-5908.

Tao, T., Gong, B. -J., and Leavis, P.C. (1990) Calcium-induced movement of troponin I relative to actin in skeletal muscle thin filament. *Science* **247**, 1339-1341

Van Eyk, J. E., and Hodges, R. S. (1988) The biological importance of each amino acid residues of the troponin I inhibitory sequence 104-115 in the interaction with troponin C and tropomyosin-actin. *J. Biol. Chem.* **263**, 1726-1732.

Van Eyk, J. E., and Hodges, R. S. (1991) A synthetic peptide of the N-terminus of actin interacts with myosin. *Biochemistry* **30**, 11676-82

Van Eyk, J. E., Sönnichsen, F. D., Sykes, B. D., Hodges, R. S. (1991) Interaction of actin 1-28 with myosin and troponin I and importance of these interaction to muscle regulation. In: Ruegg, J. C., ed, *Peptide as probes in muscle reserch*, Heidelberg, Germany: Springer-Verlag, pp. 15-31.

Wang, C. -K., and Cheung, H. C. (1986) Proximity relationship in the binary complex formed between troponin I and troponin C. *J. Mol. Biol.* **190**, 509-521.

Wang, Z., Sarker, S., Gergely, J., and Tao, T. (1990) Ca^{2+}-dependent interactions between the C-helix o troponin C and troponin I. Photocross-linking and fluorescence studies using recombinant troponin C. *J. Biol. Chem.* **265**, 4953-4957

Weeds, A. G., and Taylor, R. S. (1975) Separation of subfragment-1 isoenzymes from rabbit skeletal muscle myosin. *Nature* **257**, 54-56

White, S. P., Cohen, C., and Phillips, G. N. Jr. (1987) Structure of co-crystals of tropomyosin and troponin. *Nature* **235**, 826-828.

White, H. D., and Rayment, I. (1993) Kinetic characterization of reductively methylated myosin subfragment 1. *Biochemistry* **32**, 9859-9865.

Wilkinson, J. M., and Grand, R. J. A. (1978) Comparison of amino acid sequence of troponin I from different striated muscles. *Nature* **271**, 31-35.

Willadsen, K. A., Butters, C. A., Hill, L. E., and Tobacman, L. S. (1992) Effects of the amino-terminal region of tropomyosin and troponin T on thin filament assenbly. *J. Biol. Chem.* **267**, 23746-23752.

Winkelmann, D. A., Mekeel, H., and Rayment, I. (1985) Packing analysis of crystalline myosin subfragment-1. *J. Mol. Biol.* **181**, 487-501.

Winkelmann, D. A., Baker, T. S., and Rayment, I. (1991) Three-dimensional structure of myosin subfragment-1 from electron microscopy of sectioned crystals. *J. Cell Biol.* **114**, 701-713.

Xie, X., Harrison, D. H., Schlichting, I., Sweet, R. M., Kalabokis, V. N., Szent-Györgyi, A. G., and Cohen, C. (1994) Structure of the regulatory domain of scallop myosin at 2 Å resolution: implications for regulation. *Nature* **368**, 306-312.

Zhao, X., Kobayashi, T., Malak, H., Gryczynski, I., Lakowicz, J., Wade, R., and Collins, J. H. (1995) Calcium-induced troponin flexibility revealed by distance distribution measurements between engineered sites. *J. Biol. Chem.* **270**, 15507-15514.

Zot, A. S., Potter, J. D., and Strauss, W. L. (1987) Isolation and sequence of a cDNA clone for rabbit skeletal muscle tropopnin C: homology with calmodulin and parvalbmin. *J. Biol. Chem.* **262**, 15418-15421.

Crystallization and crystallographic techniques

Giegé, R., Lorber, B., and Dietrich, A. T. (1994) Crystallogenesis of biological macromolecules: facts and perspective. *Acta Cryst.* **D50**, 339-350.

Hope, H. (1990) Crystallography of biological macromolecules at ultra-low temperature. *Annu. Rev. Biophys. Biophys. Chem.* **19**, 107-126.

Hope, H., Frolow, F., von Boehlen, K., Makowski, I., Kratky, C., Halfon, Y., Webster, P., Bartels, K. S., Wittman, H. G., and Yonath, A. (1989) Cryocrystallography of ribosomal particles. *Acta Cryst.* **B45**, 190-199.

MacPherson, A., Malkin, A. J., and Kuznetsov, Y. G. (1995) The science of macromolecular crystallization. *Structure* **3**, 759-768.

McPherson, A. (1990) Current approaches to macromolecular crystallization. *Eur. J. Biochem.* **189**, 1-23.

Mikol, V., Hirsch, E., and Giegé, R. (1989) Monitoring protein crystallization by dynamic light scattering. *FEBS Lett.* **258**, 63-66.

Mikol, V., Hirsch, E., and Giegé, R. (1990) Diagnostic of precipitant for biomacromolecule crystallization by quasi-elastic light-scattering. *J. Mol. Biol.* **213**, 187-195.

Nakasako, M. (1995) *Methods in cryogenic protein crystallography version 1.0.* Biophysics laboratory and SR structural biology research group, Riken.

Rodgers, D. W. (1994) Cryocrystallography. *Structure* **2**, 1135-1140.

Schick, B., and Jurnak, F. (1994) Extinction of the diffraction resolution of crystals. *Acta Cryst.* **D50**, 563-568.

Sousa, R. (1995) Use of glycerol, polyols and other protein structure stabilizing agents in protein crystallization. *Acta Cryst.* **D51**, 271-277.

Teng, T. Y. (1990) Mounting of crystals for macromolecular crystallography in a free-standing thin film. *J. Appl. Cryst.* **23**, 387-391.

Trakhanov, S. and Quiocho, F. A. (1995) Influence of divalent cations in protein crystallization. *Protein Sci.* **4**, 1914-1919.

Weber, P. C. (1991) Physical principles of protein crystallization. *Advance in protein chem.* 41, 1-36.

Methods

Babbitt, P. C., West, B. L., Buecher, D. D., Kuntz, I. D., and Kenyon, G. L. (1990) Removal of a proteolytic activity associated with aggregates formed from expression of creatine kinase in Escherichia coli leads to improved recovery of active enzyme. Bio/Technology 8, 945-949.

Jacobson, G. R., Schaffer, M. H., Stark, G. R., and Vanaman, T. C. (1973) Specific chemical cleavage in high yield at the amino peptide bonds of cysteine and cystine residues. *J. Biol. Chem.* **248**, 6583-6591.

Gill, S. C., and von Hippel, P. H. (1989) Calculation of protein extinction coefficients from amino acid sequence data. *Anal. Biochem.* **182**, 319-326.

Taniguchi, H., Suzuki, M., Manenti, S., and Titani, K. (1994) A mass spectrometric study on the in vivo posttranslational modification of GAP-43. *J. Biol. Chem.* **269**, 22481-22484.

Others

Chernaia, M. M., Malcolm, B. A., Allaire, M., and James, M. N. G. (1993) Hepatitis A virus 3C protease: Some properties, crystallization and preliminary crystallographic characterization. *J. Mol. Biol.* **234**, 890-893.

Fontana, A., Fassina, G., Vita, C., Dalzoppo, D., Zamai, M., and Zambonin, M. (1986) Correlation between sites of limited proteolysis and segmental mobility in thermolysin. *Biochemistry* **25**, 1847-1851.

Iwata, S., Ostermeier, C., Ludwig, B., and Michel, H. (1995) Structure at 2.8 Å resolution of cytochrome c oxidase from *Paracoccus denitrificans*. Nature 376, 660-669.

Kautt, M. R., and Ducruix, A. (1994) Crystallization of previously desolted lysozyme in the presence of sulfate ions. *Acta Cryst.* **D50**, 366-369.

Lischwe, M., Newton, R. C., Huang, J. J., Yates, R. A., Breth, L. A., and Larsen, B. S. (1993) *Escherichia coli*: derived murine interleukin-1b with N-terminus partially Na-acetylated. *Protein Expression Purification* **4**, 499-502.

Ostermeier, C., Iwata, S., Ludwig, B., and Michel, H. (1995) F_V fragment mediated crystallization of the membrane protein bacterial cytochrome c oxidase. *Nature Struct. Biol.* **2**, 842-846.

Rould, M. A., Perona, J. J., and Steitz, T. A. (1991) Structural basis of anticodon loop recognition by glutaminyl-tRNA synthetase. *Nature* **352**, 213-218.

Rypniewski, W. R., Holden, H. M., and Raymet, I. (1993) Structural consequences of reductive methylation of lysine residues in hen egg white lysozyme: An X-ray analysis at 1.8-Å resolution. *Biochemistry* **32**, 9851-9858.

Tsunazawa, S. (1995) Amino-terminal processing of nascent proteins: their role and implication on biological function. (in Japanese)蛋白質・核酸・酵素 40, 389-398.

Zhu, L., Sage, J. T., Rigos, A. A., Morikis, D., and Champion, P. M. (1992) Comformational interconversion in protein crystals. *J. Mol. Biol.* **224**, 207-215.